Genetic regulation of the cellular and organismal response to hypertonic stress in *C. elegans*

by

Sarel Johanna Urso

B.A., Oberlin College, 2016

Submitted to the Graduate Faculty of the

School of Medicine in partial fulfillment

of the requirements for the degree of

Doctor of Philosophy

University of Pittsburgh

2021

UNIVERSITY OF PITTSBURGH

SCHOOL OF MEDICINE

This dissertation was presented

by

Sarel Johanna Urso

It was defended on

April 8, 2021

and approved by

Arohan R. Subramanya, Associate Professor, Department of Medicine, Renal-Electrolyte Division

Arjumand Ghazi, Associate Professor, Department of Pediatrics

Yang Hong, Associate Professor, Department of Cell Biology

Karen Arndt, Professor, Department of Biological Sciences

Dissertation Director: Todd Lamitina, Associate Professor, Department of Cell Biology

Genetic regulation of the cellular and physiological response to hypertonic stress in *C. elegans*

Sarel Johanna Urso, Ph.D.

University of Pittsburgh, 2021

Virtually all cells must maintain osmotic homeostasis in order to survive. Changes in extracellular osmolarity due to both physiological and pathophysiological conditions disrupt osmotic homeostasis and elicit rapid cellular responses. In particular, increased extracellular osmolarity (hypertonic stress, HTS) causes a rapid decrease in cell volume leading to increased intracellular ionic strength. One major pathway cells activate to counteract HTS involves the upregulation of genes that facilitate accumulation of small organic solutes called compatible osmolytes. Compatible osmolytes restore cell volume, decrease intracellular ionic strength, and promote proper protein folding. The mechanisms by which animals detect HTS and activate osmoprotective gene expression, including genes involved in osmolyte accumulation, remain poorly understood. Similarly to humans, *Caenorhabditis elegans* responds to HTS by synthesizing compatible osmolytes from glucose metabolic products. *C. elegans* synthesizes the compatible osmolyte glycerol by transcriptionally upregulating the enzyme that catalyzes the rate-limiting step in glycerol biosynthesis, glycerol-3-phosphate dehydrogenase (GPDH-1). To understand how the hypertonic stress response (HTSR) is coordinated in animals, I conducted a genetic screen to identify mutants with no induction of osmolyte biosynthesis gene expression (Nio mutants). In this screen I discovered ten loss-of-function (LOF) recessive single-gene mutants with impaired hypertonic induction of a *gpdh-1* reporter. In addition to a Nio phenotype, four of these mutants were unable to adapt to HTS. The phenotype-causing mutations in two of these mutants were

distinct nonsense single nucleotide polymorphisms in the conserved *O*-GlcNAc transferase OGT-1. The phenotype-causing mutations in the other two mutants were LOF missense mutations in interacting components of the 3' mRNA cleavage and polyadenylation complex. Upon further characterization, I found that *ogt-1* is required in an osmosensitive hypodermal cell signaling pathway for the post-transcriptional induction of *gpdh-1*. Surprisingly, OGT-1 does not function through its well-studied enzymatic *O*-GlcNAcylation activity in this pathway. Additionally, my data suggest that OGT-1 and the 3' cleavage and polyadenylation complex function through separate cellular pathways to regulate the HTSR. The results from my thesis project not only describe novel functions of conserved and well-studied proteins, but they also identify unusual paradigms of gene regulation that may be applicable to physiological contexts outside of the HTSR.

Table of Contents

List of Tables

List of Figures

Preface

Since the start of my journey into scientific research ten years ago, my experiences have been shaped by wonderful mentors and an amazing network of friends and family. I consider myself very lucky and I am extremely grateful to everyone who made this dissertation possible.

First and foremost, I would like to thank my doctoral advisor Dr. Todd Lamitina. Todd is a brilliant scientist, driven researcher, and truly an exceptional mentor. I am so lucky to have found the perfect lab for my graduate education. I joined Todd's lab with no experience in genetics or *C. elegans*, but thanks to countless hours spent discussing ideas, analyzing papers, and learning techniques with Todd, I am graduating as a well-rounded *C. elegans* geneticist and biologist. Todd's love and energy for science are contagious. Todd comes into lab every day genuinely excited about something, whether it be a new idea, a new discovery, or a recent baseball, running, or music - related accomplishment. This excitement is refreshing and encouraging, but above all it is inspiring. From Todd's example I have learned how to be a curious, confident, and creative scientist and I will take these skills with me into the next steps of my career.

Second, I would like to thank members of the broader University of Pittsburgh community for their academic support. Thank you to my thesis committee made up of Drs. Arohan Subramanya, Arjumand Ghazi, Yang Hong and Karen Arndt for their valued advice on my project, bringing a variety of perspectives to my research, and guiding me towards developing a focused story. This work benefited greatly from our biannual meetings. Thank you to my Cell Biology and Molecular Physiology program directors, Drs. Michael Butterworth and Adam Kwiatkowski, for their feedback on presentations, career advice, and keeping me on track to finish my doctorate.

Last, thank you to the Pittsburgh worm community, specifically the Yanowitz, Ghazi, and Gurkar labs, for sharing reagents, expertise, and good holiday party laughs with me.

Third, I would like to thank the mentors who introduced me to science and paved the way for my journey into graduate school. My scientific career started as a high school junior in Dr. Cynthia Haseltine's lab at Washington State University. Dr. Haseltine not only introduced me to research and common biological techniques, while guiding me through my own project, but her never-wavering enthusiasm and love for science also inspired me to pursue a career in science. I continued my scientific pursuits at Oberlin College and was greatly influenced by my honor's thesis advisor Dr. Lisa Ryno. Through Dr. Ryno's dedicated mentorship I learned how to contribute to a collaborative lab environment, troubleshoot, and most importantly how to tell a story through my research.

Finally, I would like to thank my support network inside and outside the lab. Thank you to my two fellow 'Lamitina Lab Rats', Dr. Paige Rudich and Carley Snoznik for being the best lab mates and friends I could have asked for. It was an honor to work alongside such smart and hard-working women. Thank you to my fellow scientists and good friends, Julia Loose and Charlie Good, for our regular hikes and valuable scientific and non-scientific chats. Last and most importantly, thank you to my family. Thank you to my parents, Dr. David Loewus and Andrea Kirchner-Loewus, for encouraging me from the beginning to be an independent thinker and hard worker and for providing me with a strong foundation from which to pursue my dreams. Thank you to my late grandparents, Drs. Frank and Mary Loewus for being my scientific role models and setting me up with my own subscription to *The Scientist* as a high schooler. Above all, thank you to my husband and biggest supporter, Josh Urso, for his unwavering love and encouragement during all the highs and lows of graduate school.

This dissertation was supported by a NIH R01GM135577 grant to Todd and a Research Advisory Council grant from the Children's Hospital of Pittsburgh to me.

List of Abbreviations

3’ UTR: 3’ untranslated region

ABA: Abscisic acid

ACE: Angiotensin-converting enzyme

Akt: Protein kinase B

AMPK: AMP-activated protein kinase

APA complex: 3’ mRNA cleavage and polyadenylation complex

APA: Alternative polyadenylation

AQP2: Aquaporin 2

AQP5: Aquaporin 5

AQP7: Aquaporin 7

AT_1: Angiotensin II receptor type I

ATM: Ataxia telangiectasia-mutated kinase

BTG1: Betaine/GABA transporter 1

CaMKIV: Calcium/calmodulin-dependent kinase

*ce*OGT-1: *C. elegans* OGT-1

CF II_m: Cleavage factor II

CF I_m: Cleavage factor I

CHO cells: Chinese hamster ovary cells

CPSF: Cleavage and polyadenylation specificity factor

CstF: Cleavage stimulation factor

DMSP: Dimethylsulfoniopropionate

DSE: Downstream element sequence

ECF: Extracellular fluid

ECM: Extracellular matrix

eIF2α: Eukaryotic translation initiation factor 2 alpha

eIF4F: Eukaryotic initiation factor 4F

eIF4GI: Eukaryotic translation initiation factor 4 gamma 1

ENac: Epithelial sodium channel

ENU: N-ethyl-N-nitrosourea

ER: Endoplasmic reticulum

ev(RNAi): *empty vector RNAi*

GFP: Green fluorescent protein

GPC: Glycerophosphocholine

GPD1: Glycerol-3-phosphate dehydrogenase (yeast)

GPDH: Glycerol-3-phosphate dehydrogenase (*C. elegans*)

HBP: Hexamine biosynthetic pathway

HCF-1: Mammalian host cell factor 1

HOG pathway: High osmolarity glycerol pathway (yeast)

*h*OGT: *H. sapians* OGT

HSPs: Heat shock proteins

HTS: Hypertonic stress

HTSR: Hypertonic stress response

LOF: Loss-of-function

LRRC8: Leucine-rich repeat containing 8A channel

MAPK: Mitogen-activated protein kinase

MEFs: Mouse embryonic fibroblasts

MNCs: Magnocellular neurosecretory cells

mOGT: Mitochondrial OGT

MscL: Mechanosensitive channel large conductance

MscS: Mechanosensitive channel small conductance

NCED: 9-*cis*-expoxycartenoid dioxygenases

ncOGT: Nucleocytoplasmic OGT

NFAT5/TonEBP: Nuclear factor of activated T cells 5/ Tonicity-responsive enhancer binding protein

NGM: Nematode growth media

Nio: No induction of osmolyte biosynthesis gene expression

NLS: Nuclear localization signal

NPA motif: Asparagine-proline-alanine motif

NTE: Neuropathy target esterase

OLVTs: Organum vasculosum of the lamina terminalis cells

ORE/TonE: Osmotic response element/tonicity enhancer element

ORG: Osmotically regulated gene

OSR: Osmotic stress resistance

OSR1: Oxidative stress responsive kinase 1

PABP: Poly(A)-binding protein

PAP: Poly(A) polymerase

PAS: Polyadenylation signal sequence

PI3K-IA: Phosphoinositide 3-kinase IA

PKA: Protein kinase A

RAA: Renin-angiotensin-aldosterone

RBPs: RNA binding proteins

RNAi: RNA interference

RR: Response regulator

RRM: RNA-recognition motif

RVD: Regulatory volume decrease

SHK: Sensor histidine kinase

SMIT: Sodium myo-inositol transporter

SNARE: Soluble N-ethylmaleimide–sensitive factor attachment protein receptor

SNP: Single nucleotide polymorphism

sOGT: Short isoform OGT

SPAK: Ste20/SPS1-related proline/alanine-rich kinase

SYMPK: Symplekin

TAUT: Taurine transporter

TMAO: Trimethylamine N-oxide

TOF: time of flight

TPR: Tetratricopeptide repeat

TRPV1: Transient receptor potential vanilloid type-1 channel

UPR: Unfolded protein response

VRAC: Volume – regulated anion channel

WNK1: Lysine deficient protein kinase 1

WT: Wild type

1.0 Introduction

Cell volume is among the most aggressively defended physiological set points. Changes in cell volume affect cellular properties vital for proper cell function such as turgor pressure, membrane tension, and increased intracellular ionic strength [1]. Among the cellular functions directly affected by cell shrinkage or swelling are protein folding [2], enzymatic function [3, 4], membrane potential [5], and cytoskeletal architecture [6]. Abrupt changes in cell volume lead to cell death if proper protective mechanisms are not engaged [7-12]. Therefore, cells in every type of organism have evolved mechanisms to adapt to and counteract changes in cellular volume. Many, but not all, of these mechanisms are highly conserved. While the physiological mechanisms used to adapt to cell volume changes have been extensively characterized in single and multicellular organisms, the regulatory pathways that are triggered by cell volume changes to initiate these adaptive mechanisms are poorly understood, especially in multicellular organisms. Using the *in vivo* model *Caenorhabditis elegans*, my project uses unbiased genetic methods to dissect the regulatory pathways governing the cellular and organismal responses to changes in cell volume caused by osmotic stress. I discovered ten mutants with distinct loss of function (LOF) mutations in seven genes that have an impaired response to increased extracellular osmolarity (hypertonic stress, HTS). Detailed characterization of four of these mutants revealed critical roles of the *O*-GlcNAc transferase OGT and the 3' mRNA cleavage and polyadenylation complex in the hypertonic stress response (HTSR). Intriguingly, I demonstrate that OGT functions through a non-canonical and post-transcriptional mechanism to regulate the HTSR. My discoveries contribute novel insights to our understanding of the HTSR in multicellular organisms and suggest

that multiple pathways are required to successfully upregulate protective gene expression during HTS.

1.1 Cell volume regulation

Cell volume is directly influenced by water movement across the plasma membrane. Cell membranes are several orders of magnitude more permeable to water than they are to ions [13, 14]. This permeability allows water to move up ionic concentration gradients, a force termed osmosis. Water therefore accumulates inside cells when extracellular ionic strength is decreased relative to intracellular ionic strength (hypotonic stress) and this results in cell swelling. Correspondingly, water leaves cells when extracellular ionic strength is increased relative to intracellular ionic strength (HTS) and this results in cell shrinkage. Cells respond to hypertonic and hypotonic stress with specific mechanisms that restore cell volume.

1.1.1 Determinants of cell membrane permeability

The permeability of the cell plasma membrane to water is determined by two main factors: fluidity of the lipid bilayer [15] and the presence of water-permeable channels (aquaporins) in the plasma membrane [16]. Generally, the more fluid the lipid bilayer, the more permeable the membrane is to nonionic molecules like water and urea. Plotting liposome fluidity against liposome permeability to water, urea, acetamide, and ammonia fits a single exponential function, implying that membrane permeability is dependent on membrane fluidity [15]. Properties of the lipid bilayer that increase its fluidity include decreased acyl chain saturation, decreased cholesterol

concentration, and decreased sphingomyelin concentration [15]. However, the positive correlation between membrane fluidity and permeability does not apply to ionic molecules such as salts [15]. The permeability of membranes to these charged molecules depends on channel and transporter activity in the membrane. Therefore, changing membrane fluidity is one way cells fine tune how rapidly nonionic molecules, most notably water, are able to move across the plasma membrane.

In addition to membrane fluidity, the presence of aquaporins in the plasma membrane also directly influences membrane water permeability [16]. Aquaporins are protein channels that allow for the passive movement of water molecules across the plasma membrane [16]. Water molecules move through aquaporins in the direction of their osmotic gradient [16]. In addition to water, some aquaporins are also passively permeable to the metabolites glycerol and urea [17]. Cells can thus regulate their permeability to nonionic molecules, such as water, by modulating the concentration of aquaporins in the plasma membrane.

Since the serendipitous discovery of the first aquaporin, Aquaporin 1, by Agre, et al. in 1987 [18], 13 mammalian channels, many of which are conserved in other organisms, have been identified that are permeable to water, glycerol and/or urea [17]. The fundamental structure of an aquaporin consists of four subunits, each subunit containing two hemipores made up of three transmembrane domains with two conserved loops containing the asparagine-proline-alanine (NPA) motif [16, 19]. The NPA motif confers specificity to the aquaporin by forming hydrogen bonds with water, glycerol, and/or urea to facilitate their movement through the channel [16, 19]. Although each aquaporin has a similar fundamental structure and function, the expression profile and physiological role of the 13 mammalian aquaporins varies across cell type [17].

Aquaporin 2 (AQP2) is expressed in the kidney renal collecting duct and plays an integral role in systemic osmotic homeostasis in mammals [20]. AQP2 is not constitutively localized in

the plasma membrane. Instead, under basal conditions AQP2 is localized primarily in intracellular vesicles where it does not function in plasma membrane permeability [20]. It is only during systemic water depletion that AQP2 is exocytosed to the apical membrane where it increases plasma membrane permeability to water and thereby allows water to be reabsorbed from the urine to replenish systemic water levels [20]. Highlighting the importance of AQP2, mice with a loss of function mutation in AQP2 have severe urine concentrating defect at birth that results in dehydration and ultimately death within 5-6 days [21]. AQP2 is therefore an example of how regulation of aquaporin number in the plasma membrane can directly influence membrane water permeability to meet the organismal needs.

Aquaporin 5 (AQP5) is another example of an aquaporin that plays a role in fluid homeostasis in mammals [22]. AQP5 functions primarily in the salivary glands to promote salivary secretion. The parotid and sublingual acinar cells of AQP5 deficient mice have decreased permeability to water, which results in decreased salivary secretion due to a low efflux of water [22].

While both AQP2 and AQP5 function primarily in water permeability, Aquaporin 7 (AQP7) is both water and glycerol permeable and is critical for glycerol homeostasis in adipose cells where it facilitates the efflux of glycerol [23, 24]. Strikingly, knock down of AQP7 in mice causes adipocyte hypertrophy and a subsequent increase in body mass due to intracellular glycerol and triglyceride accumulation [25]. Therefore, depending on its structure and cell specificity, aquaporins play a variety of physiological roles in mammals critical for water and/or glycerol homeostasis. The key function of aquaporins required for these physiological roles is the modulation of plasma membrane permeability.

Surprisingly, aquaporins are not required for osmotic homeostasis in all organisms. The small nematode *Caenorhabditis elegans* has eight aquaporins, but they are not required for adaption to osmotic stress [26]. Simultaneous knockout of all four epithelial expressed and water-permeant aquaporins in *C. elegans* leads to a slight increase in hypotonic stress sensitivity, but has no effect on HTS sensitivity or survival during either type of osmotic stress [26]. This result suggests that some organisms, including *C. elegans*, may have redundant mechanisms to alter membrane permeability or that aquaporin-mediated membrane permeability is not as important for *C. elegans* osmotic physiology.

In conclusion, the permeability of the plasma membrane to water is determined primarily by lipid bilayer composition and aquaporin concentration. The plasma membrane is significantly more permeable to water than it is to ionic molecules and this water permeability can be further increased by decreasing acyl chain saturation, cholesterol, and sphingolipid concentration and increasing aquaporin concentration in the lipid bilayer. Cells fine tune their water permeability by limiting the localization of aquaporins in the plasma membrane, as seen with AQP2, to meet organismal needs. Importantly, the permeability of the plasma membrane to water, but not ionic molecules, makes cells intrinsically sensitive to osmotic stress regardless of how lipid composition or aquaporin concentration are regulated.

1.1.2 Cells of all types respond to changes in extracellular solute concentration with the osmotic stress response

Cells are extremely sensitive to changes in osmotic homeostasis. For example, some renal cells respond to osmotic perturbations of < 3% [27]. One important consequence of osmotic stress

is that it changes cell volume [28]. Maintenance of cell volume is required for proper cell function and thus cells have evolved mechanisms to sense even small changes in cell volume and activate protective pathways. Osmotic stress can be categorized into two types: anisosmotic volume changes and isosmotic volume changes [29]. Anisosmotic volume changes are introduced by altered extracellular osmolarity; for example by increased extracellular salt concentration. Isosmotic volume changes are introduced by improper cell function; for example by inhibition of ion transporters such as the Na^+/K^+-ATPase [29]. Anisosmotic stress is the primary focus of my research project.

1.1.2.1 The hypotonic stress response

The fundamental mechanisms cells utilize to adapt to hypotonic stress are conserved across organisms. Decreased extracellular solute concentration relative to intracellular solute concentration osmotically drives water into the cell causing cell swelling. To counteract impaired cellular function due to increased cell volume, cells employ a conserved two-phase hypotonic stress response. Within seconds of hypotonic stress, cells activate the K^+-Cl^- transporter, ClC-2 Cl^- channel, and a volume – regulated anion channel (VRAC) to passively efflux K^+ ions, Cl^- ions, and nonionic molecules called compatible osmolytes from the cell [29, 30]. These transporters are stored in submembrane cytoplasmic vesicles that are quickly activated by exocytosis to the plasma membrane [29, 30]. The rapid efflux of solutes osmotically draws water out of the cell in a process called regulatory volume decrease (RVD) and this restores normal cell volume.

The molecular identity of VRAC has long remained mysterious. It has been known for over forty years that in addition to ion efflux, compatible osmolyte efflux also contributes significantly to RVD, but the volume sensitive channel (VRAC) through which compatible osmolyte efflux occurs has remained unknown [31, 32]. In the late 1990s compatible osmolyte

efflux was proposed to occur through an anion channel distinct from the volume activated ClC-2 Cl^- channel [33-35]. It was not until 2014 that an essential component of VRAC was identified: the leucine-rich repeat containing 8A channel (LRRC8) [36]. Knockdown of LRRC8 slows ionic and compatible osmolyte efflux from cells and prevents cells from undergoing RVD during hypotonic stress, suggesting that LRRC8 is a required component of VRAC [36]. However, it is still not understood how LRRC8 is activated by increased cell volume.

In addition to the immediate RVD that occurs in response to hypotonic stress, cells also employ a second slower phase of adaptation to hypotonic stress. In this second phase of adaption, cells inhibit the accumulation of intracellular compatible osmolytes by downregulating the transcription of compatible osmolyte biosynthetic enzymes and compatible osmolyte transporters [33]. By decreasing the intracellular accumulation of compatible osmolytes, cells decrease intracellular osmolarity to match the decreased extracellular osmolarity and thus restore normal water content and cell volume.

Hypotonic stress is induced either anisosmotically by decreased extracellular osmolarity or isosmotically by impaired cell function. Anisosmotic hypotonic stress occurs when the water content of the extracellular fluid is increased or the solute concentration of the extracellular fluid is decreased. Isosmotic hypotonic stress occurs when the ion transport into or out of the cell is activated or inhibited respectively [29]. For example, activation of the epithelial sodium channel ENaC increases sodium transport into the cell causing cell swelling [37]. Correspondingly, inhibition of the Na^+/K^+-ATPase decreases sodium transport out of the cell also causing cell swelling [38]. Both anisosmotic and isosmotic hypotonic stress activate the two-phased adaptation pathways discussed above.

1.1.2.2 The hypertonic stress response

HTS is the opposite of hypotonic stress and is characterized by increased extracellular relative to intracellular solute concentration. HTS results in rapid cell shrinkage and increased intracellular ionic strength [28]. To avoid the cellular toxicity associated with HTS - induced cell shrinkage, cells employ a two-phase adaptative response [7, 8]. Similarly to the hypotonic stress response, within seconds of HTS cells influx sodium and chloride through the Na^+-K^+-$2Cl^-$ cotransporter [39], Na^+/ H^+ exchanger [40], and Cl^-/HCO_3^- exchanger [29, 41, 42]. Increased intracellular ion concentration osmotically drives water into the cell to counteract cell shrinkage. Intracellular sodium is quickly replaced by intracellular potassium through sodium-induced activation of the Na^+/K^+-ATPase [41, 43]. The second, slower phase of the HTSR involves the accumulation of compatible osmolytes [44]. In this phase, the transcription of compatible osmolyte biosynthesis genes and/or compatible osmolyte transporters is increased over the minutes and hours following HTS [45]. Compatible osmolytes eventually replace the intracellular ions that were accumulated during the first phase of the HTSR so that cell volume and intracellular ionic strength are restored to homeostatic setpoints [41, 46].

Regulation of the HTSR in metazoans is poorly understood. The ion transporters that mediate rapid ion influx during HTS are regulated primarily by phosphorylation and several of the required kinases have been identified, as is discussed in subsequent sections [47, 48]. However, it is unknown whether these kinases themselves are the osmosensing proteins (osmosensors) or whether other osmosensors exist that activate these kinases during HTS. Similarly, one transcription factor that upregulates compatible osmolyte accumulation gene transcription in the second phase of the HTSR has been identified in mammals, but it remains poorly understood how this transcription factor itself is activated [49]. Furthermore, this transcription factor is only found

in mammals. Whether or not other conserved mechanisms for regulation of osmosensitive gene expression exist is not known. The objective of my thesis project is to re-examine the functional requirements for a conserved aspect of the HTSR by taking an unbiased forward genetic approach in the multicellular animal model *C. elegans*. While this type of approach has defined HTSR mechanisms in unicellular organisms and plants, I am the first to apply such approaches in an animal model.

1.2 Intracellular compatible osmolyte accumulation is a widespread mechanism cells use to adapt to hypertonic stress

Intracellular compatible osmolyte accumulation is an essential component of the HTSR. Compatible osmolytes are small organic molecules whose intracellular concentration tracks the extracellular solute concentration to maintain appropriate intracellular water content [44]. Most compatible osmolytes have a net neutral charge at physiological pH and do not interact with charged cell metabolites or components [44]. Unlike inorganic ion accumulation, intracellular compatible osmolyte accumulation, even at molar concentrations, does not interfere with enzymatic activity or protein folding [3, 4, 50]. The second phase of the HTSR, in which intracellular ions are replaced by compatible osmolytes, is therefore critical for sustained adaptation to HTS because high intracellular ion concentration is detrimental to the function and folding of proteins required for proper cell function [4].

In virtually all organisms, compatible osmolytes are intracellularly accumulated by transcriptional upregulation of biosynthetic enzymes or transporter proteins that mediate their influx [44]. Different organisms and even distinct cell types within a single organism have varying

preferences for compatible osmolyte accumulation [51]. Several bacteria, for example *Escherichia coli*, first accumulate compatible osmolytes from their environment by upregulating the corresponding transporters. However, if their environment lacks the necessary compatible osmolytes, these bacteria upregulate biosynthetic enzymes to make their own [52]. Yeast and plants, on the other hand, accumulate compatible osmolytes primarily by upregulating biosynthetic enzymes regardless of the compatible osmolyte content of their environment [52, 53]. In mammals, some cells upregulate biosynthesis enzymes, while others upregulate transporters to accumulate compatible osmolytes [52]. A key readout for the HTSR that I use in my thesis project is the genetic upregulation of osmolyte biosynthetic enzyme upregulation in *C. elegans*.

Even though compatible osmolytes are accumulated to extremely high concentrations inside cells without negatively affecting cellular functions, most compatible osmolytes are not completely inert [44]. In addition to protecting cells against HTS, compatible osmolytes in plants function as antioxidants to scavenge free radicals [54, 55]. In marine invertebrates living in hydrothermal vents and cold seeps, compatible osmolytes, such as hypotaurine and thiotaurine, function in sulphide/sulphate detoxication to protect cells from high sulfur levels [56, 57]. In these same deep sea marine organisms, another compatible osmolyte, trimethylamine N-oxide (TMAO) stabilizes proteins to counteract protein damage due to hydrostatic pressure [58]. Finally, compatible osmolytes also function in defense. Unicellular algae accumulate the compatible osmolyte dimethylsulfoniopropionate (DMSP) during HTS. DMSP not only protects unicellular algae from HTS, but also from predators. Cell lysis activates cleavage of DMSP into the gas dimethyl sulfide (DMS), which deters predators [59, 60]. Therefore, while compatible osmolytes are essential for the HTSR, they also benefit cells in other ways.

1.2.1 The chemical diversity of compatible osmolytes

There is significant chemical diversity among compatible osmolytes. Generally compatible osmolytes can be grouped into four categories: polyols (e.g. glycerol, sucrose, inositol, and sorbitol), free amino acids and amino acid derivatives (e.g. taurine, beta-alanine, glycine, proline), urea and methylamines (e.g. trimethylamine N-oxide (TMAO), betaine, sacrosine), and small carbohydrates (e.g. trehalose) [44, 51]. Urea alone is denaturing, but simultaneous accumulation of urea and TMAO in a 2:1 urea:TMAO ratio, such as in marine organisms, counteracts the denaturing effects of urea and allows it to function as a compatible osmolyte [44, 51]. The majority of compatible osmolytes are utilized in multiple organisms. Betaine is used as a compatible osmolyte in all kingdoms of life. Similarly, taurine is accumulated in most marine and mammalian organisms. In contrast, urea is not widely used as a compatible osmolyte, except in cartilaginous fish, where it is accumulated with TMAO [51, 55]. A single organism can also accumulate multiple types of compatible osmolytes. The mammalian kidney alone accumulates myo-inositol, sorbitol, glycerophosphorylcholine (GPC), glycine betaine, and taurine [55]. While there is striking chemical diversity in compatible osmolytes, they all share the property that they can be accumulate to molar concentrations in cells to maintain osmotic homeostasis.

One explanation for the chemical diversity of compatible osmolytes is that they evolved with organisms to be compatible with specific enzymes. However, it has since been demonstrated that the compatibility of osmolytes is general and not specific towards enzymes of particular cell types or species. The hypertonic growth of *E. coli* depleted of its preferred compatible osmolytes betaine and proline can be rescued by a variety of compatible osmolytes not naturally used by *E. coli* [61]. Similarly, in cultured mammalian kidney cells that preferentially synthesize sorbitol during HTS, cell growth due to inhibition of sorbitol synthesis can be rescued with glycine betaine

[62]. Therefore, compatible osmolytes likely evolved chemical diversity not because they only function in specific cell types, but because different cells and organisms have different diets, metabolisms, and environments that make some compatible osmolytes more accessible than others [51].

1.2.2 Compatible osmolytes function as chemical chaperones

In addition to tracking extracellular solute concentration and restoring cell volume homeostasis, compatible osmolytes also function as chemical chaperones to promote proper protein folding. The first experiments to demonstrate this showed that compatible osmolytes glycerol and TMAO protect proteins from thermal denaturation [63, 64] and reduce the rate of scrapie prion formation [65]. It has since been demonstrated that compatible osmolytes stabilize proteins by interacting unfavorably with the peptide backbone. This unfavorable interaction causes proteins to fold more tightly to shield the peptide backbone from interactions with compatible osmolyte molecules. In this way, compatible osmolytes increase the Gibbs free energy required to shift a protein from the folded to unfolded state and this enhances the relative stability of the folded state [66]. In contrast to compatible osmolytes, inorganic ions interact favorably with the protein backbone and promote protein denaturation [51]. Therefore, accumulation of compatible osmolytes during HTS not only restores cell volume, but also promotes protein homeostasis.

Compatible osmolytes can be categorized into four groups based on their protein stabilizing properties as measured by the biophysical Tanford's transfer model [67]. First, there are compatible osmolytes, such as sorbitol and sucrose that stabilize proteins. Even though these compatible osmolytes interact favorably with amino acid side chains, which alone is denaturing,

their unfavorable interaction with the peptide backbone is stronger. Therefore proteins exclude these compatible osmolytes from their peptide backbones by folding and the Gibbs free energy required to unfold the protein is increased [67]. Second, there are compatible osmolytes that only moderately stabilize proteins because their unfavorable interactions with the peptide backbone barely outcompete their favorable interactions with amino acid side chains. Examples of osmolytes that fall into this second category include glycerol, glycine betaine, and proline [67]. Third, there is one compatible osmolyte that is denaturing on its own: urea. Nonpolar amino acid side chains and the peptide backbone interact with urea to promote protein unfolding [67]. Finally, there are counteracting compatible osmolytes. The most notable examples of these are TMAO and urea, which are found to promote protein folding in cartilaginous fish when in a 2:1 urea: TMAO ratio. TMAO offsets the favorable interactions between urea and the protein backbone so that protein folding is promoted. In the absence of urea, TMAO precipitates proteins because it "overstabilizes" protein folding [67]. Therefore, TMAO requires the presence of a counteracting solute like urea to be beneficial. Trehalose is another example of an "overstabilizing" solute and can function with the counteracting solute urea to promote protein homeostasis [55, 68]. In conclusion, although compatible osmolytes act as chemical chaperones to different degrees, most contribute to protein homeostasis when accumulated to high concentrations, such as during HTS.

Chemical chaperones are distinct from protein chaperones in three ways. First, protein chaperones bind misfolded proteins in an energetic (ATP-dependent) or regulated process and aid in their folding, whereas chemical chaperones promote protein folding by their passive (non-energetic) exclusion from proteins [69]. Second, protein chaperones are catalytic, allowing them to be present in substantially lower concentrations than chemical chaperones and still maintain protein homeostasis. Third, the driving forces for chemical chaperones on protein folding are

continuous. In contrast, protein chaperones act temporarily on proteins and once their interaction with the protein is lost, the driving forces for protein misfolding continue to persist [69]. Chemical chaperones and protein chaperones therefore both function in protein homeostasis, but the mechanisms through which they operate are distinct.

1.3 Regulation of the osmotic stress response has been well characterized in bacteria, yeast, and plants.

Over the last fifty years, detailed pathways regulating the HTSR in bacteria, yeast, and plants have been elucidated primarily through genetic methods. Specifically, unbiased forward genetic screens have been instrumental in the characterization of these pathways. Forward genetic screens are powerful because they allow the organism to reveal what is required for a pathway in a physiologically relevant context. Driven by the success of this approach in other organisms, my thesis project takes advantage of the power of unbiased genetic screens and the genetic manipulability of *C. elegans* to characterize the HTSR in an animal system for the first time.

Despite the evolutionary distance between bacteria, yeast, and plants, all utilize two-component signal transduction systems to modulate gene expression during HTS. The prototypical two component transduction system consists of a sensor histidine kinase (SHK) and a response regulator (RR). A stimulus is sensed by the input domain of the SHK and this causes auto-phosphorylation of its histidine kinase catalytic domain. The phosphoryl group is then transferred to the receiver domain of the RR to activate its nuclear translocation and subsequent gene regulation [70]. While this is the basic organization of a two-component signal transduction

system, more complex variations commonly exist, such as in the HTSR, as is highlighted in the subsequent sections.

1.3.1 Regulation of the osmotic stress response in bacteria

The bacterial hypo- and hypertonic stress responses are made up of the same general themes as that of other organisms. Bacteria respond to hypotonic stress by rapidly effluxing cytoplasmic solutes to relieve cell swelling . Among the effluxed cytoplasmic solutes are ions and the compatible osmolytes proline, glycine betaine, and trehalose [71, 72]. This efflux occurs through two mechanosensitive channels: mechanosensitive channel small conductance (MscS) and mechanosensitive channel large conductance (MscL) [73-75]. Multiple members of the MscS family are expressed in bacteria, archaea, fungi, and plants, while only a single member of the MscL family is expressed in bacteria and fungi [76]. Proteins related to MscS are predicted to exist in mammals as well [77]. MscS and MscL are large channels that are permeable to molecules less than 1000 Da, including proline, potassium, glutamate, trehalose, and ATP [76]. Both channels are necessary for an effective hypotonic stress response in bacteria, as loss of their activity results in increased sensitivity to hypotonicity and retention of cytoplasmic solutes like potassium [75].

To date, more is known about the regulation of MscL than MscS. MscL exists in a closed conformation in the plasma membrane under basal conditions [78]. Data from liposomes suggests that MscL is activated directly by changes in the lipid bilayer and its activation does not require additional proteins [74]. The open conformation of MscL is promoted by both the thinning of the lipid bilayer and the increased curvature of the lipid bilayer due to asymmetry in lipid composition [79]. However, it is hypothesized that increased curvature of the lipid bilayer is the primary driving

force for MscL opening because in liposomes, increased bilayer curvature traps MscL in the open state, whereas thinning of the lipid bilayer alone is not sufficient to have this effect [79]. MscL thus directly senses biophysical changes in the cell caused by hypotonic stress and is itself an osmosensor.

Like the bacterial hypotonic stress response, the bacterial HTSR follows the same themes as that of other organisms. Bacteria respond to HTS with a rapid initial response followed by a slower sustainable response. Cell shrinkage induced by HTS causes the immediate intracellular accumulation of potassium via activation of ion transporters to restore cell volume [80]. To prevent a shift in membrane potential caused by positively charged potassium, cells synthesize the counter-ion glutamate [80]. Within two hours of HTS, intracellular potassium glutamate is replaced by intracellular compatible osmolytes. Specifically, bacteria increase uptake of proline and betaine from their environment by upregulating the corresponding transporters [81, 82]. However, if their environment does not contain proline or betaine, bacteria accumulate intracellular trehalose via synthesis [80]. Accumulation of these compatible osmolytes restores bacterial cell volume without increasing intracellular ionic strength and thereby provides a sustainable adaptive response.

1.3.1.1 Hypertonicity induced gene expression in bacteria

Transcriptional regulation is an essential aspect of the HTSR in bacteria. Osmotically induced gene expression is the primary way compatible osmolyte accumulation is regulated during the second phase of the HTSR, but it also plays an important role in the initial phase of potassium accumulation. Bacteria have four potassium transporter systems, Kdp, TrkA, TrkD, and TrkF that facilitate potassium accumulation during HTSR [83]. Three of the four transporter systems, TrkA, TrkD, and TrkF are primarily regulated post-transcriptionally during HTSR to facilitate a rapid

influx of potassium [83]. However, the Kdp potassium transport system is genetically regulated during HTSR and serves as a backup system if satisfactory potassium levels are not reached by the other transport systems [83, 84]. Expression of the Kdp operon (*kdpFABC*) is dependent on two factors: intracellular potassium levels and a two component signal transduction system [85-89]. *kdp* expression is inhibited by increased potassium to prevent its activation in conditions of adequate intracellular potassium concentration [85]. The two component signal transduction system that also regulates expression of *kdpFABC* is made of an inner membrane-localized SHK, KdpD, and a DNA binding cytosolic RR, KdpE [86]. Both *kdpD* and *kdpE* are localized on an operon adjacent to the *kdpFABC* operon [87]. During conditions of HTS and low intracellular potassium concentration, KdpD is activated via autophosphorylation to subsequently phosphorylate KdpE [88]. Phosphorylated KdpE binds the regulatory sequence upstream of *kdpFABC* to induce its transcription and thereby increase Kdp transporter protein concentration at the plasma membrane to facilitate potassium influx [89]. In this way, the Kdp transporter system is genetically activated by HTS and fine-tuned by intracellular potassium concentration.

In the second phase of the HTSR, bacteria accumulate the compatible osmolytes proline and betaine through osmotically regulated gene expression [81, 82]. HTS increases the expression of *proP* and *proU*, which encode two betaine/proline transport systems [90, 91]. Increased intracellular proline and betaine in turn repress transcriptional induction of *proP* and *proU* in a negative feedback loop [85]. The transcription of *proP* during HTS is regulated by its P1 promoter [92]. During isosmotic conditions, the cAMP receptor protein CRP (CRP-cAMP) binds the ProP P1 promoter to repress its transcription [93, 94]. Intracellular potassium glutamate accumulation during HTS destabilizes the association between CRP-cAMP and the ProP P1 promoter, allowing for its transient transcription [93, 94]. Similarly to ProP, ProU transcription is induced by

increased intracellular potassium glutamate concentration during HTS [95-97]. However, unlike ProP, ProU can be upregulated in a cell-free, protein-free system by addition of only potassium glutamate, suggesting potassium glutamate itself is able to increase *proU* transcription without any protein factors [96]. ProP and ProU genetic upregulation are the primary ways bacteria accumulate proline and betaine when these two compatible osmolytes exist in their environment.

A final example of osmosensitive gene expression in bacteria is the OmpF and OmpC porin system. Both OmpF and OmpC are trimers that form pores in the outer membrane and allow passive diffusion of small hydrophilic molecules less than 650 kDa in size [98, 99]. *ompC* and *ompF* are upregulated during hypertonic and hypotonic stress respectively, but their precise roles in these osmotic stress responses remain unknown [100-102]. Despite their unknown physiological role, the two component signal transduction system that regulates *ompF* and *ompC* transcription during osmotic stress has been well characterized. During HTS, the inner membrane localized SHK, EnvZ, undergoes autophosphorylation and subsequently phosphorylates the cytoplasmic RR OmpR [103]. Phosphorylation of OmpR causes it to bind the upstream regulatory regions of *ompC* and *ompF* [104, 105]. OmpR activates the transcription of *ompC* and represses the transcription of *ompF* [101, 102]. Therefore, OmpC levels are increased during HTS and OmpF levels are increased during hypotonic stress. The OmpC/OmpF system in bacteria is an example of how one signal transduction pathway is harnessed to simultaneously regulate two proteins in opposing ways.

1.3.2 Regulation of the osmotic stress response in *Saccharomyces cerevisiae*

Of all organisms, the osmotic stress response has been the most thoroughly characterized in *Saccharomyces cerevisiae* (yeast). Yeast genetics, specifically the power of forward genetic

screens, has provided a powerful platform to characterize the regulatory pathways controlling ion and compatible osmolyte accumulation and efflux [106-111]. Additionally, yeast utilize one compatible osmolyte during osmotic stress - glycerol - which provides a quantifiable readout of the stress response [53].

The hypotonic stress response in yeast has two phases. In the acute response, cell swelling is reversed by efflux of the compatible osmolyte glycerol from the cell via the Fps1p aquaglyceroporin [112]. Within three minutes of hypotonic stress, 50% of intracellular glycerol is effluxed from wild type (WT) cells. In contrast *fps1pΔ* mutants take over two hours to remove this same amount of glycerol [112]. Furthermore, *fps1pΔ* mutants are unable to survive levels of hypotonic stress that 100% of WT yeast are able to tolerate [112]. Therefore, glycerol efflux, specifically through the Fps1p aquaglyceroporin, is essential for the initial phase of the hypotonic stress response in yeast.

In addition to compatible osmolyte efflux, yeast respond to hypotonic stress with a slower, more sustained response in which they repair cell wall damage caused by cell swelling. Specifically, hypotonic stress upregulates *och1*, which encodes a *cis*-Golgi localized mannosyltransferase [113]. Och1 is required for N-linked glycosylation of secreted and transmembrane proteins, a process vital for cell wall maintenance [113]. Failure to maintain cell wall integrity is detrimental to subsequent hypotonic challenges as highlighted by *pkc1Δ* mutants, which are sensitive to hypotonicity due to an impaired cell wall [114]. Overexpression of the Och1 pathway in the *pkc1Δ* mutant rescues its hypotonic sensitivity, further suggesting that maintenance of cell wall integrity is a critical defense against hypotonic stress [114, 115].

Like the hypotonic stress response, the HTSR in yeast is composed of two phases. In the seconds immediately following HTS, yeast increase intracellular ion concentration to counteract

cell shrinkage. Unlike bacteria, which accumulate ions by activating plasma membrane ion channels, yeast activate the vacuolar Na^+/H^+ exchanger Nhx1. Nhx1 transports sodium into the vacuole to maintain cellular water content, without exposing cytoplasmic proteins to high ionic strength [116]. Consequently, *nhx1Δ* mutants are slow growing in the initial phase after HTS because they are unable to rapidly reverse cell shrinkage [116]. Yeast mutants with a defective vacuole also have increased sensitivity to acute HTS, highlighting the importance of the vacuole in initial intracellular ion accumulation [107].

Another mechanism yeast use to prevent intracellular ion concentration from getting destructively high, is to activate the plasma membrane Nha1 Na^+/H^+ antiporter and Tok1 potassium channel [117]. Nha1 and Tok1 mediate the efflux of sodium and potassium respectively to lower cytoplasmic ionic strength. Both these permeability pathways are activated via phosphorylation by the p38 MAPK homolog and master osmotic regulator Hog1 [117]. In conclusion, like in bacteria, the initial phase of the HTSR in yeast is made up of intracellular ion accumulation, but these ions accumulate primarily in the vacuole instead of the cytoplasm. Yeast fine tune cytoplasmic ion concentration via the vacuolar Nhx1 exchanger and the plasma membrane Nha1 antiporter and Tok1 channel.

In the hours following HTS, yeast initiate a second phase of the HTSR that facilitates long-term cellular adaptation. These adaptive responses depend on transient modulation of gene expression. Over 300 mRNAs are differentially regulated by HTS in yeast. Among these genes are cell cycle progression genes and osmolyte accumulation genes [118-120]. In response to HTS, yeast downregulate the cell cycle regulators *cln1*, *cln2*, and *clb5* and upregulate *cln3* to temporarily delay the cell cycle in the G1 stage. Resumption of the cell cycle occurs when cell volume and ionic strength are restored to homeostatic set points by intracellular compatible osmolyte

accumulation [121]. Specifically, yeast upregulate the glycerol biosynthetic enzyme glycerol-3-phosphate dehydrogenase (*GPD1*) to facilitate intracellular accumulation of the glucose metabolite glycerol [122]. Genes that increase glycerol synthesis capacity such as glucose transporters and glucose metabolic enzymes are also upregulated, but to a lesser extent than *GPD1* [118]. Furthermore, to prevent glycerol efflux during HTS, the aquaglyceroporin Fps1p is closed [112, 123]. Glycerol accumulation in yeast is essential for survival in hypertonic conditions [122].

1.3.2.1 The high osmolarity glycerol mitogen-activated protein kinase pathway in yeast

ORG expression critical for the yeast HTSR is regulated by the p38 MAPK yeast homolog Hog1 [124]. Hog1 was identified almost three decades ago through an unbiased forward genetic screen in yeast [106]. This forward genetic screen identified mutants that failed to grow in **h**igh **o**smolarity media due to impaired **g**lycerol accumulation. Both *hog1Δ* and its downstream target *pbs2Δ* (originally named *hog4Δ*) mutants were picked up in the screen [106]. Not only did this genetic screen identify Hog1 as an essential regulator of the HTSR in yeast, but it also defined a new class of conserved kinases, the p38 MAPKs. The discovery of Hog1 led to dozens of subsequent forward genetic screens that were ultimately used to characterize the rest of the Hog1 regulatory pathway and the HTSR (Fig 1.3.1) [106-111]. Therefore, unbiased genetic methods in yeast not only led to the characterization a novel osmosensing pathway, but also to the identification of a new class of conserved kinases, p38 MAPKs, which are now known to be involved in many important cellular processes outside of the HTSR.

Hog1 regulates ORGs by interacting with several structurally unrelated transcription factors [125-128]. For example, upregulation of the glycerol biosynthetic enzyme *GPD1* during HTS requires a physical interaction between phosphorylated Hog1 and the transcription factor Hot1 [128]. Hot1 recruits activated Hog1 to the promoters of osmolyte biosynthetic enzymes such

as *GPD1* [128]. The recruitment of Hog1 to ORG promoters by osmotically regulated transcription factors and the corresponding upregulation of ORGs such as *GPD1* is required for adaptation to HTS in yeast [108].

The MAPK pathway that regulates Hog1 has been extensively characterized in yeast. Hog1 is regulated by two redundant signaling pathways that converge on Pbs2, a MAPKK and direct activator of Hog1 (Fig 1.3.1) [106, 110, 129, 130]. The first branch regulating Hog1 activation is a complex two component signal transduction system made up of the transmembrane hybrid histidine kinase Sln1, the cytoplasmic proteins Ypd1 and Ssk1, and the redundant conserved MAPKKKs Ssk2/Ssk22. During basal isosmotic conditions, Sln1 is activated to undergo autophosphorylation [111]. Activated Sln1 transfers a phosphoryl group to the nucleocytoplasmic protein Ypd1, which consequently phosphorylates Ssk1 to inactivate it [111]. During HTS, Sln1 is never activated, causing the active, unphosphorylated, form of Ssk1 to accumulate [110]. Double dephosphorylated dimers of Ssk1 phosphorylate the redundant MTK1 homologs and MAPKKKs Ssk2 and Ssk22, which phosphorylate the MKK homolog and MAPKK Pbs2 [109, 131]. Phosphorylated Pbs2 in turn binds, phosphorylates, and activates Hog1 [130].

In addition to regulating HTS induced gene expression through Hog1, Sln1 also regulates hypotonic stress induced gene expression through the transcription factor Skn7 [113]. Intracellular accumulation of glycerol by inhibition of the aquaglyceroporin Fps1p activates Sln1 autophosphorylation and subsequent phosphorylation of Ypd1 [132]. In addition to Ssk1, Ydp1 has another phosphorylation target: the nuclear transcription factor Skn7 [133]. Phosphorylation of Skn7 by Ypd1 activates hypotonic gene expression, such as upregulation of *OCH1*, the mannosyltransferase required for cell wall biosynthesis [113]. Therefore, yeast use the Sln1 -

Ypd1 pathway to regulate both Hog1 activation during HTS and Skn7 activation during hypotonic stress.

In addition to the Sln1 pathway, Hog1 activation during HTS is also regulated by the Sho1 branch, which is redundant to the Sln1 pathway (Fig 1.3.1). The transmembrane proteins Msb2, Hkr1, and Sho1 act as putative osmosensors in this branch of the pathway [134]. Msb2 and Hkr1 are functionally redundant mucin-like proteins [134]. Sho1 is a scaffolding protein that is also considered an osmosensor because it can activate Hog1 in the absence of Msb2 and Hkr1 [135]. Msb2, Hkr1, and Sho1 sense HTS and recruit the small GTPase Cdc42 to the plasma membrane and activate it [136]. The activation of Cdc42 is also dependent on the integral membrane protein Opy2 [137]. Activated Cdc42 binds and activates the p21-activated kinases Ste20/Cla4 [138, 139]. The Cdc42-Ste20/Cla4 complex and Opy2 in turn bind and recruit the MAPKKK Ste11 and its complexed protein Ste50 to the plasma membrane via binding to the cytoplasmic domain of Sho1 [138, 140]. The interaction of all of these proteins at the plasma membrane allows Ste20/Cla4 to phosphorylate and activate the MAPKKK Ste11 [141]. Activated Ste11 phosphorylates the MAPKK Pbs2, which also binds the cytoplasmic domain of Sho1 [138]. Finally, activated Pbs2 phosphorylates and activates Hog1 [106, 130]. Therefore, the Sln1 and Sho1 branches converge on the MAPKK Pbs2 to activate the MAPK Hog1 (Fig 1.3.1).

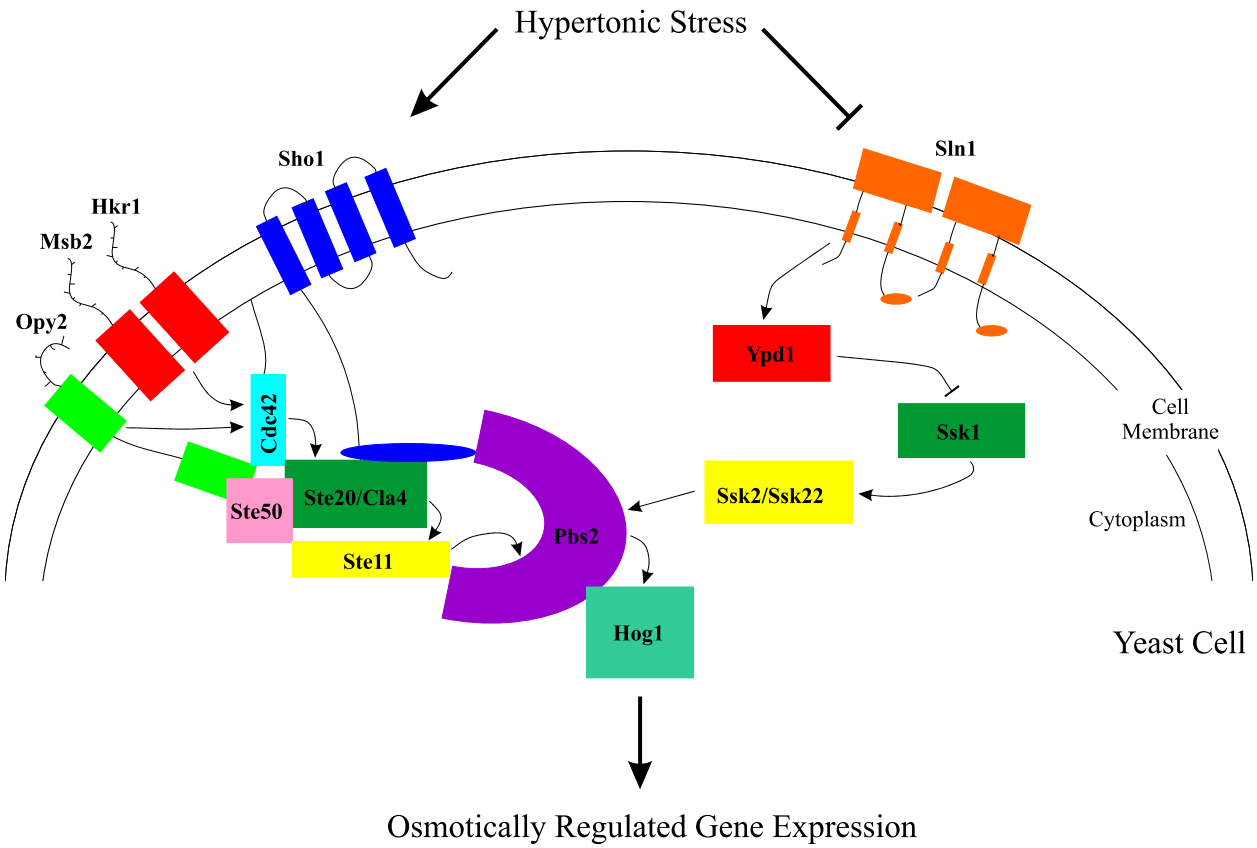

Figure 1.3.1 The high osmolarity glycerol (HOG) osmosensing pathway in yeast

The redundant Sho1 and Sln1 MAP kinase pathways converge on Pbs2 to regulate the expression of osmoprotective genes in yeast.

Hog1 is phosphorylated by Pbs2 at two sites to activate it and induce its translocation into the nucleus, where it regulates gene expression [142, 143]. Both the phosphorylation of Hog1 and its catalytic activity are required for its nuclear translocation [144]. In addition to regulating gene expression in the nucleus, phosphorylated Hog1 also functions in the cytoplasm to activate the Nha1 and Tok1 ion transporters, which mediate efflux of excess sodium and potassium [117]. After osmotic balance is reestablished, either by a return to isosmotic conditions or by sufficient intracellular accumulation of glycerol, Hog1 activity returns to basal levels because the Sln1/Sho1 pathways are no longer activated and Hog1 is exported from the nucleus [143]. Furthermore, to

bring the system back to its original state, Hog1 is dephosphorylated by the type 2C Ser/Thr phosphatase family members Ptc1, Ptc2, and Ptc3 and by the protein tyrosine phosphatase family members Ptp2 and Ptp3 [145, 146]. The return of Hog1 back to its original state primes it to respond to dynamic osmotic conditions.

The successful identification and characterization of the Hog1 osmosensing pathway in yeast illustrates how valuable unbiased forward genetic methods are for dissecting intricate stress response pathways. However, it is still unclear if Hog1-like proteins and homologous signaling mechanisms are utilized in animals during hypertonic stress. In my project, I harness the same unbiased genetic methods used to characterize the yeast Hog1 pathway to identify HTSR signaling pathways in the multicellular animal *C. elegans*. Just as the discovery of Hog1 was not only important to the yeast HTSR, but also to the characterization p38 MAPKs, my research may yield protein functions and paradigms important to areas of biology outside of the animal HTSR.

1.3.3 Regulation of the osmotic stress response in plants

Conditions that plants face commonly in nature, such as drought and increased soil salinity, induce osmotic stress that is detrimental to plant survival [147]. Plants have therefore evolved elaborate adaptive responses to osmotic stress. Unlike bacteria and yeast, the multicellularity of plants allows them to compartmentalize the osmotic stress response to distinct tissues [148]. Although this compartmentalization contributes to the complexity of the osmotic stress response in plants, the fundamental processes plants use are similar to bacteria and yeast.

During hypotonic stress, caused for example by increased rain, plants counteract cell swelling in an analogous way to bacteria. Like bacteria, plants express homologs of MscS that facilitate the efflux of solutes during hypotonic stress [149]. Knockout of MscS channels in

Arabidopsis results in persistent cell swelling that can be rescued by increasing extracellular osmolarity [150].

Plants also exhibit similarity with other organisms, specifically yeast, in the mechanisms they use to respond to HTS. Immediately following HTS, *Arabidopsis thaliana* sequesters sodium in the vacuole via the Na^+/H^+ antiporter AtNHX1. AtNHX1 is a functional homologue of Nhx1 in yeast and is expressed in the root, shoot, leaf, and flower tissues of *Arabidopsis* [151]. Vacuolar sodium sequestration increases intracellular ion concentration and thus water content without exposing cytoplasmic proteins to high ionic strength. Overexpression of *AtNHX1* in *Arabidopsis* confers resistance to HTS, supporting its role in the HTSR [151]. Like yeast, plants also efflux sodium from the cytoplasm to fine tune intracellular ion concentration during HTS. SOS1 is the plasma membrane localized Na^+/H^+ antiporter through which sodium is extruded. SOS1 is genetically upregulated in root and shoot tissue during HTS and mutations that affect its function lead to HTS sensitivity [152]. Within a few hours of HTS, plants, like all organisms, accumulate compatible osmolytes to maintain cell volume. Due to the diversity of plant metabolisms and environmental conditions, plants use a variety of compatible osmolytes including proline, glycine betaine, mannitol, glucose, and fructose [153-155].

Osmolyte accumulation is genetically regulated in plants. There are several signaling pathways that regulate hypertonic induced gene expression including osmolyte accumulation genes [156]. Most, but not all, of these signaling pathways are dependent on the stress-signaling hormone abscisic acid (ABA) [156, 157]. ABA is accumulated by plants in all tissues during HTS in response to decreased cell volume and turgor pressure [158, 159]. However, the proteins that sense these cell changes and activate ABA accumulation have not been identified.

ABA is synthesized by aldehyde oxidases, but none of the aldehyde oxidases have increased activity or protein levels during HTS [160]. Instead, an upstream cleavage step carried out by 9-*cis*-expoxycartenoid dioxygenases (NCED) is the rate-limiting step in ABA synthesis [161]. NCED3 is transcriptionally upregulated within fifteen minutes of plant dehydration [162, 163]. Correspondingly, overexpression of *NCED3* in *Arabidopsis* increases ABA abundance and HTS tolerance [162]. After osmotic homeostasis is achieved, ABA is catabolized to an inactive form by oxidation or conjugation. A key part of this catabolism pathway includes the ABA 8'-hydroxylases CYP707As [164]. *CYP707A3* is transcriptionally upregulated within thirty minutes of the reestablishment of osmotic homeostasis and knockout of *CPY707A3* results in the retainment of high ABA levels after recovery from HTS [165]. Retainment of ABA in *cpy707a3* mutants likely makes them less sensitive to subsequent HTS [165]. Dynamic ABA accumulation is therefore required for osmotically regulated gene expression in plants and facilitates survival during HTS [166].

AREB/ABF transcription factors are activated during HTS in an ABA dependent manner. AREB/ABF transcription factors regulate the expression of many ORGs, including the upregulation of compatible osmolyte accumulation genes [167]. Knockout or inactivation of AREB/ABF transcription factors results in defective ABA accumulation, osmotically induced gene expression, proline accumulation, and growth during HTS [167, 168]. ABA activates AREB/ABF transcription factors through a well-characterized pathway. ABA binds the PYR/PYL/RCAR family of steroidogenic acute regulatory protein–related lipid–transfer (START) domain-containing soluble receptors [169]. When bound to ABA, these receptors inhibit protein phosphatase 2Cs (PP2Cs). PP2Cs normally inhibit SNF1-related protein kinase 2s (SnRK2s), but because ABA inhibits PP2Cs, SnRK2s become activated during HTS [169-171]. Active SnRK2s

in turn phosphorylate and activate AREB/ABF transcription factors, which bind G-box-like-*cis*-acting elements called ABA-responsive elements (ABREs) in the promoters of target genes [172, 173].

Not all osmotically induced genes have ABREs. Some genes, like the osmotically protective BURP domain (named for its four members: BNM2, USP, RD22, and PG1β) protein *RD22*, are upregulated in an ABA-dependent, AREB/ABF-independent manner [174]. *RD22* is upregulated by the basic helix-loop-helix (bHLH)-related MYC2 and MYB-related MYB2 transcription factors via MYC and MYB recognition sites in its promoter [174]. Overexpression of MYC2 and MYB2 increases *RD22* expression to facilitate the maintenance of chlorophyll integrity during HTS [174, 175]. In addition to ABA-dependent gene expression, the MYC2 transcription factor regulates several other plant hormone signaling pathways, such as those involved in plant defense and development [176].

Although most hypertonicity induced gene expression in plants is ABA dependent, there are also key ABA-independent pathways [156]. The CBF/DREB1/DREB2 transcription factors are activated during HTS in plants in an ABA-independent manner to regulate osmotically induced gene expression [177]. These transcription factors bind C-repeat (CRT)/dehydration-responsive elements (DREs) in genes to upregulate them [178]. Overexpression of *CBF/DREB1/DREB2* transcription factors results in increased drought (HTS) tolerance, suggesting that the upregulation of key osmoprotective genes are dependent on this pathway [179].

Additionally, a yeast-like two component signal transduction system has been identified in plants that activates hypertonicity induced gene expression. AtHK1 was identified in *Arabidopsis* as a transmembrane hybrid histidine kinase similar to Sln1 in yeast [180]. Like Sln1, AtHK1 is in an active state during isosmotic conditions and in an inactive state during hypertonic conditions

[180]. In fact, AtHK1 can activate Hog1 in *sln1Δ sho1Δ* mutant yeast, supporting it functional conservation with Sln1 [180]. AtHK1 may function upstream of AREB/ABF and CBF/DREB1/DREB2 transcription factors, because *AtHK1* mutants fail to activate these transcription factors and the upregulation of their downstream gene targets to the same extent as WT plants [181].

1.3.4 Conclusions

In conclusion, regulation of the osmotic stress response in bacteria, yeast, and plants has been extensively genetically characterized over the last several decades. Such genetic analyses are more challenging to execute in most animals, including mammals. Therefore, genetic dissection of these osmotically induced pathways in animals has remained largely incomplete. The objective of my research project is to fill this gap in knowledge using the genetically amenable small animal *C. elegans* to identify key components of HTSR regulatory pathways. Similar to the examples just discussed for bacteria, yeast, and plants, my research uses unbiased genetic screening approaches to characterize proteins, mechanisms, and eventually pathways required for activation of the metazoan HTSR.

1.4 Regulation of the osmotic stress response in mammals

Like bacteria, yeast, and plants, mammals respond to osmotic stress with a cellular adaptive response to counteract cell volume and intracellular ionic strength changes. However, unlike these other organisms, mammals regulate their extracellular fluid (ECF) osmolarity systemically in

addition to cellularly. Mammals maintain their ECF osmolarity within a tight range. Although there is slight variation among species, all mammals have an ECF osmolarity around 300 mosmol kg^{-1} under normal conditions [182]. Even small deviations (< 10%) in osmolarity can have detrimental consequences to sensitive tissues like the brain [183]. Simple acts such as strenuous exercise in the heat or increased sodium intake can acutely increase plasma osmolarity 1-3% [184, 185]. Therefore, mammals have evolved sophisticated mechanisms to systemically regulate osmolarity. Moreover, mammalian tissues are capable of responding to osmotic stress at the cellular level. These cellular osmotic stress responses are most relevant to tissues that experience physiological osmotic fluctuations, such as the kidney, and during diseases that affect systemic or tissue osmolarity, such as hyper- and hyponatremia. The following section will focus on systemic osmoregulation in mammals, while the subsequent section with focus on cellular osmoregulation in mammals. The two primary pathways regulating systemic plasma osmolarity in mammals are the vasopressin – AQP2 and renin-angiotensin-aldosterone signaling axes.

1.4.1 The vasopressin – AQP2 axis and the renin – angiotensin – aldosterone axis regulate systemic plasma osmolarity in mammals

Mammals sense systemic plasma osmolarity in two areas of the brain: the organum vasculosum of the lamina terminalis cells (OVLTs) in the AV3V region and the magnocellular neurosecretory cells (MNCs) in the supraoptic nucleus of the hypothalamus [185-187]. OLVTs and MNCs are unique among mammalian cells because they are the only cells that do not counter osmotically-induced changes in cell volume with adaptive mechanisms. Instead the volume of these cells changes proportionally to the ECF osmolarity and this allows them to sense systemic osmotic changes [188, 189]. Specifically, decreased cell volume leads to increased nonselective

cation channel conductance, membrane depolarization and activation of OLVTs and MNCs [187, 189-192]. Cell volume changes and not intracellular ionic strength changes activate OLVTs and MNCs because decreasing OLVT or MNC cell volume with suction or negative pressure is sufficient to activate these neurons [189, 193].

The transient receptor potential vanilloid type-1 (TRPV1) channel is proposed to be the osmosensing entity in OLVTs and MNCs. When the TRPV1 channel is knocked out or inactivated, the volume of OLVTs and MNCs still decreases with increasing ECF osmolarity, but nonselective cation conductance, membrane potential, and action potential firing rate are not increased in these cells [189, 190, 194]. Thus the TRPV1 channel is required for OLVT and MNC activation. In particular an intact microtubule-TRPV1 interaction is required for hypertonic activation of MNCs [195]. Activated OLVTs and MNCs facilitate water reabsorption in the kidney via the hormone vasopressin to correct systemic hypertonic plasma [196-199].

The antidiuretic hormone, vasopressin, is synthesized in MNCs [196-199]. There are at least three stimuli that modulate the synthesis of vasopressin. First, as discussed above MNCs directly sense increases in ECF osmolarity and synthesize vasopressin in response to cell shrinkage [187, 198, 199]. Second, the osmosensitive OLVT neurons can activate MNCs. OLVT neuronal axons project into the supraoptic nucleus and increase the firing rate of MNCs when they become activated by increased ECF osmolarity [200]. Third, astrocytes surrounding MNCs release the compatible osmolyte taurine in an osmolarity dependent manner [201]. Taurine binds inhibitory glycine receptors on MNCs to inactivate them. Hypertonic ECF inhibits taurine release from these astrocytes and this promotes the activation of MNCs [201, 202].

After vasopressin synthesis, MNCs package vasopressin molecules into large dense core vesicles that are subsequently transported to axon terminals [198]. These MNC axon terminals

project into the posterior pituitary, allowing vesicles filled with vasopressin to be exocytosed into fenestrated capillaries [203-205]. Exocytosis of vasopressin is calcium dependent and driven by MNC action potentials initiated in the soma [206]. Following release into the blood stream, vasopressin binds V_2 G-protein coupled receptors on the basolateral side of principal cells in the renal collecting duct of the kidney [207, 208]. Binding of vasopressin to V_2 receptors leads to adenylyl cyclase activation, increased cyclic AMP concentration and activation of protein kinase A (PKA) [20, 207, 209]. Activated PKA phosphorylates AQP2 and increases its translocation to the apical membrane [20, 209]. Increased AQP2 at the apical membrane in turn increases water reabsorption by the collecting duct to correct systemic hypertonic ECF [20].

In contrast to the vasopressin – AQP2 axis, which is activated by increased systemic ECF osmolarity, the renin-angiotensin-aldosterone (RAA) signaling axis is activated by decreased plasma volume [210]. The RAA signaling axis responds to decreased plasma volume and functions to increase sodium reabsorption in the collecting duct of the kidney via the hormone aldosterone and regulators angiotensin I and II [211]. Low salt intake activates the proteolytic cleavage of angiotensinogen by the enzyme renin to form angiotensin I [212, 213]. Renin is synthesized, stored, and secreted from juxtaglomerular cells of the kidney and angiotensinogen is secreted into circulation by liver cells [214]. Angiotensin I is subsequently converted to angiotensin II by angiotensin-converting enzyme (ACE). ACE is secreted into circulation by both kidney and lung cells [215]. Angiotensin II binds type I receptors (AT_1) in the zona glomerulosa of the adrenal gland to stimulate aldosterone secretion [216-220]. To promote sodium reabsorption in the kidney, aldosterone binds the mineralocorticoid receptor (MR) in the cortical collecting duct of the kidney [221]. Binding of aldosterone to MR increases the number of epithelial sodium channels (ENaC) in the apical membrane of principal renal collecting duct cells and increases

ENaC transcription [222-224]. ENaC facilitates sodium reabsorption in the kidney [223]. In this way, aldosterone increases plasma volume and ECF osmolarity in response to systemic hypotonic stress.

1.4.2 The cellular response to osmotic stress in mammals

Even though mammals tightly regulate systemic ECF osmolarity, all mammalian cells, with the exception of OLVTs and MNCs, have the capacity to respond to osmotic stress at the cellular level. This cellular response allows mammalian cells to survive during diseases in which systemic osmoregulatory mechanisms are unable to reestablish osmotic homeostasis, such as during hypernatremia, or in tissues that require drastic osmotic fluctuations for normal function, such as in the kidney. Similarly to bacteria, yeast, and plants, the cellular HTSR in mammals consists of an initial regulatory volume increase phase followed by a slower osmolyte accumulation phase. Although the transcription factor Nuclear Factor of Activated T Cells 5 (NFAT5)/Tonicity-Responsive Enhancer Binding protein (TonEBP) has been identified as a master regulator of the HTS response in mammals, the osmosensing pathways upstream of NFAT5, including the osmosensor that activates NFAT5, has not been fully characterized [49, 225]. Furthermore, NFAT5 is not conserved in all metazoans, which indicates there may be more ancient NFAT5-independent HTSR regulatory mechanisms. Therefore, much about the precise signaling pathways that sense and initiate ORG expression in animals still remain elusive. My thesis project seeks to fill these gaps in knowledge by studying ORG expression in *C. elegans*. Since *C. elegans* do not express a homolog of NFAT5, it provides a platform from which to investigate NFAT5-independent mechanisms regulating ORG expression. Additionally, *C. elegans* provides powerful genetic means to identify conserved osmosensitive signaling pathways

upstream of NFAT5-dependent or -independent gene expression. Through the use of *C. elegans*, my objective is to characterize conserved regulatory mechanisms governing the HTSR in animals.

1.4.2.1 Regulatory volume increase in mammals

The initial response to HTS in mammalian cells, like in other organisms, is a rapid influx of ions to counteract cell shrinkage. Within thirty seconds of HTS induction by 500 mM sorbitol or sodium chloride, mammalian cells activate the lysine deficient protein kinase 1 (WNK1) by autophosphorylation [226]. WNK1 subsequently phosphorylates the Ste20/SPS1-related proline/alanine-rich kinase (SPAK) and the oxidative stress responsive kinase 1 (OSR1) [227, 228]. Activated SPAK and OSR1 phosphorylate the Na-K-Cl cotransporter NKCC1, which mediates the influx of sodium to correct cell shrinkage [47, 48, 229].

WNK1 activation peaks around two minutes following HTS and is sustained for up to eighty minutes [226]. Although the specific mechanisms by which HTS activates WNK1 are not well understood, two key observations have provided clues about its regulation. First, WNK1 activation has been shown to occur independently of the three canonical mammalian MAPK signaling pathways, classical MAPK (ERK), C-Jun N-terminal kinase (JNK), and p38, which commonly regulate stress responsive signaling pathways [226]. Second, HTS causes diffuse cytoplasmic WNK1 to condense into reversible membraneless liquid droplets [230]. These condensates may colocalize with clathrin and the trans-Golgi network [226]. Formation of these phase separated WNK1 structures trigger activation of the WNK1/SPAK/OSR1/NKCC1 pathway [230]. Furthermore, optogenetic experiments have demonstrated that it is specifically molecular crowding caused by HTS induced cell shrinkage that promotes WNK1 puncta formation [230]. Therefore, WNK1 is intrinsically sensitive to HTS and may itself serve as the osmosensor required to activate NKCC1 and correct cell shrinkage.

In addition to mammals, the WNK1 pathway is required for acute cell volume recovery in other organisms, such as *C. elegans* [231]. *C. elegans* have a single SPAK-like protein, GCK-3, which is required for acute volume recovery and survival during HTS. *gck-3* mutants exhibit greater shrinkage and reduced volume recovery during HTS compared to WT animals [231]. Furthermore, GCK-3 interacts physically with WNK-1 in *C. elegans* and *wnk-1* mutants have a qualitatively similar HTS sensitivity as *gck-3* mutants. Genetic epistasis experiments indicate that WNK-1 and GCK-3 function in the same HTSR pathway in *C. elegans*, like they do in mammals [231]. The evolutionary conservation of the hypertonicity induced WNK1 pathway highlights the importance of acute volume recovery in the HTSR.

1.4.2.2 Intracellular compatible osmolyte accumulation in mammals

Within a few hours of HTS, intracellular ions accumulated during the acute phase of the HTSR are replaced with compatible osmolytes [232]. As discussed previously, the intracellular accumulation of compatible osmolytes protects cells against HTS - induced shrinkage, without increasing intracellular ionic strength. Therefore compatible osmolytes enable a long-term adaptive strategy for cells in hypertonic environments. In mammals, each cell type accumulates a different combination of compatible osmolytes during HTS. For example, renal medullary cells accumulate sorbitol, glycine betaine, myo-inositol, taurine, and glycerophosphocholine (GPC) [233]. The brain accumulates myo-inositol, glutamate, glutamine, taurine, and creatine [32]. Liver endothelial cells accumulate glycine betaine, myo-inositol, and taurine [234]. Since compatible osmolytes are often interchangeable in their protection during HTS, it is not completely understood why different mammalian cells accumulate different compatible osmolytes. One hypothesis is that a cell's metabolism and/or extracellular matrix (ECM) composition determine which compatible osmolytes it uses [51].

Five of the most common compatible osmolytes found in mammals are sorbitol, betaine, myo-inositol, taurine, and GPC. Sorbitol is accumulated intracellularly during HTS via increased synthesis. HTS activates upregulation of aldose reductase, which catalyzes the rate-limiting step of sorbitol synthesis from glucose [235, 236]. In contrast to sorbitol, myo-inositol is accumulated intracellularly via increased transport from the ECF. The source of this myo-inositol is either diet or lipid degradation pathways [237]. HTS increases transcription of the sodium myo-inositol transporter (*SMIT)*, which couples import of myo-inositol to the concentration gradient of sodium [236, 238, 239]. Like myo-inositol, taurine and betaine are accumulated intracellularly via transport from the ECF. The primary source of both these compatible osmolytes is dietary [240, 241]. HTS increases transcription of the taurine transporter (*TAUT)* and the betaine/GABA transporter 1 (*BTG1*), which couple taurine and betaine import to the sodium and chloride concentration gradients respectively [236, 242-245]. Finally, GPC is accumulated intracellularly by both increased synthesis and decreased breakdown of phosphatidylcholine. HTS increases transcription of the enzyme that synthesizes GPC, neuropathy target esterase (NTE*)*, and decreases transcription of the enzyme that breaks down GPC, GPC-choline-phosphodiesterase (GDPD5) to cumulatively increase GPC accumulation [52, 246-248]. Importantly, the genetic regulation of all these osmolyte accumulation genes is regulated by the transcription factor NFAT5 [49, 236, 243].

1.4.2.3 NFAT5 regulates protective gene expression during hypertonic stress in mammals

NFAT5, part of the Rel family of transcriptional activators, is a master regulator of osmotically regulate gene (ORG) expression in mammals [225]. Mammalian kidney cells, specifically those in the inner medulla of the kidney are routinely exposed to ECF osmolarities of almost six times normal plasma osmolarity [249]. NFAT5 plays a critical role in kidney cells to regulate the expression of over one hundred ORGs, including compatible osmolyte accumulation

genes, under physiological conditions [236]. Importantly, NFAT5 is expressed and functions in most cell types, not just those of the kidney [250]. Many tissues can experience changes in the osmolarity of their micro-environment and therefore require NFAT5 -dependent hypertonic adaptive pathways [251].

NFAT5 is required both *in vitro* and *in vivo* for ORG upregulation [49, 252]. Knockout of NFAT5 in cell culture impairs the upregulation of ORGs, including osmolyte accumulation genes [236]. Correspondingly, in response to HTS, WT cells increase NFAT5 protein levels four-fold and increase NFAT5 nuclear accumulation ten-fold to upregulate ORG expression [250]. Under isotonic conditions NFAT5 is equally distributed in the cytoplasm and nucleus [250]. Supporting the *in vitro* NFAT5 observations, NFAT5 is activated in the inner medulla of the mouse kidney during dehydration [253]. Unlike in cell culture, *in vivo* activation of NFAT5 consists only of NFAT5 nuclear enrichment and not of increased NFAT5 protein expression [253]. Homozygous NFAT5 null mice exhibit decreased upregulation of ORGs, including compatible osmolyte accumulation genes, during dehydration-induced HTS [49]. This decreased ORG upregulation manifests itself physiologically by primarily affecting the kidney because this tissue experiences large osmotic variations. NFAT5 null mice have kidney hypoplasia, altered medullary morphology, and increased apoptosis of inner medullary cells [49]. NFAT5 is therefore a critical architect of the HTSR in mammalian cells.

Compatible osmolyte accumulation genes make up an important portion of NFAT5-dependent ORGs. As mentioned previously, NFAT5 regulates the hypertonicity-induced expression of enzymes responsible for compatible osmolyte accumulation such as aldose reductase, SMIT, TAUT, and NTE. However, NFAT5 also regulates dozens of other genes induced by HTS [236]. It is the cumulative effect of all these genes that protects cells from HTS.

Several heat shock proteins (HSPs), such as HSP70, αB-crystallin, a HSP40 called HLJ1, and HSP110 members Osp94 and HSP105B are upregulated as part of the HTSR in an NFAT5-dependent manner [254-258]. These heat shock proteins collectively function to protect cells from protein damage caused by high intracellular ionic strength. Also among the genes that NFAT5 induces the transcription of is *AQP2*. Whereas vasopressin is required for acute activation of AQP2 in systemic osmoregulation, NFAT5 is required for increased *AQP2* expression after twenty-four hours of HTS to maintain water reabsorption in the collecting duct [259]. Interestingly, there are also several genes that are upregulated in an NFAT5-independent manner during HTS. The mechanism by which these genes are upregulated is not known [236].

NFAT5 target genes have at least one DNA motif called an osmotic response element (ORE) or tonicity enhancer element (TonE) in their promoter [260, 261]. The sequence of the consensus ORE/TonE is (A/C/G/T)GGAAA(A/T) (A/G/T)(A/C/T)(A/C)C(A/C/G/T) [261]. Binding of NFAT5 to OREs/TonEs does not require phosphorylation because NFAT5 treated with calf intestinal phosphatase binds ORE/TonE DNA elements in binding assays [262].

As with all transcription factors, NFAT5 functions in the nucleus to activate ORG upregulation. Even though binding of NFAT5 to OREs/TonEs does not require phosphorylation, nuclear translocation of NFAT5 is regulated by hypertonicity-induced phosphorylation. The kinetics of NFAT5 phosphorylation during HTS correlate temporally with NFAT nuclear localization [262]. Since NFAT5 is too big to diffuse in and out of the nucleus, nuclear translocation of NFAT5 requires an N-terminal nuclear localization signal and an auxiliary export domain [263]. One way phosphorylation of NFAT5 may facilitate its nuclear localization is by exposing these nuclear localization domains to nuclear import machinery.

Ataxia telangiectasia-mutated kinase (ATM) is partially required for the nuclear translocation of NFAT5 [264]. However it is unclear whether ATM directly phosphorylates NFAT5 because consensus ATM phosphorylation sites have not been identified in the portion of NFAT5 required for ATM regulation [264]. Nevertheless, cells without ATM have reduced nuclear enrichment of NFAT5, suggesting that ATM directly or indirectly regulates NFAT5 nuclear enrichment [264]. Since NFAT5 nuclear localization is not completely eliminated in *ATM* null cells, other unknown factor(s) are also required for NFAT nuclear translocation [264].

In addition to phosphorylation and nuclear localization, activation of NFAT5's three transactivation domains stimulates ORG upregulation. The transactivation domains of NFAT5 mediate interactions between NFAT5 and its activators to induce gene expression. As ECF hypertonicity increases, the activity of one of NFAT5's three transactivation domains increases and this is dependent on several regulators [265]. Although these regulators are each required for full activation of NFAT5, none of them is alone sufficient to activate NFAT5 [266]. Furthermore, there is a lack of direct evidence that many of these regulators interact with NFAT5 [267]. Therefore, although the role of NFAT5 in the mammalian HTSR has been studied for over twenty years, a comprehensive genetic characterization of the regulatory pathways upstream of NFAT5, if such pathways exist, has remained elusive.

There are at least five kinases that have been implicated in NFAT5 regulation via its transactivation domain. Inhibition of the cAMP-dependent PKA, p38 MAPK, Src tyrosine kinase Fyn, ATM, or phosphoinositide 3-kinase IA (PI3K-IA) decreases the transactivation activity of NFAT5 and upregulation of ORGs during the HTSR [265, 268-270]. All five of these kinases are activated by HTS, suggesting they may act upstream of NFAT5 [124, 265, 270-272]. However, only PKA and ATM have been shown via coimmunoprecipitation to physically interact with

NFAT5 either directly or indirectly [269]. Furthermore, ATM and PI3K-IA are the only two kinases that have been suggested to function together to regulate hypertonic activation of NFAT5. Knockout of PI3K-IA decreases NFAT5 activation in an ATM dependent manner [270]. Therefore it is likely that multiple parallel pathways involving these kinases regulate NFAT5 activation during the HTSR.

While study of NFAT5 activity has proven to be an important tool for characterizing regulation of the HTSR in mammals, it has not led to a detailed understanding of the pathway. Despite decades of study, significant work is still required to dissect apart the pathways regulating NFAT5 activity, understand the requirement for seemingly redundant pathways, and identify the osmosensor(s) that activate these pathways. These studies may be limited due to possible genetic redundancy, NFAT5-independent pathways, and the absence of *in vivo* context in cell culture. My project seeks to address these limitations and study regulation of the HTSR using a fundamentally different approach that does not rely on NFAT5 activity. Instead, I use unbiased genetic approaches in *C. elegans* to characterize pathways regulating the HTSR. Such approaches allow for investigation of the HTSR in an *in vivo* context and have the potential to offer new perspectives on the HTSR [273].

1.4.3 Physiological exposure of mammalian cells to osmotic stress

All mammalian cells, with the exception of osmosensing neurons, are able to detect HTS and initiate protective ORG expression [250, 251, 267]. However, due to systemic osmoregulation, only some cells are routinely exposed to HTS under physiological conditions [251, 267]. Cells in the inner medulla of the kidney are exposed to the most drastic osmotic fluctuations in mammals. Cells at the tip of the renal inner medulla are commonly exposed to

osmolarities of up to 1,744 mosmol kg^{-1}, in contrast the plasma osmolarity of about 300 mosmol kg^{-1} [249]. Hypertonic ECF in the inner medulla is a normal part of kidney physiology, as it drives water reabsorption in the collecting duct during antidiuresis. Depending on the state of diuresis, kidney cells are therefore routinely exposed to large fluctuations in ECF osmolarity and must modulate expression of protective genes, including osmolyte accumulation genes to survive and adapt [41].

Other mammalian cells that are exposed to HTS under physiological conditions include cells in lymphoid tissues and the liver [251]. Both liver and lymphoid tissues have high metabolic activities and cell densities, two factors that increase hypertonicity of the ECF [251]. Cells in the thymus and spleen can be exposed to ECF osmolarities of up to 330 mosmol kg^{-1} [251]. Partial loss of NFAT5 activity impairs lymphocyte function supporting a critical role of NFAT5 in the adaptation of lymphocytes to hypertonic environments [251].

1.4.4 Pathophysiological exposure of mammalian cells to osmotic stress

Mammalian cells are also exposed to osmotic stress during disease. In certain mammalian diseases, such as hypernatremia, hyponatremia, and ischemia reperfusion injury, systemic regulation of ECF osmolarity and the cellular HTSR are insufficient to avoid acute cellular and tissue damage due to osmotic stress. Hypernatremia is a condition in which plasma osmolarity is hypertonic due to a net water loss or sodium gain [274]. Chronic hypernatremia is caused gradually over several days and is most common in infants and elderly people because they miss or are unable to communicate early symptoms [274, 275]. Diarrhea and thirst impairment/dehydration are the most common causes of hypernatremia in infants and the elderly

respectively. However, hypernatremia can also be a side effect of other diseases such as Cushing's syndrome, Guillain-Barre syndrome, and diabetes insipidus [274].

The symptoms of hypernatremia correlate in severity with how quickly plasma osmolarity is changed. The brain is the most susceptible organ to hypernatremia because hypernatremia causes brain shrinkage [274, 276, 277]. Although brain cells adapt quickly to HTS by accumulating compatible osmolytes, rapid and drastic increases in hypertonicity, as seen in hypernatremia, can overwhelm these adaptive responses [274, 276]. Correspondingly, most symptoms of hypernatremia are neurological [274, 277]. These symptoms start with lethargy and irritability and progress to muscle rigidity, tremors, seizures and eventually death if plasma hypertonicity is not corrected [274]. The treatment for hypernatremia is a slow administration of hypotonic fluids. Hypotonic fluids decrease plasma hypertonicity. However, because compatible osmolytes accumulated intracellularly in the brain take up to two days to return to normal levels, rapid administration of hypotonic fluids can cause cerebral edema, which leads to convulsions, coma and even death [275, 278]. Therefore, hypernatremia, especially in severe cases in which plasma osmolarity exceeds 377 mosmol kg^{-1}, requires slow, monitored correction [277].

In contrast to hypernatremia, hyponatremia is characterized by hypotonic plasma due to excess water intake or reduced sodium intake [279]. Hyponatremia is the most common cause of brain swelling [279]. It is most frequently caused by psychotic polydipsia (excessive water intake that is most common in psychiatric patients), renal failure, use of thiazide diuretics, osmotic diuresis, and inappropriate secretion of vasopressin due to a head trauma, brain tumor, or cerebrovascular accident [279]. The first symptoms of hyponatremia are brain swelling, depression of sensorium, and seizures [280]. Acute hyponatremia results in death in over half of cases because ECF hypotonicity progresses quicker than the ability of the brain to mount an

adaptive response [280]. However, chronic, slow onset, hyponatremia rarely leads to death or symptoms, because brain cells have time to efflux ions and compatible osmolytes to reestablish osmotic homeostasis [32, 280]. Following the same principles of hypernatremia, hyponatremia is corrected via the slow infusion of hypertonic saline [281]. If hypertonic saline is administered too rapidly, brain dehydration resulting in demyelinating brain lesions and a 40% death rate occurs [282]. Therefore, like hypernatremia, hyponatremia requires a deliberate, slow correction to appropriately leverage the osmotic stress response to restore homeostasis.

Finally, another common cause of osmotic stress in mammals is ischemia reperfusion injury. Ischemia reperfusion injury is caused by insufficient blood supply to an organ, most commonly the heart, kidneys, lung, and brain [283]. Strokes and myocardial infarction are examples of conditions that cause ischemia reperfusion injury [283]. Unlike hypernatremia and hyponatremia, which are caused by anisosmotic osmotic changes, ischemia reperfusion injury is caused by isosmotic cell volume changes. Insufficient blood supply to an organ causes a switch from aerobic to anaerobic metabolism in the affected tissues and this leads to Na^+/K^+-ATPase failure due to decreased ATP production [284, 285]. Failure of the Na^+/K^+-ATPase triggers a loss in the transmembrane ionic gradient because sodium is no longer pumped out of the cells. The net result is increased intracellular sodium concentration, which results in hypotonic stress-induced cell swelling [286].

The swelling of endothelial cells during ischemia blocks small blood vessels and causes “no-reflow” after reperfusion of the affected tissue. Thus, even when blood supply to the affected tissue is fixed, blood is still unable to access cells in the tissue because of endothelial cell swelling [287]. Ischemia reperfusion injury can be avoided by exposing affected cells to acute HTS to decrease cell swelling. This is most effectively done with mannitol or glucose injections [288].

1.4.5 Conclusions

Mammalian organisms, unlike bacteria, yeast, and plants, maintain a systemic plasma osmolarity of about 300 mosmol kg^{-1} via the vasopressin and aldosterone hormone signaling pathways. However, individual mammalian cells still maintain the ability to respond and adapt to osmotic stress and this is critical for their survival. Cells such as those in the kidney, lymphoid tissues, and liver are routinely exposed to HTS and all cells are exposed to osmotic stress during diseases in which systemic osmotic regulation is insufficient to maintain ECF osmolarity. While the transcription factor NFAT5 has emerged as a key regulator of the cellular HTSR in mammals, much remains unknown about its regulation. Specifically, it remains elusive how mammalian cells sense HTS, how these osmosensitive signals are transmitted to the kinases upstream of NFAT5, and if there are NFAT5-independent mechanisms cells use to regulate ORG expression. My thesis project will address these unknowns using the invertebrate animal *C. elegans*.

1.5 *C. elegans* provides a powerful *in vivo* model system to study genetic regulation of the hypertonic stress response

C. elegans is a multicellular transparent small nematode that was first cultivated for laboratory research by Sydney Brenner in the 1970s [289]. Brenner was interested in mapping out the structure of the nervous system and chose *C. elegans* as an animal model because of its relatively simple nervous system and genetic manipulability [289]. Since Brenner's introduction of *C. elegans* to the scientific community, this model organism has proved instrumental in the discovery of diverse conserved cellular pathways. Discoveries using *C. elegans* have been

recognized with three separate Nobel Prizes. First, in the 2002 Nobel Prize, Brenner was recognized for establishing *C. elegans* as a model system [289], John E. Sulston was recognized for creating a cell linage map [290, 291], and H. Robert Horvitz was recognized for describing a conserved pathway regulating programmed cell death [292-294]. The identification of the cell death pathway has since played a key role in understanding human diseases, such as neurodegenerative disease, in which programmed cell death pathways are aberrantly activated [295]. Second, in 2006 Andrew Z. Fire and Craig C. Mello were awarded the Nobel Prize for their discovery of RNA interference (RNAi) [296]. RNAi has since become an important tool, not only in basic research, but in therapeutics as well [297]. Finally, Martin Chalfie was acknowledged with the 2008 Nobel Prize in Chemistry for his development of green fluorescent protein (GFP) as a genetic tool. Chalfie used *C. elegans* to demonstrate that GFP could be used to visualize neuronal gene expression in live cells [298]. These Nobel Prize winning discoveries, combined with countless other discoveries in *C. elegans*, illustrate the value of this small nematode in science.

Multiple experimental attributes make *C. elegans* uniquely suited to answer genetic questions, particularly those related to understanding stress response pathways such as the HTSR. The first and perhaps greatest advantage of *C. elegans* is its optical transparency throughout its entire lifecycle. This transparency allows scientists to view all *C. elegans* cells under the microscope in living animals without perturbing the ECM, cell interactions, or tissue integrity. Furthermore, fluorescently tagged proteins in these cells can be viewed at single cell and subcellular resolution. The optical transparency of *C. elegans* made the high-throughput genetic screen that was the basis for my thesis project possible. Using the COPAS Biosort I sorted thousands of living *C. elegans* based on the expression of a GFP tagged gene in the hypodermis without dissecting or perturbing the cells. I was able to not only detect GFP in the hypodermis of

living animals, but also sort out animals based on GFP intensity. Another benefit of using an optically transparent model organism is that fluorescently tagged protein localization can be visualized in living animals through imaging. In my thesis project, I utilized this advantage to determine the localization of proteins required for the HTSR.

A second advantage of *C. elegans* is its hermaphroditic genetics. *C. elegans* produces germline oocytes and sperm cells, allowing it to self-fertilize once it reaches adulthood [289]. In its self-reproductive lifespan of about six days a *C. elegans* produces 200-300 self-offspring [299]. Because of its hermaphroditic mode of reproduction, each of these offspring is genetically representative of the maternal genotype. In combination with standard genetic tools, such as genetic balancers and markers, this mode of reproduction enables simple maintenance and identification of heterozygous and homozygous mutations within a population of animals. However, male *C. elegans* can also arise through errors of meiosis and mate with hermaphrodites to produce 50% male offspring [289]. The existence of males allows mutations to be moved into and out of different genetic backgrounds through standard genetic crossing methods. The ability of *C. elegans* to both self- and cross- fertilize made it possible for me to isolate clonal populations of *C. elegans* from a single animal in the forward genetic screen that was the basis for my thesis project. These characteristics also made it possible to rapidly determine if my isolated mutants exhibited Mendelian segregation properties consistent with single gene recessive phenotype-causing mutations.

A third advantage of *C. elegans* is its compact genome. The genome of *C. elegans*, which was completed in 1998, consists of roughly 20,000 protein coding genes and about 1,300 non-protein coding genes in just over 100 million base pairs of DNA [300-302]. Included in the non-protein coding genes are 590 transfer RNAs, 275 ribosomal RNAs, 140 trans-spliced leader RNAs,

120 miRNAs, 70 spliceosomal RNAs, and 30 snoRNAs [302]. Even though humans and *C. elegans* have a similar number of protein-coding genes, *C. elegans* package their genes in thirty-fold less DNA [300]. The compact nature of the *C. elegans* genome makes whole genome sequencing relatively quick and inexpensive. Additionally, about 80% of protein-coding *C. elegans* genes have human homologs, suggesting that many aspects of this organism's physiology are conserved across evolution [303]. The compact and stable nature of the *C. elegans* genome, along with inexpensive whole-genome resequencing allowed me to efficiently sequence the genomes of over a dozen HTSR defective mutants and identify mutations in genes involved in the HTSR.

Finally, a fourth advantage of *C. elegans* is its multicellularity. An adult hermaphroditic *C. elegans* develops from an embryo to an adult with 959 somatic cells in just over three days at the standard cultivation temperature of 20°C [304, 305]. Adult animals contain neurons, glial, muscle, intestinal, and hypodermal cells that are very similar to their counterparts in mammals [306]. The outer layer of these adult animals is a collagen-rich cuticle made of hundreds of ECM proteins [307]. This structure provides protection against harmful pathogens, leverage for muscle contraction and motility, and sensors for detection of stressors [308-310]. Therefore, unlike single cell model systems such as yeast, *C. elegans* provides a platform from which to characterize intercellular signaling pathways, such as paracrine and endocrine signaling events, in the context of the native ECM. This platform was critical to my thesis project because it allowed me to study the involvement of multiple cell types in the HTSR and do so in the context of the ECM, which plays an important functional role in the HTSR.

Unbiased genetic screens in *C. elegans* have been instrumental for understanding the regulation of key conserved physiological stress responsive pathways [311-314]. Most of these

screens utilize a common phenotypic strategy. First, they identify key transcriptional targets that are upregulated by the stressor. Second, they generate transgenic animals that express GFP under control of a stress-inducible promoter. Finally, they screen for mutants or RNAi knockdowns that either constitutively activate or inhibit stress-inducible expression of the reporter based on GFP expression. While conceptually simple, these types of *in vivo* high-throughput screening approaches are only possible in *C. elegans* due to its optical transparency.

The conserved pathways regulating the oxidative stress response transcriptional regulator, SKN-1 (Nrf homolog), have been extensively characterized through unbiased genetic strategies in *C. elegans.* SKN-1 is required for both the upregulation of phase II detoxification genes during xenobiotic and oxidative stresses and for the upregulation of proteasomal subunits during proteasomal disruption [315, 316]. Additionally, knockdown of *skn-1* decreases lifespan, suggesting that SKN-1 dependent gene expression mediates longevity [315]. Fluorescent reporter – based genetic screens have been instrumental in understanding how SKN-1 is regulated during control and stress conditions. The phase two detoxification gene *gst-4* is specifically and robustly upregulated during oxidative stress in a SKN-1 dependent manner, making it an ideal reporter candidate for a genetic screen [311]. Indeed, an RNAi screen using a *gst-4p::GFP* reporter identified several genes that constitutively activate reporter expression during control conditions [311]. Upon further examination of these genes, SKN-1 target gene expression and nuclear localization were found to be negatively regulated by a proteasomal degradation pathway involving the WD40 protein WDR-23 [311]. This result suggests that SKN-1 is constitutively localized to the nucleus, but it is unable to accumulate during control conditions due to a WDR-23 dependent proteasomal degradation pathway. Therefore, a *C. elegans* RNAi screen was the

first to identify proteasomal degradation as a method of SKN-1 regulation and it paved the way for characterization of conserved pathways in other organisms.

Furthermore, another RNAi screen using the SKN-1 dependent phase II detoxification gene reporter, *gcs-1p::GFP*, led to the discovery that genes involved in translation and ribosomal assembly also negatively regulate SKN-1 dependent gene transcription [312]. RNAi knockdown of translation initiation factors in the eukaryotic initiation factor 4F (eIF4F) and pre-initiation complexes resulted in constitutive SKN-1 dependent gene expression and increased lifespan in a SKN-1 dependent manner [312]. The results from this RNAi were not only the first to suggest that SKN-1 mediates lifespan extension in animals with inhibited translation, but they also revealed the complexity of SKN-1 regulation.

Finally, in addition to these RNAi based screens, forward mutagenesis screens have also been instrumental towards characterizing SKN-1 regulation. The proteasomal subunit gene *rpt-3* is upregulated in a SKN-1 dependent manner during proteasomal disruption [313]. Therefore, in *C. elegans* with genetically disrupted proteasomes, *rpt-3::GFP* is constitutively expressed. Animals constitutively expressing *rpt-3::GFP* were used in a forward mutagenesis based genetic screen to identify mutants with impaired *rpt-3::GFP* induction. This genetic screen revealed a critical role of the ER in SKN-1 regulation [313]. An ER-associated isoform of SKN-1 and ER-mediated post-translational modifications of SKN-1 are required for SKN-1 dependent transcriptional responses during proteasomal disruption [313]. This genetic screen not only identified a novel form of SKN-1 regulation, but it also uncovered potential therapeutic targets upstream of SKN-1/Nrf that could be used in cancers resistant to proteasomal inhibitors.

Similarly to the oxidative stress response, genetic screening approaches in *C. elegans* have also played a critical role in defining the Ire1 branch of the endoplasmic reticulum (ER) unfolded

protein response (UPR) [314]. The heat shock protein gene *hsp-4* is strongly upregulated by ER stress in an *ire-1* dependent manner in *C. elegans* [314]. This robust and specific upregulation makes *hsp-4p::GFP* an excellent reporter for forward genetic screens. A forward genetic screen in mutants that constitutively upregulated *hsp-4p::GFP* led to the discovery that the X-box binding protein -1 (XBP-1) is required for the IRE-1 dependent UPR transcriptional response [314]. IRE-1 was subsequently shown to cleave XBP-1 into its active form during ER stress in both *C. elegans* and mammals [314]. Therefore, as is often the case with genetic screens in *C. elegans*, this *hsp-4p::GFP* fluorescence based forward genetic screen was critical towards identifying a conserved physiological pathway and it led to a broader understanding of this pathway not only in *C. elegans*, but in mammals as well.

The oxidative and ER stress response illustrate the power of unbiased genetic screening strategies in *C. elegans* for understanding the regulation of physiological stress-responsive signaling pathways. Often these unbiased genetic screens reveal unexpected novel signaling mechanisms that would have taken longer to uncover using traditional biochemical or cell biological methods. My thesis project applies genetic screens, similar to those used to characterize these oxidative and ER stress responses, to the HTSR in *C. elegans* in order to identify signaling pathways regulating ORG expression. By taking an unbiased screening approach, I identified surprising and unexpected new genes and pathways required for the HTSR. My thesis focuses on two such pathways, one involving the *O*-GlcNAc transferase OGT-1 and one involving the 3'mRNA cleavage and polyadenylation complex.

1.5.1 The hypertonic stress response in *C. elegans*

HTS is induced in *C. elegans* by increasing the osmolarity of its environment. True isotonicity for *C. elegans* is not known. However, most studies of the *C. elegans* HTSR consider standard Nematode Growth Media (NGM), which contains ~50 mM NaCl and has an osmolarity of ~170 mOsm, to be isotonic [317]. HTS is typically elicited by raising NaCl concentrations. HTS causes at least three distinct organismal phenotypes in *C. elegans*, depending on the relative increase and duration of exposure. First, acute HTS (>500 mM NaCl) can lead to death of the organism within 24 hours [318]. Second, acute exposure to non-lethal HTS (i.e. adaptation, 200 mM NaCl) allows animals to subsequently survive a normally lethal HTS for naïve animals [318]. Third, chronic exposure to non-lethal HTS (250 mM NaCl) elicits adaptive mechanisms that enable growth and development over multiple generations [319]. Specific and sometimes overlapping molecular mechanisms mediate each of these organismal responses.

Immediately upon exposure to HTS, the body cavity of *C. elegans* shrinks as water leaves [318]. This HTS - induced cell shrinkage activates the conserved 'With No Lysine' protein kinase 1 (WNK-1) pathway [231]. The WNK-1 cell volume recovery pathway is the initial cellular response to HTS that mediates the influx of ions (and osmotically obliged water) into the cell to quickly restore cell volume. In mammals, cell shrinkage activates auto-phosphorylation of WNK-1 [226, 320]. Phosphorylated WNK-1 subsequently phosphorylates and activates SPAK and OSR1 [227, 228]. Finally, SPAK and OSR1 phosphorylate and activate the Na – K – Cl cotransporter NKCC1, which mediates the influx of sodium and water to correct cell shrinkage [47, 48, 229]. The WNK-1 pathway is also activated in *C. elegans* following HTS [231]. Although the WNK-1 pathway acutely restores cell volume, the activation of WNK-1 targets increases

intracellular ionic strength due to the influx of sodium ions. Increased intracellular ionic strength interferes with many cellular processes such as protein folding and enzyme activity [3, 4]. While the WNK1 pathway is important for the acute phase of the HTSR, other pathways appear to mediate long-term aspects of the HTSR that replace inorganic ions with compatible solutes.

1.5.1.1 Compatible osmolyte accumulation in *C. elegans* during hypertonic stress

Glycerol is the primary compatible osmolyte used by laboratory-reared *C. elegans* to adapt to HTS [318]. This is similar to yeast, which also utilize glycerol [53]. Although mammals do not utilize glycerol as an osmolyte, they do take a similar metabolic approach to osmolyte production by breaking down glucose to produce sorbitol [235]. In this respect, *C. elegans* may represent an evolutionary intermediate in terms of mechanisms of HTS adaptation. Intracellular glycerol concentration tracks extracellular osmolarity and accumulates on the order of hours in *C. elegans* [317, 318]. When *C. elegans* acclimated to a hypertonic environment is transferred back to normal growth conditions, glycerol levels drop due to glycerol efflux [318]. Therefore, glycerol accumulation in *C. elegans* is dynamic.

C. elegans biosynthesizes glycerol via transcriptional upregulation of a glycerol-3-phosphate dehydrogenase homolog (*gpdh*) [318]. GPDH catalyzes the rate-limiting step in glycerol biosynthesis [321]. Therefore, upregulation of *gpdh* enhances the rate of glycerol production. There are two classes of eukaryotic GPDH enzymes, a cytosolic NADH-dependent form and a mitochondrial FAD-dependent form. NADH – and FAD – dependent GPDHs together make up the 'glycerol – phosphate shuttle' that is critical for cellular glucose metabolism [322, 323]. NADH – dependent GPDH reduces dihydroxyacetone (DAP) to glycerol-3-phosphate (G3P)

while oxidizing NADH to NAD, and FAD – dependent GPDH oxidizes G3P to DAP while reducing FAD to $FADH_2$ [323]. Only NADH – dependent GPDH is involved in the HTSR [318].

There are two NADH-dependent *gpdh* genes in the *C. elegans* genome encoded by *gpdh-1* and *gpdh*-2 [317, 318]. During the HTSR, *gpdh-2* exhibits little to no upregulation [317]. This contrasts with *gpdh-1*, which is upregulated > 20 - 50 – fold within the first three hours of HTS exposure [319, 324]. Notably, loss of *gpdh-1* does not significantly reduce steady state whole animal glycerol levels in response to HTS, although the rate of glycerol accumulation is slowed [317]. *gpdh-1* mutants do exhibit a mild defect in their ability to acutely adapt to HTS, showing that *gpdh-1* does play a functionally significant role the HTSR [319]. However, animals lacking both *gpdh-1* and *gpdh-2* exhibit a ~50% reduction in steady-state glycerol levels [317]. This suggests that *gpdh-2* can function redundantly with *gpdh-1* in HTS-induced glycerol production. It also suggests the existence of *gpdh*-independent mechanisms for glycerol production.

A transcriptional reporter for *gpdh-2* is constitutively expressed in the intestine, hypodermis, and excretory cell and is not substantially upregulated by HTS [317]. On the other hand, a *gpdh-1* transcriptional reporter is virtually undetectable under control conditions but is strongly induced in the hypodermis and intestine during HTS [317]. This reporter is specifically induced by HTS since it is not induced by other cellular stressors, such as heat shock, ER stress, or oxidative stress. Interestingly, the *gpdh-1* reporter is not activated in other tissues, such as the muscle, neurons, or germline [317]. This suggests a model in which the hypodermis and intestine, which are environmentally exposed epithelial tissues that are the first to encounter HTS, are the primary sites of glycerol production. Glycerol is then shunted out of the basolateral membrane into the pseudocoelomic space, where it can be accumulated by non-glycerol producing cells, such as muscle and neurons, via passive uptake mechanisms. In support of such a model, glycerol

permeant aquaglyceroporins are localized to the basolateral epithelial membrane, while water permeant aquaporins are present on the apical membrane [26]. This could provide a permeability pathway for the efflux of glycerol out of the intestine as well as an influx pathway for osmotically driven water movement.

1.5.1.2 Osmotically regulated genes in *C. elegans*

gpdh-1 is one of 324 ORGs in *C. elegans* [324]. Several of these upregulated ORGs suggest there may be other interesting physiological mechanisms involved in the *C. elegans* HTSR. For example, the H^+-coupled myo-inositol transporter *hmit-1.1* is upregulated >100-fold by HTS. The kinetics of *hmit-1.1* upregulation differ from those of *gpdh-1* in that *hmit-1.1* upregulation peaks at later timepoints than *gpdh-1* [324]. While myo-inositol is a major osmolyte in mammalian cells and is accumulated via transcriptional upregulation SMIT [238, 239], there is no evidence that *C. elegans* accumulate myo-inositol under laboratory conditions [318]. However, myo-inositol is a major breakdown product of plant organic material, which is present in many, if not all, of the sites where *C. elegans* are known to inhabit [325-327]. Therefore, the upregulation of *hmit-1.1* may indicate that *C. elegans* in the wild can utilize myo-inositol as an osmolyte in addition to glycerol, but that it is unable to use myo-inositol in the laboratory since it is absent from the cultivation conditions.

Many genes upregulated by HTS are also upregulated during bacterial and fungal infection in *C. elegans*. This does not include *gpdh-1* or *hmit-1.1*, which appear to be exclusively upregulated by HTS. Instead, many of these co-regulated genes are components of the *C. elegans* innate immune response, such as members of the neuropeptide-like protein (*nlp*) and caenicin (*cnc*) gene families [324]. Some pathogens, such as the fungal pathogen *Drechmeria coniospora*,

physically penetrate the cuticle as part of the infection process [308, 328]. Since both pathogens and the HTS impinge on the specialized *C. elegans* ECM that forms the cuticle, this supports the hypothesis that upregulation of some ORGs may be triggered via hypertonicity- or pathogen-induced disruptions in the cuticle. Consistent with this hypothesis, several mutants affecting structural components of the cuticle, including many collagen-encoding *dpy* genes (i.e. *dpy-7*, *-8*, *-9*, and *-10*), constitutively activate the *C. elegans* HTSR [310, 317, 324]. One possible interpretation of these genetic findings is that the cuticle is a water impermeant cell wall-like structure that slows the movement of water out of the underlying tissues during HTS. However, the cuticle is permeable to many small molecule dyes [329], suggesting that smaller molecules, such as water, can move through this structure with relative ease, although such permeability could be dynamically regulated by HTS. Moreover, enhancing cuticle permeability does not alter the HTS phenotype of *C. elegans* mutants [329]. Another possible hypothesis that is consistent with such observations is that the cuticle functions as a mechanical osmosensor whose shape, tension, and/or connections to the underlying hypodermis are influenced by changes in the hypodermal tissue volume. Whether or not HTS itself leads to specific disruption of the cuticle and how such disruptions might couple to signaling pathways that activate ORGs is not yet known.

1.5.1.3 Transcriptional regulation of the *C. elegans* hypertonic stress response

For over a decade, our lab has taken advantage of the strong and specific upregulation of *gpdh-1* and the power of unbiased genetic screens in *C. elegans* to characterize the genetic pathways regulating the HTSR, specifically ORG expression [317, 329]. The first screen for regulators of the HTSR utilized genome-wide RNAi screening to identify genes that when inhibited caused upregulation of a *gpdh-1p::GFP* reporter under isotonic conditions [317]. This

screen identified over one hundred genes negatively regulating *gpdh-1* and other ORG expression [317]. Surprisingly, most of the genes identified in this screen fell into two classes.

The first class of osmotic regulators included protein homeostasis genes involved in RNA processing, protein synthesis, protein folding, and protein degradation [317]. One hypothesis to explain this discovery is that cells sense HTS and upregulate *gpdh-1* expression through detection of stress- induced protein damage. While protein damage can be replicated by inhibition of protein homeostasis genes, other stressors, such as heat shock, also cause protein damage but nevertheless fail to upregulate *gpdh-1* expression [317]. This suggests that HTS causes a type of protein damage that differs from other types of protein damage and specifically activates the HTSR without activating other stress response pathways. In support of this hypothesis is the observation that HTS causes a model protein (polyQ) to form aggregates [330, 331]. These polyQ aggregates differ from aggregates caused by other stressors in both *C. elegans* and mammalian cells in their morphology, solubility, and ubiquitination characteristics, suggesting they are a unique aggregate species [330, 331]. Additional studies show that endosomal sorting pathways and lysosomes clear existing protein damage to facilitate survival and adaptation during HTS [332]. However, when genes involved in degradation are inhibited, protein damage accumulates and *C. elegans* can no longer survive or adapt to HTS [332]. These data clearly reveal an important role for maintenance of the proteome in the regulation of the *C. elegans* HTSR.

In a mechanism likely related to HTSR-induced accumulation of damaged proteins, regulation of protein translation also has a critical role in the HTSR [333, 334]. Global protein translation is inhibited ~50% by mild HTS (200 mM NaCl) [334]. Moreover, pharmacological inhibitors of translation lead to a mild upregulation of *gpdh-1* mRNA even in the absence of HTS, suggesting a direct signaling link between HTS-induced translation inhibition and regulation of

the ORG *gpdh-1* [334]. HTS-induced translational inhibition requires phosphorylation of eukaryotic translation initiation factor 2 alpha (eIF2α) by the kinase GCN-2 and its accessory protein GCN-1 and loss of *gcn-1* or *gcn-2* reduces HTS-induced *gpdh-1* expression by ~50% [334]. GCN-1/2 appear to act in the same pathway as WNK-1 (Section 1.5.1) since *gcn-1* mutants are non-additive with *wnk-1* knockdown [334]. How this pathway for HTS-induced translational inhibition is linked to transcriptional regulation of *gpdh-1* is currently unknown.

The second large class of genes that negatively regulate *gpdh-1* gene expression and the HTSR are genes encoding secreted extracellular proteins [317]. These extracellular proteins are synthesized by the hypodermis and secreted from the apical membrane to generate the specialized *C. elegans* ECM called the cuticle [307]. This ECM is shed and resynthesized during each of the four larval molts that occur in *C. elegans* development [309]. The precise organization and makeup of the cuticle differs between these developmental stages. However, by adulthood the cuticle contains hundreds of ring-like annular furrows that form circumferential-oriented ingressions along the length of the animals [309]. One of the most abundant structural components of the cuticle are collagen proteins, which are encoded by many genes in *C. elegans* [335]. Mutations in several of these collagen genes lead to alterations in body shape [336, 337]. Interestingly, mutations in collagen genes that disrupt specifically the annular furrow (*dpy-2, -7, -8, -9,* and *-10*) [310] activate *gpdh-1* expression under isotonic conditions and cause the accumulation of massive amounts of glycerol [310, 317]. As a result, these mutants retain motility in extremely hypertonic environments (500 mM NaCl), whereas WT animals rapidly paralyze [310, 317]. This suggests that the annular furrow plays an important role in the *C. elegans* HTSR. However, animals with LOF mutations in other secreted proteins, such as the mucin-like protein OSM-8, the notch ligands OSM-7 and OSM-11, and the novel secreted protein OSR-1 exhibit

qualitatively normal furrows, but also activate *gpdh-1* expression, accumulate glycerol, and are osmotic stress resistant [317, 324, 329, 338-340]. One possibility is that these non-furrow disrupting ECM proteins act to couple furrow-based osmosensing to the underlying hypodermis through detection of HTS-induced structural changes. Direct tests of this mechanically-based osmosensing model are still needed.

The genetic origins of several HTSR-regulated extracellular genes reveal connections between whole-animal HTS adaptation and behavioral responses that allow *C. elegans* to avoid hypertonic environments. *osm-7, -8,* and *-11* were isolated in a forward genetic screen for osmotic avoidance abnormal (*osm*) mutants [341]. While wild-type animals crawl away from hypertonic stimuli, *osm* mutants fail to avoid these stimuli. Hypertonic avoidance behavior depends on the ciliated ASH sensory amphid neurons [342]. There are three classes of *osm* genes that differ based on their effects on the ASH neuron. The first and second class of *osm* genes function cell autonomously in the ASH neurons to regulate cilia formation and cell signaling respectively [343, 344]. In contrast, the third class of *osm* genes, which includes *osm-7, -8,* and *-11* is not expressed in the ASH neurons and mutations in these genes do not affect the ASH neurons. Instead, these genes are expressed in the hypodermis, where they function to inhibit the expression of *gpdh-1* and glycerol accumulation [329, 338]. The hypodermal expression of these class three *osm* genes suggests that an unidentified paracrine factor(s) signals from the hypodermis to the ASH neurons during HTS to modulate behavior. One possibility is that this paracrine factor is glycerol itself because glycerol could blunt amphid neuron volume changes upon hypertonic exposure when present at high levels. In addition, there is some evidence that retrograde signaling occurs, i.e. that ASH neurons signal to osmosensitive tissues to modify the HTSR. The class two *osm* gene, *osm-9*, encodes a transient receptor potential channel, TRPV, that is expressed in ASH neurons to

facilitate ASH-dependent signaling [343]. Surprisingly, *osm-9* mutants are not only behaviorally *osm*, but they also constitutively upregulate the ORG *aqp-8* in osmosensitive tissues [345] and have improved acute survival during HTS due to decreased protein damage [346]. Therefore, unidentified paracrine factors signal from the ASH neurons to the osmosensitive tissues of *osm-9* mutants to modulate cellular physiology. The *osm* paradigm provides a unique opportunity to investigate how hypodermis-based physiological information is integrated to modulate neuronal-based behavior and vice versa. It also highlights the importance of investigating the HTSR at the organismal level, where behavior and physiology can be studied together.

The class three gene *osm-8* has been studied in significant molecular detail to understand its role in the HTSR. *osm-8* encodes a small hypodermally – secreted mucin protein [329]. Like the other class three *osm* mutants, *osm-8* mutants constitutively induce ORGs, including *gpdh-1*, accumulate large amounts of glycerol during control conditions, and are resistant to normally lethal levels of HTS [329]. To identify genes that may function downstream of the secreted *osm-8* gene to transduce signals from outside the cell to the nucleus, our lab performed an unbiased RNAi screen for suppressors of *osm-8* mutants. Inhibition of the multi-pass transmembrane patched – related protein 23 (*ptr-23*) completely suppressed many *osm-8* phenotypes, including constitutive *gpdh-1* induction, glycerol accumulation, and the osmotic stress resistance (OSR) phenotype [329]. However, *ptr-23* did not suppress the induction of all ORGs, since many innate immunity genes upregulated in *osm-8* mutants were similarly upregulated in *osm-8; ptr-23* double mutants [329]. Therefore, a subset of ORGs must be regulated in a *ptr-23* – independent manner. Furthermore, *ptr-23;osm-8* double mutants still induce the *gpdh-1* reporter during HTS, suggesting that the HTSR does not exclusively require *ptr-23* [329]. These two observations indicate that

there are multiple redundant pathways regulating the HTSR and at least one of them is independent of *ptr-23*.

While unbiased genetic screens have revealed valuable information about the HTSR, the specific signaling pathways that control upregulation of *gpdh-1* and/or other ORGs have not yet been identified. In yeast and mammals, MAPK – dependent signaling pathways are known to regulate HTS – dependent transcription. The p38 MAPK activates hypertonic induction of the mammalian transcription factor NFAT5/TonEBP [347, 348] and the p38 MAPK homolog, HOG1, regulates the transcription of ORGs during HTS in yeast [106]. Despite the roles of MAPK signaling in the yeast and mammalian HTSR, there is little evidence that MAPK signaling is involved in the *C. elegans* HTSR. MAPK signaling components have thus far not been isolated in genetic screens for regulators of the HTSR, although we note that such screens have not yet reached saturation [317, 329]. Moreover, knockdown of p38 signaling pathway components in *osm-7* and *osm-11* mutants has no effect on acute or chronic OSR [338]. Similarly, p38 MAPK signaling is not involved in induction of the ORG, *nlp-29*, by HTS despite being required for induction of *nlp-29* during fungal infection [349]. However, MAPK signaling is involved in the chronic survival of *osr-1* mutants on HTS [340] and the survival of WT animals during desiccation [350]. Therefore, MAPKs may be involved in the *C. elegans* HTSR, but they are unlikely to be a major contributor to the transcriptional upregulation of ORGs during HTS.

In mammals, the rel family transcription factor NFAT5 is directly responsible for the transcriptional upregulation of many genes by HTS [236]. However, the *C. elegans* genome does not contain rel family transcription factors. While the tonicity-responsive transcription factor in *C. elegans* is currently unknown, promoter analysis of *C. elegans* ORGs has provided some candidates. The promoters of *C. elegans* ORGs are highly enriched for GATA-type transcription

factor binding sites [324]. RNAi screening identified the GATA erythroid-like factors ELT-2 and ELT-3 as being required for HTS-induced upregulation of a *gpdh-1* transcriptional reporter [324]. *elt-2* is expressed in the intestine and mediates intestinal upregulation of *gpdh-1*, while *elt-3* is expressed in the hypodermis and is required for hypodermal upregulation of *gpdh-1* [324]. Both these transcription factors function downstream of the ECM proteins that negatively regulate the HTSR, but it is unknown if they are required for all HTSR pathways [324]. An alternative hypothesis is that *elt-2* and *elt-3* are required for intestinal and hypodermal differentiation and development but are not the physiological targets of the HTSR [351, 352]. Future studies using CRISPR/Cas9 to tag native alleles of *elt-2* and *elt-3* followed by cell biological and biochemical analysis in the presence and absence of HTS are needed to determine if HTS leads to changes in the localization and/or activity of *elt-2/3*, as has been shown for other stress-responsive transcription factors [315, 353].

In conclusion, protein homeostasis and extracellular proteins inhibit HTSR-induced transcriptional responses. While it is tempting to speculate that increased protein damage functions as the illusive "osmosensor" during HTS, it is unlikely to be the primary way cells sense HTS because it is prominent only at extremely high levels of HTS [330, 331]. Another hypothesis is that cells sense HTS through changes in ECM structure. The annular furrow in the ECM has been linked to the HTSR, but it remains unknown if changes in its structure during HTS trigger the HTSR . Finally, in addition to understanding how cells sense HTS, a transcription factor(s) specific to ORG induction remains to be identified. ELT-2 and ELT-3 are required for intestinal and hypodermal ORG induction respectively. However, since they are also generally required for transcription in these tissues, it is unknown whether they themselves are activated in a specific way by HTS or function with other HTS – specific factors [351, 352]. Continued unbiased genetic

screening efforts, which is the greatest strength of the *C. elegans* model system, should help to identify HTSR relevant transcription factors, signaling pathways, and other proteins involved in signaling the transcriptional response to HTS.

1.5.2 Conclusions

Our lab was the first to harness the power of genetic screens in *C. elegans* to characterize the HTSR. Transcriptionally, the HTSR is under strong negative regulation. Regulation of protein homeostasis genes, which oppose protein damage and synthesis, negatively regulate the HTSR transcriptional response through *gcn-1/2* and *gck-3/wnk-1* signaling pathways. Extracellular proteins inhibit *gpdh-1* transcriptional induction under isotonic conditions through a pathway involving a transmembrane protein and GATA-type transcription factors. Additional independent pathways also regulate the transcription of other ORGs. Therefore, genetic screens performed to date have revealed the existence of at least two transcriptional HTSR pathways in *C. elegans* [273].

In my thesis project, I build on our previous success of using unbiased genetic screens to understand negative regulation of the HTSR in *C. elegans* by using the same fundamental strategies to understand the positive regulation of this stress response. Using *gpdh-1p::GFP* fluorescent reporter expression as a read-out for the HTSR, I conducted a forward genetic screen for mutants that have an impaired HTSR. My unbiased genetic screen led to the discovery of three unexpected genes affecting two biological pathways. One gene is the sole *C. elegans* homolog of the conserved *O*-GlcNAc transferase OGT and the other two genes are interacting proteins within the 3' mRNA cleavage and polyadenylation complex. Neither of these pathways have previously been linked to the HTSR. Understanding how these genes contribute to the HTSR is the goal of my thesis project and will contribute fundamentally new insights into this stress response pathway.

1.6 The *O*-GlcNAc transferase OGT

Post-translational modifications play key roles in cellular processes such as stress responses. One recently discovered post-translational modification is the addition of a single ring sugar motif, ß-linked N-acetylglucosamine (*O*-GlcNAc), to serine and threonine residues of intracellular proteins [354]. *O*-GlcNAcylation was first described in 1984 following a serendipitous discovery in lymphocytes and it was subsequently observed to be abundant in the nucleus and cytoplasm of a variety of cell types [355-358]. Similarly to other post-translational modifications, *O*-GlcNAcylation modifies the function, localization, and stability of proteins [354]. In 1997, the sole enzyme that *O*-GlcNAcylates proteins, *O*-GlcNAc transferase (OGT), was cloned in mammals and *C. elegans* [359, 360]. Shortly after, the sole enzyme that removes *O*-GlcNAc, *O*-GlcNAcase (OGA), was discovered and cloned [361]. OGT and OGA are ubiquitously expressed in the somatic tissues of all metazoans and are absent from yeast genomes [360-362]. Together these two enzymes regulate O-GlcNAc homeostasis, which is important to a variety of cellular processes including metabolism, stress responses, and proteostasis [354].

1.6.1 Evolutionary conservation of OGT protein structure and function

The structure of OGT is highly conserved among metazoans with up to 80% identity between organisms [359]. OGT is made up of an N-terminal tetratricopeptide repeat (TPR) domain, a nuclear localization signal (NLS), and C-terminal catalytic domain [360, 363]. *C. elegans* and human OGT shares 89% identity in the TPR domain and 74% identity in the catalytic domain [319].

The N-terminal TPR domain of OGT is made up of 12.5 repeats, each with 34 amino acids, that mediate the recognition and binding of *O*-GlcNAcylation substrates to OGT [364-366]. Together these repeats are arranged in anti-parallel α-helices that form two flexible right-handed superhelices with substrate-interacting asparagine residues lining the inner protein binding groove [367]. The large surface area and conformational flexibility of the TPR domain facilitates interactions with a wide range of substrates. In addition to substrate recognition, the TPR domain is required for OGT trimerization [368]. While trimerization is not required for *O*-GlcNAcylation activity, trimerization increases the affinity of OGT for its *O*-GlcNAc donor uridine diphosphate *N*-acetylglucosamine (UDP-GlcNAc) [368]. This suggests that multimerization regulates OGT activity. Deletion analysis demonstrates that TPRs 2 - 6 are sufficient to mediate binding of OGT to substrates [366], but all TPRs are required for OGT trimerization [368].

Another important domain within OGT is the NLS. OGT is localized in both the nucleus and cytoplasm and it therefore must be shuttled between these two cellular compartments [359]. In the cytoplasm, OGT modifies hundreds of enzymes and structural proteins to modulate cellular pathways such as those involved in metabolism, protein expression, and cell stress responses [354]. In the nucleus, OGT has two broad functions. It modifies nuclear pore proteins to modulate nuclear envelope permeability and it modifies transcription and chromatin factors to regulate gene expression [369]. The *O*-GlcNAc modification is associated with the chromatin of hundreds of gene promoters and is required for proper transcriptional regulation of these genes [370]. OGT has been shown to recruit transcriptional repressors to gene promoters through both *O*-GlcNAcylation-dependent and -independent mechanisms [371]. Additionally, within the nucleus, there is interplay between *O*-GlcNAcylation and phosphorylation of the C-terminal domain (CTD) of RNA Polymerase II (RNAP II). *O*-GlcNAcylation of RNAP II is required for assembly of the

preinitiation transcriptional complex and knockdown of *ogt* decreases transcription about 50% [372].

The nuclear localization of OGT is facilitated by a three amino acid NLS motif, DFP (aa 451-453), located within the TPR domain [363]. In addition to the NLS, nuclear localization of OGT requires *O*-GlcNAcylation of Ser389 in the TPR domain [363]. It is hypothesized that *O*-GlcNAcylation at this residue causes a conformational change in OGT that exposes the NLS to importin α5, which interacts with OGT via the DFP motif to transport OGT into the nucleus [363].

Finally, located at the C-terminal end of OGT is the catalytic glycosyltransferase domain. This domain binds UDP-GlcNAc and the substrate to catalyze the addition of *O*-GlcNAc [373]. A strict OGT substrate binding motif has not been identified, but many of its substrates have amino acids that promote an extended conformation, like proline, flanking the *O*-GlcNAcylated residue [373]. Structurally, the catalytic domain is made up of Rossmann-like folds (a layered sandwich-like tertiary structure made up of alternating α-helices and ß-sheets) and α-helices with His498 acting as the catalytic base [373]. The Rossmann-like folds function to bind nucleotides such as UDP-GlcNAc [374]. The catalytic domain alone is sufficient to *O*-GlcNAcylate synthetic peptides *in vitro* [365], but the TPR domain is required *in vivo* [319].

The single mammalian *ogt* gene encodes four isoforms of OGT that vary only in the length of their TPR domains [359, 364]. The canonical nucleocytoplasmic isoform of OGT (ncOGT), isoform 3, has 12.5 TPRs and regulates global cellular *O*-GlcNAcylation [364]. A second nucleocytoplasmic isoform, isoform 1, is identical to isoform 3 except that it has ten fewer amino acids in its TPR domain. Isoforms 1 and 3 function interchangeably. Additionally, there is a shorter mitochondrially localized isoform of OGT (mOGT) that contains TPRs 5 – 12.5 and an N-terminal mitochondrial targeting sequence [364]. TPRs 5 - 7 of mOGT are sufficient for substrate

binding [365]. Consistent with its mitochondrial localization, mOGT regulates mitochondrial membrane structure and function via *O*-GlcNAcylation of mitochondrially-encoded proteins [375]. Finally, the shortest isoform of OGT (sOGT) is nucleocytoplasmic and contains TPRs 11 – 12.5. The function(s) of sOGT remains largely unknown, but evidence suggests that it negatively regulates ncOGT O-GlcNAcylation activity by directly interacting with ncOGT [376]. In contrast to mammals, only one isoform of OGT have been experimentally verified in *C. elegans*. *C. elegans* OGT-1 is nucleocytoplasmic and has high homology to mammalian ncOGT isoforms 1 and 3 [360].

1.6.2 The cellular functions of OGT

Although *O*-GlcNAcylation was the first discovered function of OGT and has long been considered the primary function of OGT, research in the last twenty years has revealed additional catalytic and non-catalytic functions of OGT. My thesis project describes a novel non-catalytic role of OGT in the HTSR. Using unbiased genetic approaches in *C. elegans*, I discovered a critical role of OGT in regulating protein expression of the osmolyte biosynthetic enzyme GPDH-1 during HTS. Surprisingly, the function of OGT in the HTSR does not depend on the catalytic activity of OGT, but it does depend on the presence of the protein – protein interacting tetratricopeptide repeat (TPR) domain. Therefore, my thesis project demonstrates that OGT engages in important molecular functions outside of its well described roles in post-translational *O*-GlcNAcylation.

1.6.2.1 The *O*-GlcNAcylation function of OGT

OGT was first discovered because of its *O*-GlcNAcylation activity [355]. Unlike canonical glycosylation, which occurs in the secretory pathway, OGT glycosylates thousands of intracellular

nuclear, cytoplasmic, and mitochondrial proteins [354]. OGT is the only protein that catalyzes the addition of the single ring sugar motif, *O*-GlcNAc, to serine and threonine residues of proteins [359]. Correspondingly, only one enzyme, OGA, catalyzes the removal of *O*-GlcNAc from proteins [361]. Together OGT and OGA establish a dynamic *O*-GlcNAcylation environment within cells.

The source of *O*-GlcNAc in cells is UDP-GlcNAc [377]. The catalytic domain of OGT binds UDP-GlcNAc to facilitate the addition of O-GlcNAc to proteins and the energetically favorable release of UDP [373]. UDP-GlcNAc is synthesized from glucose, amino acids, fats, and nucleotides by the hexamine biosynthetic pathway (HBP) [378]. About 2 – 5% of intracellular glucose enters the HBP and becomes *O*-GlcNAc [379]. O-GlcNAc synthesis, and the HBP as a whole, is therefore sensitive to the nutrient and metabolic status of the cell. In fact, diets high in fat and sugar have been shown to increase global O-GlcNAcylation without affecting OGT or OGA protein levels [380].

O-GlcNAcylation is regulated in several different ways. As alluded to above, the first way *O*-GlcNAcylation is regulated is by the nutrient status of the cell. Hyperglycemic conditions increase flux through the HBP, leading to a greater intracellular concentration of UDP-GlcNAc [354]. Increased intracellular UDP-GlcNAc in turn results in higher OGT activity and affinity of OGT for its substrates [368]. Paradoxically, glucose deprivation also increases *O*-GlcNAcylation [381]. This increase in *O*-GlcNAcylation is due not to increased flux through the HBP, but to the transcriptional upregulation of OGT by the AMP-activated protein kinase (AMPK). Glucose deprivation activates AMPK to increase OGT transcript and protein levels [382]. One hypothesis is that increased *O*-GlcNAcylation in these glucose poor conditions protects proteins from degradation, as has been shown in other contexts [383]. Therefore, *O*-GlcNAcylation is regulated

both through intracellular UDP-GlcNAc levels and OGT transcription, depending on the nutrient status of the cell. However, these are not the only factors regulating the catalytic function of OGT.

O-GlcNAcylation activity is also regulated through post-translational modification of OGT. OGT is phosphorylated under several different conditions to increase its *O*-GlcNAcylation activity. Calcium/calmodulin – dependent protein kinase (CaMKIV) phosphorylates and activates OGT during potassium chloride – induced neuronal depolarization [384]. OGT activation in these neurons is required for Ca^{2+} – dependent gene induction, such as the upregulation of genes involved in nerve tissue remodeling and neuronal plasticity [384]. Another kinase that phosphorylates and activates OGT is the circadian rhythm regulator glycogen synthase kinase 3β (GSK3β) [385]. GSK3β activity oscillates in a circadian pattern, thereby causing the activity of its targets, such as OGT, to oscillate with circadian time as well [385]. *O*-GlcNAcylation of mammalian clock proteins plays a critical role in the timing and length of each circadian phase [385]. Finally, AMPK also phosphorylates OGT to regulate its nuclear localization and global substrate selectivity during stress conditions such as glucose deprivation [386]. Together these examples show that phosphorylation is one way that cells regulate OGT function.

In addition to phosphorylation, OGT activity is also modulated via *O*-GlcNAcylation. Multiple sites on OGT are *O*-GlcNAcylated to regulate its nuclear localization and substrate selectivity [387]. *O*-GlcNAcylation of Ser389 in the TPR domain of OGT exposes the NLS and is required for the nuclear localization of OGT [363]. Furthermore, *O*-GlcNAcylation of the short isoform of OGT at Thr12 and Ser56 changes the substrate selectivity of sOGT and the latter promotes cell proliferation and cell cycle progression [388]. Therefore, the catalytic activity of OGT itself plays an autoregulatory role in confining OGT to specific cellular localizations and substrates.

The final way in which *O*-GlcNAcylation is regulated is via protein – protein interactions. A p38 MAPK interaction with the C-terminus of OGT is required for activation of OGT in low glucose conditions [382]. This interaction with p38 is independent of phosphorylation, as OGT is not a phosphorylation target of p38 [382]. The interaction between p38 and OGT is required for the *O*-GlcNAcylation of specific substrates, such as Neurofilament H, but not for the binding of OGT to these substrates [382]. Two other proteins that regulate *O*-GlcNAcylation via direct interactions with OGT are the targeting regulatory subunit of the PP1-beta serine/threonine phosphatase (MYPT1) and the transcriptional coactivating arginine methyltransferase CARM1 [389]. Both these proteins change the substrate selectivity of OGT without changing its intrinsic catalytic activity. It is hypothesized that MYPT1 and CARM1 enable OGT substrate specificity by acting as adaptor proteins between OGT and particular substrates [389]. However the nature of these substrates remains to be characterized.

Since OGT modifies Ser and Thr residues of target substrates, the *O*-GlcNAc modification can compete with phosphorylation for modification of the same residue or influence modification of adjacent residues. The crosstalk between these two PTMs is complicated and specific to the target protein. At a global level, increasing *O*-GlcNAcylation decreases phosphorylation at some sites, while increasing it at others [390]. In many cases, *O*-GlcNAcylation and phosphorylation are not mutually exclusive. For example, neurofilament proteins are simultaneously phosphorylated and *O*-GlcNAcylated in the same protein domains [391].

However, cross-talk between *O*-GlcNAcylation and phosphorylation does occur when there is steric hindrance, modification of the same residue, or *O*-GlcNAcylation of the kinase. For example, the CTD of RNAP II is dynamically *O*-GlcNAcylated at Thr4 and phosphorylated at Ser2 and Ser5 [392, 393]. However, *O*-GlcNAcylation is not detected on phosphorylated RNAP

II and vice versa due to steric hindrance between the added phosphates and *O*-GlcNAc [393]. *O*-GlcNAcylation of the RNAP II CTD is required for proper assembly of the preinitiation complex and subsequent gene transcription [372]. Additionally, the same residue on a protein can be the target of both phosphorylation and *O*-GlcNAcylation. Thr58 on the protooncogene c-Myc can be phosphorylated or *O*-GlcNAcylated depending on the nutrient status of the cell [394, 395]. During serum starvation, Thr58 is *O*-GlcNAcylated and during serum stimulation Thr58 is phosphorylated. Therefore, mutually exclusive phosphorylation and *O*-GlcNAcylation can act as a rheostat for the nutrient status of the cell [395]. Finally, *O*-GlcNAcylation influences phosphorylation when the kinase itself is *O*-GlcNAcylated to modify its activity. This occurs with CaMKIV, which is *O*-GlcNAcylated at a position that directly blocks its catalytic activity and prevents it from phosphorylating substrates [396]. Phosphorylation of CaMKIV in turn prevents this inhibitory *O*-GlcNAcylation and allows it to remain active[396].

In conclusion, the *O*-GlcNAcylation activity of OGT integrates inputs, such as the nutrient status of the cell and circadian rhythm, to modulate a variety of cellular signaling pathways. Although progress has been made in understanding the mechanisms of OGT regulation and the cross talk between *O*-GlcNAcylation and phosphorylation, much is still not understood about this widespread PTM. In particular, there is still much to learn about how one enzyme can achieve specificity to thousands of substrates, how the activities of OGT and OGA influence one another, and how the methods of OGT regulation are integrated together. Continued research on this unique form of glycosylation from a biochemical, genetic, and physiological perspective will be useful to answering these questions.

1.6.2.2 The proteolytic function of OGT

In addition to the reversible *O*-GlcNAc PTM, OGT also catalyzes a non-reversible proteolytic event. It binds and proteolytically cleaves one known target, the mammalian host cell factor 1 (HCF-1) [397, 398]. HCF-1 is synthesized as a large precursor protein and must be cleaved at six central amino acid repeats ($HCF\text{-}1_{PRO}$) by OGT to be activated in mammals [399]. Once cleaved, the N - and C – terminal HCF-1 subunits remain non-covalently associated and promote passage through the Gl and M phase of the cell cycle respectively [399-401]. Interestingly, OGT is only required to cleave HCF-1 in mammals. *Drosophila* utilize another enzyme, Taspase1, to cleave HCF-1 [402] and HCF-1 in *C. elegans* is expressed in its active form and thus does not need to be cleaved [403].

OGT uses the same active site for HCF-1 proteolysis as it uses for canonical *O*-GlcNAcylation [404]. In fact, OGT proteolytically cleaves HCF-1 via the non-canonical *O*-GlcNAcylation of a glutamate in HCF-1 [404]. This *O*-GlcNAcylated glutamate creates a high energy pyroglutamate species that causes spontaneous amide hydrolysis of HCF-1 [405]. In support of this model, the addition of uncleavable UDP-5SGlcNAc to cells inhibits HCF-1 cleavage [404].

While the proteolytic activity of OGT is important in mammalian biology, it appears to be obsolete in invertebrates such as *C. elegans*. Therefore, the proteolytic activity of OGT is likely not involved in the HTSR. In mammals, the proteolytic and *O*-GlcNAcylation activity of OGT can be inhibited by a single amino acid change in the C-terminal catalytic domain (K842M) [406]. Even though OGT does not cleave HCF-1 in *C. elegans,* this residue is in a highly conserved region of OGT and can be mutated in *C. elegans* OGT-1 (K957M) to completely inhibit any potential

OGT-1 proteolytic activity [319]. In my thesis project we use this amino acid change to demonstrate that OGT proteolytic activity is not required in the HTSR.

1.6.2.3 The non-catalytic functions of OGT

Finally, in addition to its catalytic activities, OGT also has non-catalytic functions. These non-catalytic functions of OGT have only recently been described and the exact non-catalytic mechanism(s) remain poorly understood [371, 407, 408]. However, it has been hypothesized that OGT may act as a scaffolding and/or adaptor protein via its N-terminal TPR domain. In fact, it has been demonstrated that the TPR domain of OGT is sufficient to repress transcription in mammalian cells via an interaction with the corepressor mSin3A. The first six TPRs of OGT recruit mSin3A to promoters to repress transcription in both histone deacetylase dependent and independent pathways [371]. Therefore, the catalytic activity of OGT is not required for mSin3A gene transcriptional repression.

OGT has also been shown to function non-catalytically in mammalian cell adhesion. Specifically, OGT inhibits the formation of the E-cadherin/catenin complex in H1299 cells by binding and inhibiting p120, which stabilizes the complex [407]. Although it was not explicitly tested, inhibition of the E-cadherin/catenin complex by OGT is hypothesized to decrease E-cadherin/catenin mediated cell adhesion and thus promote metastasis in cancer cells [407]. Interestingly, WT and catalytically impaired OGT (OGT H558A) inhibit this E-cadherin/catenin complex to the same extent suggesting that the catalytic activity of OGT is not required for this OGT function [407]. However, it remains unknown if the TPR domain is required for this interaction. Experiments with a truncated TPR domain would help to address this question.

Additionally, the physiological consequences of this noncatalytic role of OGT still need to be addressed.

Another described non-catalytic function of OGT is in the GABAergic motor neurons of *C. elegans* [408]. OGT forms a complex with the HECT family ubiquitin ligase EEL-1 to facilitate proper neuronal function [408]. Overexpression of catalytically impaired or dead OGT-1 (H612A or K957M respectively) in *ogt-1* mutants rescues the impaired GABAergic motor neuron function, demonstrating that the catalytic activity of OGT is dispensable for this phenotype [408]. As with the function of OGT in cell adhesion, it is not known if OGT functions in the GABAergic neurons through a mSin3A – like mechanism that requires only the TPR domain.

Although several examples of non-catalytic OGT function have been described, there is very little mechanistic insight into this newly discovered function of OGT. The most is known about the role of OGT in transcriptional repression, where it acts as an adaptor protein via its first six TPRs to recruit mSin3A to the promoter of genes. Whether OGT acts as an adaptor protein via its TPR domain in cell adhesion and GABAergic neurons remains to be explored. In my thesis research, through unbiased genetic screens, we discovered another non-catalytic function of OGT. The TPR, but not catalytic activity, of OGT is required for ORG protein expression in the HTSR. The requirement of the TPR domain suggests that OGT may function as an adaptor – like protein in the HTSR similar to its function in mSin3A - mediated transcriptional repression. However, continued genetic and biochemical experiments are required to more thoroughly mechanistically characterize the role of OGT in the HTSR.

1.6.3 The role of OGT in cellular processes

Due to its wide variety of substrates, OGT is involved in numerous aspects of cell biology and physiology including insulin signaling, neurobiology, autophagy, and cellular stress responses. The majority of these cellular processes require the *O*-GlcNAcylation activity of OGT, but it is important to note that in several of the studies a complete OGT knockout, which ablates all OGT functions, was used . Therefore, in many cases, the described cellular roles of OGT could be due to either catalytic or non-catalytic OGT functions. However, my thesis project describes a new role of OGT in cell physiology that does not require its catalytic activity. The diverse involvement of OGT in cell signaling highlights the multi-faceted nature of this enzyme and its importance in cellular function.

1.6.3.1 OGT and insulin signaling

In mammals, elevated *O*-GlcNAcylation due to increased flux through the HBP, inhibition of OGA, or overexpression of *Ogt* suppresses insulin signaling [409-411]. Specifically, *O*-GlcNAcylation of protein kinase B (Akt) inhibits its phosphorylation and activation by the PDK1 kinase in adipocyte cell culture and mice [410, 412]. Since phosphorylated Akt activates glucose uptake, *O*-GlcNAcylation of Akt inhibits glucose uptake and results in insulin resistance [410, 412]. Additionally, knockout of *ogt-1* suppresses the Dauer phenotype in *C. elegans* containing loss of function mutations in the IGFR homolog DAF-2 and increases glycogen stores in WT *C. elegans*, suggesting that OGT-1 also suppresses insulin signaling in *C. elegans* [413].

In addition to Akt, several other components of the insulin signaling pathway, including Foxo1 and Irs1, are also *O*-GlcNAcylated [410, 414, 415]. Like Akt, *O*-GlcNAcylation of these proteins affects their phosphorylation status and inactivates them [410, 414, 415]. Physiologically,

OGT acts in a negative feedback pathway to dampen insulin signaling. Insulin stimulates the PI3 kinase to produce PIP3 at the plasma membrane which recruits OGT to the plasma membrane via a unique C-terminal phosphoinositide binding domain [416]. Once at the plasma membrane, OGT *O*-GlcNAcylates components of the insulin signaling pathway to inhibit insulin-stimulated glucose uptake [416].

Unlike in mammals and *C. elegans*, where OGT suppresses insulin signaling, *O*-GlcNAcylation in *Drosophila* appears to activate insulin signaling. In particular, *O*-GlcNAcylation of Akt in Drosophila enhances its phosphorylation and thus activation [417]. These contradictory results highlight the complex and species specific interplay between *O*-GlcNAcylation and insulin signaling. Additionally, an important consideration with all of these studies connecting OGT to insulin signaling is that although *O*-GlcNAcylation was measured and correlated with these pathways, none of these studies explicitly tested whether catalytically dead, but otherwise functional, OGT could operate in these pathways. A demonstration that catalytically dead OGT is unable to modulate insulin signaling would strengthen the argument that the *O*-GlcNAcylation activity of OGT mediates this cellular pathway.

1.6.3.2 OGT and the nervous system

Research primarily in *C. elegans* has demonstrated the importance of OGT in the nervous system. Knockout of *ogt-1* in *C. elegans* increases neuronal axon regeneration after neuronal laser ablation by promoting a switch from mitochondrial oxidative phosphorylation to glycolysis [418]. Interestingly, knockout of *oga-1*, which correspondingly results in increased *O*-GlcNAcylation, also increases neuronal axon regeneration but through a distinct mechanism that involves modulation of mitochondrial dynamics [418]. The effects of *ogt-1* and *oga-1* knockdown on

neuronal regeneration are dependent on AKT and SGK1 insulin signaling pathways respectively [418]. While the roles of OGT-1 and OGA-1 in neuronal regeneration are presumed to be via their *O*-GlcNAcylation and *O*-GlcNAcase activities respectively, this has not been explicitly demonstrated by either identifying *O*-GlcNAcylated targets or testing catalytically inhibited *ogt-1* mutants.

In addition to neuron regeneration, OGT is involved in cognitive function in both *C. elegans* and mammals. In *C. elegans*, OGT-1 functions in primary sensory neurons to regulate a type of learning called habituation [419]. Habituation describes the phenomenon whereby the response of an organism to repeated stimuli decreases over time. OGT-1 inhibits habituation at short interstimulus intervals and promotes habituation at long interstimulus intervals [419]. The molecular mechanisms through which OGT-1 operates to regulate habituation remain unknown. In mice, *Ogt* knockout in the hippocampus causes premature aging phenotypes and impairs learning and memory [420]. Correspondingly, overexpression of *Ogt* in the hippocampus of older mice partially rescues age related cognitive decline [420]. *O*-GlcNAcylation in the hippocampus decreases as animals age, suggesting that the *O*-GlcNAcylation activity of OGT may mediate the learning and memory phenotypes in *ogt* knockout and aging mice [420]. However, the catalytic involvement of OGT in hippocampal function has not been explicitly demonstrated and therefore it cannot be ruled out that another non-catalytic function of OGT mediates memory and learning in mice.

Finally as described in Section 1.6.2.3, OGT-1 is required for proper GABAergic motor neuron function in *C. elegans* through an interaction with the ubiquitin ligase EEL-1 that does not require the catalytic *O*-GlcNAcylation activity of OGT-1 [408]. As these several examples indicate, OGT is required in a wide range of neuronal processes. However, the mechanistic details

of how OGT functions in the nervous system are largely undescribed. In particular, it is often assumed that the *O*-GlcNAcylation function of OGT is the critical function. However, OGT knockout models remove all OGT functions and therefore they cannot be used to attribute phenotypes to *O*-GlcNAcylation defects. Instead, inhibition of the catalytic activity of OGT using biochemical or genetic CRISPR/Cas9 approaches should be used to dissect apart the roles of OGT in the nervous system.

1.6.3.3 OGT and autophagy

In *C. elegans*, *Drosophila*, and mammals, OGT inhibits autophagy. *ogt-1* mutant *C. elegans* have increased starvation-induced autophagy and clearance of proteotoxic proteins [421]. Knockdown of *ogt* in *Drosophila* increases the number of autophagic structures, while *ogt* overexpression correspondingly decreases autophagesome and autolysosome number basally and following starvation [422]. Furthermore, in *Drosophila*, *ogt* overexpression decreases the expression of autophagy-related proteins, suggesting that OGT may regulate autophagy at the transcriptional level [422]. In contrast, in *C. elegans* and mammalian cells there is substantial evidence that OGT directly *O*-GlcNAcylates autophagy proteins to regulate autophagic flux [423]. Specifically, OGT inhibits the maturation of autophagosome into autolysosomes by *O*-GlcNAcylating the soluble N-ethylmaleimide–sensitive factor attachment protein receptor (SNARE) complex [423]. The SNARE complex mediates the fusion of autophagosomes with lysosomes to create the autolysosome. However, *O*-GlcNAcylation of one of its components, SNAP-29, inhibits SNARE complex formation and thus autophagy [423]. During conditions that promote autophagy, such as starvation, *O*-GlcNAcylation of SNAP-29 is decreased [423]. While four *O*-GlcNAcylated residues on SNAP-29 have been mapped out and mutation of these *O*-GlcNAcylated residues has been shown to decrease SNARE complex assembly and promote

autophagy, it has not been explicitly shown that catalytically-dead OGT is unable to inhibit autophagy [423]. Such an experiment is needed to unequivocally support the hypothesis that the *O*-GlcNAcylation activity of OGT is required to regulate autophagy.

1.6.3.4 OGT and cellular stress responses

Finally, OGT regulates several cellular stress responses via its *O*-GlcNAcylation activity. The fast and dynamic nature of *O*-GlcNAcylation is well suited to facilitate rapid activation and suppression of these pathways in response to changes in cellular conditions. In particular, distinct roles for OGT in the cellular responses to oxidative stress, heat shock, ER stress, and infection have been described. First, OGT-1 functions in the oxidative stress response in *C. elegans* by *O*-GlcNAcylating the oxidative stress response master regulator and nuclear factor-erythroid-related-factor (Nrf) homolog SKN-1 [424]. *O*-GlcNAcylation of SKN-1 at Ser470 and Thr493 increases during oxidative stress and promotes its nuclear localization by sterically inhibiting SKN-1 phosphorylation at Ser483 by GSK-3 [424]. Ser483 phosphorylation by GSK-3 functions under basal conditions to inhibit SKN-1 nuclear accumulation [425].

OGT has also been implicated in the heat shock response in mammalian cells. However, there is conflicting data about the mechanisms by which OGT functions in this response. Most recently, a post-transcriptional role of OGT in the heat shock response has been described in mouse embryonic fibroblasts (MEFs). In this study, knockout of *Ogt* in MEFs decreased chaperone (e.g. Hsp70 and Hsp25) protein induction during heat shock, but had no effect on the mRNA induction of these chaperones [426]. OGT regulates this heat shock chaperone protein induction by *O*-GlcNAcylating eukaryotic translation initiation factor 4 gamma 1 (eIF4GI) at Ser68 [426]. *O*-GlcNAcylation of eIF4GI at this residue dissociates it from poly(A)-binding protein 1 (PABP1), which functions in stress granules to bring the 5’ and 3’ ends of RNA together to facilitate cap-

dependent translation [426]. Dissociation of eIF4GI and PABP1 thereby dissolves the stress granules and releases stress-induced mRNAs trapped in the stress granules to facilitate the selective translation of stress – induced mRNAs, such as those encoding Hsp70 and Hsp25 [426].

However, earlier studies conflict with a post-transcriptional role of OGT in the heat shock stress response. One study found that OGT was required for the transcriptional upregulation of eighteen molecular chaperones during heat stress in MEFs [427]. OGT facilitates the induction of these chaperones by stimulating the phosphorylation of GSK-3, which in turn inhibits it and prevents it from phosphorylating HSF-1 at Ser303 [427]. Phosphorylation of HSF-1 at this site is inhibitory for the downstream induction of chaperones and therefore inhibiting this phosphorylation correspondingly activates chaperone transcriptional induction [427]. Furthermore, another study found that knockout of *Ogt* in Chinese hamster ovary (CHO) cells decreased their survival during heat stress, but had no effect on heat shock chaperone protein induction, including Hsp70 [428]. Instead, knockout of OGT increased protein aggregation during heat stress, which decreased cell survival [428].

While there are conflicting data about how OGT regulates the heat shock response, it is clear that OGT is required for mammalian cells to mount a normal response to and survive heat shock. In particular, there is consensus that the *O*-GlcNAcylation activity of OGT is required in this response, although this has not been thoroughly tested using a catalytic dead version of OGT. However, whether OGT acts through a transcriptional, post-transcriptional, protein homeostasis, or combined mechanism remains unclear. A multi-faceted involvement of OGT in the heat shock response likely explains these seemingly contradictory results.

As with the heat shock response, there is also evidence that OGT post-transcriptionally regulates the ER UPR [429]. During ER stress in mammalian cells OGT *O*-GlcNAcylates eIF2α

at three residues [429]. The *O*-GlcNAcylation of eIF2α inhibits its phosphorylation at Ser51. Since phosphorylation of eIF2α promotes the selective translation of stress-induced pro-apoptotic mRNAs like C/EBP homologous protein (CHOP), *O*-GlcNAcylation inhibits the translation of these pro-apoptotic factors and thus protects cells from apoptosis during ER stress [429].

Finally, OGT has been implicated in the innate immune response during bacterial infection in *C. elegans* [430]. *ogt-1* mutants have decreased survival during exposure to *Staphylococcus aureus*, but interestingly not during exposure to *Pseudomonas aeruginosa* [430]. Therefore OGT-1 is required for pathogen specific innate immunity. OGT-1 does not function in this innate immune response through a p38 MAPK pathway, even though p38 MAPK signaling is integral to the innate immune response to *S. aureus* [430]. Rather, OGT facilitates the survival of *C. elegans* during exposure to *S. aureus* through a pathway with the innate immunity regulator and *C. elegans* *β*-catenin homolog BAR-1 [430].

In conclusion, OGT is involved in several different cellular stress responses including the oxidative stress response, the heat shock response, the ER stress response, and pathogen infection. The involvement of OGT in all these stress responses is presumed to be via its *O*-GlcNAcylation activity. This has been tested in all cases except for the pathogen response by mutating OGT substrate residues to prevent their *O*-GlcNAcylation. Work from my thesis project adds to the list of stress responses in which OGT is involved. I found that OGT is critical to the HTSR. OGT is required for both organismal adaptation to HTS and the upregulation of the protective compatible osmolyte accumulation protein GPDH-1. As in the case of the heat shock and ER stress response, I present evidence that OGT functions through a post-transcriptional mechanism to regulate this protective protein upregulation. However, unlike the stress responses OGT has previously been implicated in, I demonstrate that the *O*-GlcNAcylation activity of OGT is dispensable for the

HTSR. This suggests that OGT functions through a unique mechanism, different from that of the other stress responses, to regulate the HTSR.

1.6.4 The essential function of OGT

Ogt is an essential gene in almost all metazoans. *C. elegans* is the only organism that expresses *ogt*, but that does not require OGT for cellular viability [413]. Expression of *Ogt* is required for the completion of embryogenesis in *Drosophila* [431] and for cell division and cell cycle progression in mammalian cells [432]. Knockout of *Ogt* in replicating mammalian cells causes cell death [433]. Furthermore, even though postmitotic mammalian cells are able to survive without *Ogt*, their function is significantly impaired. Mice with neuronal specific *Ogt* knockout survive ten days, but have compromised locomotion and neuronal defects [432]. Likewise, knockout of *Ogt* in mice cardiomyocytes from the start of development leads to increased fibrosis, apoptosis, and hypertrophy, altered gene expression, and increased cell stress activation in the heart [434]. The heart function in these animals is so poor that only 12% survive to 4 weeks old. Additionally, conditional knockout of *Ogt* in adult cardiomyocytes has no short term effects, but within a month results in cardiomyopathy [434]. Therefore, even in non-replicating cells, OGT is required for proper cell function.

It is largely unknown whether *O*-GlcNAcylation, proteolysis of HCF-1, or a non-catalytic function of OGT is essential in mammalian cells. If *O*-GlcNAc cycling is required for cell viability, then disruption of the enzyme that removes *O*-GlcNAc, OGA, should also impede cell division. However, unlike *Ogt* knockout mice, *Oga* knockout mice have a limited capacity to develop. They have stunted growth and die within a day of birth, but their cells nevertheless retain the ability to divide [435]. Furthermore, treatment of cells with an uncleavable UDP-GlcNAc

analog, Ac_4-*5S*GlcNAc, significantly decreases *O*-GlcNAcylation, but does not affect the proliferation of CHO cells, suggesting that these cells do not require *O*-GlcNAcylation for cell division [436]. In contrast to these data, there is also some evidence that *O*-GlcNAcylation is required for the essential functions of OGT. Decreasing intracellular UDP-GlcNAc levels by knocking out glucosamine-6-phosphate (*EMeg32*), which is required for UDP-GlcNAc synthesis, reduces proliferation in MEF cells [437]. Interestingly, *EMeg32* knockout cells still retain 2 – 33% of the normal intracellular UDP-GlcNAc concentration [437]. This observation may explain why proliferation is reduced and not completely inhibited in these cells and suggests there is a redundant pathway for UDP-GlcNAc synthesis . Finally, inhibition of OGT *O*-GlcNAcylation activity with the small molecule OSMI-1 decreases CHO cell viability to 50% within 24 hours, supporting the requirement of *O*-GlcNAcylation activity for cellular viability [438]. However, a small molecule structurally related to OSMI-1 that did not inhibit OGT *O*-GlcNAcylation activity affected cell viability to the same extent as OSMI-1, suggesting that OSMI-1 functions through an OGT-1 independent pathway to regulate cell viability [438]. The mechanism of OSMI-1 inhibition has not been determined and it thus cannot be ruled out that OSMI-1 inhibits other OGT functions, such as its proteolytic and non-catalytic functions. Therefore, whether or not *O*-GlcNAcylation is required for cellular viability remains an open question.

Proteolysis of HCF-1 by OGT is likely not the essential function of OGT in mammalian cells. Cleavage of HCF-1 by OGT is not required for cell cycle progression in mammalian cells [400]. Furthermore, HCF-1 depleted cells have impaired cytokinesis, which results in a binucleation phenotype that is not seen in *Ogt* knockout cells [400]. Therefore, cells lacking HCF-1 do not display the same phenotypes as cells lacking OGT, suggesting that inhibited HCF-1 cleavage is not what leads *Ogt* knockout cells to die. Finally, as with *O*-GlcNAcylation activity,

treatment of cells with the UDP-GlcNAc analog Ac_4-5*S*GlcNAc inhibits the proteolytic activity of OGT, but does not affect the proliferation of CHO cells [404, 436]. These data in combination suggest that the proteolytic activity of OGT is not required for cellular viability.

Since neither the *O*-GlcNAcylation nor the proteolytic activity of OGT appear to be required for cell proliferation, this suggests that OGT may function via a non-catalytic mechanism to facilitate cell survival. The details of this non-catalytic mechanism remain uncharacterized, but may involve protein interactions via the TPR domain of OGT. It is also not understood why, in contrast to other metazoans, *ogt-1* knockout *C. elegans* appear grossly WT. My thesis project begins to address these question because we discovered that, while *ogt-1* is not essential in *C. elegans* under normal isotonic laboratory conditions, it is essential for *C. elegans* survival in hypertonic environments. Since the HTS and cell division both affect cell volume, this suggests that OGT may more broadly be required for cell volume regulation in all metazoans.

1.6.5 Conclusions

OGT was first discovered because of its catalytic *O*-GlcNAcylation activity, but it clearly has other non-enzymatic functions. The rapid nature of this PTM, in combination with its sensitivity to the nutrient status of the cells, implicates it in numerous cellular pathways including stress responses and insulin signaling. While the nature of OGT's involvement in these cellular pathways has benefitted greatly from the availability of *Ogt* knockout cells/organisms and tagged OGT proteins, many questions still remain about how OGT is regulated and how OGT achieves substrate specificity. Importantly, *O*-GlcNAcylation is not the only function of OGT. OGT also proteolytically cleaves one target protein, HCF-1, and has largely uncharacterized non-catalytic roles in cells. Furthermore, *Ogt* is essential in all metazoans except for *C. elegans.* The required

function(s) of OGT in these organisms are not well understood, but several pieces of evidence suggest that the catalytic activities of OGT are dispensable for cell viability.

In my thesis project I demonstrate that OGT is essential in the HTSR. My findings not only add to the growing list of cellular pathways OGT plays a role in, but they also describe a novel non-catalytic function of OGT that requires the TPR domain. Furthermore, the requirement for OGT during HTS in *C. elegans* and during cell division in mammalian cells supports the hypothesis that OGT is generally required for cell volume regulation because both cell division and HTS impact cell volume. However, significant work is still required to understand the precise role OGT may play in cell volume regulation.

1.7 The 3'mRNA cleavage and polyadenylation complex

In my genetic screen for regulators of the *C. elegans* HTSR, I identified mutations in two interacting components of the 3' mRNA cleavage and polyadenylation complex (*cpf-2* and *symk-1*) that blocked hypertonic induction of *gpdh-1* and prevented adaptation to hypertonic environments. This was a surprising discovery because it implicates a protein complex that is required for most types of gene expression in the specific upregulation of ORGs. The unbiased forward genetic screens I performed in *C. elegans* was essential for this discovery because the null phenotype for the genes in this complex is lethal. Therefore, the role of these genes in the HTSR was only revealed due to the discovery of unique LOF missense alleles that did not completely ablate their essential functions.

Adenine nucleotide repeat sequences (poly(A) sequences) on the 3' end of mRNA transcripts were first discovered in the mid twentieth century through analysis of thymus extract

[439]. The nuclear and cytoplasmic localization of these poly(A) mRNA 3' tails led to the hypothesis that eukaryotic precursor mRNA molecules are co-transcriptionally cleaved and polyadenylated to create the mature mRNA species [440, 441]. This 3' mRNA cleavage and polyadenylation of transcripts is required to promote the transcriptional termination, nuclear export, protection from degradation by 3' exonucleases, and translation of mRNA in the cytoplasm [442-445].

More than 80 proteins in mammals make up the 3' mRNA cleavage and polyadenylation complex and facilitate its two enzymatic activities, cleavage and polyadenylation [446, 447]. The mammalian 3' mRNA cleavage and polyadenylation complex contains eight major subcomplexes each made up of multiple proteins: the cleavage and polyadenylation specificity factor (CPSF), the cleavage stimulation factor (CstF), cleavage factor I (CF I_m), cleavage factor II (CF II_m), poly(A) polymerase (PAP), poly(A) binding protein (PABP), symplekin (SYMPK), and RNAP II [447]. The CPSF complex recognizes the polyadenylation signal sequence (PAS) at the 3' end of mRNA, recruits the other components of the larger 3' mRNA cleavage and polyadenylation complex to the PAS, and catalyzes 3' cleavage of the mRNA [448]. Once recruited by the CPSF complex, the CstF complex binds the mRNA via its N-terminal RNA-recognition motif (RRM) [449] and the two CF complexes (CF I_m and CF II_m) stabilize these RNA interactions while SYMPK stabilizes the entire structure [442, 450, 451]. PAP is a template independent polymerase that poly-adenylates the 3' end of mRNAs [452]. The entire 3' mRNA cleavage and polyadenylation complex is assembled on the CTD of RNAP II [453, 454]. The association of any one of these subcomplexes with RNA is weak, but together they form a stable and high affinity interaction [448].

1.7.1 Mechanism of 3' mRNA cleavage and polyadenylation

The first step in 3' mRNA cleavage and polyadenylation is recognition of the 3' untranslated region (3' UTR). This is most frequently done via the presence of a PAS in the 3' UTR. The PAS is highly conserved and 10-30 nucleotides upstream of the mRNA cleavage site [455]. The canonical PAS sequence in mammalian cells is AAUAAA, although some variation in this sequence is tolerated [442, 447, 456]. The 3' UTR is also defined by the downstream element sequence (DSE), which is located about 30 nucleotides downstream of the cleavage site [457]. The DSE is less well conserved than the PAS, but it is generally a GU or U rich sequence [457]. Finally, there is the actual cleavage site which is located between the PAS and DSE in the 3' UTR and this is where the poly(A) tail is added onto the mRNA. While the cleavage site is not very well conserved, the most optimal cleavage occurs between adjacent C and A nucleotides [455].

The assembly of the large 3' mRNA cleavage and polyadenylation complex begins when the CPSF complex co-transcriptionally binds the PAS in the 3' UTR [458] . The CPSF subunits CPSF160 and FIP1 alone are able to bind the PAS sequence on the mRNA, but they require the other components of the CPSF complex to bind with full affinity and specificity [459, 460]. Once bound to the PAS, the CPSF complex recruits the rest of the 3' mRNA processing complex in a SYMPK dependent manner [461]. SYMPK is an adaptor protein that interacts with several components of the 3' mRNA cleavage and polyadenylation complex to facilitate its assembly. SYMPK is required for both the cleavage and polyadenylation of the mRNA [461]. The interaction between the CPSF complex and the transcript is further enhanced by the recruitment and subsequent interaction of the CstF complex with the DSE [462]. Among the proteins recruited to the PAS are the CF I_m and CF II_m complexes, which stabilize the CPSF-CstF interaction, bind the

mRNA, and are required for mRNA cleavage [450]. Additionally, the CTD of RNAP II interacts with CPSF and CstF to stabilize formation of the entire complex [454].

Once the 3' mRNA cleavage and polyadenylation complex has been fully assembled, the endonuclease CPSF-73 cleaves the mRNA at the cleavage site [463]. CPSF-73 contains metallo-beta-lactamase and beta-CASP domains that are known endonucleases and CPSF-73 alone is therefore sufficient to cleave mRNA *in vitro* [463]. After the mRNA is successfully cleaved, the CPSF complex remains bound to the PAS and recruits PAP [460]. CPSF anchors PAP to the mRNA so that it can use ATP to add 150-250 adenosines to the 3' end of the transcript in a template-independent manner [448, 464]. Without CPSF, PAP has no specificity for mRNA substrates [458, 464]. PABP functions with PAP to regulate the length of the poly(A) tail and increase the efficiency with which PAP lengthens the poly(A) tail [465].

Before the newly polyadenylated transcript can be exported from the nucleus, the 3' mRNA cleavage and polyadenylation complex must be disassembled. Disassembly is poorly understood in mammalian cells. However, data from yeast suggest that CF II_m (PcfII in yeast) binds the RNAP II CTD to initiate disassembly of the complex and transcriptional termination [466]. Additionally, there is evidence that the entire 3' mRNA cleavage and polyadenylation complex does not dissociate from the mRNA [467]. At least a few cleavage and polyadenylation factors, such as CF I_m 68, remain associated with the mRNA and act as adaptors for the mRNA export receptor NXF1/TAP to promote export of the processed mRNA [467].

1.7.2 Alternative polyadenylation

Virtually all eukaryotic mRNAs are processed by the 3' mRNA cleavage and polyadenylation complex, with histone encoding mRNAs representing an important exception

[468]. Interestingly, many mRNA transcripts contain more than one PAS [469, 470]. This allows for modulation of the polyadenylation site, a phenomenon called alternative polyadenylation (APA). APA is carried out by the 3' mRNA cleavage and polyadenylation complex, which has led the field to refer to it as the APA complex [471]. At least 79% of transcripts in mammals [469] and 40% of transcripts in *C. elegans* undergo APA [470]. APA functions to regulate gene expression and/or increase the diversity of transcripts made from a single gene.

APA can occur in two distinct ways. First, genes can have multiple PAS sites in the 3' UTR (3' UTR APA) [472, 473]. This creates mRNA isoforms with the same coding sequence but short or long 3' UTRs. Long 3' UTRs contain sequences that are subject to post-transcriptional regulation by miRNA, RNA binding proteins, and long non-coding RNAs that may be lacking in short mRNAs [474]. Additionally, long 3' UTRs can alter several aspects of mRNA biology, including stability, translation, localization, and nuclear export [471, 475]. Since short 3' UTRs can escape these additional layers of regulation, they are often more stable and are therefore present under conditions necessitating rapid translation, such as in stress responses and proliferation [474, 476].

A second type of APA is termed Upstream Region APA (UR-APA). This type of APA differentially utilizes PAS sequences upstream of coding exons [472]. This results in mRNA isoforms that encode different protein sequences, as well as different 3' UTRs. UR-APA proteins can carry out different cellular functions, including activation or inhibition of cellular signaling or even auto-regulation of APA itself [477, 478]. Therefore, both 3' UTR APA and UR-APA can have major consequences for cellular and organismal biology.

APA is regulated primarily in two ways. First, expression of the APA complex can be modulated to affect PAS usage. In general, decreased expression of the APA complex promotes

distal PAS usage and increased expression of the APA complex promotes proximal PAS usage [479, 480]. This trend can be explained by the observation that the APA complex generally has a higher affinity for the distal PAS than the proximal PAS [473, 481]. Therefore, when the cleavage and polyadenylation machinery is not the limiting factor, the first (most proximal) PAS encountered by the machinery is used. However, in actuality the relationship between expression of the APA complex and PAS usage is much more complicated than these general trends imply. For example, knockdown of specific subunits of the CF I_m subcomplex decreases expression of the APA complex [482, 483]. This should lead to increased utilization of distal PAS sites and longer mRNAs. However, the opposite is observed, i.e. CF I_m knockdown leads to increased usage of proximal PAS sites and thus to global shortening of 3' UTRs [482, 483]. This is hypothesized to be due to the recognition of specific sequences enriched near the distal PAS by the CF I_m subunits. Therefore, when these subunits are expressed, global use of distal PAS sequences is promoted [482, 483].

APA is also regulated through auxiliary factors, in particular RNA binding proteins (RBPs). RBPs can both inhibit APA complex formation at canonical PAS sites [484] and promote 3' mRNA processing complex formation at alternative PAS sites [485]. RBPs that regulate splicing also regulate APA because there is often interplay between splicing and APA, particularly in the case of UR-APA. Intronic PAS usage increases in genes with weak intronic 5' splice sites and when splicing is inhibited by knockdown of RBPs that promote splicing [486, 487]. This increase in UR-APA when splicing is inhibited may represent redundancy to ensure proper protein expression [486, 487]. In addition to splicing RBPs, other RBPs such as SR proteins [488] and embryonic lethal abnormal vision (ELAV) proteins [489], also regulate APA in a context

dependent manner. The exact mechanisms by which these RBPs regulate APA are largely unknown.

The APA complex is able to modulate gene expression through APA. For example, the CstF subunit CstF-64 regulates the expression of membrane-bound and secreted immunoglobulin M heavy chain (IgM H-chain) through APA [490]. Low CstF-64 levels promote the expression of membrane-bound IgM H-chain from a distal higher affinity PAS [490]. In contrast, during B cell activation, the expression of *CstF-64* is increased and this promotes the expression of secreted IgM H-chain from a proximal lower affinity PAS because it is the first encountered PAS [490]. In this way, the APA complex is able to directly influence IgM H-chain isoform expression. Surprisingly, despite being required for general gene expression, knockdown of *CstF-64* by 10% specifically affects *IgM H-chain* expression in B cells, without affecting the expression of other genes [490]. One hypothesis that may explain this specific effect is that CstF-64 has a lower affinity for the PAS sites in the *IgM H-chain* transcript than it does for other transcripts and therefore *IgM H-chain* PAS sites are more drastically affected by CstF-64 knockdown [490].

APA also affects expression of the cytoskeletal protein ankyrin in *C. elegans* [491]. There are three isoforms of ankyrin expressed via different PAS site usage. Expression of the longest ankyrin isoform, giant ankyrin, in neurons facilitates stabilization of the mature *C. elegans* nervous system by preventing neuronal growth cone growth [491]. Casein kinase 1δ (CK1δ) promotes the formation of giant ankyrin by inhibiting usage of the most proximal and middle PAS in the ankyrin transcript [491]. Therefore, *ck1δ* mutants exhibit paralysis and disordered nervous system phenotypes [491]. However, missense mutations in several APA complex components or in ankyrin's proximal PAS sites themselves suppress the *ck1δ* mutant phenotypes because they allow

read through of the most proximal PAS sites, which leads to expression of the giant ankyrin isoform [491].

APA is also utilized by cells to change gene expression during cellular stress responses [492]. For example, arsenic induced oxidative stress causes global shortening of 3' UTRs via APA [476]. Transcripts with shorter 3' UTRs are generally more stable than transcripts with longer 3'UTRs [474]. Therefore by biasing towards short 3' UTRs via APA, cells preserve transcripts crucial for the oxidative stress recovery process [476]. Following a similar theme, APA allows for the increased expression of *Hsp70.3* during ischemia and heat shock [493]. These cellular stresses promote the usage of a proximal PAS to create *Hsp70.3* transcripts with short 3' UTRs [493]. These shortened 3' UTRs make the *Hsp70.3* transcripts more stable because they do not contain the miRNA targeting sites and other cis elements found in the longer 3' UTR [493]. Interestingly, the transcription factor that regulates *Hsp70.3* transcription, HSF1, interacts with the APA complex components SYMPK, CstF-64, and CPSF during heat shock [493]. This supports the hypothesis that the 3' mRNA cleavage and polyadenylation complex is recruited to the *Hsp70.3* transcript by HSF1 [493].

1.7.3 Conclusions

The APA complex is required for the addition of 3' poly(A) tails onto mRNA transcripts prior to their export form the nucleus. Despite the general requirement for this complex in the modification of all transcripts exiting the nucleus, knockdown of components of the 3' APA complex affects the expression of specific genes via APA. Therefore, modulation of the 3' APA complex is a way for cells to post-transcriptionally regulate gene expression. However, the mechanisms through which this occurs are still largely undefined.

Intriguingly, I identified unique LOF missense alleles of two conserved components of the APA complex, SYMPK (SYMK-1 in *C. elegans*) and CstF-64 (CPF-2 in *C. elegans*), in a forward genetic screen for genes required for ORG induction in *C. elegans*. These components of the APA complex are also required for *C. elegans* to adapt to HTS. We do not know how these missense alleles affect the functions of SYMK-1 and CPF-2 or their interactions with other members of the 3' mRNA processing complex. Additionally, we do not know if they function in the same pathway as OGT in the HTSR. However, the identification of these proteins as critical to the HTSR suggests that, as with other cellular stress responses, APA may be involved in the regulation of ORGs during HTS.

1.8 Conclusions

The HTSR is a conserved and essential way in which cells counter the decreased cell volume and increased intracellular ionic strength that occur when extracellular solute concentration is increased. A conserved physiological component of the HTSR is the intracellular accumulation of compatible osmolytes. These small organic solutes are accumulated to molar concentrations within cells without affecting general cellular functions and are required for long term adaptation to HTS. Importantly, these compatible osmolytes are universally accumulated via the transcriptional upregulation of either osmolyte transport proteins or biosynthetic enzymes. Osmolyte accumulation genes are among hundreds of genes differentially regulated by HTS. Therefore upon sensing increases in extracellular osmolarity, cells transmit signals to the nucleus to modulate gene expression.

Many of the signaling proteins and transcription factors that make up osmosensitive signaling pathways have been characterized in single celled organisms and plants. However these pathways are less well understood in multicellular organisms. In mammals, a master transcriptional regulator of the HTSR, NFAT5, has been identified. However, not all genes are upregulated during HTS in a NFAT5 dependent manner in mammals and not all multicellular organisms express rel family transcription factors like NFAT5. Therefore, other mechanisms to modulate gene expression during HTS must exist. Furthermore, even in the case of NFAT5 dependent osmosensitive gene expression, the proteins and mechanisms cells use to sense increases in extracellular osmolarity and how these signals are integrated to activate NFAT5 are poorly understood.

In my thesis project I identified three novel proteins regulating both ORG induction and physiological adaptation during HTS in *C. elegans*. These proteins include the *O*-GlcNAc transferase OGT-1 and two interacting components of the APA complex: CPF-2 and SYMK-1. OGT is a highly conserved enzyme that *O*-GlcNAcylates serine and threonine residues of hundreds of intracellular proteins, proteolytically cleaves the cell cycle regulator HCF-1, and functions non-catalytically as a putative scaffolding protein. Through these functions OGT regulates diverse cellular processes including metabolism, gene expression, and cellular stress responses. Importantly, OGT function is required in mammalian cells for cell division. While research in the field has largely focused on the catalytic activities of OGT, its non-catalytic functions are less well understood. In particular, it is unknown how widespread the non-catalytic activity of OGT is, which protein domains are required for its non-catalytic function, and if the non-catalytic function of OGT is essential for mammalian cell division. My thesis project begins to address these questions. I found that OGT is required for the post-transcriptional induction of the

osmoprotective gene GPDH-1 and the long term viability of *C. elegans* in hypertonic conditions. Surprisingly, this function of OGT in the HTSR is independent of its *O*-GlcNAcylation and proteolytic catalytic activities. However, it requires the protein interacting TPR domain of OGT. These discoveries were only possible in *C. elegans* because, unlike other organisms, *ogt* null mutants are uniquely viable under control conditions. Furthermore, the conditional requirement for *ogt* expression during HTS in *C. elegans* provides a valuable platform from which to investigate the conserved essential functions of OGT.

The other two proteins I identified as being required for the HTSR, the cleavage stimulation factor subunit 2 homolog CPF-2 and the symplekin homolog SYMK-1, are part of the conserved APA complex. This complex is required for the cleavage and polyadenylation of most mRNAs prior to their export from the nucleus. Because many transcripts have multiple PAS sites in their 3' UTR and/or coding sequence, the APA complex can regulate gene expression by altering 3' UTR length and protein isoform expression. Additionally, despite the general requirement for the APA complex in mRNA processing, mutations in components of the APA complex have been shown to preferentially change the expression of particular genes. Changes in PAS site usage by the APA complex can be induced by cellular stress to modulate gene expression. Therefore, the APA complex is a highly dynamic multi-faceted complex with functions that extend beyond general mRNA processing. However, the mechanisms through which this complex regulates inducible gene expression are not well understood. In my thesis project, I describe two novel missense alleles of *cpf-2* and *symk-1* that impair ORG induction and physiological adaptation to HTS. These two missense alleles will not only allow us to characterize a potential role of APA in the HTSR, but they will also provide clues to how the APA complex modulates the expression of specific genes despite being required for general mRNA processing.

2.0 Results

We employed unbiased genetic methods in *C. elegans* to characterize the metazoan HTSR. In response to HTS, *C. elegans* induces the robust upregulation of the osmolyte accumulation gene *gpdh*-1. To characterize the cellular pathways required for *gpdh-1* upregulation, we designed a forward genetic screen to identify mutants with impaired hypertonic induction of *gpdh-1*. I focused on three mutants from this screen because they not only had impaired hypertonic induction of *gpdh-1p::GFP*, but they were also unable to acutely adapt to HTS. Upon further characterization of these three mutants I identified novel and unexpected HTSR regulatory pathways.

2.1 Identification of mutant *C. elegans* with impaired induction of the hypertonic stress response through an unbiased, fluorescence based, forward genetic screen

In *C. elegans*, HTS rapidly and specifically upregulates expression of the osmolyte biosynthesis gene *gpdh-1*, which we visualized with a *gpdh-1p::GFP* transcriptional reporter. To optimize this reporter for genetic screening, we added a *col-12p::dsRed* reporter, whose expression is not affected by HTS and serves as an internal control for non-specific effects on gene expression. This dual reporter strain (*drIs4*) expresses only dsRed under isotonic conditions and both dsRed and GFP under hypertonic conditions, with very few animals exhibiting an intermediate phenotype (Fig 2.1.1A, 2.1.1B, and 2.1.1C). A *gpdh-1p::GPDH-1-GFP* translational reporter (*kbIs6*) is also

upregulated by HTS, but exhibits more variability than the *drIs4* transcriptional reporter (Fig 2.1.1D, 2.1.1E, and 2.1.1F).

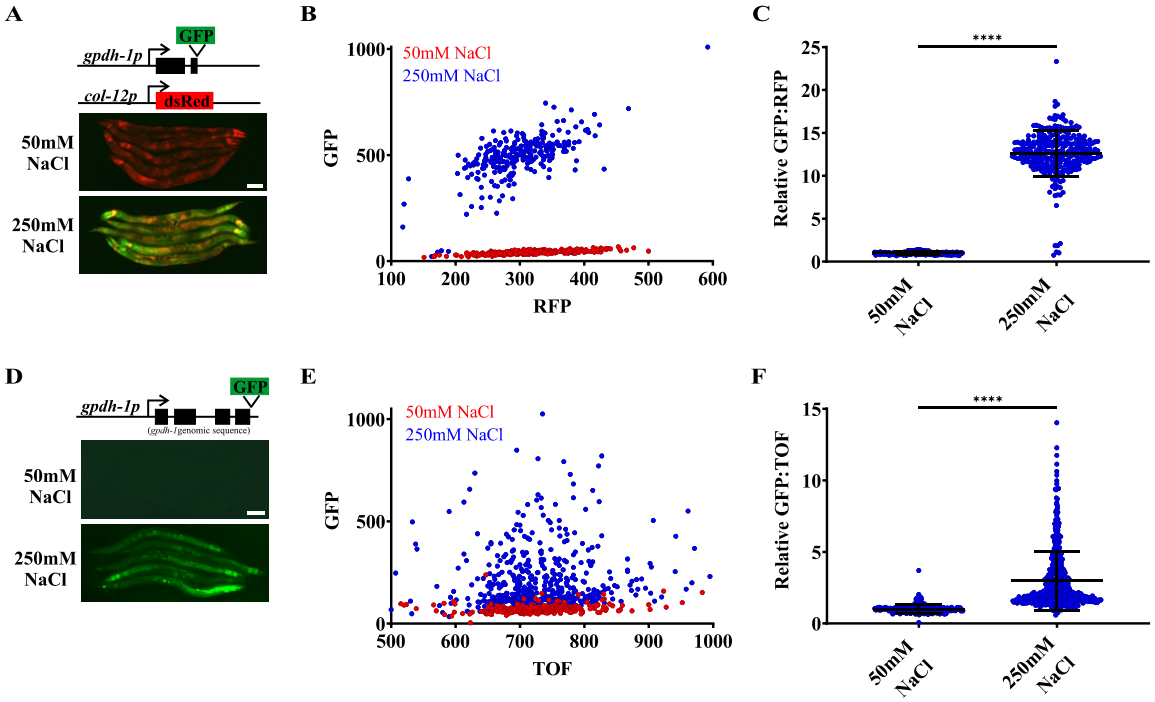

Figure 2.1.1 *gpdh-1* transcriptional and translational reporters are upregulated by HTS

(A) Wide-field fluorescence microscopy of day 2 adult animals expressing *drIs4* (*col-12p::dsRed;gpdh-1p::GFP*) exposed to 50 or 250 mM NaCl for 18 hours. Images depict merged GFP and RFP channels. Scale bar = 100 microns. (B) COPAS Biosort quantification of GFP and RFP signal in day 2 adult animals expressing *drIs4* exposed to 50 or 250 mM NaCl NGM plates for 18 hours. Each point represents the quantified signal from a single animal. N ≥ 276 for each group. (C) Population mean of the normalized GFP/RFP ratio from data in B. Data are expressed as mean ± S.D. with individual points shown. **** - $p < 0.0001$ (Mann-Whitney test). (D) Wide-field fluorescence microscopy of day 2 adult animals expressing *kbIs6 (gpdh-1p::GPDH-1-GFP)* translational fusion protein exposed to 50 or 250 mM NaCl NGM plates for 18 hours. Scale bar = 100 microns. (E) COPAS Biosort quantification of GFP and time of flight (TOF) signal in day 2 adult animals expressing the *kbIs6* translational fusion protein exposed to 50 or 250 mM NaCl NGM plates for 18 hours. N ≥ 276 for each group. (F) Population mean of the normalized GFP/TOF ratio from data in E. Data are expressed as mean ± S.D. **** - $p < 0.0001$ (Mann-Whitney test).

Taking advantage of the binary nature of GFP activation by HTS in the *drIs4* strain, we designed an unbiased F_2 forward genetic screen for mutants that fail to activate GFP expression during HTS, but still express RFP (No induction of osmolyte biosynthesis gene expression or Nio mutants). Briefly, I mutagenized hermaphrodite animals with N-ethyl-N-nitrosourea (ENU) and screened the F_2 generation as day one adults exposed to 250 mM NaCl agar plates for ~18 hours (Fig 2.1.2A). From this screen of ~120,000 haploid genomes, I identified ten mutants that failed to activate *gpdh-1p::GFP* during HTS, but that still expressed *col-12p::dsRed* (Fig 2.1.2B and 2.1.2C). I determined that these ten mutants contained recessive single-gene mutations by crossing each mutant back to WT males and testing the *gpdh-1p::GFP* phenotypes of their cross-progeny and the self progeny of those cross progeny during HTS. If an individual Nio mutant is a recessive allele of a single gene, then the number of Nio (impaired *gpdh-1p::GFP* induction on 250 mM NaCl NGM plates) males from a cross of *nio* x WT (i.e *nio*/+) should be 0% and the number of Nio animals among self progeny of *nio*/+ hermaphrodites should be about 25% (Table 2.1.1). After determining that these ten mutants had recessive single gene phenotype-causing mutations, I used genetic complementation testing to demonstrate that they represented seven genes, *nio-1* through *nio-7* (Table 2.1.2). To do this genetic complementation testing, I crossed each Nio mutant to each other Nio mutant two times, once as a hermaphrodite and once as a heterozygous male. Mutant crosses complemented (i.e. phenotype causing mutations are in different genes) when 0% of progeny were Nio and failed to complement (i.e. phenotype causing mutations are in the same gene) when ~50% of progeny were Nio (Table 2.1.2).

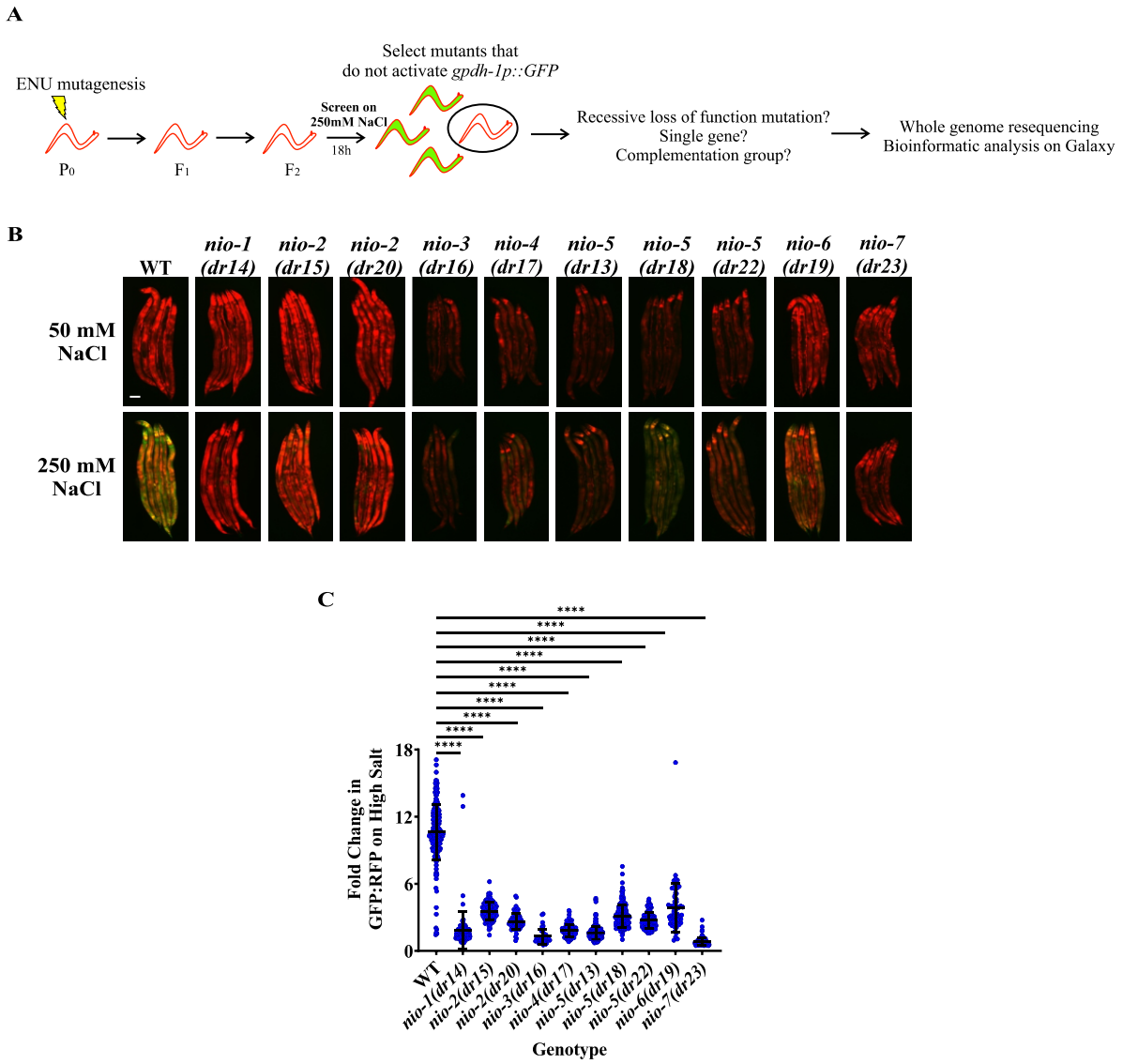

Figure 2.1.2 Seven *nio* genes are required for the upregulation of the *gpdh-1* transcriptional reporter by HTS

(A) ENU-based forward genetic screening strategy and mutant identification workflow. (B) Wide-field fluorescence microscopy of day 2 adult *drIs4* and *nio;drIs4* mutant animals exposed to 50 or 250 mM NaCl NGM plates for 18 hours. Images depict merged GFP and RFP channels. Scale bar = 100 microns. (C) COPAS Biosort quantification of GFP and RFP signal in day 2 adult animals expressing *drIs4* or *nio;drIs4* exposed to 250 mM NaCl NGM plates for 18 hours. Data are represented as the relative fold induction of normalized GFP/RFP ratio on 250 mM NaCl plates versus 50 mM NaCl NGM plates. Each point represents the quantified signal from a single animal. Data are expressed as mean ± S.D. **** - $p < 0.0001$ (Kruskal-Wallis test with post hoc Dunn's test). $N \geq 38$ for each group.

Table 2.1.1 The genetics of the *nio* genes are consistent with recessive single gene alleles

* = data not collected. The ENU round and plate the mutant was isolated from are indicated in brackets.

Strain	Outcross	Number of Nio males from a cross of *nio* x WT	Number of Nio among self progeny of *nio*/+
nio-5(dr13) [ENU2 9a#1]	#1	0/30 (0%)	6/29 (21%)
	#2	0/20 (0%)	9/36 (25%)
	#3	0/25 (0%)	12/40 (30%)
nio-1(dr14) [ENU1 5i#4]	#1	1/20 (5%)	5/27 (19%)
	#2	0/15 (0%)	6/37 (16%)
	#3	0/20 (0%)	9/50 (18%)
nio-2(dr15) [ENU2 4g#2]	#1	0/30 (0%)	8/27 (30%)
	#2	0/20 (0%)	7/34 (21%)
	#3	0/15 (0%)	13/65 (20%)
nio-3(dr16) [ENU1 2c#4]	#1	0/20 (0%)	6/30 (20%)
	#2	0/7 (0%)	9/36 (25%)
	#3	0/6 (0%)	9/45 (20%)
nio-4(dr17) [ENU2 6a#5]	#1	0/9 (0%)	9/56 (16%)
	#2	0/6 (0%)	6/30 (20%)
	#3	0/20 (0%)	8/35 (23%)
nio-5(dr18) [ENU2 7a#2]	#1	0/10 (0%)	16/41 (39%)
	#2	0/15 (0%)	6/23 (26%)
	#3	0/12 (0%)	13/65 (20%)
nio-6(dr19) [ENU3 3d#2]	#1	0/18 (0%)	4/18 (22%)
	#2	*	4/16 (25%)
	#3	0/20 (0%)	15/70 (21%)
nio-2(dr20) [ENU3 2c#2]	#1	0/20 (0%)	3/17 (18%)
	#2	*	7/34 (21%)
	#3	0/15 (0%)	17/70 (24%)
nio-5(dr22) [ENU4 5a#1]	#1	0/12 (0%)	5/21 (24%)
	#2	0/20 (0%)	5/15 (33%)
	#3	0/34 (0%)	16/40 (40%)
nio-7(dr23) [ENU4 7c#2]	#1	0/9 (0%)	6/50 (12%)
	#2	0/20 (0%)	8/50 (16%
	#3	0/9 (0)%)	8/45 (18%)

Table 2.1.2 Genetic complemention of the *nio* alleles

Fractions represent the number of animals with a Nio phenotype (impaired *gpdh-1p::GFP* induction on 250 mM NaCl NGM plates) over the total number of animals observed. Males were heterozygous for the *nio* mutation. Mutant crosses that failed to complement are highlighed in yellow. * = mate was unsuccessful. ** = numbers were not recorded

Mutant A (hermaphrodite)

Mutant B (male)	*dr14*	*dr15*	*dr16*	*dr13*	*dr17*
dr14	17/36 (47%)	0/35 (0%)	0/36 (0%)	0/24 (0%)	*
dr15	0/36 (0%)	13/29 (45%)	0/37 (0%)	0/33 (0%)	0/10 (0%)
dr16	0/30 (0%)	0/33 (0%)	16/34 (47%)	0/35 (0%)	0/7 (0%)
dr13	0/24 (0%)	0/23 (0%)	0/28 (0%)	14/30 (47%)	0/7 (0%)
dr17	0/34 (0%)	0/38 (0%)	0/31 (0%)	0/34 (0%)	8/18 (44%)
dr18	0/35 (0%)	0/31 (0%)	0/21 (0%)	15/29 (52%)	2/8 (25%)
dr19	1/36 (3%)	0/32 (0%)	0/18 (0%)	1/30 (3%)	0/8 (0%)
dr20	0/22 (0%)	13/31 (42%)	0/18 (0%)	0/22 (0%)	0/20 (0%)
*dr22***	(~0%)	(~0%)	(~0%)	(~50%)	(~0%)
*dr23***	(~0%)	(~0%)	(~0%)	(~0%)	(~0%)

Mutant A (hermaphrodite)

Mutant B (male)	*dr18*	*dr19*	*dr20*	*dr22***	*dr23***
dr14	0/23 (0%)	0/37 (0%)	0/26 (0%)	(~0%)	(~0%)
dr15	0/36 (0%)	0/32 (0%)	7/38 (18%)	(~0%)	(~0%)
dr16	0/36 (0%)	0/32 (0%)	0/36 (0%)	(~0%)	(~0%)
dr13	9/32 (28%)	0/35 (0%)	0/32 (0%)	(~50%)	(~0%)
dr17	1/27 (4%)	0/35 (0%)	0/36 (0%)	(~0%)	(~0%)
dr18	13/27 (48%)	1/33 (3%)	0/23 (0%)	(~50%)	(~0%)
dr19	0/38 (0%)	6/21 (29%)	0/35 (0%)	(~0%)	(~0%)
dr20	0/30 (0%)	0/26 (0%)	13/30 (43%)	(~0%)	(~0%)
*dr22***	(~50%)	(~0%)	(~0%)	(~50%)	(~0%)
*dr23***	(~0%)	(~0%)	(~0%)	(~0%)	(~50%)

Since the *nio* genes were required for induction of the *gpdh-1p::GFP* transcriptional reporter by HTS, we hypothesized that they were also required for induction of endogenous *gpdh-1* mRNA by HTS. To test this, I used qPCR to measure the amount of *gpdh-1* mRNA in each Nio mutant. Surprisingly, I found that *gpdh-1* mRNA was still upregulated by HTS in the majority of the Nio mutants (Fig 2.1.3A). *nio-3(dr16)* and *nio-7(dr23)* were the only two Nio mutants that appeared to have reduced *gpdh-1* mRNA during HTS, however neither reduction was statistically significant compared to WT animals (mean ± S.D. of fold change in *gpdh-1* mRNA on high salt –

WT 17.8 ± 4.3, *nio-3(dr16)* 7.9 ± 0.2, *nio-7(dr23)* 2.5 ± 0.3). Consistent with endogenous *gpdh-1* mRNA levels, I also observed that GFP mRNA derived from the overexpressed *gpdh-1p::GFP* reporter *drIs4* was upregulated by HTS in *nio-1* through *nio-7*, even though GFP fluorescence in these strains was strongly reduced (Fig 2.1.2B, 2.1.2C and 2.1.3B). As was the case with *gpdh-1* mRNA, *nio-3(dr16)* and *nio-7(dr23)* were the only two Nio mutants with reduced (albeit not a statistically significant reduction compared to WT animals) *GFP* mRNA during HTS (mean ± S.D. of fold change in *GFP* mRNA on high salt – WT 12.9 ± 2.8, *nio-3(dr16)* 10.7 ± 1.3, *nio-7(dr23)* 3.5 ± 3.3). These data unexpectedly suggest that the majority of the *nio* genes are required for hypertonic induction of *gpdh-1p::GFP* reporter protein expression, but not endogenous *gpdh-1* or HTS reporter derived *GFP* mRNA.

To further understand the requirements of the *nio* genes in the HTSR, I examined the physiological phenotypes of each Nio mutant in response to HTS. *C. elegans* upregulates osmosensitive genes, including *gpdh-1*, to survive and adapt to hypertonic challenges. Survival and adaptation can be measured in several ways. Survival measures the ability of animals grown under standard laboratory isotonic conditions to survive a 24 hour exposure to an indicated level of HTS [318]. Acute adaptation measures the ability of animals to activate adaptive responses that permit survival under normally lethal hypertonic conditions using a pre-conditioning stimulus [318]. Chronic adaptation measures the ability of animals to develop under non-lethal hypertonic conditions [319].

I found that loss of the *nio* genes had no effect on the survival of *C. elegans* during increasing levels of HTS. *nio-4(dr17)* mutants did have reduced survival during HTS, but they also had reduced survival under isotonic conditions (Fig 2.1.3C). This results suggests that the health of *nio-4(dr17)* mutants is generally compromised regardless of the tonicity of their

environment. In contrast to the survival assay, five out of the seven *nio* genes were implicated in acute adaptation to HTS. *nio-4* and *nio-6* had a moderate acute adaptation phenotype, whereas *nio-2*, *nio-3*, and *nio-7* mutants were almost completely unable to maintain movement on normally lethal levels of HTS even though they received a pre-conditioning stimulus (Fig 2.1.3D). The severe acute adaptation phenotype of *nio-2, nio-3,* and *nio-7*, in combination with the *gpdh-1p::GFP* phenotype, suggests that these three Nio mutants contain mutations in genes required for both osmoprotective gene expression and physiological adaptation to HTS.

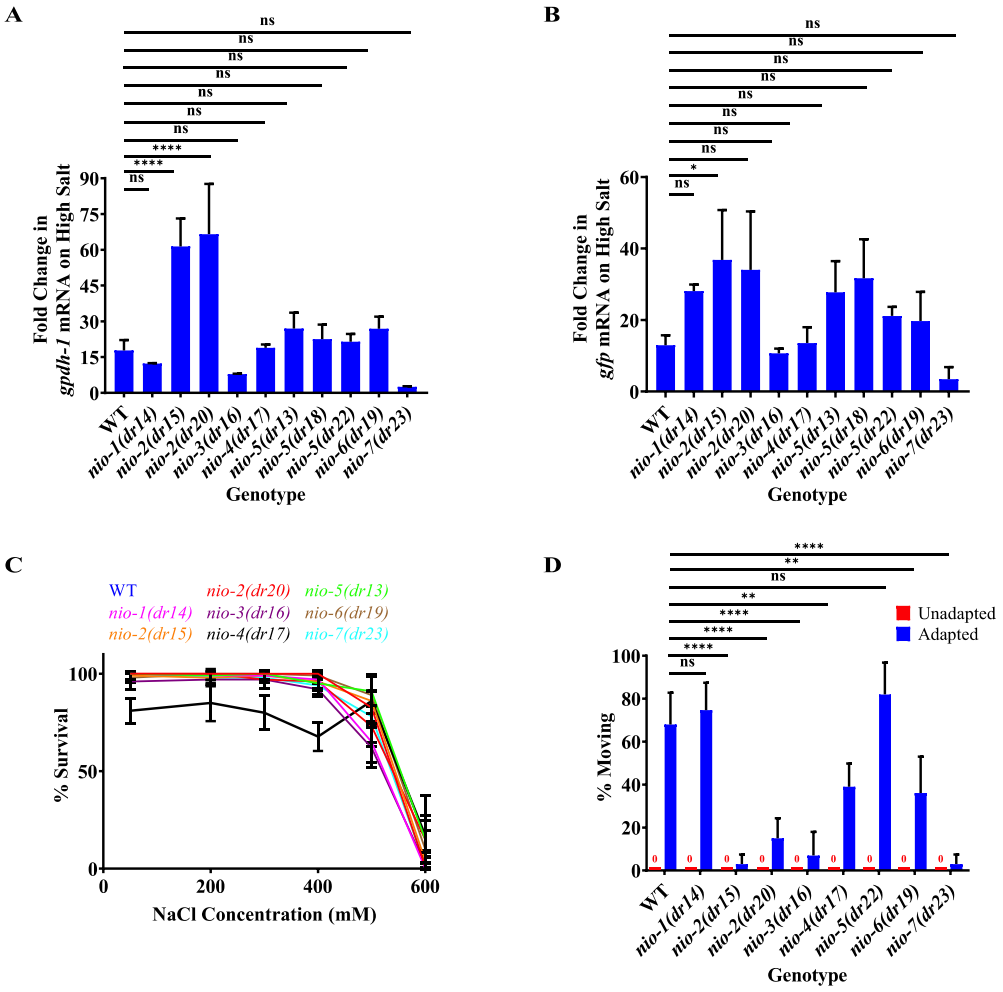

Figure 2.1.3 The majority of Nio mutants upregulate osmosensitive mRNAs, exhibit normal survival, and are able to acutely adapt to HTS

(A) qPCR of *gpdh-1* mRNA from WT and *nio* mutant day 2 adult animals expressing *drIs4* exposed to 250 mM NaCl NGM plates for 24 hours. Data are represented as fold induction of mRNA on 250 mM NaCl relative to 50 mM NaCl. Data are expressed as mean ± S.D. **** - $p < 0.0001$, ns = nonsignificant (One-way ANOVA with post hoc Tukey's test). $N \geq 3$ biological replicates of 35 animals for each group. (B) qPCR of *GFP* mRNA from WT and *nio* mutant day 2 adult animals expressing *drIs4* exposed to 250 mM NaCl NGM plates for 24 hours. Data are represented as fold induction of mRNA on 250 mM NaCl relative to 50 mM NaCl. Data are expressed as mean ± S.D. * - $p < 0.05$, n.s. = nonsignificant (One-way ANOVA with post hoc Tukey's test). $N \geq 3$ biological replicates of 35 animals for each group. (C) Percent survival of day 2 adult animals expressing *drIs4* exposed to 100 – 600 mM NaCl NGM plates for 24 hours. Strains include WT and the *nio* mutants expressing *drIs4*. Data are expressed as mean ± S.D. N = 5

replicates of 20 animals for each salt concentration. (D) Percent of moving unadapted and adapted day 3 adult animals exposed to 600 mM NaCl NGM plates for 24 hours. Strains include WT and the *nio* mutants expressing *drIs4*. Data are expressed as mean ± S.D. **** - $p < 0.0001$, ** - $p < 0.01$, ns = nonsignificant. N = 5 replicates of 20 animals for each strain.

In order to identify the phenotype-causing mutations in the Nio mutants, we had the genome of each mutant sequenced. Using bioinformatics, I compared the single nucleotide polymorphisms (SNPs) in each Nio mutant to the SNPs in the *drIs4* starting strain to find genes with homozygous mutations not present in the *drIs4* starting strain. My bioinformatic analysis identified hundreds of homozygous SNPs in each mutant that were not in the starting *drIs4* strain (Table 2.1.3). A common practice in forward genetic screens is to cross isolated mutants back to WT animals (backcrossing) several times to decrease background mutations. Each Nio mutant was therefore backcrossed three times prior to sequencing. However, the sequencing results suggest that at least for *nio-1(dr14)* and *nio-2(dr20)* mutants, backcrossing did not have a large effect on mutant SNP number (Table 2.1.3).

Table 2.1.3 Number of unique homozygous SNPS in each Nio mutant

SNPs in the *drIs4* strain were subtracted from SNPs in the WT strain (N2) to identify SNPs unique to *drIs4*. These SNPs in *drIs4* were then subtracted from the SNPs in each Nio mutant to identify SNPs unique to each Nio mutant.

Mutant	# of SNPs
drIs4	359
nio-1(dr14)	311
nio-1(dr14) no backcross	329
nio-2(dr15)	259
nio-2(dr20)	340
nio-2(dr20) no backcross	386
nio-3(dr16)	267
nio-4(dr17)	363
nio-5(dr13)	261
nio-5(dr18)	244
nio-5(dr22)	321
nio-6(dr19)	328
nio-(dr23)	411

To simplify analysis of the whole genome sequencing data, I mapped the *nio* genes to specific chromosomes using *C. elegans* balancer strains harboring chromosomal translocations or inversions. Using the *mIn1* strain, which carries an inversion of a region of chromosome II, I determined that *nio-6(dr19)* was the only *nio* gene located on chromosome II. Using the *nT1* (chromosome IV/V translocation) strain and the *hT2* (chromosome I/III translocation) strains I mapped *nio-3(dr16)* to chromosome III and *nio-7(dr23)* to chromosome V. Furthermore, since each Nio mutant segregated with traditional Mendelian genetics, I was able to rule out gene candidates on chromosome X, as hemizygous X/null males did not exhibit a Nio phenotype. Finally, I used the results from the genetic complementation testing to further narrow down the phenotype-causing *nio* gene candidates. A list of phenotype-causing *nio* gene candidates for each strain can be found in Table 2.1.4. Since the *nio-2*, *nio-3*, and *nio-7* mutants had both impaired hypertonic induction of the *gpdh-1p::GFP* reporter and acute adaptation to HTS, we chose to focus on these three mutants to further characterize the HTSR.

Table 2.1.4 *nio* gene candidates (SNPs)

Genes in each strain with homozygous missense, nonsense, or splicing mutations that are predicted to be LOF. Bolded genes have mutations that are found in multiple strains that complement (i.e. strains that have different phenotype causing mutations). Underlined genes have mutations that are found in multiple strains that fail to complement (i.e. strains that have the same phenotype-causing mutations). * - The *C01B10.3* genes is adjacent to the *drh-2* pseudogene.

Mutant	*nio-1(dr14)*	*nio-2(dr15)*	*nio-2(dr20)*	*nio-3(dr16)*	*nio-4(dr17)*	*nio-5(dr13)*	*nio-5(dr18)*	*nio-5(dr22)*	*nio-6(dr19)*	*nio-7(dr23)*
nio gene candidates	*Y54E10A.23* *rcq-5* *C01G12.16* *C28A5.6* *C27F2.8* *adr-2* *gsp-2* *alh-12* *C07H6.4* *cdc-25.3* *R10E11.9* ***srv-19*** *H24K24.2* *ZC178.2* *F40F9.11* *unc-41* *F28H7.2* *nas-17* *C55A6.3* *mans-2* *T04H1.11* *C54D10.17* *F20G2.3* *B0391.1* *C14A6.9* *Y80D3A.8*	*cpt-3* *ogt-1* *T07C4.3* *Y41C4A.11* *Y111B2A.24* ***srv-19*** ***Y80D3A.8***	*ubr-1* *stam-1* *let-607* *sec-8* *Y47H9C.9* *F08A8.4* *Y53G8AR.6* *amx-1* *dex-1* ***nono-1*** *ogt-1* *Y69A2AR.25* *C55C3.72* ***srv-19*** *sss-1* *Y57G11C.1143* *Y105C5B.1420* ***alh-2*** *srx-86* *Y80D3A.8*	*ZK1025.1* *cpf-2* ***srv-19*** *clx-1* *Y105C5B.1420* *srx-9* *srbc-9*	*C36F7.5* *Y54E5B.5* *Y55B1BR.2* *pef-1* *Y47D3B.23* ***srv-19*** *sss-1* *21ur-1385* ***alh-2*** *Y40B10A.9* *srt-13* *C14C11.2* *ZC178.2* *sup-37* *srt-18* *pqn-63* *C08B6.14* *T04F3.1* *K01D12.5* *F09F3.5* *R02D5.7* *T08G3.7* ***Y80D3A.8***	***nono-1*** *Y47D3B.14* ***srv-19*** *C01B10.3** *T05A12.3* *catp-7* *Y80D3A.8*	*dig-1* ***srv-19*** *drh-2** *str-219* *F35H10.10* *K09B11.5* *C52D10.10* ***alh-2*** *ZC178.2* ***Y80D3A.8***	*gcy-35* *fkh-7* ***srv-19*** *drh-2** *F42A9.6* *C33A12.16* *F13B12.2* *T12G3.4* *Y57G11C.36* ***alh-2***	*kpc-1* *F33E2.10* *hinf-1* *sdz-3* *Y57A10A.27* *usp-14* ***dig-1*** ***srv-19*** *pqn-79* ***alh-2*** ***Y80D3A.8***	*gls-1* *C39B5.6* ***dig-1*** *ZK370.8* *Y55F3C.17* ***srv-19*** *hcf-1* *Y105C5B.1420* *srw-7* *C49G7.1* *nhr-181* *mut-14* *alh-4* *C50E3.5* *ncx-10* *symk-1* *tag-196* *R03H4.8* *ptr-1* *gcy-6* *twk-12* *T16G1.6* *mes-4* *F20G2.1* *clec-232* *Y69H2.21,Y69H2.25* *Y39B6A.21* *nhr-266*

2.2 The *O*-GlcNAc transferase OGT-1 is required post-transcriptionally for the hypertonic induction of GPDH-1 and physiological adaptation to hypertonic stress

In the forward genetic screen for Nio mutants, I identified two recessive alleles, *dr15* and *dr20,* that genetically failed to complement (Tables 2.1.1 and 2.1.2). Whole genome sequencing and bioinformatics revealed that *dr15* and *dr20* contained distinct nonsense mutations (R267STOP and Q600STOP respectively) in the gene encoding the *O*-GlcNAc transferase *ogt-1* (Table 2.1.4, Fig 2.2.1A). Two independently isolated *ogt-1* deletion alleles, *ok430* and *ok1474,* as well as WT worms exposed to *ogt-1(RNAi),* also exhibited a Nio phenotype (Fig 2.2.1A, 2.2.1B, 2.2.1C, 2.2.1D). The *ok430* and *ok1474* alleles failed to complement the *dr15* and *dr20* alleles, supporting the hypothesis that the loss of *ogt-1* function is the basis for the Nio phenotype (Table 2.2.1). Consistent with this hypothesis, transgenic overexpression of *ogt-1* in the *ogt-1(dr20)* mutant led to supra-physiological rescue of hypertonic *gpdh-1p::GFP* induction (Fig 2.2.1E). Finally, CRISPR reversion of the *dr20* Q600STOP mutation back to WT was sufficient to rescue the *ogt-1* Nio phenotype, indicating that ENU induced mutations in the background of these animals do not contribute to the Nio phenotype (Fig 2.2.1F). In combinations, these results support the hypothesis that *ogt-1* is required for hypertonic induction of *gpdh-1p::GFP*.

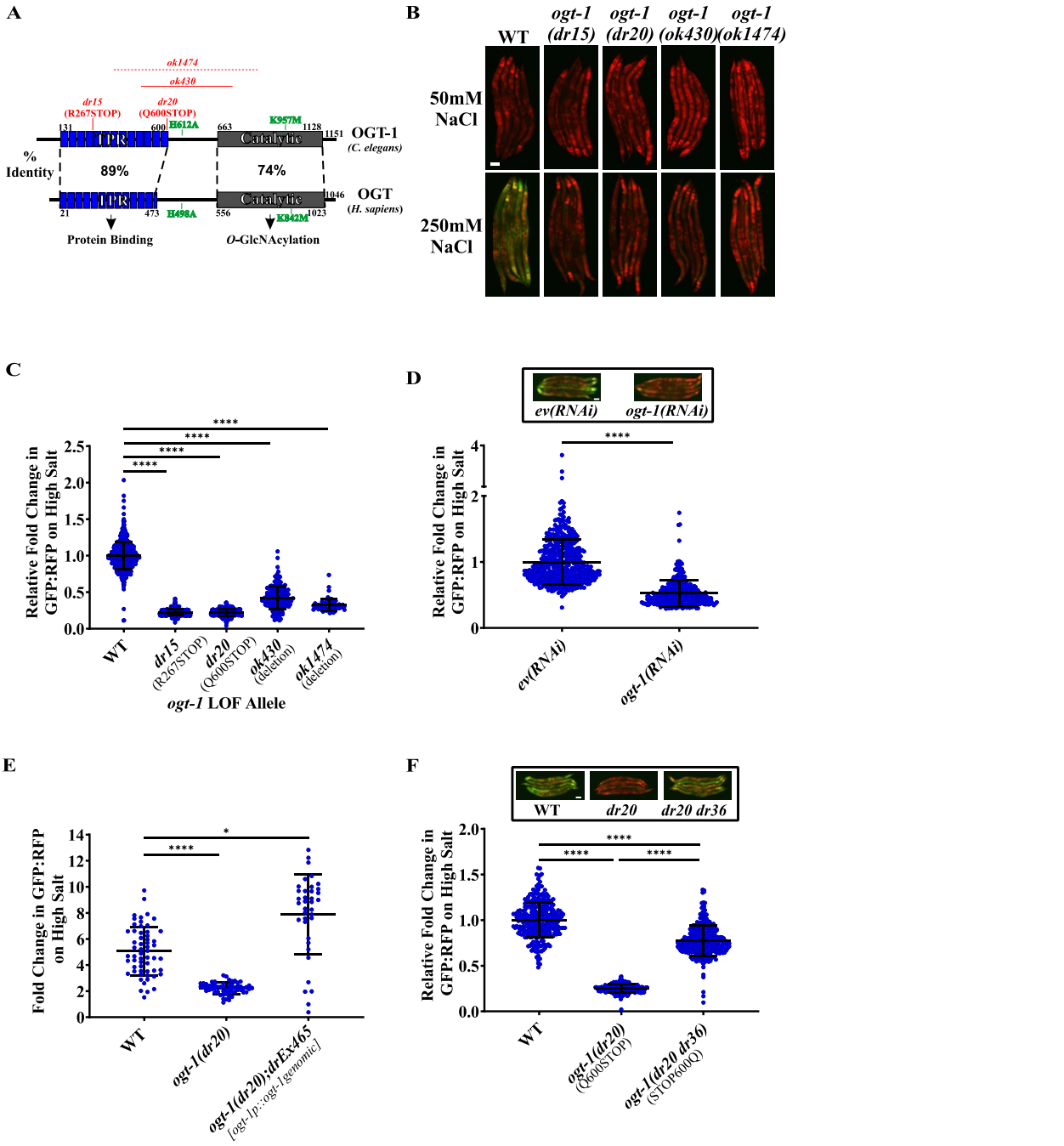

Figure 2.2.1 The conserved *O*-GlcNAc transferase OGT-1 is required for the upregulation of the *gpdh-1p::GFP* transcriptional reporter by HTS.

(A) *C. elegans* and *Homo sapians* OGT protein domain diagrams detailing the positions of the two LOF *ogt-1* alleles identified in the screen (*dr15* and *dr20*), two independently isolated *ogt-1* deletion mutations (*ok430* and *ok1474)*, and the two mutations that disrupt catalytic activity of the enzyme (H612A and K957M). The precise breakpoints of

ok1474 have not been determined. (B) Wide-field fluorescence microscopy of day 2 adult *drIs4* and *ogt-1;drIs4* mutant animals exposed to 50 or 250 mM NaCl NGM plates for 18 hours. Images depict merged GFP and RFP channels. Scale bar = 100 microns. (C) COPAS Biosort quantification of GFP and RFP signal in day 2 adult animals expressing *drIs4* or *ogt-1;drIs4* exposed to 250 mM NaCl NGM plates for 18 hours. Data are represented as the relative fold induction of normalized GFP/RFP ratio on 250 mM NaCl NGM plates versus 50 mM NaCl NGM plates, with WT induction set to 1. Each point represents the quantified signal from a single animal. Data are expressed as mean ± S.D. **** - $p < 0.0001$ (Kruskal-Wallis test with post hoc Dunn's test). $N \geq 62$ for each group. (D) COPAS Biosort quantification of GFP and RFP signal in day 2 adult WT animals expressing *drIs4* exposed to 250 mM NaCl NGM plates for 18 hours. Animals were grown on *empty vector (RNAi) (ev(RNAi))* or *ogt-1(RNAi)* plates for multiple generations. Data are represented as fold induction of normalized GFP/RFP ratio on 250 mM NaCl NGM plates relative to on 50 mM NaCl NGM plates. Each point represents the quanitfied signal from a single animal. Data are expressed as mean ± S.D. **** - $p < 0.0001$ (Mann-Whitney test). $N \geq 334$ for each group. *Inset:* Wide-field fluorescence microscopy of day 2 adult animals expressing *drIs4* exposed to 250 mM NaCl NGM plates for 18 hours. Animals were grown on *ev(RNAi)* or *ogt-1(RNAi)* plates for multiple generations. Images depict merged GFP and RFP channels. Scale bar = 100 microns. (E) COPAS Biosort quanitification of GFP and RFP signal in day 2 adult animals expressing *drIs4* exposed to 250 mM NaCl NGM plates for 18 hours in the indicated genetic background. *drEx465* is an extrachromosomal array expressing a 10.3 Kb *ogt-1* genomic DNA fragment containing ~2 Kb upstream and ~1 Kb domnstream of the *ogt-1* coding sequence. Data are represented as fold induction of normalized GFP/RFP ratio on 250 mM NaCl NGM plates relative to on 50 mM NaCl NGM plates. Each point represents the quantified signal from a single animal. Data are expressed as mean ± S.D. **** - $p < 0.0001$, * - $p < 0.05$ (Kruskal-Wallis test with post hoc Dunn's test). $N \geq 37$ for each group. (F) COPAS Biosort quanitification of GFP and RFP signal in day 2 adult animals expressing *drIs4* or *drIs4;ogt-1(dr20)* exposed to 50 or 250 mM NaCl NGM plates for 18 hours. *ogt-1(dr20 dr36)* is a strain in which the *dr20* mutation is converted back to WT using CRISPR/Cas9 genome editing. Data are represented as relative fold induction of normalized GFP/RFP ratio on 250 mM NaCl NGM plates versus 50 mM NaCl NGM plates, with WT fold induction set to 1. Each point represents the quantified signal from a single animal. Data are expressed as mean ± S.D. **** - $p < 0.0001$ (Kruskal-Wallis test with post hoc Dunn's test). $N \geq 170$ for each group. *Inset:* Wide-field fluorescence microscopy of day 2 adult animals expressing *drIs4* in the WT or

indicated *ogt-1* mutant background exposed to 250 mM NaCl NGM plates for 18 hours. Images depict merged GFP and RFP channels. Scale bar = 100 microns.

Table 2.2.1 Genetic complementation of the *ogt* alleles

Fractions represent the number of animals with a Nio phenotype (impaired *gpdh-1p::GFP* induction on 250 mM NaCl NGM plates) over the total number of animals counted. Males were heterozygous for the *nio* mutation. Mutant crosses complemented (i.e. phenotype causing mutations are in different genes) when 0% of progeny were Nio and failed to complement (i.e. phenotype causing mutations are in the same gene) when ~50% of progeny were Nio.

		Mutant A (hermaphrodite)			
		dr15	*dr20*	*ok430*	*ok1474*
Mutant B (male)	*dr15*	8/18 (44%)	13/31 (42%)	6/12 (67%)	8/20 (40%)
	dr20		11/28 (39%)	9/32 (28%)	12/33 (36%)
	ok430			3/10 (30%)	13/27 (48%)
	ok1474				14/22 (64%)

To determine if *ogt-1* is required specifically for HTSR induced reporter expression or more generally for stress-inducible reporter expression, I examined the requirement for *ogt-1* in the heat shock and ER stress responses. *ogt-1* was not required for activation of other stress inducible reporters since inhibition of *ogt-1* resulted in a small but significant increase in the heat shock inducible GFP reporter and had no effect on the ER stress inducible GFP reporter (Fig 2.2.2A, 2.2.2B, 2.2.2C, and 2.2.2D). Additionally, I used a GFP reporter for the expression of the antimicrobial peptide *nlp-29 (frIs7)* to examine if *ogt-1* is required for the induction of other osmotically induced reporters. *nlp-29p::GFP* is induced by several stressors including HTS. *ogt-1(RNAi)* did not prevent *nlp-29p::GFP* upregulation by HTS and in some cases led to a small but significant increase in the hypertonic induction of this reporter. In conclusion, these results suggest that *ogt-1* is required specifically for the upregulation of *gpdh-1p::GFP* reporter expression during HTS.

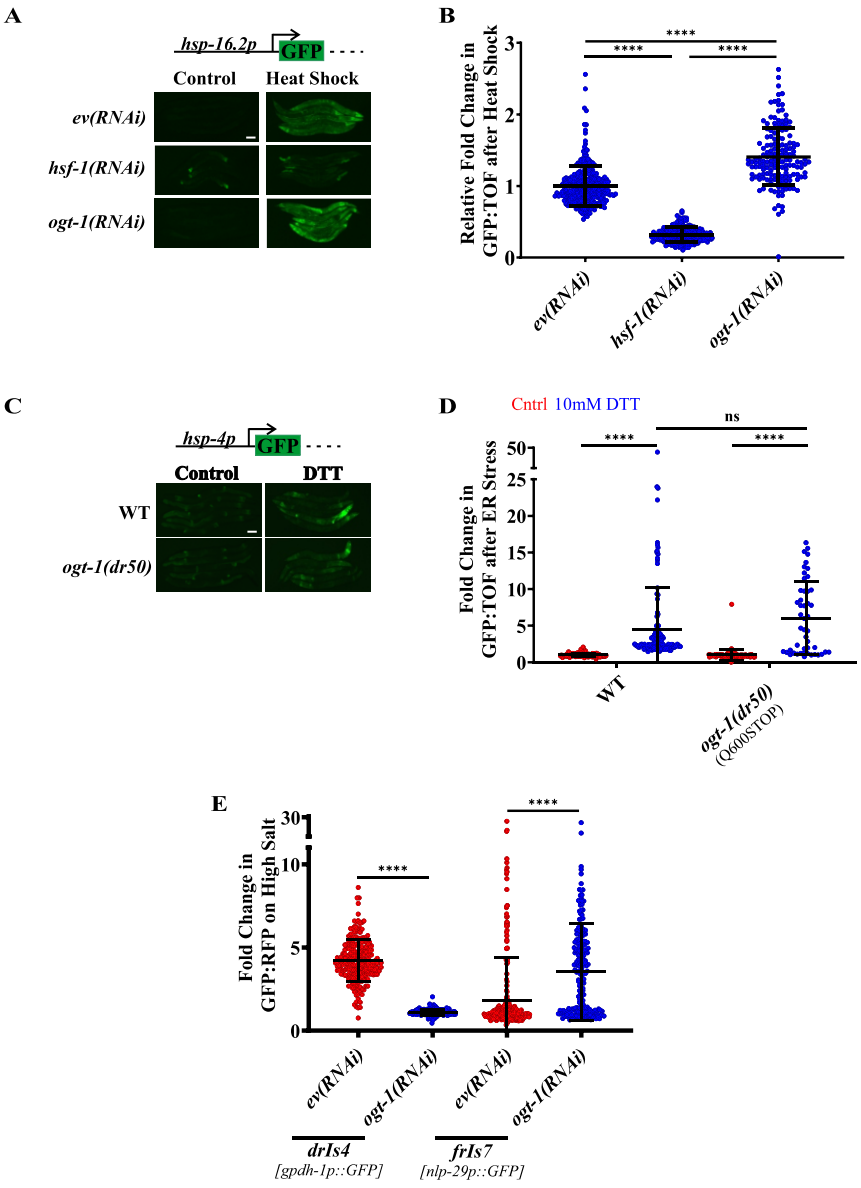

Figure 2.2.2 *ogt-1* is not required for the upregulation of transcriptional reporters by heat shock or ER stress or for the upregulation of the *nlp-29p::GFP* reporter by HTS.

(A) Wild-field fluorescence microscopy of day 2 adult animals expressing *hsp-16.2p::GFP (gpIs1)* grown on *ev(RNAi), ogt-1(RNAi),* or *hsf-1(RNAi)* plates and exposed to control or heat shock conditions (35˚C for 3 hours, 18 hour recovery at 20˚C). Images depict the GFP channel, since there is not a normalizing RFP reporter in these strains. Scale bar = 100 microns. (B) COPAS Biosort quantification of GFP and TOF signal from animals in (A). Data are represented as fold induction of normalized GFP/TOF ratio of animals exposed to heat shock conditions relative to animals exposed to control conditions. Each point represents the quantified signal from a single animal. Data are

expressed as mean ± S.D. **** - $p < 0.0001$ (Kruskal-Wallis test with post hoc Dunn's test). $N \geq 158$ for each group. (C) Wide-field fluorescence microscopy of day 2 adult animals expressing *hsp-4p::GFP (zcIs4)* exposed to DTT plates for 18 hours. The *ogt-1(dr50)* allele carries the same homozygous Q600STOP mutation as the *ogt-1(dr20)* allele and was introduced using CRISPR/Cas9. Images depict the GFP channel. Scale bar = 100 microns. (D) COPAS Biosort quantification of GFP and TOF signal from animals in (C). Data are represented as fold induction of normalized GFP/TOF ratio of animals exposed to DTT plates relative to animals exposed to control plates. Each point represents the quantified signal from a single animal. Data are expressed as mean ± S.D. **** - $p < 0.0001$, ns = nonsignificant (Kruskal-Wallis test with post hoc Dunn's test). $N \geq 48$ for each group. (E) COPAS Biosort quantification of GFP and RFP signal from day 2 animals expressing *gpdh-1p::GFP (drIs4)* or *nlp-29p::GFP (frIs7)* exposed to 250 mM NaCl for 18 and 24 hours respectively [349]. Data are represented as fold induction of normalized GFP/RFP ratio of animals exposed to 250 mM NaCl plates relative to animals exposed to 50 mM NaCl plates. Each point represents the quantified signal from a single animal. Data are expressed as mean ± S.D. **** - $p < 0.0001$ (Kruskal-Wallis test with post hoc Dunn's test). $N \geq 173$ for each group.

2.2.1 OGT-1 is required for osmosensitive GPDH-1-GFP protein expression, but not osmosensitive transcription in a sequence-independent manner

Since *ogt-1* is required for induction of the *gpdh-1p::GFP* transgenic reporter by HTS, I hypothesized that endogenous osmosensitive mRNAs would not be upregulated in *ogt-1* mutants. To test this, I used qPCR to measure the expression levels of several previously described mRNAs that are induced by HTS. Surprisingly, I found that *gpdh-1* was still upregulated by HTS in all four *ogt-1* mutants following 24 hours of HTS (Fig 2.2.3A). In fact, *ogt-1* mutants upregulated *gpdh-1* mRNA levels to a greater extent than WT animals during HTS. Consistent with this, I also observed that GFP mRNA derived from the overexpressed *gpdh-1p::GFP* reporter *drIs4* was upregulated by HTS in all four *ogt-1* mutants even though GFP protein levels were strongly reduced (Fig 2.2.3B, 2.2.1B, and 2.2.1C). Furthermore, *gpdh-1* mRNA was upregulated in *ogt-*

1(dr20) mutants after only three hours of HTS (Fig 2.2.3C). Therefore, *ogt-1* mutant animals, like WT animals, likely activate the cellular pathways required for *gpdh-1* mRNA induction soon after exposure to HTS and they maintain high *gpdh-1* mRNA levels for an extended period of time. Finally, osmotically induced mRNA expression of *nlp-29* and *hmit-1.1* mRNA was also increased in *ogt-1(dr20)* mutants (Fig 2.2.3D and 2.2.3E), suggesting that osmosensitive mRNAs are upregulated in *ogt-1* mutants despite the reduction in *gpdh-1p::GFP* protein levels.

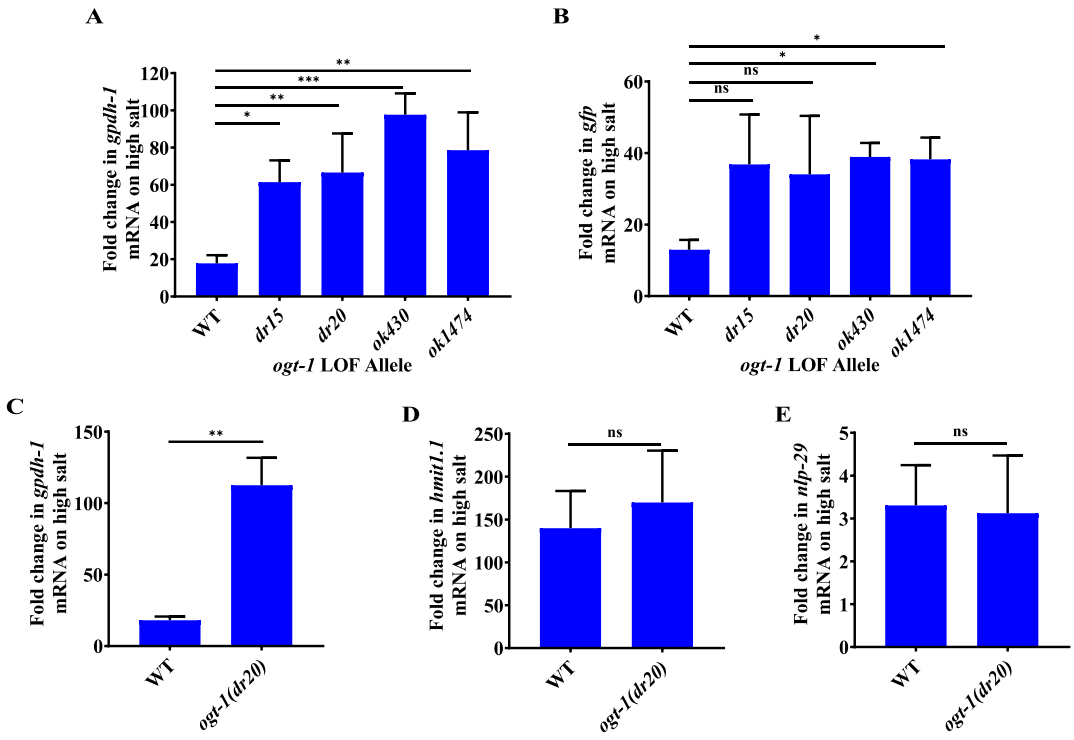

Figure 2.2.3 *ogt-1* is not required for the upregulation of ORG mRNA transcripts by HTS

(A) qPCR of *gpdh-1* mRNA from WT and *ogt-1* mutant day 2 adult animals expressing *drIs4* exposed to 250 mM NaCl NGM plates for 24 hours. Data are represented as fold induction of RNA on 250 mM NaCl relative to 50 mM NaCl. Data are expressed as mean ± S.D. *** - $p < 0.001$, ** - $p < 0.01$, * < 0.05 (One-way ANOVA with post hoc Tukey's test). $N \geq 3$ biological replicates of 35 animals for each group. (B) qPCR of *GFP* mRNA from WT and *ogt-1* mutant day 2 adult animals expressing *drIs4* exposed to 250 mM NaCl NGM plates for 24 hours. Data are represented as fold induction of RNA on 250 mM NaCl relative to 50 mM NaCl. Data are expressed as mean ± S.D. * $p < 0.05$, ns = nonsignificant (One-way ANOVA with post hoc Tukey's test). $N \geq 3$ biological replicates of 35 animals for each group. (C) qPCR of *gpdh-1* mRNA from WT and *ogt-1* mutant day 2 adult animals expressing *drIs4* exposed to 250 mM NaCl NGM plates for 3 hours. Data are represented as fold induction of RNA on 250 mM NaCl relative to 50 mM NaCl. Data are expressed as mean ± S.D. ** - $p < 0.01$ (Student's two-tailed t-test). $N \geq 3$ biological replicates of 35 animals for each group. (D) qPCR of *hmit-1.1* mRNA from WT and *ogt-1* mutant day 2 adult animals expressing *drIs4* exposed to 250 mM NaCl NGM plates for 24 hours. Data are represented as fold induction of RNA on 250 mM NaCl relative to 50 mM NaCl. Data are expressed as mean ± S.D. ns = nonsignificant (Student's two-

tailed t-test). N ≥ 3 biological replicates of 35 animals for each group. (E) qPCR of *nlp-29* mRNA from WT and *ogt-1* mutant day 2 adult animals expressing *drIs4* exposed to 250 mM NaCl NGM plates for 24 hours. Data are represented as fold induction of RNA on 250 mM NaCl relative to 50 mM NaCl. Data are expressed as mean ± S.D. ns = nonsignificant (Student's two-tailed t-test). N ≥ 3 biological replicates of 35 animals for each group.

To further examine how OGT-1 affects the coupling between HTS induced mRNA and protein expression, I measured GFP protein levels in an *ogt-1* mutant (*dr34*; CRISPR/Cas9 knock-in of the *dr20*(Q600STOP mutation)) expressing a GPDH-1 translational reporter (GPDH-1::GFP). As I observed for the *gpdh-1p::GFP* transcriptional reporter, *ogt-1(dr34)* mutants failed to induce the GPDH-1::GFP protein in response to HTS (Fig 2.2.4A). However, the mRNA from this translational reporter was still induced to WT levels (Fig 2.2.4B). mRNA induction of the translational reporter did not exceed WT levels like I saw for the transcriptional reporter for unknown reasons. Importantly, the requirement for *ogt-1* in the HTS is not transgene dependent because *ogt-1* is also required for the hypertonic induction of a CRISPR/Cas9 engineered endogenously expressed GPDH-1::GFP fusion protein, which I confirmed to be functional based on its ability to exhibit acute adaptation to HTS (Fig 2.2.4C and 2.2.6E). Like in the transcriptional and translational reporters, *gpdh-1::GFP* mRNA levels of the *gpdh-1::GFP* CRISPR allele were induced to WT levels or higher during HTS (Fig 2.2.4D and 2.2.4E). In conclusion, these results suggest that *ogt-1* functions downstream of osmosensitive mRNA upregulation to regulate hypertonic GPDH-1 protein induction.

One possibility to explain these results is that *ogt-1* mutants aberrantly activate protein degradation pathways that decrease GPDH-1 protein levels. To test this possibility, I inhibited proteasomal degradation and autophagy in *ogt-1* mutants with *rpn-8(RNAi)* and *lgg-1(RNAi)* respectively [423, 494]. I hypothesized that if these degradation pathways decreased GPDH-1

protein levels in the *ogt-1* mutants, then inhibiting these pathways would rescue *gpdh-1p::GFP* expression in *ogt-1* mutants. However, *rpn-8(RNAi)* and *lgg-1(RNAi)* did not increase *gpdh-1p::GFP* expression in *ogt-1* mutants, suggesting that these pathways are not regulated by OGT-1 during the HTSR (Fig 2.2.4F and 2.2.4G). Therefore, OGT-1 functions downstream of osmosensitive mRNA upregulation, but upstream of osmosensitive GPDH-1-GFP protein expression during the HTSR.

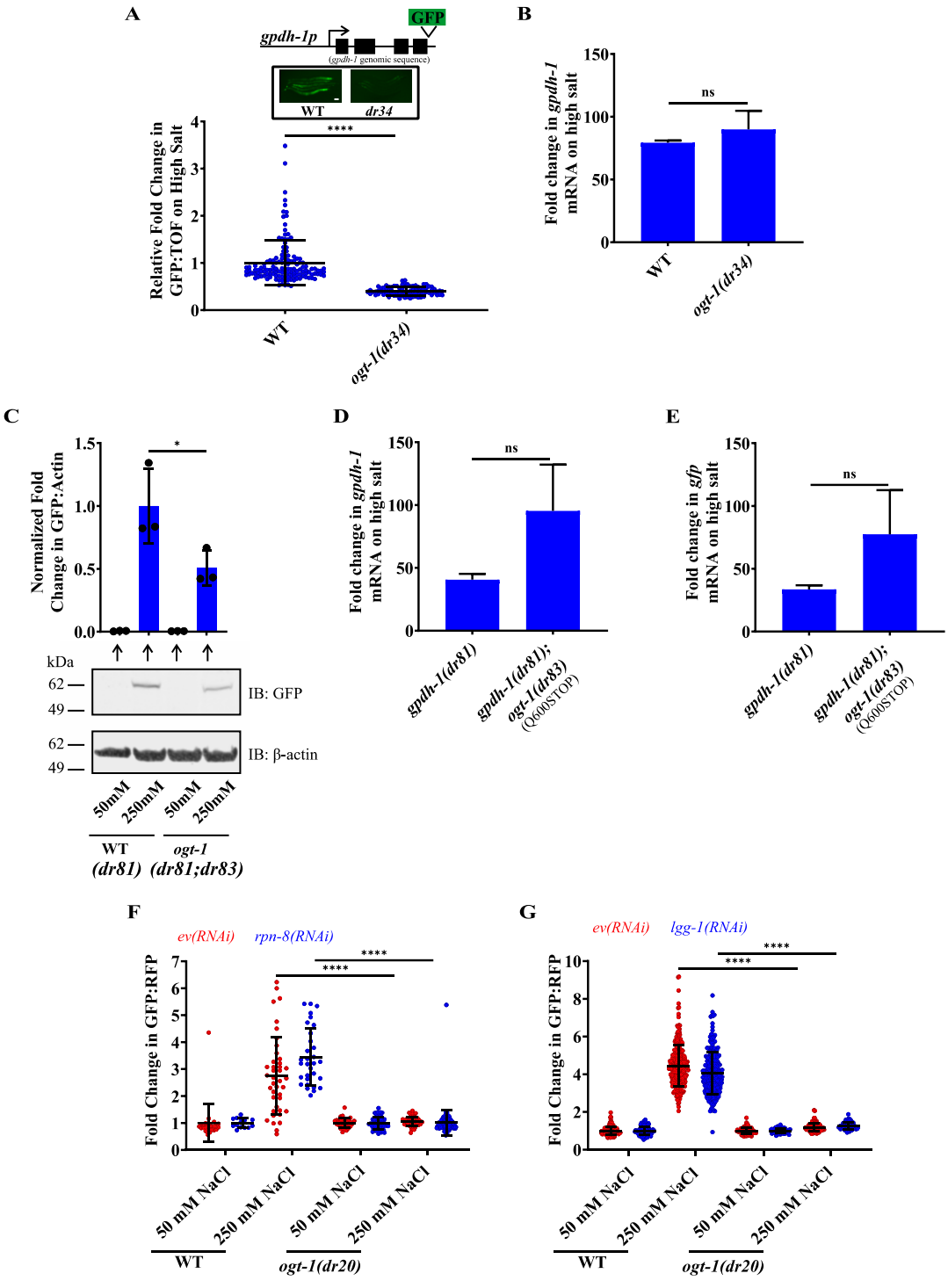

Figure 2.2.4 OGT-1 functions post-transcriptionally to regulate osmosensitive GPDH-1 protein expression

(A) COPAS Biosort quantification of GFP and TOF signal in day 2 adult animals expressing the *kbIs6* GPDH-1 translational fusion exposed to 250 mM NaCl NGM plates for 18 hours. The *ogt-1(dr34)* allele carries the same

homozygous Q600STOP mutation as the *ogt-1(dr20)* allele and was introduced using CRISPR/Cas9. Data are represented as relative fold induction of normalized GFP/TOF ratio on 250 mM NaCl NGM plates versus 50 mM NaCl NGM plates. Each point represents the quantified signal from a single animal. Data are expressed as mean ± S.D. **** - $p < 0.0001$ (Mann-Whitney test). $N \geq 84$ for each group. *Inset:* Wide-field fluorescence microscopy of day 2 adult animals expressing the *kbIs6* translational fusion protein exposed to 250 mM NaCl NGM plates for 18 hours. Scale bar = 100 microns. (B) qPCR of *gpdh-1* mRNA from day 2 adult animals expressing the *kbIs6* translational fusion exposed to 250 mM NaCl NGM plates for 24 hours. Strains include WT and *ogt-1(dr34).* The *ogt-1(dr34)* allele is the *dr20* point mutation introduced using CRISPR/Cas9. Data are represented as fold induction of RNA on 250 mM NaCl relative to 50 mM NaCl. Data are expressed as mean ± S.D. ns = nonsignificant (Student's two-tailed t-test). N = 3 biological replicates of 35 animals for each group. (C) Immunoblot of GFP and β-actin in lysates from day 2 adult animals exposed to 50 mM or 250 mM NaCl for 18 hours. The animals express a CRISPR/Cas9 edited knock-in of GFP into the endogenous *gpdh-1* gene (*gpdh-1(dr81)). ogt-1* carries the *dr83* allele, which is the same homozygous Q600STOP mutation as the *ogt-1(dr20)* allele and was introduced using CRISPR/Cas9. *Top:* Normalized quantification of immunoblots. * - $p < 0.05$ (Two-way ANOVA with post hoc Tukey's test). *Bottom:* Representative immunoblot. N = 3 biological replicates. (D) qPCR of *gpdh-1* mRNA in day 2 adult animals exposed to 250 mM NaCl NGM plates for 24 hours. The animals express a CRISPR/Cas9 edited knock-in of GFP into the endogenous *gpdh-1* gene (*gpdh-1(dr81)). ogt-1* carries the *dr83* allele, which is the same homozygous Q600STOP mutation as the *ogt-1(dr20)* allele and was introduced using CRISPR/Cas9. Data are represented as fold induction of RNA on 250 mM NaCl relative to 50 mM NaCl. Data are expressed as mean ± S.D. ns = nonsignificant (Student's two-tailed t-test). $N \geq 3$ biological replicates of 35 animals for each group. (E) qPCR of *GFP* mRNA in day 2 adult animals exposed to 250 mM NaCl NGM plates for 24 hours. The animals express a CRISPR/Cas9 edited knock-in of GFP into the endogenous *gpdh-1* gene (*gpdh-1(dr81)). ogt-1* carries the *dr83* allele, which is the same homozygous Q600STOP mutation as the *ogt-1(dr20)* allele and was introduced using CRISPR/Cas9. Data are represented as fold induction of RNA on 250 mM NaCl relative to 50 mM NaCl. Data are expressed as mean ± S.D. ns = nonsignificant (Student's two-tailed t-test). $N \geq 3$ biological replicates of 35 animals for each group. (F) COPAS Biosort quantification of GFP and RFP signal in day 2 adult animals expressing *drIs4* exposed to 50 and 250 mM NaCl NGM plates for 18 hours. Animals were placed on *ev(RNAi)* or *rpn-8(RNAi)* plates as L1s. Data are represented as normalized fold induction of GFP/RFP ratio on 250 mM or 50 mM NaCl RNAi plates

relative to on 50 mM NaCl RNAi plates. Each point represents the quantified signal from a single animal. Data are expressed as mean ± S.D. **** - $p < 0.0001$ (Kruskal-Wallis test with post hoc Dunn's test). $N \geq 14$ for each group. (G) COPAS Biosort quanitification of GFP and RFP signal in day 2 adult animals expressing *drIs4* exposed to 50 and 250 mM NaCl NGM plates for 18 hours. Animals were placed on *ev(RNAi)* or *lgg-1(RNAi)* plates as L1s. Data are represented as normalized fold induction of GFP/RFP ratio on 250 mM or 50mM NaCl RNAi places relative to on 50 mM NaCl RNAi plates. Each point represents the quantified signal from a single animal. Data are expressed as mean ± S.D. **** - $p < 0.0001$ (Kruskal-Wallis test with post hoc Dunn's test). $N \geq 47$ for each group.

Since our evidence thus far suggested that *ogt-1* is required for translation of the *gpdh-1p::GFP* transcript into protein, I next considered which portion of the *gpdh-1p::GFP* transcript was required for *ogt-1* regulation during HTS. The *gpdh-1p::GFP* reporter (*drIs4)* that was the basis for my forward genetic screen contained the *gpdh-1* 5' UTR, start ATG codon, and a small portion of the *gpdh-1* coding sequence fused to GFP (Fig 2.2.5). This *gpdh-1p::GFP* reporter is referred to as the WT *gpdh-1p::GFP* reporter here. As previously shown, hypertonic induction of GFP was reduced in animals expressing this WT *gpdh-1p::GFP* reporter upon knock down of *ogt-1* with RNAi (Fig 2.2.1D and Fig 2.2.5). Similarly, animals expressing truncated *gpdh-1p::GFP* reporters missing the *gpdh-1* coding sequence (ΔCDS *gpdh-1p::GFP* reporter) or both the *gpdh-1* coding sequence and 5' UTR (Δ5' UTR *gpdh-1p::GFP* reporter) also had decreased GFP induction when *ogt-1* was knocked down with RNAi (Fig 2.2.5). Since transcripts derived from the Δ5' UTR *gpdh-1p::GFP* reporter contained no mRNA sequence unique to the *gpdh-1* transcript, this result surprisingly indicates that OGT-1 requires no part of the *gpdh-1* mRNA sequence to regulate *gpdh-1* protein expression. Therefore OGT-1 may regulate the hypertonic induced translation of the GPDH-1 protein through an indirect mechanism.

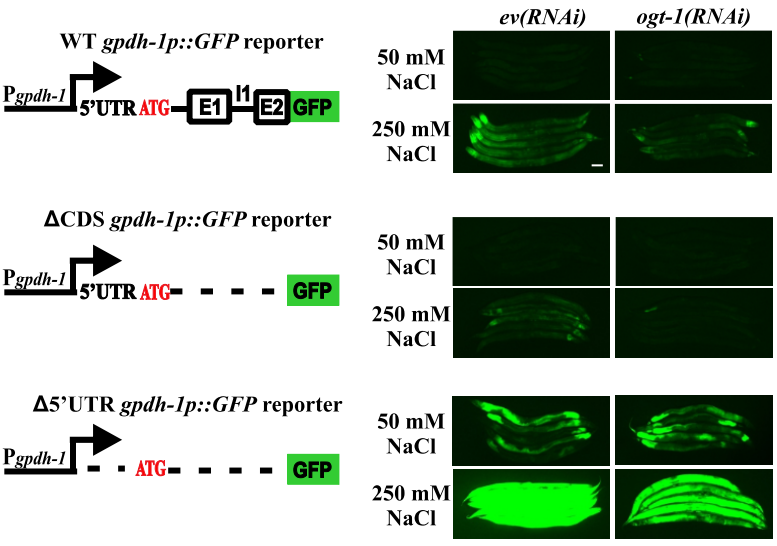

Figure 2.2.5 OGT-1 regulates hypertonic induction of the *gpdh-1* transcriptional reporter in a sequence independent manner

Wide-field fluorescence microscopy of day 2 adult animals expressing the indicated *gpdh-1p::GFP* transcriptional reporters (extrachromosomal arrays) exposed to 50 or 250 mM NaCl NGM plates for 18 hours. Animals also express a the *myo2p::mCherry* extrachromosomal array as a co-injection marker. All images are exposure matched. Scale bar = 100 microns. In the diagrams P = promoter, E = exon, and I = intron.

2.2.2 Physiological and genetic adaptation to hypertonic stress requires *ogt-1*

C. elegans upregulates osmosensitive genes, including *gpdh-1*, to survive and adapt to hypertonic challenges. As mentioned previously (Section 2.1), survival, acute adaptation, and chronic adaptation all measure the physiological phenotypes of *C. elegans* during HTS. I found that loss of *ogt-1/nio-2* had no effect on survival during HTS (Fig 2.1.3C). In contrast, loss of *ogt-1* blocked both acute and chronic adaptation to HTS (Fig 2.2.6A and 2.2.6B). Chronic HTS did not alter *ogt-1(dr20)* egg laying under hypertonic conditions compared to WT animals (Fig

2.2.6C). However, embryo development during HTS, but not in isotonic conditions, was inhibited in *ogt-1(dr20)* animals (Fig 2.2.6D). Therefore, the chronic adaptation phenotype of *ogt-1(dr20)* mutants is likely caused by the inability of *ogt-1* mutants to develop during chronic HTS. The acute adaptation phenotype was rescued by CRISPR reversion of the *dr20* Q600STOP mutation to WT (Fig 2.2.6E). Interestingly, the acute adaptation phenotype of *ogt-1* mutants must extend beyond its effects on *gpdh-1*, since the acute adaptation phenotype of a *gpdh-1* presumptive null mutant was not as severe as that observed in an *ogt-1* mutant (Fig 2.2.6A).

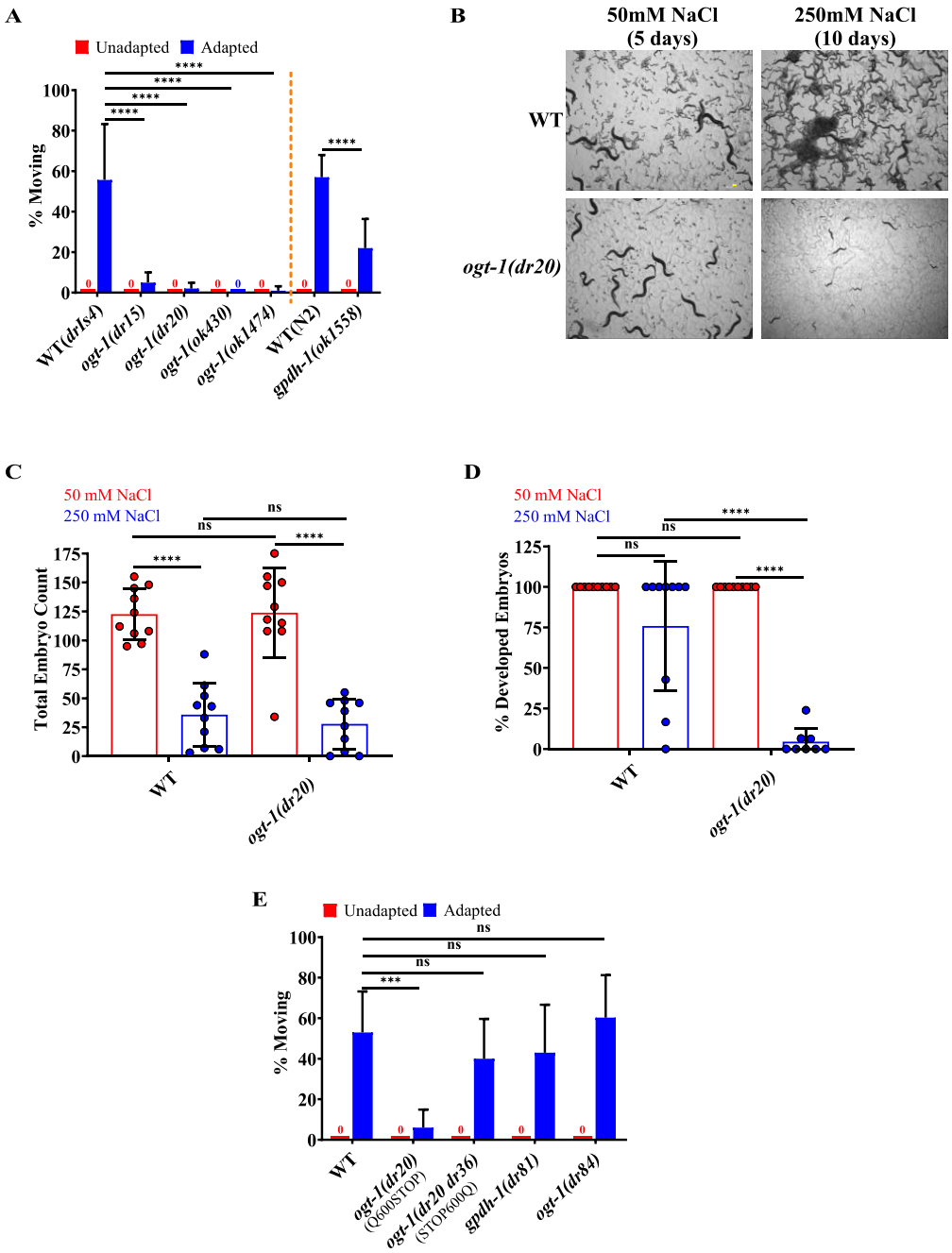

Figure 2.2.6 *ogt-1* is required for physiological acute and chronic adaptation to HTS

(A) Percent of moving unadapted and adapted day 3 adult animals exposed to 600 mM NaCl NGM plates for 24 hours. Strains expressing *drIs4* are on the left of the dashed orange line and those not expressing *drIs4* are on the right. *ok1558* is an out-of-frame deletion allele that generates a premature stop codon in exon 2 of *gpdh-1* and is therefore a likely null allele. Data are expressed as mean ± S.D. **** - $p < 0.0001$ (Two-way ANOVA with post hoc Tukey's

test.). N = 5 replicates of 20 animals for each strain. (B) Brightfield microscopy images of animals grown on 50 mM or 250 mM NaCl for 5 and 10 days respectively. Strains include WT (*drIs4)* and *ogt-1(dr20);drIs4.* Scale bar = 100 microns. (C) Percent of progeny laid. L4 animals were placed on 50 or 250 mM NaCl and the total number of eggs laid were counted each day as described in the 'Methods'. Data are expressed as mean ± S.D. **** - $p < 0.0001$, ns = nonsignificant (Two-way ANOVA with post hoc Tukey's test). N = 10 independent broods for each strain. (D) Percent of progeny that developed into L4s. L4 animals were placed on 50 or 250 mM NaCl and the total number of eggs laid and progeny that developed into L4s were counted each day as described in the 'Methods'. Data are expressed as mean ± S.D. **** - $p < 0.0001$, ns = nonsignificant (Two-way ANOVA with post hoc Tukey's test). N = 10 independent broods for each strain. (E) Percent of moving unadapted and adapted day 3 adult animals exposed to 600 mM NaCl NGM plates for 24 hours. *ogt-1(dr20 dr36)* is a strain in which the *dr20* mutation was converted back to WT using CRISPR/Cas9 genome editing. The *gpdh-1(dr81)* allele is a CRISPR/Cas9 edited C-terminal knock-in of GFP into the endogenous *gpdh-1*. The *ogt-1(dr84)* allele is a CRISPR/Cas9 edited C-terminal knock-in of GFP into the endogenous *ogt-1*. Data are expressed as mean ± S.D. *** - $p < 0.001$, ns = nonsignificant (Two-way ANOVA with post hoc Tukey's test). N = 5 replicates of 20 animals for each strain.

In addition to physiological exposures, adaptation to HTS can also be induced genetically via LOF mutations in several hypodermis expressed secreted extracellular proteins. These mutants exhibit maximal induction of *gpdh-1* mRNA and accumulation of glycerol [324, 329]. As a result, these mutants are constitutively adapted to survive normally lethal levels of HTS. To test if *ogt-1* is required for genetic adaptation to HTS, I introduced the *ogt-1(dr20)* mutation into *osm-8(dr9)* or *osm-11(n1604)* mutants. Both *osm-8* and *osm-11* mutants exhibit constitutively elevated *gpdh-1p::GFP* expression under isotonic conditions [324, 329]. However, *gpdh-1p::GFP* levels were significantly reduced in *osm-8;ogt-1* and *osm-11;ogt-1* double mutants (Fig 2.2.7A and 2.2.7B). Consistent with this observation, the ability of *osm-8* mutants to survive a lethal HTS was suppressed in the *osm-8;ogt-1* double mutants (Fig 2.2.7C). These data suggest that *ogt-1* is

required for both physiological adaptation to HTS and genetic adaptation to HTS caused by loss of the extracellular proteins OSM-8 and OSM-11.

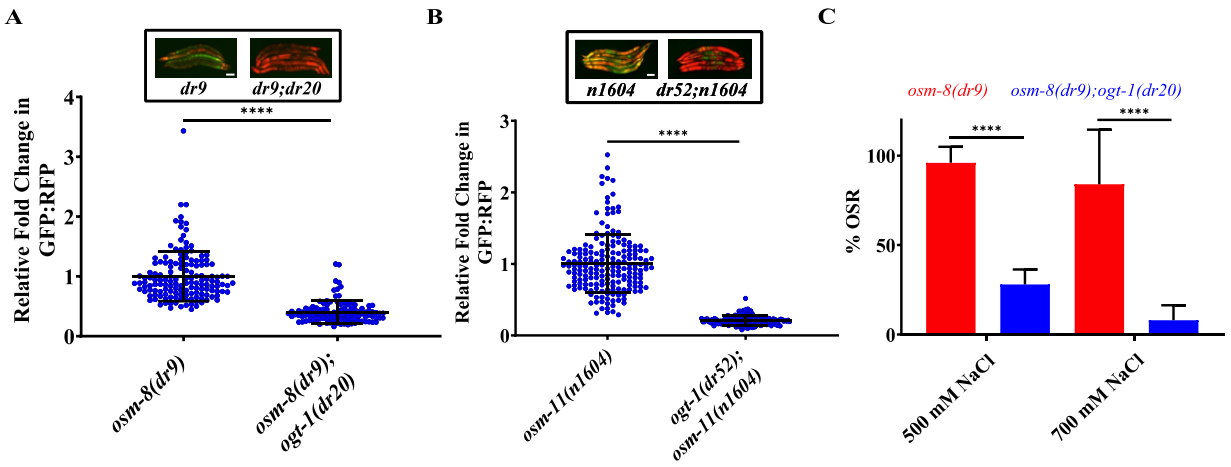

Figure 2.2.7 *ogt-1* is required for genetic adaptation to HTS

(A) COPAS Biosort quantification of GFP and RFP signal in day 2 adult animals expressing *drIs4* exposed to 50 mM NaCl NGM plates. Data are represented as the fold induction of normalized GFP/RFP ratio on 50 mM NaCl NGM plates with *osm-8(dr9)* set to 1. *osm-8(dr9)* was isolated in a previous genetic screen for new *osm-8* alleles but encodes the same mutation as the *n1518* reference allele. Each point represents the quantified signal from a single animal. Data are expressed as mean ± S.D. **** $p < 0.0001$ (Mann-Whitney test). $N \geq 109$ for each group. *Inset:* Wide-field fluorescence microscopy of day 2 adult animals expressing *drIs4* exposed to 50 mM NaCl NGM plates. Images depict merged GFP and RFP channels. Scale bar = 100 microns. (B) COPAS Biosort quantification of GFP and RFP signal in day 2 adult animals expressing *drIs4* exposed to 50 mM NaCl NGM plates. Data are represented as the fold induction of normalized GFP/RFP ratio on 50 mM NaCl NGM plates with *osm-11(n1604)* set to 1. The *ogt-1(dr52)* allele carries the same homozygous Q600STOP mutation as the *ogt-1(dr20)* allele, which was introduced using CRISPR/Cas9. Each point represents the quantified signal from a single animal. Data are expressed as mean ± S.D. **** $p < 0.0001$ (Mann-Whitney test). $N \geq 163$ for each group. *Inset:* Wide-field fluorescence microscopy of day 2 adult animals expressing *drIs4* exposed to 50 mM NaCl NGM plates. Images depict merged GFP and RFP channels. Scale bar = 100 microns. (C) Percent of moving (OSR) day 1 animals after exposure to 500 mM NaCl or 700 mM NaCl for 10 minutes. Data are represented as mean ± S.D. **** p – 0.0001 (Two-way ANOVA with post hoc Tukey's test). N = 5 replicates of 10 animals for each strain.

2.2.3 Non-canonical activity of *ogt-1* in the hypodermis regulates *gpdh-1* induction by hypertonic stress through a functionally conserved mechanism

I next investigated the functional requirements of OGT-1 in the HTSR. First, knock down of *ogt-1* during post-developmental stages with *ogt-1(RNAi)* was sufficient to cause a Nio phenotype. This result suggests that OGT-1 is not required for the establishment of developmental structures necessary for responding to HTS and that it is instead required acutely in the HTSR (Fig 2.2.8A).

In *C. elegans*, a CRISPR generated OGT-1-GFP allele is functional and is ubiquitously expressed throughout somatic cells in the nucleus, consistent with previous observations [362] (Fig 2.2.10B and 2.2.6E). Therefore, I used tissue specific promoters to test which tissues require *ogt-1* expression for *gpdh-1* induction by HTS. The expression of *ogt-1* from either its native promoter or a hypodermal specific promoter was sufficient to rescue *gpdh-1* induction by HTS in *ogt-1* LOF mutants (Fig 2.2.8B and 2.2.8C). Expression of *ogt-1* from an intestinal specific promoter or a muscle specific promoter caused weak but statistically significant rescue (Fig 2.2.8C). Expression of *ogt-1* in the neurons did not rescue. Since *gpdh-1* is induced by HTS in the hypodermis, these results suggest that *ogt-1* primarily acts cell autonomously in the hypoderm to regulate osmosenstive protein expression.

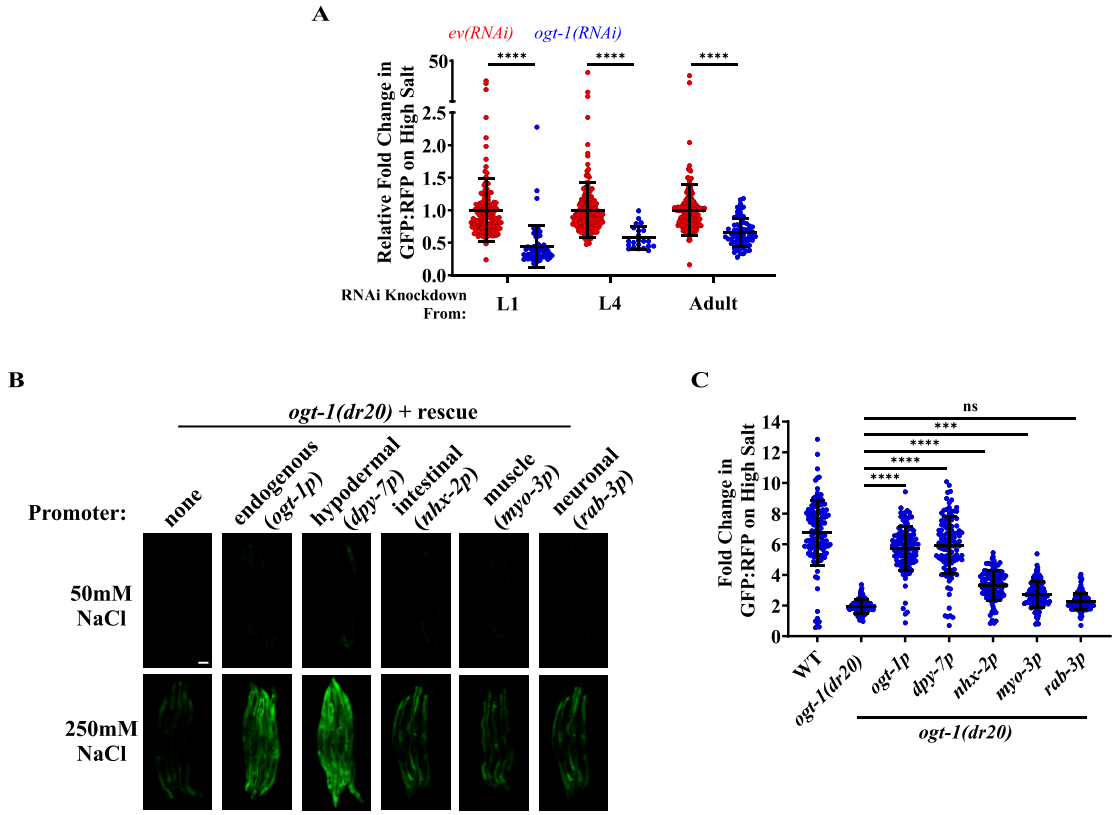

Figure 2.2.8 *ogt-1* expression is required acutely in the hypodermis for hypertonic induction of *gpdh-1p::GFP*

(A) COPAS Biosort quantification of GFP and RFP signal in day 2 adult animals expressing *drIs4* exposed to 50 or 250 mM NaCl NGM plates for 18 hours. Animals were placed on *ev(RNAi)* or *ogt-1(RNAi)* plates at the indicated stage. Data are represented as normalized fold induction of GFP/RFP ratio on 250 mM NaCl RNAi plates relative to on 50 mM NaCl RNAi plates, with *ev(RNAi)* set to 1 for each RNAi timepoint. Each point represents the quantified signal from a single animal. Data are expressed as mean ± S.D. **** - $p < 0.0001$ (Mann-Whitney test). $N \geq 144$ for each group. (B) Wide-field fluorescence microscopy of day 2 adult animals expressing *drIs4* exposed to 50 or 250 mM NaCl NGM plates for 18 hours. Strains express *ogt-1* cDNA from the indicated tissue-specific promoter. Images depict the GFP channel only for clarity. The RFP signal was unaffected in these rescue strains (not shown). Scale bar = 100 microns. (C) COPAS Biosort quantification of GFP and RFP signal in day 2 adult animals expressing *drIs4* exposed to 250 mM NaCl NGM plates for 18 hours. Data are represented as normalized fold induction of GFP/RFP ratio on 250 mM NaCl NGM plates relative to 50 mM NaCl NGM plates. Each point represents the quantified signal

from a single animal. Data are expressed as mean ± S.D. *** - $p < 0.001$, **** < 0.0001, ns = nonsignificant (Kruskal-Wallis test with post hoc Dunn's test). $N \geq 110$ for each group.

Given that *C. elegans* OGT-1 is highly conserved with human OGT (Fig 2.2.1A), I asked if human OGT could functionally replace *C. elegans* OGT-1 (*ce*OGT-1) in the HTSR. Overexpression of a human *Ogt* cDNA (*hs*OGT) from the native *C. elegans ogt-1* promoter exhibited weak but statistically significant rescue of *gpdh-1p::GFP* induction by HTS in an *ogt-1* LOF mutant (Fig 2.2.9A and 2.2.9B). Unexpectantly, catalytically inhibited human OGT (OGT H498A) rescued *gpdh-1p::GFP* induction by HTS in an *ogt-1(dr20)* LOF mutant to the same extent as WT human OGT (Fig 2.2.9A and 2.2.9B). To further test the requirement for OGT-1 *O*-GlcNAcylation in the HTSR, I CRISPR engineered catalytically inactive mutations into the endogenous *C. elegans ogt-1* locus (H612A and K957M, equivalent to human H498A and K842M respectively). Surprisingly, only the K957M mutation completely suppressed *O*-GlcNAcylation activity (Fig 2.2.10A). The H612A mutation reduced *O*-GlcNAcylation but did not eliminate it (Fig 2.2.10A). However, neither the K957M nor the H612A mutation altered OGT-1 protein levels or nuclear localization (Fig 2.2.10B). In agreement with the results from the catalytically inhibited human OGT rescue experiments, *C. elegans* expressing catalytically impaired alleles of endogenous *ogt-1* induced *gpdh-1p::GFP* during HTS and had normal acute adaptation during HTS (Fig 2.2.10C, 2.2.10D, and 2.2.10E). In conclusion, a non-catalytic function of OGT-1 in the hypodermis is required for osmosensitive protein induction by HTS and this function may be conserved from *C. elegans* to humans.

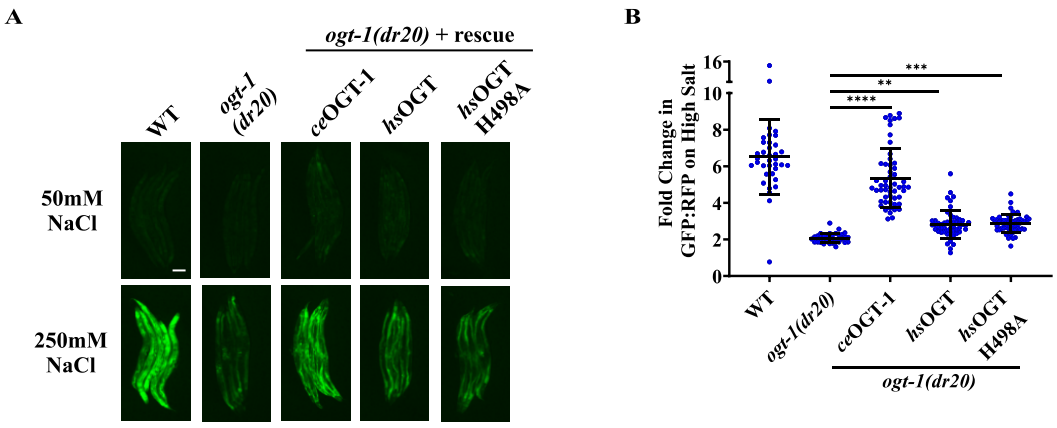

Figure 2.2.9 Overexpression of human *Ogt* partially rescues hypertonic induction of *gpdh-1p::GFP*

(A) Wide-field fluorescence microscopy of day 2 adult animals expressing *drIs4* exposed to 50 or 250 mM NaCl NGM plates for 18 hours. For the WT and catalytically inactive human rescue strains, we expressed a human cDNA (*hs*OGT) corresponding to isoform 1 of OGT using an extrachromosomal array. Images depict the GFP channel only for clarity. The RFP signal was unaffected in these rescue strains (not shown). Scale bar = 100 microns. (B) COPAS Biosort quantification of GFP and RFP signal in day 2 adult animals expressing *drIs4* exposed to 250 mM NaCl NGM plates for 18 hours. Data are represented as normalized fold induction of GFP/RFP ratio on 250 mM NaCl NGM plates relative to 50 mM NaCl NGM plates. Each point represents the quantified signal from a single animal. Data are expressed as mean ± S.D. **** - $p < 0.0001$, *** - $p < 0.001$, ** - $p < 0.01$ (Kruskal-Wallis test with post hoc Dunn's test). $N \geq 40$ for each group.

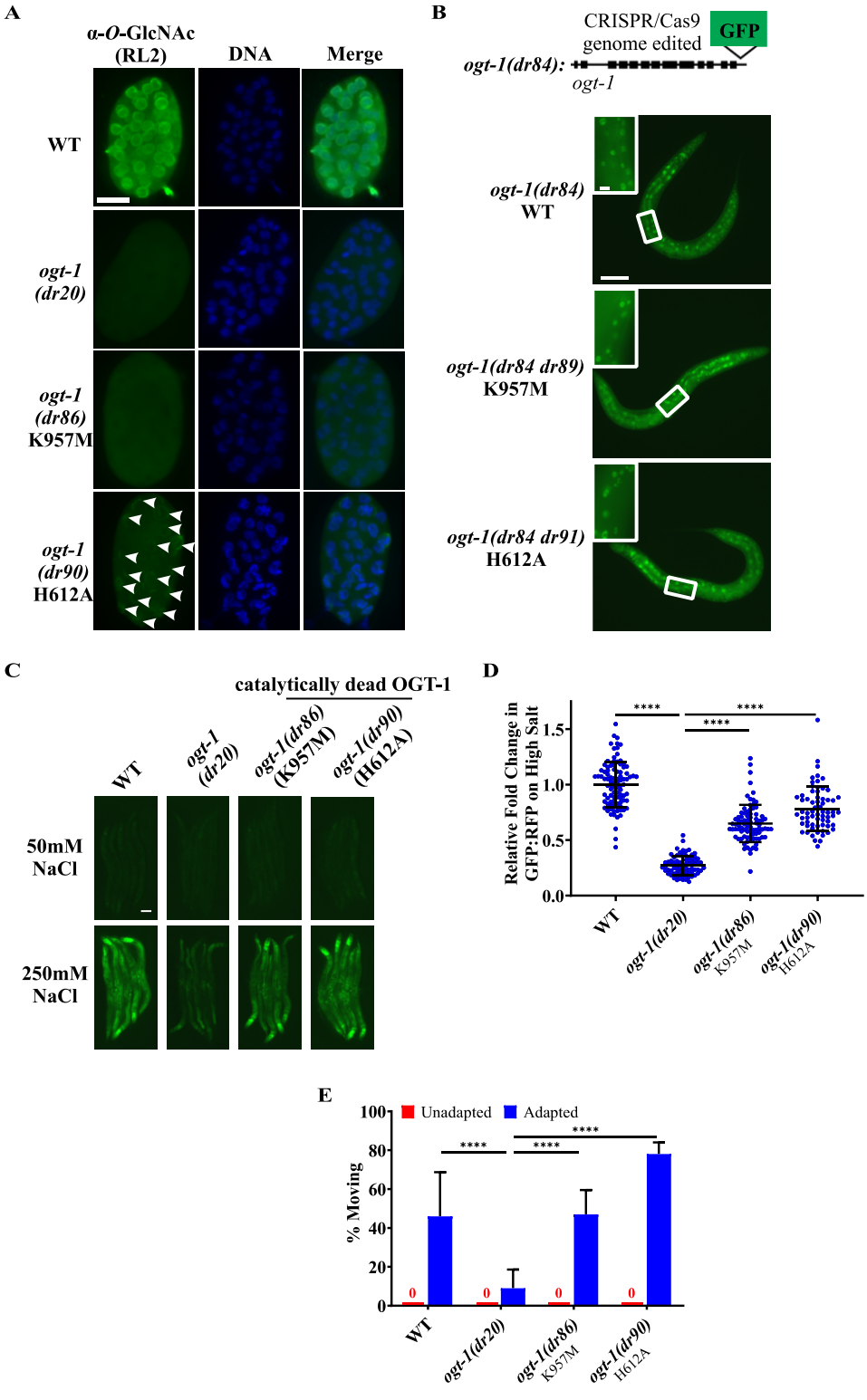

Figure 2.2.10 OGT-1 functions through a non-catalytic mechanism to regulate hypertonic induction of *gpdh-1p::GFP* and adaptation to HTS

(A) Wide-field fluorescence microscopy of fixed and stained embryos. RL2 was used to stain for nuclear pore *O*-GlcNAc modifications and Hoechst 33258 was used to visualize the DNA. Images are exposure matched. White arrowheads indicate RL2 staining in OGT-1^{H612A} embryos. Scale bar = 10 microns. (B) Wide-field fluorescence microscopy of day 1 adult animals expressing endogenously CRISPR/Cas9 GFP tagged OGT-1 exposed to 50 mM NaCl NGM plates. Scale bar = 100 microns. Images are exposure matched. *Inset:* Zoomed in images of the boxed area. Scale bar = 10 microns. (C) Wide-field fluorescence microscopy of day 2 adult animals expressing *drIs4* exposed to 50 or 250 mM NaCl NGM plates for 18 hours. Images depict the GFP channel only for clarity. The RFP signal was unaffected in these rescue strains (not shown). Scale bar = 100 microns. (D) COPAS Biosort quantification of GFP and RFP signal in day 2 adult animals expressing *drIs4* exposed to 250 mM NaCl NGM plates for 18 hours. Data are represented as the fold induction of normalized GFP/RFP ratio on 250 mM NaCl NGM plates relative to 50 mM NaCl NGM plates, with WT induction set to 1. Each point represents the quantified signal from a single animal. Data are expressed as mean ± S.D. **** - $p < 0.0001$ (Kruskal-Wallis test with post hoc Dunn's test). $N \geq 81$ for each group. (E) Percent of moving unadapted and adapted day 3 adult animals expressing *drIs4* exposed to 600 mM NaCl NGM plates for 24 hours. Data are expressed as mean ± S.D. **** - $p < 0.0001$ (Two-way ANOVA with post hoc Tukey's test). N = 5 replicates of 20 animals for each strain.

In addition to the catalytic domain of OGT, another functionally important domain in OGT is the tetratricopeptide repeat (TPR) domain [366]. This domain mediates protein-protein interactions thought to be important for the binding of *O*-GlcNAcylation substrates. To determine if the TPR domain is also required for the HTSR in *C. elegans*, I used CRISPR to engineer a complete deletion of the TPR domain in the *ogt-1* locus (ΔTPR (128aa-583aa)). The ΔTPR mutation suppressed *O*-GlcNAcylation completely (Fig 2.2.11A). However, it did not alter OGT-1-GFP protein levels or localization (Fig 2.2.11B). *C. elegans* expressing the *ogt* ΔTPR allele (*ogt-1(dr93))* had impaired *gpdh-1p::GFP* induction during HTS and impaired adaptation during HTS (Fig 2.2.11C, 2.2.11D and 2.2.11E). Therefore, a TPR-dependent, *O*-GlcNAcylation-independent function of OGT-1 is required in the HTSR.

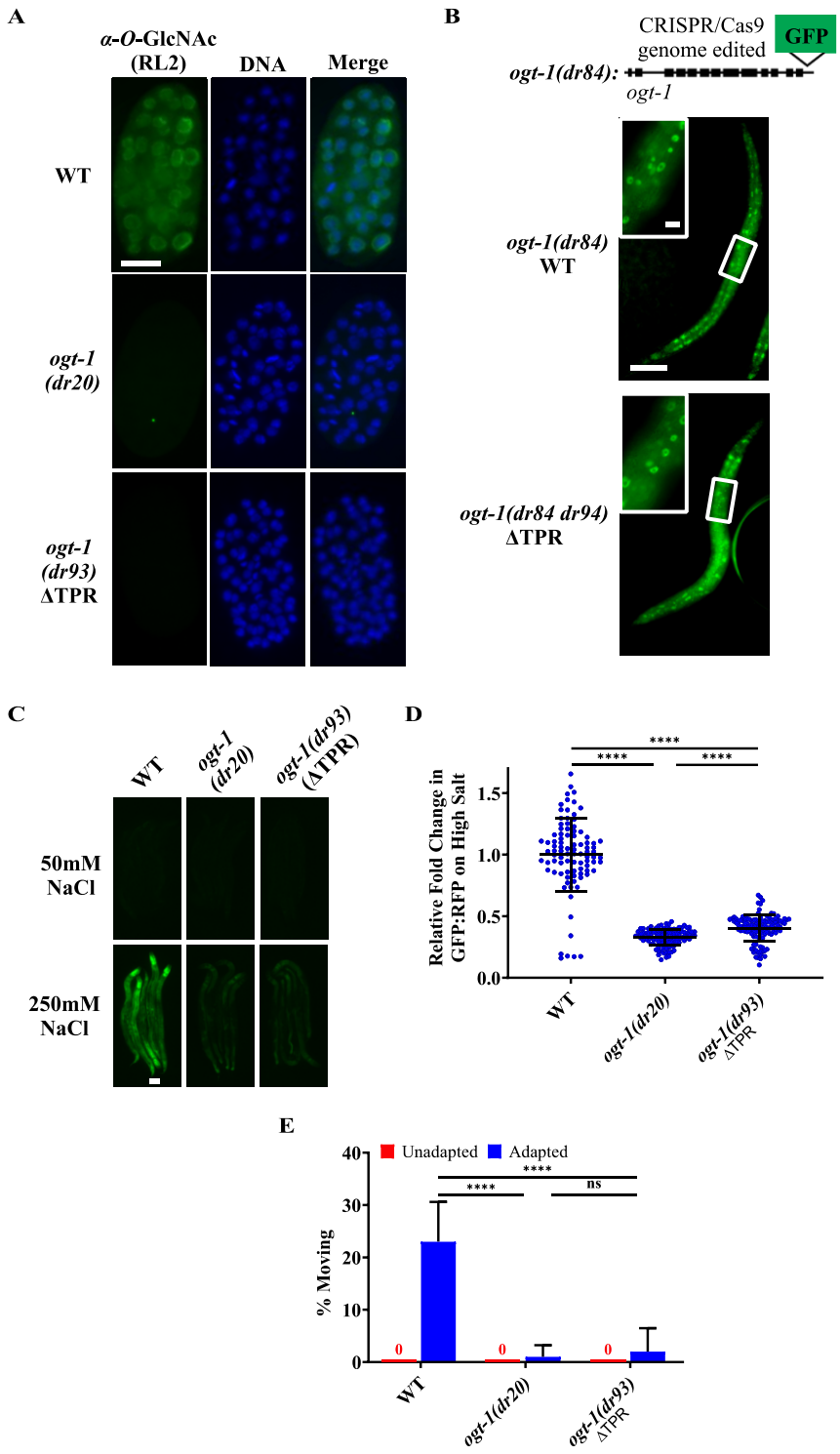

Figure 2.2.11 The tetratricorepeat domain of OGT-1 is required for hypertonic induction of *gpdh-1p::GFP* and adaptation to HTS

(A) Wide-field fluorescence microscopy of fixed and stained embryos. RL2 was used to stain for nuclear pore *O*-GlcNAc modifications and Hoechst 33258 was used to visualize the DNA. Images are exposure matched. Scale bar = 10 microns. (B) Wide-field fluorescence microscopy of day 1 adult animals expressing endogenously CRISPR/Cas9 GFP tagged OGT-1 exposed to 50 mM NaCl NGM plates. Scale bar = 100 microns. Images are exposure matched. *Inset:* Zoomed in images of the boxed area. Scale bar = 10 microns. (C) Wide-field fluorescence microscopy of day 2 adult animals expressing *drIs4* exposed to 50 or 250 mM NaCl NGM plates for 18 hours. Images depict the GFP channel only for clarity. The RFP channel was unaffected in these rescue strains (not shown). Scale bar = 100 microns. (D) COPAS Biosort quantification of GFP and RFP signal in day 2 adult animals expressing *drIs4* exposed to 250 mM NaCl NGM plates for 18 hours. Data are represented as the fold induction of normalized GFP/RFP ratio on 250 mM NaCl relative to on 50 mM NaCl NGM plates, with WT induction set to 1. Each point represents the quantified signal from a single animal. Data are expressed as mean ± S.D. **** - $p < 0.0001$ (Kruskal-Wallis test with post hoc Dunn's test). $N \geq 92$ for each group. (E) Percent of moving unadapted and adapted day 3 adult animals expressing *drIs4* exposed to 600 mM NaCl NGM plates for 24 hours. Data are expressed an mean ± S.D. **** - $p < 0.0001$, ns = nonsignificant (Two-way ANOVA with post hoc Tukey's test). N = 5 replicates of 20 animals for each strain.

2.3 Interacting components of the 3' mRNA cleavage and polyadenylation complex are required for the hypertonic induction of GPDH-1 and physiological adaptation to hypertonic stress

In our forward genetic screen for Nio mutants I identified two recessive mutants, *nio-3(dr16)* and *nio-7*(*dr23)*, that exhibited impaired hypertonic induction of *gpdh-1p::GFP* and adaptation to HTS (Fig 2.1.2C and 2.1.3D). Through whole genome sequencing, bioinformatics, and RNAi screening of *nio* gene candidates, I found that the phenotype causing mutations in *nio-3(dr16)* and *nio-7(dr23)* were both missense mutations in interacting components of the conserved

3’ mRNA cleavage and polyadenylation complex (APA complex). Our analysis revealed that a G42E mutation in the mammalian cleavage stimulation factor subunit 2 (CSTF2/CstF-64) homolog CPF-2 and a R580W mutation in the mammalian symplekin (SYMPK) homolog SYMK-1 caused *nio-3(dr16)* and *nio-7(dr23)* mutants respectively to have an impaired HTSR (Fig 2.3.1, 2.1.2B, 2.1.2C, 2.1.3D, Table 2.1.1, 2.1.2, 2.1.3, and 2.1.4). Consistent with the hypothesis that these missense alleles cause a LOF phenotype, RNAi knockdown of *cpf-2* and *symk-1*, which produces genetic LOF, also inhibited the hypertonic induction of *gpdh-1p::GFP* (Fig 2.3.2A and 2.3.2B). Furthermore, transgenic overexpression of a *cpf-2* DNA fragment in *nio-3(dr16)* mutants and a *symk-1*-containing fosmid in *nio-7(dr23)* mutants rescued hypertonic induction of *gpdh-1p::GFP* (Fig 2.3.2C, 2.3.2D, and 2.3.2E).

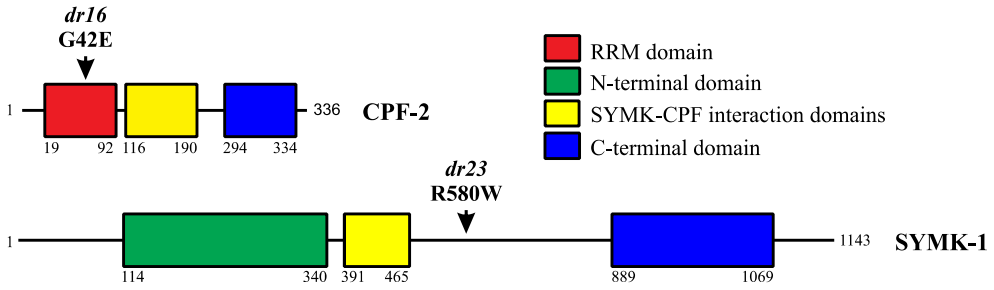

Figure 2.3.1 The *nio-3(dr16)* and *nio-7(dr23)* mutants contain distinct LOF mutations in the CstF-64 homolog *cpf-2* and the symplekin homolog *symk-1* respectively that impair the HTSR

C. elegans CPF-2 and SYMK-1 protein domain diagrams detailing the positions of the two LOF alleles identified in the screen (*dr16* and *dr23*).

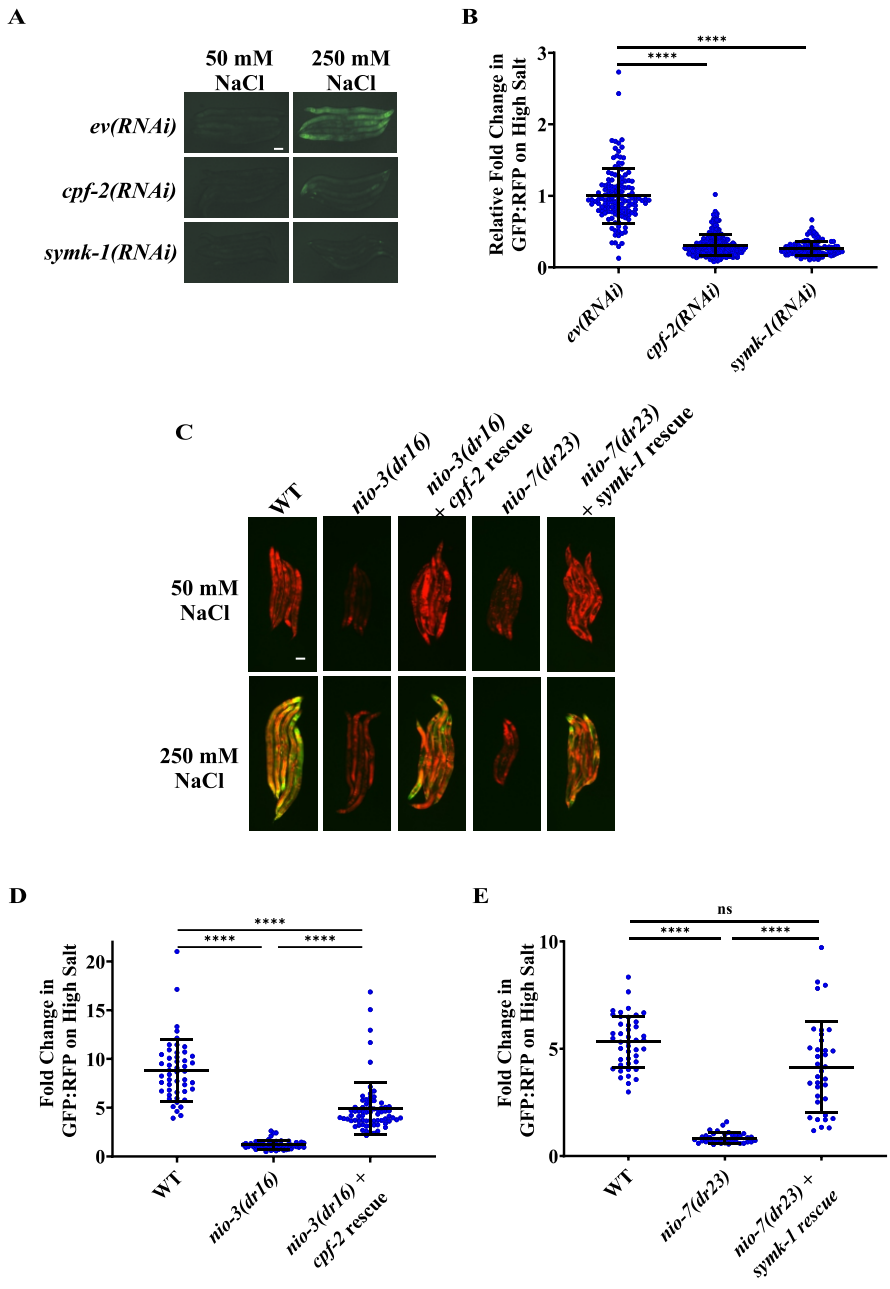

Figure 2.3.2 *cpf-2* and *symk-1* are required for hypertonic induction of *gpdh-1p::GFP*

(A) Wild-field fluorescence microscopy of day 2 adult WT animals expressing *drIs4* grown on *ev(RNAi)* or *ogt-1(RNAi)* plates and exposed to 50 or 250 mM NaCl. Images depict the GFP channel only for clarity. Scale bar = 100 microns. (B) COPAS Biosort quantification of GFP and RFP signal in day 2 adult WT animals expressing *drIs4* grown on *ev(RNAi)* or *ogt-1(RNAi)* plates and exposed to 250 mM NaCl NGM plates for 18 hours. Data are represented as fold induction of normalized GFP/RFP ratio on 250 mM NaCl RNAi plates relative to on 50 mM NaCl

RNAi plates, with WT fold induction on *ev(RNAi)* and 250 mM NaCl set to 1. Each point represents the quantified signal from a single animal. Data are expressed as mean ± S.D. **** - $p < 0.0001$ (Kruskal-Wallis test with post hoc Dunn's test). $N \geq 99$ for each group. (C) Wide-field fluorescence microscopy of day 2 adult WT, *nio-3(dr16)* and *nio-7(dr23)* mutant animals exposed to 50 or 250 mM NaCl NGM plates for 18 hours. The *cpf-2* rescue animals express an extrachromosomal array with a *cpf-2* genomic DNA fragment containing ~2 Kb upstream and ~1 Kb domnstream of the coding sequence. The *symk-1* rescue animals express a fosmid containing the *symk-1* genomic sequence. All strains express *drIs4.* Images depict merged GFP and RFP channels. Scale bar = 100 microns. (D) COPAS Biosort quantification of GFP and RFP signal in day 2 adult animals expressing *drIs4* exposed to 250 mM NaCl NGM plates for 18 hours. The *cpf-2* rescue animals express an extrachromosomal array with a *cpf-2* genomic DNA fragment containing ~2 Kb upstream and ~1 Kb domnstream of the coding sequence. Data are represented as the fold induction of normalized GFP/RFP ratio on 250 mM NaCl relative to on 50 mM NaCl NGM plates. Each point represents the quantified signal from a single animal. Data are expressed as mean ± S.D. **** - $p < 0.0001$ (Kruskal-Wallis test with post hoc Dunn's test). $N \geq 49$ for each group. (E) COPAS Biosort quantification of GFP and RFP signal in day 2 adult animals expressing *drIs4* exposed to 250 mM NaCl NGM plates for 18 hours. The *symk-1* rescue animals express a fosmid containing the *symk-1* genomic sequence. Data are represented as the fold induction of normalized GFP/RFP ratio on 250 mM NaCl relative to on 50 mM NaCl NGM plates. Each point represents the quantified signal from a single animal. Data are expressed as mean ± S.D. **** - $p < 0.0001$, ns = nonsignificant (Kruskal-Wallis test with post hoc Dunn's test). $N \geq 35$ for each group.

Similarly to *ogt-1, cpf-2* and *symk-1* are required for hypertonic induction of the *gpdh-1p::GPDH-1-GFP* translational reporter (*kbIs6*) (Fig 2.3.3). Additionally, since *nio-3(dr16)* and *nio-7(dr23)* mutants have an acute HTS adaptation phenotype, this suggests that *cpf-2* and *symk-1*, like *ogt-1*, are required physiologically during HTS (Fig 2.1.3D). However, unlike *ogt-1* mutants, *nio-3/cpf-2(dr16)* and *nio-7/symk-1(dr23)* mutants have slightly reduced hypertonic induction of endogenous *gpdh-1* RNA and GFP RNA derived from the *gpdh-1p::GFP* reporter compared to WT animals (mean ± S.D. of fold change in *gpdh-1* RNA on high salt – WT 17.8 ±

4.3, *cpf2/nio-3(dr16)* 7.9 ± 0.2, *symk-1/nio-7(dr23)* 2.5 ± 0.3, mean ± S.D. of fold change in *GFP* RNA on high salt – WT 12.9 ± 2.8, *cpf-2/nio-3(dr16)* 10.7 ± 1.3, *symk-1*/*nio-7(dr23)* 3.5 ± 3.3) (Fig 2.1.3A and 2.1.3B). However, these reductions were not statistically significant when compared with all the *nio* mutants (Fig 2.1.3A and 2.1.3B). These results in combination suggest that in contrast to *ogt-1*, *cpf-2* and *symk-1* may function to regulate the mRNA induction of *gpdh-1* during HTS.

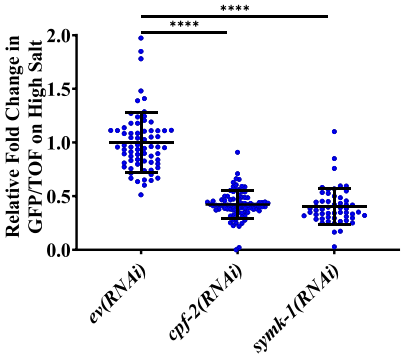

Figure 2.3.3 *cpf-2* and *symk-1* are required for hypertonic induction of *gpdh-1p::GPDH-1-GFP*

COPAS Biosort quantification of GFP and TOF signal in day 2 adult animals expressing the *kbIs6* GPDH-1 translational fusion grown on *ev(RNAi)* or *ogt-1(RNAi)* and exposed to 250 mM NaCl NGM plates for 18 hours. Data are represented as relative fold induction of normalized GFP/TOF ratio on 250 mM NaCl NGM plates versus 50 mM NaCl NGM plates, with WT induction on *ev(RNAi)* and 250 mM NaCl set to 1. Each point represents the quantified signal from a single animal. Data are expressed as mean ± S.D. **** - $p < 0.0001$ (Kruskal-Wallis test with post hoc Dunn's test). $N \geq 54$ for each group.

To begin investigating the dynamics and interplay of the APA complex and OGT-1 in the HTSR, I studied the localization of CPF-2 and OGT-1 during isotonic and hypertonic conditions. In isotonic conditions a functional endogenously CRISPR/Cas9 tagged tagRFP-CPF-2 allele had a diffuse nuclear localization in the hypodermis, intestine and germline (Fig 2.3.4A, 2.3.4B, and 2.3.4C). In the same strain in isotonic conditions, an endogenously CRISPR/Cas9 tagged OGT-

1-GFP allele had a similar nuclear localization as tagRFP-CPF-2, except that it was not detectably expressed in the germline (Fig 2.3.4A, 2.3.4B, and 2.3.4C). In response to HTS of 600 mM NaCl for 24h, both tagRFP-CPF-2 and OGT-1-GFP formed nuclear puncta. Puncta formation of both these proteins was most robust in the hypodermis, but it also occurred in intestinal cells (Fig 2.3.4A and 2.3.4B). Neither tagRFP-CPF-2 nor OGT-1-GFP formed puncta in the germline in response to HTS (Fig 2.3.4C). Interestingly, the tagRFP-CPF-2 and OGT-1-GFP puncta that formed in the hypodermis did not co-localize with one another (Fig 2.3.4A). These results suggest that HTS causes the redistribution of both CPF-2 and OGT-1 into distinct nuclear compartments in the hypodermis. However, the specific characteristics and functional significance of these nuclear puncta remain unknown.

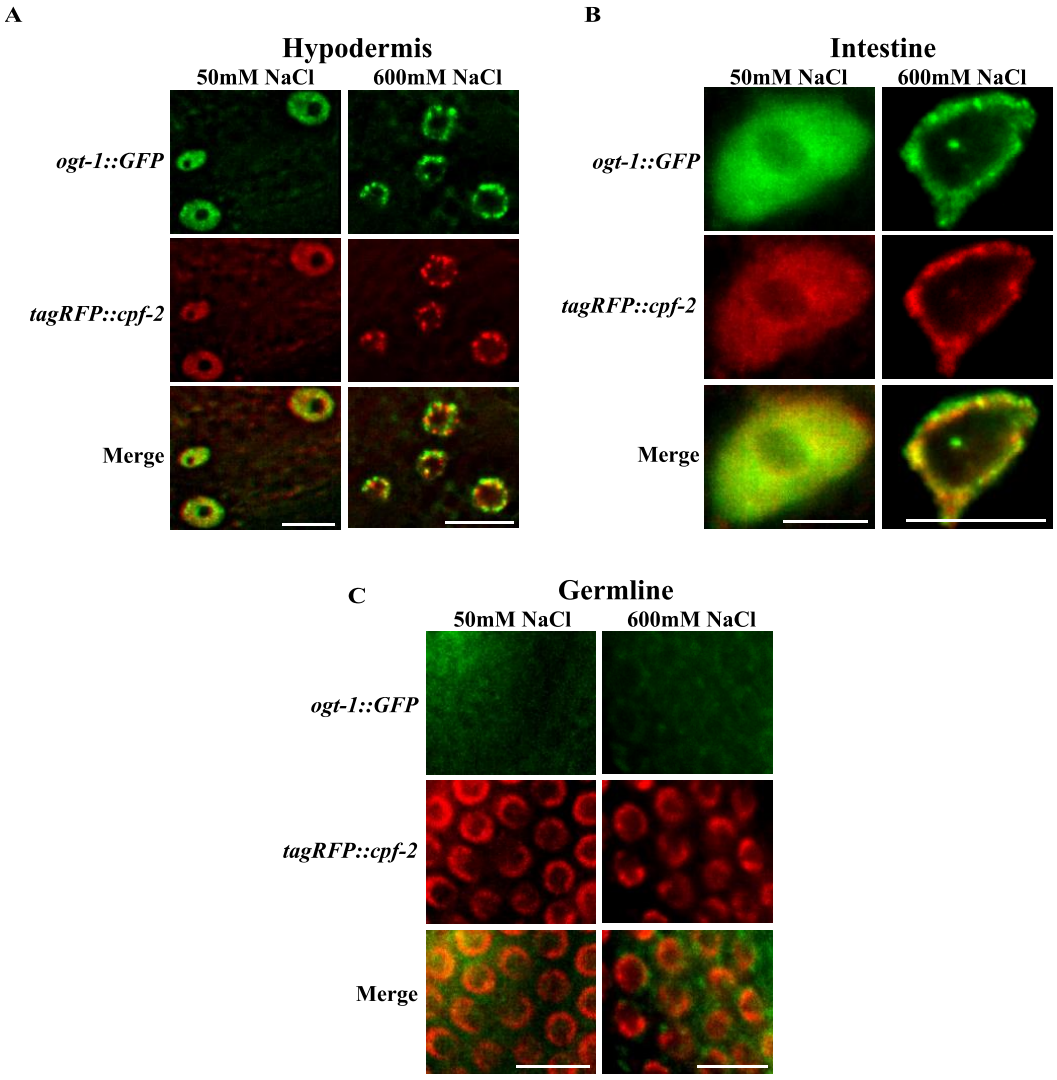

Figure 2.3.4 CPF-2 and OGT-1 form puncta during HTS that do not colocalize

(A) Wide-field fluorescence microscopy of hypodermal cells from day 2 adult animals exposed to 600 mM NGM NaCl plates for 24 hours. Animals express functional endogenously CRISPR/Cas9 GFP tagged OGT-1 and tagRFP tagged CPF-2. Images are exposure matched. Images depict GFP, RFP, and merged channels. Scale bar = 10 microns. (B) Wide-field fluorescence microscopy of intestinal cells from day 2 adult animals exposed to 600 mM NGM NaCl plates for 24 hours. Animals express functional endogenously CRISPR/Cas9 GFP tagged OGT-1 and tagRFP tagged CPF-2. Images are exposure matched. Images depict GFP, RFP, and merged channels. Scale bar = 10 microns. (C) Wide-field fluorescence microscopy of germline cells from day 2 adult animals exposed to 600 mM NGM NaCl plates

for 24 hours. Animals express functional endogenously CRISPR/Cas9 GFP tagged OGT-1 and tagRFP tagged CPF-2. Images are exposure matched. Images depict GFP, RFP, and merged channels. Scale bar = 10 microns.

3.0 Discussion

The maintenance of cell volume is critical to cellular function because it directly influences protein folding [2], enzymatic activity [3, 4], membrane potential [5] and cytoskeletal architecture [6]. Therefore, virtually all cells have evolved protective mechanisms to counteract changes in cell volume. These mechanisms are mostly conserved across cell types and organisms and have been extensively characterized over the last several decades. However, the cellular pathways that regulate these protective mechanisms remain poorly understood. In my thesis project, I employed unbiased genetic methods in the small metazoan *C. elegans* to identify the cellular pathways regulating the response to cell volume changes, specifically those induced by HTS.

3.1 Identification of mutant *C. elegans* with impaired induction of the hypertonic stress response through an unbiased fluorescence based forward genetic screen

To characterize the metazoan HTSR, I conducted an unbiased forward genetic screen in *C. elegans* to identify mutants with impaired induction of osmosensitive gene expression. I identified ten single gene recessive mutants with decreased induction of the osmolyte accumulation gene reporter *gpdh-1p::GFP* during HTS. I refer to this phenotype as the Nio (no induction of osmolyte accumulation) phenotype. Genetic complementation analysis revealed that these ten Nio mutants represented seven *nio* genes and there were two alleles of *nio-2* and three alleles of *nio-5*. Surprisingly, hypertonic induction of endogenous *gpdh-1* mRNA and GFP mRNA derived from the *gpdh-1p::GFP* reporter continued to be upregulated in the majority of the Nio mutants.

Additionally, none of the Nio mutants had a survival phenotype and only three Nio mutants had a severe acute adaptation phenotype during HTS. The identification of several mutants with both impaired genetic and physiological induction of the HTSR highlights the feasibility of our genetic screening strategy.

However, there are likely additional *nio* genes that remain to be identified because our genetic screen did not reach saturation. A forward genetic screen is saturated when several alleles of the same genes are identified instead of alleles of new genes. Saturation indicates that all the genes in a pathway, at least all the genes that can be isolated through genetic screening methods, have been found. For example, in my genetic screen I did not identify predicted members of the HTSR pathway such as genes that encode transcription factors or extracellular proteins. Continued Nio screening may uncover these predicted HSTR factors and provide a more detailed understanding of the HTSR pathway.

Forward genetic screening methods in *C. elegans* have been used for decades to understand genetic pathways [311-314]. The beauty of the forward genetic screen is that it is an unbiased approach to let the organism and/or cells reveal what genes are important for a phenotype. Therefore, it is common to uncover unanticipated cellular pathways and mechanisms of gene regulation through forward genetic screens. Despite not reaching saturation, my Nio screen was no exception as it provided me with unexpected results. We designed the Nio screen with the expectation that we would identify genes, such as transcription factors, required for the transcriptional upregulation of *gpdh-1* during HTS. However, to our surprise the majority of the *nio* genes I identified were not required for hypertonic upregulation of *gpdh-1* mRNA, despite being required for induction of *gpdh-1p::GFP* reporter fluorescence. *nio-3* and *nio-7* were the only two *nio* genes that were likely required for induction of *gpdh-1* mRNA, as both these mutants

had a slightly decreased fold induction of *gpdh-1* mRNA during HTS, although not statistically significant when compared with all the Nio mutants. Therefore, instead of isolating the expected candidates, our genetic screen revealed that the HTSR pathway is more nuanced than we anticipated.

The results from our Nio screen unexpectedly suggest that in the majority of Nio mutants, regulation of the overexpressed *gpdh-1p::GFP* reporter protein is distinct from regulation of *gpdh-1* mRNA during HTS. One possible explanation for this phenomenon is that the Nio mutants contain transgene suppressor mutations. Although forward genetic screens can provide an unbiased lens into cellular pathways, they are limited by the screening method, i.e. you get what you screen for. Transgene suppressor mutations inhibit the expression of overexpressed transgenes, such as the *gpdh-1p::GFP* reporter, without affecting endogenous gene expression. However, three pieces of evidence suggest that the Nio mutants do not contain transgene suppressor mutations. First, transgene suppressor mutations would also inhibit expression of the *col-12p::dsRed2* reporter, which was not the case in the Nio mutants. Second, transgene suppressor mutations would inhibit hypertonic induction of GFP mRNA derived from the *gpdh-1p::GFP* reporter. However, the Nio mutants upregulated GFP mRNA during HTS. Finally, although we did not examine this in all of the Nio mutants, *nio-2* mutants expressed GFP reporters other than the *gpdh-1p::GFP* reporter at WT levels or higher, supporting the conclusion that fluorescent reporter expression is not generally affected in the Nio mutants. Therefore, it is unlikely that the Nio mutants contain transgene suppressor mutations.

Since our evidence indicates that reporter fluorescence is not generally inhibited in the Nio mutants because they do not contain transgene suppressor mutations, this suggests that the majority of the *nio* genes may be required post-transcriptionally for hypertonic GPDH-1 protein expression

(Table 3.1.1). While we provide evidence that *nio-2/ogt-1* mutants have decreased GPDH-1 protein expression during HTS, this still needs to be explicitly tested in the remaining Nio mutants. If all the Nio mutants have decreased hypertonic induction of GPDH-1 like *nio-2* mutants, this would surprisingly suggest that the HTSR is under strong post-transcriptional regulation. Although evidence exists that other cellular stress responses, such as the heat shock and ER stress response, are regulated post-transcriptionally via modulation of translation initiation factors [426, 495], this is the first evidence that the HTSR is also under post-transcriptional control.

C. elegans upregulates osmosensitive genes, including *gpdh-1*, to survive and adapt to HTS [317, 318]. Survival is the ability of animals grown in isotonic conditions to survive a 24 hour exposure to HTS [318]. Adaptation is measured as either acute or chronic adaptation. Acute adaptation is the ability of animals to upregulate adaptative responses that facilitate survival under normally lethal HTS after a pre-conditioning stimulus [318]. Chronic adaptation is the ability of animals to develop under continuous non-lethal HTS [319].

The survival of all seven Nio mutants did not depend on environmental hypertonicity (Table 3.1.1). This result was not surprising since *gpdh-1* null mutants also do not have a survival phenotype [317]. However, despite their WT survival during HTS, five out of the seven Nio mutants and *gpdh-1* null mutants had an acute adaptation phenotype (Table 3.1.1). *nio-2, -3,* and *-7* mutants had the most severe phenotype, with virtually no ability to adapt to HTS, suggesting that these genes regulate more than just *gpdh-1* to facilitate adaptation to HTS. Interestingly, *nio-1* and *nio-5* mutants did not have an impaired ability to adapt to HTS, despite having impaired hypertonic *gpdh-1p::GFP* reporter induction. This lack of an acute adaptation phenotype suggests that *nio-1* and *nio-5* mutants retain enough GPDH-1 activity to accumulate sufficient glycerol over

a 24 hour period to facilitate acute adaptation to HTS. Therefore, *nio-1* and *nio-5* are likely only partially required for GPDH-1 induction during HTS.

Table 3.1.1 Summary of the Nio mutant phenotypes

The genetic and physiological phenotypes of each Nio mutant are summarized.

Mutant	*gpdh-1p::GFP* reporter fluorescence induction by HTS?	*gfp* mRNA induction by HTS?	*gpdh-1* mRNA induction by HTS?	HTS acute survival phenotype?	HTS acute adaptation phenotype?	HTS chronic adaptation phenotype?
nio-1(dr14)	No	Yes	Yes	No	No	Unknown
nio-2(dr15/dr20)	No	Yes	Yes	No	Yes	Yes
nio-3(dr16)	No	Reduced	Reduced	No	Yes	Unknown
nio-4(dr17)	No	Yes	Yes	No	Yes	Unknown
nio-5(dr13/dr18/dr22)	No	Yes	Yes	No	No	Unknown
nio-6(dr19)	No	Yes	Yes	No	Yes	Unknown
nio-7(dr23)	No	Reduced	Reduced	No	Yes	Unknown

In conclusion, our Nio screen revealed that *gpdh-1* induction during HTS is under post-transcriptional regulation by several *nio* genes. Although we are still in the preliminary stages of characterizing many of these Nio mutants, the results from this screen represent the first indication that the HTSR is under post-transcriptional control. Post-transcriptional regulation of cellular stress responses is a relatively new and growing field of study and it will be interesting to determine the post-transcriptional mechanisms at play in the HTSR. Further characterization of *nio-2/ogt-1* mutants has provided us with a platform from which to start answering these questions.

3.1.1 Future directions

Since our Nio screen did not reach saturation, continued Nio screening will likely reveal additional genes and/or cellular pathways that regulate the HTSR. In our initial iteration of the Nio screen, we screened animals for decreased *gpdh-1p::GFP* expression during HTS. However,

in future Nio screens it will be useful to screen animals for both decreased *gpdh-1p::GFP* expression and impaired adaptation during HTS in order to identify *nio* genes that are required for both the genetic and physiological components of the HTSR. This modification to the genetic screen should enrich for bona fide components of the HTSR pathway. Through this type of screen I expect the newly identified *nio* genes to fall into one of two categories: those that are required for both the mRNA and protein induction of *gpdh-1* during HTS (like *cpf-2* and *symk-1*) and those that are required for only the protein induction of *gpdh-1* during HTS (like *ogt-1*). By carrying the Nio screen out to saturation we will identify genes that function with *ogt-1*, the APA complex, or in different pathways to regulate the HTSR.

3.2 The *O*-GlcNAc transferase OGT-1 is required post-transcriptionally for the hypertonic induction of GPDH-1 and physiological adaptation to hypertonic stress

In our unbiased forward genetic screen for mutants that disrupt osmosensitive expression of a *gpdh-1p::GFP* reporter in *C. elegans* (Nio mutants), I identified multiple alleles of the *O*-GlcNAc transferase OGT-1 . *ogt-1* likely functions as a key signaling component of the HTSR, since post-developmental knockdown of *ogt-1* was sufficient to cause the Nio phenotype. Furthermore, *ogt-1*-dependent signaling in the HTSR is required in the hypodermis, a known osmosensitive tissues in *C. elegans* [317, 329]. The mechanism by which *ogt-1* regulates hypertonicity induced gene expression was unexpected. *ogt-1* mutants exhibited hypertonicity induced upregulation of stress response mRNAs. However, the level of at least one reporter protein, GPDH-1::GFP, was significantly reduced, suggesting *ogt-1* acts via a post-transcriptional mechanism(s). Interestingly, *ogt-1* was not required for hypertonic induction of the *nlp-29::GFP*

reporter, suggesting that the effect of *ogt-1* is linked to *gpdh-1* and not GFP. Additionally, *ogt-1* mutants were completely unable to adapt and develop in hypertonic environments and this correlated with an inability of *ogt-1* mutants to properly upregulate the translation of osmoprotective proteins such as GPDH-1-GFP. Intriguingly, I demonstrated that the function of *ogt-1* in the HTSR did not require *O*-GlcNAcylation catalytic activity. This non-catalytic function of OGT-1 may be conserved with humans as both WT and catalytically inactive human OGT partially rescued the *C. elegans ogt-1* Nio phenotype. However, *C. elegans* expressing OGT-1 without the TPR domain were Nio, suggesting that unlike the catalytic activity, the TPR domain is required for the HTSR (Figure 3.2.1).

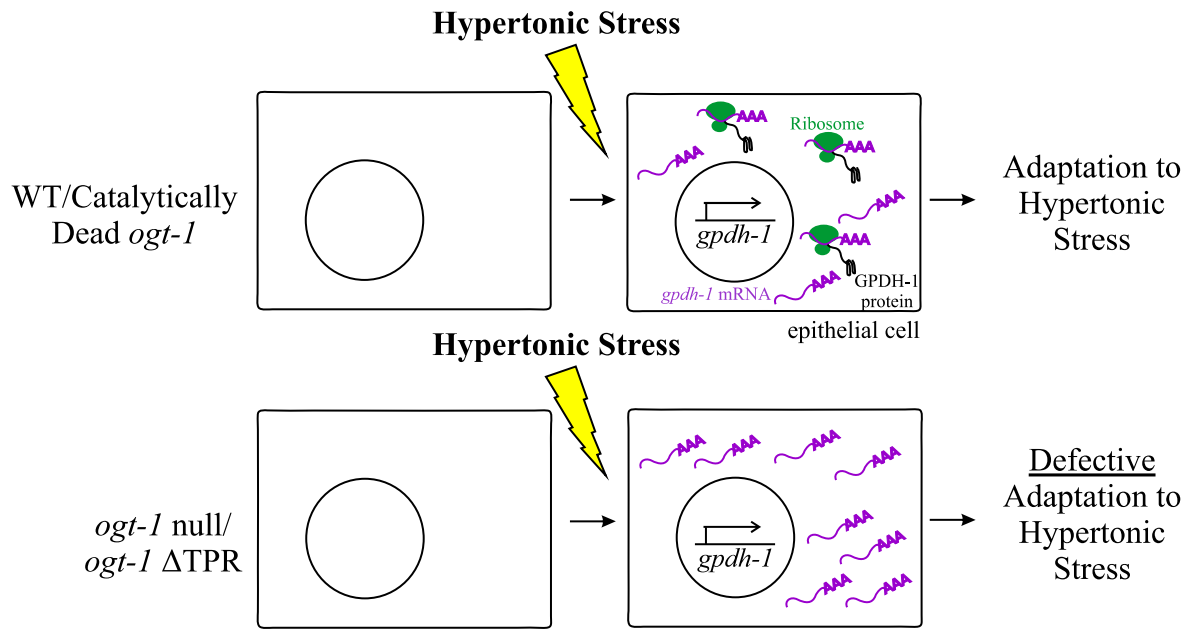

Figure 3.2.1 A non-catalytic function of *ogt-1* is required to couple HTS induced transcription and translation to enable physiological adaptation to HTS.

WT animals exposed to HTS induce the transcription of osmosensitive mRNAs, such as *gpdh-1*. These mRNAs are rapidly translated into protein by the ribosome, facilitating adaptation to HTS. Loss of *ogt-1* does not interfere with HTS induced transcription. Rather, loss of *ogt-1* decreases HTS induced protein levels. *ogt-1* may facilitate stress-induced translation via several potential mechanisms, including regulation of mRNA cleavage and 3' UTR usage, mRNA export, intiation factor interactions, or ribosomal elongation of the transcript. Importantly, the TPR domain, but not the *O*-GlcNAcylation function of OGT-1 is required in the HTSR.

C. elegans is the primary genetic model system for studies of *ogt-1* because it is the only known organism in which loss of *ogt-1* is viable [413, 433]. This has allowed many previous studies to parse the roles of *ogt-1* in lifespan [370, 496, 497], metabolism [413], innate immunity [430], behavior [419], neuron function [408, 418], stress responses [424, 498, 499], cell fate [362, 500], and autophagy [423]. Importantly, most of these studies utilized global *ogt-1* knockdown, which eliminates both *O*-GlcNAcylation-dependent and -independent functions of *ogt-1*. The

missense alleles generated here will provide powerful tools for differentiating between catalytic and non-catalytic functions. Further structure-function studies are needed to determine if the hypertonic functions of *ogt-1* can be molecularly separated from its *O*-GlcNAcylation-dependent functions. If these non-catalytic regions are conserved, such mutations could provide important new insights into the physiological role of non-catalytic OGT functions in humans.

My studies revealed a critical and previously unappreciated condition-specific role of OGT-1 in adaptation to HTS. This phenotype is completely penetrant and one of the strongest *ogt-1* phenotypes described to date. Although their ability to survive acute HTS is unaffected, *ogt-1* mutants are unable to adapt and develop following extremely mild shifts in extracellular osmolarity (250 mM NaCl). Such conditions have minimal effects on the ability of WT animals to adapt and develop [317]. This suggest a critical physiological role of *ogt-1* in the ability of *C. elegans* to survive in the wild, since *C. elegans* are continuously exposed to fluctuating environmental salinity in its native ecosystems [501]. Given that both *C. elegans* and human OGT are able to rescue the Nio phenotype of *ogt-1* mutants in *C. elegans*, we speculate that OGT plays an ancient and conserved biological function in response to environmental and physiological perturbations in osmotic homeostasis.

In mammals, OGT is essential to cell division, a physiological process that involves tight regulation of cell volume [11, 433, 502, 503]. Therefore, we speculate that OGT may be required for mammalian cell division for the same reason it is essential for adaptation to HTS in *C. elegans*: it plays a critical role in cell volume regulation. One reason mammalian cells may be unable to divide without OGT is because they cannot properly regulate cell volume during cell division. In *C. elegans*, unlike in mammals, *ogt-1* is not an essential gene [413, 433]. I hypothesize that the osmotic homogeneity of standard *C. elegans* lab culture conditions allows *ogt-1* mutants to survive

and propagate normally. However, under hypertonic conditions, *ogt-1* becomes an essential gene in *C. elegans*, like it is in humans. It will be interesting to explore the roles and requirements of OGT in cell volume regulation in mammalian cells and tissues.

Knockout of OGT in mammalian cells leads to a rapid loss of cellular viability [433]. This phenotype is largely thought to be due to loss of *O*-GlcNAcylation activity. However, data from human cells suggest that *O*-GlcNAcylation activity may not be the essential function of OGT. For example, exposure of mammalian cells to the *O*-GlcNAc inhibitor Ac_4-5*S*GlcNAc largely blocks *O*-GlcNAcylation, but cellular viability and division are unaffected [436]. Additionally, cells and humans carrying inherited catalytic point mutations in OGT associated with intellectual disability are viable [504]. My data show that the role of OGT-1 in the *C. elegans* HTSR is also independent of catalytic activity. Such catalytically-independent roles of OGT-1 have also been described in the context of synaptic regulation [408], cell adhesion [407], and transcriptional repression [371]. If the evolutionarily critical role of OGT in mammalian cells is related to its ability to regulate cell volume, my data suggest that such functions are independent of *O*-GlcNAcylation activity. These non-catalytic functions of OGT and the protein domains that regulate these functions are largely unexplored. The *C. elegans* Nio phenotype may provide a powerful genetic system for identifying new domains important for OGT function via targeted and unbiased genetic screening strategies.

Cell volume regulation during environmental stress requires upregulation of osmoprotective proteins, including those that regulate osmolyte accumulation. In almost all cases, these genes are upregulated at the transcriptional level [324]. My findings are the first evidence that this pathway is also under post-transcriptional control. OGT-1 is required for the accumulation of a GFP tagged GPDH-1 protein during HTS, but not for the upregulation of *gpdh-1* mRNA. Interestingly, this is not a complete elimination of GPDH-1-GFP protein induction and

even if it were, *gpdh-1* null mutants retain significant hypertonic adaptation potential, whereas *ogt-1* mutants are completely adaptation deficient. Alternatively, OGT-1 may in fact regulate *gpdh-1* mRNA at the transcriptional level but only in specific tissues, such as the hypodermis. Upregulation of *gpdh-1* in other tissues, like the intestine, may mask such tissues specific regulation. Nevertheless, my results suggest that OGT-1 regulation of the HTSR is likely to extend beyond its effects on GPDH-1 induction. The nature of these additional targets and/or mechanisms is currently unknown.

The regulation of stress responsive gene expression by OGT is not a new paradigm. Previous data has shown that it plays both a transcriptional and post-transcriptional role in stress response gene expression. For example, OGT-1 *O*-GlcNAcylates the oxidative stress responsive transcription factor SKN-1 to facilitate upregulation of antioxidant gene transcription [424]. On the other hand, OGT regulates ER stress response [495] and heat shock response [426] gene expression post-transcriptionally by *O*-GlcNAcylating translation initiation factors to selectively facilitate translation of stress induced mRNAs. Importantly, all of the previously described roles of OGT in stress responses require *O*-GlcNAcylation. While our data suggests that OGT-1 also functions in the HTSR through a post-transcriptional mechanism, this mechanism is fundamentally different from that of the oxidative, heat shock, and ER stress responses because it does not require *O*-GlcNAcylation activity. Further mechanistic studies are needed to define the *O*-GlcNAcylation-independent downstream targets of OGT-1 and cellular mechanisms required for osmoprotective protein expression.

Since the discovery of OGT, *C. elegans* have been an important tool for characterizing the role of OGT in cell signaling because it is the only known organism in which genetic loss of OGT generates viable cells and organisms [360, 413]. However, it is still unknown why *ogt-1* null *C.*

elegans, in contrast to every other metazoan, is viable [505]. One possibility is that the evolutionarily conserved role of *ogt-1* in cell volume regulation during HTS contributes to the essential role of OGT in all metazoans, including *C. elegans*. However, several key questions about the osmoprotective nature of OGT still remain. First, while canonical OGT-1-dependent *O*-GlcNAcylation is dispensable for the HTSR, it remains unclear which functions of OGT-1 are important to this physiological process. Although OGT-1 can catalyze a unique type of proteolysis event, this activity is not thought to occur in *C. elegans* [403]. Regardless, the K957M mutation eliminates the known proteolytic activity of OGT-1 [404], but does not exhibit a Nio phenotype, suggesting that OGT-1 proteolysis is also not required in the HTSR. Future studies, utilizing both targeted *ogt-1* deletion alleles and unbiased genetic screens for new *ogt-1* missense mutations with a Nio phenotype, should help to define the structural requirements of OGT-1 in the HTSR. Second the precise post-transcriptional mechanism(s) that OGT-1 regulates to control GPDH-1 protein expression remains unknown. Such mechanisms could include mRNA cleavage and polyadenylation site usage, mRNA nuclear export, selective interactions between ribosomes and stress-induced mRNAs, or regulated proteolysis of stress-induced proteins such as GPDH-1. While most of these potential mechanisms await testing, we found that autophagic or proteasome-mediated proteolysis did not appear to be involved. Finally, it remains unclear which genes *ogt-1* coordinates with to regulate HTS signaling. Future studies analyzing new Nio mutants should shed light on these interactions.

In conclusion, our unbiased genetic screening approaches in *C. elegans* have revealed a previously unappreciated requirement for non-canonical OGT signaling in a critical and conserved aspect of cell physiology. The primary function of OGT has long been assumed to be due to it catalytic *O*-GlcNAcylation activity. However, as I and others have shown, OGT also has critical

and conserved non-catalytic functions that warrant further study [371, 407, 408]. It is vital that future studies involving OGT utilize point mutants that differentiate canonical from non-canonical functions rather than OGT knockouts, which ablate both. As my studies have shown, such approaches could reveal new roles for this key protein in unexpected aspects of cell physiology.

3.2.1 Future directions

While I was the first to discover and characterize the role of OGT-1 in the HTSR, the mechanism through which OGT-1 operates to regulate this cellular stress response are still unknown. Defining the function(s) of OGT-1 that is required in the HTSR, characterizing the OGT-1-dependent osmosensitive cellular pathway(s), and identifying the post-transcriptional step(s) of osmosensitive gene expression that requires *ogt-1* will shed mechanistic insights into the role of this protein in the HTSR.

The most obvious first step in identifying the non-catalytic function(s) of OGT-1 required in the HTSR is to better delineate the OGT-1 structure-function relationships with respect to the Nio phenotype. In particular, mutations that are Nio, but preserve the catalytic activity of OGT-1 are of interest, because these will be the first known mutations that uncouple the catalytic and non-catalytic functions of OGT-1. I demonstrated that a complete deletion of the OGT-1 TPR domain inhibits the HTSR pathway and OGT-1 catalytic activity. However, it will be interesting to use CRISPR/Cas9 to determine what portion of the TPR domain is required in the HTSR and if smaller TPR deletions also affect the catalytic activity of OGT-1. One hypothesis is that OGT-1 regulates the HTSR via only a portion of its TPR domain, similarly to mSin3A-dependent transcriptional repression, which only requires the first six TPRs of OGT. Additionally, it will be important to mutate the NLS with CRISPR/Cas9 to test if the nuclear localization of OGT-1 is required in the

HTSR. Finally, although I demonstrated that the catalytic activity of OGT-1 is not required in the HTSR pathway, it is unknown if other functions of the catalytic domain, such as its substrate binding functions, are required in this response. Using CRISPR/Cas9 to test the effect of a catalytic domain deletions on the HTSR will address this unknown. These structure-function experiments will provide valuable insights into the required functions of OGT-1 in the HTS.

Another way to define which functions of OGT-1 are required in the HTSR is to examine OGT-1 localization during HTS more closely. OGT-1 has a diffuse nuclear localization in somatic tissues during isotonic conditions. In response to HTS, I observed the relocalization of OGT-1 into nuclear puncta in the hypodermis. Determining if these OGT-1 nuclear puncta are required for the HTSR will provide further insights into the functional requirements of OGT-1 in the HTSR. If the relocalization of OGT-1 into nuclear puncta is disrupted in ΔTPR mutants (which are Nio), but not catalytic mutants (which are not Nio), this suggests that OGT-1 nuclear puncta may be functionally required in the HTSR. Such a finding would for the first time provide a means by which to monitor the precise kinetics of the HTSR via live-cell imaging of the nuclear puncta.

In addition to the functional requirements of OGT-1 in the HTSR, the OGT-1-dependent cellular pathways that regulate the HTSR have not been characterized. Identifying the proteins that OGT-1 interacts with directly or indirectly to regulate the HTSR is critical for understanding how OGT-1 facilitates osmosensitive protein expression and adaptation to HTS. Co-immunoprecipitation experiments in WT and ΔTPR OGT mutant animals can be used to determine if *ogt-1* regulates the HTSR through stable interactions with other proteins. Additionally, an *ogt-1* suppressor screen will reveal the dependence of the HTSR on weak or indirect interactions with OGT-1. Mutants that suppress the *ogt-1* adaptation phenotype could be bypass suppressors that activate compensatory pathways or epistatic suppressors that activate genes in the same pathway

downstream of *ogt*-1/increase levels of proteins to facilitate interactions normally driven by *ogt-1*. Identification of either of these types of mutants would be informative towards understanding the mechanistic nature of the *ogt-1*-dependent osmosensitive pathway.

Finally, moving forward it will be important to characterize the post-transcriptional mechanism(s) under OGT-1 control. Despite upregulating *gpdh-1* mRNAs during HTS, *ogt-1* mutants have impaired hypertonic induction of GPDH-1 protein and this impaired protein induction is not dependent on proteosome or autophagy – mediated degradation pathways. This suggests that *ogt-1* is required for the translation of accumulated *gpdh-1* mRNAs into protein. However, it remains unknown if *ogt-1* is required for *gpdh-1* mRNA processing, nuclear export, or ribosome/translation initiation factor – transcript interactions during HTS. Previous reports have implicated OGT-1 in the regulation of stress-responsive protein expression during the heat shock and ER stress responses via *O*-GlcNAcylation of translation initiation factors. My discovery of a non-catalytic role of OGT-1 in the HTSR is the first indication that OGT-1 also regulates stress responsive protein expression via an unknown *O*-GlcNAcylation-independent mechanism.

To test if *ogt-1* is required for osmosensitive mRNA processing, RT-PCR combined with 3' and 5' rapid amplification of cDNA ends (RACE) can be used. Sequencing of the 3' and 5' ends of transcripts in *ogt-1* mutants during HTS through 3' and 5' RACE will determine if *ogt-1* is required for the 3' polyadenylation or the 5' methylguanosine capping of osmosensitive transcripts. Additionally, to determine if *ogt-1* is required for osmosensitive mRNA export, RNA FISH can be used. RNA FISH allows for the visualization of mRNA transcripts in cells. If *ogt-1* mutants have impaired nuclear export of *gpdh-1* transcripts, these transcripts should be enriched in the nucleus. Unfortunately, my early attempts to visualize mRNA using RNA FISH probes specific for *gpdh-1* transcripts were not successful. Alternatively, interactions between OGT-1

and the translation machinery may be required for osmosensitive protein expression. This possibility can be tested by examining the colocalization and co-immunoprecipitation of WT (non-Nio) and ΔTPR OGT-1-GFP (Nio) with fluorescently tagged ribosomes and translation factors during HTS. Colocalization and co-immunoprecipitation of WT OGT-1-GFP, but not ΔTPR OGT-1-GFP, with the translation machinery during HTS would suggest that OGT-1 may function through the translation complex to post-transcriptionally regulate *gpdh-1* expression. In conclusion, determining how OGT-1 regulates osmosensitive protein induction through a combination of structure-function studies, genetics, and cell imaging approaches could reveal a novel HTSR pathway and expand our understanding of the non-canonical functions of OGT-1.

3.3 Interacting components of the 3' mRNA cleavage and polyadenylation complex are required for the hypertonic induction of GPDH-1 and physiological adaptation to hypertonic stress

In addition to *ogt-1*, our Nio screen identified mutations in two interacting components of the APA complex that impair hypertonic induction of the *gpdh-1p::GFP* reporter and acute adaptation to HTS. Specifically, a G42E missense mutation in the cleavage stimulation factor 64 kDa subunit (CstF-64) homolog CPF-2 and a R580W missense mutation in the symplekin homolog SYMK-1 led to decreased hypertonic induction of *gpdh-1* transcriptional (*gpdh-1p::GFP*) and translational (*gpdh-1p::GPDH-1::GFP*) reporters in *C. elegans*. Unlike *ogt-1* mutants, which continued to upregulate *gpdh-1* mRNA during HTS, the *cpf-2* and *symk-1* Nio mutants had a slightly reduced induction of *gpdh-1* mRNA during HTS compared to WT animals. While this

phenotype needs to be examined more thoroughly, it suggests that these APA complex proteins may be required transcriptionally for osmosensitive gene expression. Additionally, endogenously tagged OGT-1-GFP and tagRFP-CPF-2 relocalized from a diffuse nuclear pattern into nuclear puncta in the hypodermis during HTS. However, these puncta did not colocalize, suggesting that OGT-1 and CPF-2 do not interact during HTS. In conclusion, the identification of the *cpf-2* and *symk-1* missense alleles in our Nio screen add the HTSR to the growing list of cellular stress responses regulated by the APA complex.

The 3' end processing of mRNA by the APA complex is required for the expression of most genes [468]. Additionally, the presence of multiple PAS sequences in the majority of transcripts [469, 470] allows the APA complex to fine tune and change gene expression in response to factors such as cell stress and metabolic state [474, 476]. In this way, cells use 3' mRNA processing by the APA complex to diversify the transcripts expressed from a single gene. Alternative polyadenylation is therefore a ubiquitous and essential cellular process [442]. The composition, enzymatic activities, and global targets of the APA complex are the primary focus of APA research. However, an understanding of how this complex alters APA usage in specific physiological contexts is largely lacking. This is primarily because APA knockouts are lethal in every system, including *C. elegans* [442]. Our Nio screen identified unusual missense alleles in APA components that are viable, which will allow us to study the function-specific and tissue-specific roles for APA. They also provide a unique opportunity to identify specific APA targets and mechanistically test how APA events in specific target genes affect the physiological response to HTS *in vivo.*

There are several hypotheses as to how the *cpf-2* and *symk-1* Nio mutations might disrupt alternative polyadenylation. One possibility is that these mutations cause destabilization and

degradation of the APA complex. This hypothesis can be tested by measuring the effect of the Nio mutations on protein abundance of endogenously tagged *cpf-2* and *symk-1* alleles. Another hypothesis is that the *cpf-2* and *symk-1* Nio mutations disrupt APA complex subunit interactions. To test this, the endogenously tagged alleles can be used to measure co-localization between the Nio *cpf-2*/*symk-1* alleles and the APA complex under basal and hypertonic conditions. A final testable hypothesis is that the *cpf-2* and *symk-1* Nio mutations affect APA complex localization. During HTS, we observed the relocalization of tagRFP-CPF-2 into nuclear puncta. Therefore, to test this hypothesis, we can measure the effect of the Nio mutations on the kinetics, reversibility, and diffusion characteristics of the hypertonicity induced tagRFP-CPF-2 foci. These structure function studies are only possible due to the APA complex missense alleles that were isolated in our Nio screen and they will provide important information about the functional requirements of the APA complex in the HTSR.

In addition to the functional requirements of the APA complex, the target(s) of the APA complex required for the HTSR also remains unknown. Since the APA complex cleaves and polyadenylates the 3' UTR of mRNA, it is conceivable that the *cpf-2* and *symk-1* Nio mutations prevent the proper 3' processing of a transcript(s) required for the HTSR. One possibility is that the processing of *gpdh-1* itself by the APA complex is required in the HTSR. However, this is not the case because the 3' UTR of the *gpdh-1p::GFP* reporter that was the basis for my Nio screen does not contain the *gpdh-1* 3' UTR sequence. Instead, it contains the *unc-54* 3' UTR sequence. This generic *unc-54* 3' UTR is commonly used in overexpressed reporter constructs because it simplifies the cloning process. In fact, the control *col-12p::dsRed* reporter I used in the genetic screen also contains the generic *unc-54* 3' UTR instead of the endogenous *col-12* 3' UTR. Because both the *gpdh-1p::GFP* and *col-12p::dsRed* reporters contain the *unc-54* 3' UTR, but only

induction of the *gpdh-1p::GFP* reporter is decreased during HTS in the *cpf-2* and *symk-1* Nio mutants, this suggests that the generic *unc-54* 3' UTR is not regulated by the APA complex. These data suggest that the APA complex likely regulates a factor upstream of *gpdh-1* (Factor X) instead of modulating the 3' UTR of *unc-54* or *gpdh-1* itself.

There are two main models by which the APA complex could regulate the HTSR. In the first model, full expression of the APA complex facilitates the cleavage and polyadenylation of Factor X at the first PAS encountered on the transcript, a low affinity proximal PAS, and this produces a stable functional protein that can then go on to activate *gpdh-1* induction. This model assumes that the *cpf-2* and *symk-1* Nio mutations decrease expression of the APA complex as a whole and therefore promote its binding to the distal PAS of Factor X. Since long 3' UTRs are subject to greater regulation by miRNAs and RNA binding proteins and intrinsically less stable than short 3' UTRs [474, 475], this model suggests that Factor X transcripts are less stable in the *cpf-2* and *symk-1* Nio mutants and thereby cause impaired induction of *gpdh-1*. This model therefore hypothesizes that the *cpf-2* and *symk-1* Nio mutations influence the alternative polyadenylation of Factor X to a greater extent than the alternative polyadenylation of other transcripts. A paradigm similar to this is seen with the 3' mRNA processing of IgM H-chain in mammals (Section 1.7.2). The second model to explain how the APA complex may regulate the HTSR is more general. It hypothesizes that the *cpf-2* and *symk-1* Nio mutants reduce APA below a threshold that is insufficient for stress-induced APA but provides enough APA to avoid lethality. In this model the *cpf-2* and *symk-1* Nio mutants identified in our Nio screen are likely to exhibit other known APA reduction-of-function mutant phenotypes. Testing for these phenotypes will help us characterize the mechanism(s) by which APA regulates the HTSR.

Genetic screens commonly identify genes in the same cellular pathways [313]. If *ogt-1* and the APA complex function in the same pathway, they should exhibit similar cellular and molecular phenotypes. One possibility is that these proteins are in the same physical complex and co-localize *in vivo.* Endogenously tagged OGT-1-GFP and tagRFP-CPF-2 are both nuclear localized and they form puncta during HTS. Furthermore, these hypertonically induced puncta are most pronounced in the hypodermis, which is where OGT-1 functions to regulate the HTSR. However, OGT-1-GFP and tagRFP-CFP-2 puncta do not overlap in the hypodermis suggesting that OGT-1 and CPF-2 are not localized to the same complex during HTS. Another prediction is that if *ogt-1* and the APA complex work through the same pathway, they might exhibit similar molecular phenotypes. In *ogt-1* mutants, *gpdh-1* mRNA continues to be upregulated during HTS even though GPDH-1 protein is not. In contrast, in *cpf-2* and *symk-1* Nio mutants, the upregulation of *gpdh-1* mRNA is slightly reduced compared to WT animals during HTS. While the *gpdh-1* mRNA levels in APA complex mutants needs to be examined more closely, these divergent phenotypes suggest that OGT-1 and the APA complex may act in different genetic pathways to regulate the HTSR. Testing the genetic interactions between *ogt-1* and the APA complex through epistasis experiments will provide further insights into this hypothesis.

In conclusion, through an unbiased approach, I identified two interacting components of the APA complex as regulators of the HTSR. Missense mutations in the cleavage stimulation complex subunit CPF-2 and the adaptor protein SYMK-1 caused impaired hypertonic induction of *gpdh-1* and adaptation to HTS. Although we do not know how these missense mutations affect the APA complex, we hypothesize that they may affect APA complex protein abundance, subunit interactions, and/or localization. The endogenously tagged tagRFP-CPF-2 allele that we made is an important tool for answering these questions. We also do not know how the APA complex is

required for the HTSR. However, the generic nature of the *gpdh-1p::GFP* reporter 3' UTR suggests that the APA complex regulates a signaling protein upstream of *gpdh-1* instead of modifying the 3' UTR of *gpdh-1* itself. Furthermore, the absence of colocalization between tagRFP-CPF-2 and OGT-1-GFP during HTS and the different effects of *cpf-2/symk-1* and *ogt-1* mutants on hypertonic *gpdh-1* mRNA induction suggest that OGT-1 and the APA complex may function in distinct cellular pathways to regulate the HTSR. Since complete knockout of APA complex genes is lethal in animals including *C. elegans*, it was only possible to discover the requirement of the APA complex in the HTSR because of the non-null missense mutations in *cpf-2* and *symk-1* we identified in our screen. These missense mutations therefore provide a unique tool that will not only be useful for further characterizing the role of the APA complex in the HTSR, but also for understanding the broader cell biological and physiological functions of the APA complex.

3.3.1 Future directions

Several key questions about the *cpf-2* and *symk-1* Nio alleles and the role of APA in the HTSR remain. 1. How do the *cpf-2* and *symk-1* Nio mutations affect the biochemical properties of the APA complex? 2. Are *cpf-2* and *symk-1*, like *ogt-1*, required acutely in the hypodermis during HTS? 3. What is the target(s) of the APA complex required to facilitate the HTSR? Each of these questions can be answered through well-established techniques in *C. elegans.* The first question can be addressed using endogenous fluorescently tagged CPF-2 and SYMK-1 to determine the effect of the *cpf-2* and *symk-1* missense Nio alleles on the APA complex. Several possibilities exist for how these missense alleles could impact the APA complex. They may cause destabilization of the APA complex, affect APA subunit interactions, or affect APA localization.

Each of these possibilities is testable using a combination of imaging and biochemical approaches with endogenous fluorescently tagged CPF-2 and SYMK-1 alleles.

Next, it is necessary to examine the temporal and spatial requirements of CPF-2 and SYMK-1 in the HTSR to more precisely define the requirement of these proteins and the APA complex in the HTSR. *ogt-1* and previously identified regulators of the HTSR function in the hypodermis to modulate osmosensitive signaling pathways [319, 324, 329]. If *cpf-2* and *symk-1* expression are also required in the hypodermis to regulate HTSR pathways, this would support the hypothesis that the hypodermis is the primary site of osmosensitive signaling. This hypothesis can be tested using tissue-specific rescue of *cpf-2* and *symk*-1. Additionally, characterizing the temporal requirements of *cpf-2* and *symk-1* expression during the HTSR is necessary to determine if the APA complex is required for cell signaling events immediatly following HTS or if it is required developmentally to facilitate later HTSRs. An acute requirement for *cpf-2* and *symk-1* expression during HTS suggests that the APA complex dynamically responds to HTS to modulate osmosensitive gene expression and physiological adaptation to HTS.

Finally, the hypothesis that APA of unknown target(s) during HTS is required for osmosensitive gene expression and adaptation to HTS needs to be tested. While our data suggests that *gpdh-1* does not undergo APA during the HTSR, the stability of factor(s) upstream of *gpdh-1* may be modulated by APA. Enrichment of transcripts for 3' UTR polyA sequences followed by RNA sequencing in WT and APA complex Nio mutants in control and hypertonic conditions will allow for the quantification of shifts in APA utilization by HTS. While unlikely, the identification of a single APA event with functional consequences during HTS would be a major breakthrough in both the osmotic stress and APA fields because it would suggest a novel mechanism for the regulation of the HTSR.

3.4 Conclusions

Study of the HTSR in *C. elegans*, primarily through unbiased genetic screens, has revealed both post-transcriptional and transcriptional regulation of osmosensitive gene expression. Through my doctoral studies I discovered that the HTSR is post-transcriptionally regulated by a novel non-catalytic function of the *O*-GlcNAc transferase enzyme (OGT). In addition, I found that the transcriptional induction of the HTSR requires the 3' mRNA cleavage and polyadenylation complex (APA complex). Previous studies from our lab also suggest that the HTSR is under strong negative transcriptional regulation. Protein homeostasis genes, which oppose protein damage and new protein synthesis, negatively regulate the HTSR transcriptional response through a GCN-1/2 and WNK-1/GCK-3-dependent pathway. Additionally, ECM proteins inhibit *gpdh-1* transcriptional induction under isotonic conditions through a pathway involving a transmembrane protein and a GATA-type transcription factor. Therefore, genetic screens performed to date have revealed the existence of at least four basic HTSR pathways in *C. elegans* (Fig 3.4.1).

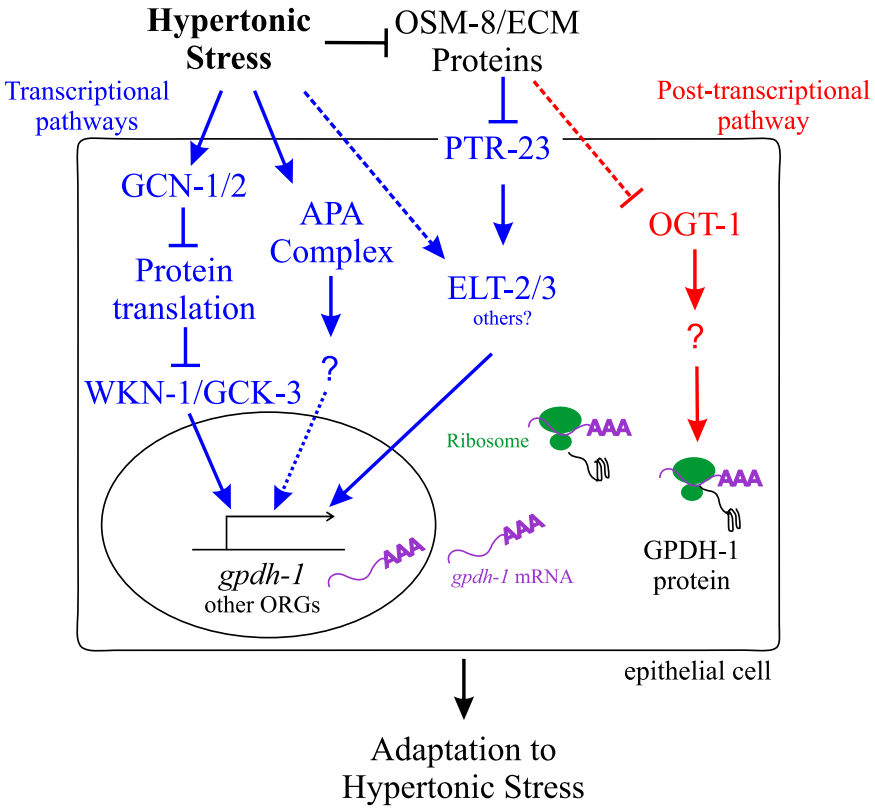

Figure 3.4.1 HTSR pathways in *C. elegans*

The induction of ORGs, such as *gpdh-1*, during HTS is regulated through both transcriptional and post-transcriptional mechanisms. At least three pathways regulate the transcriptional induction of *gpdh-1*. First, inhibition of proteins that maintain protein folding and new protein synthesis activate *gpdh-1* expression. HTS-induced decreases in protein translation lead to increased *gpdh-1* transcription through a *gcn-1/2* and *wnk-1/gck-3* dependent pathway. Additionally, while significant work shows that HTS causes unique types of protein damage and inhibition of protein homeostasis genes activates the HTSR, the specific signaling mechanisms linking HTS-induced protein damage to *gpdh-1* upregulation are not known. Second, two interacting components of the APA complex, SYMK-1 and CPF-2, are required for transcriptional induction of the HTSR through an unknown mechanism. The requirement of the APA complex in the HTSR needs to be examined more closely, but I speculate that a transcript(s) upstream of ORGs is alternatively polyadenylated to facilitate the HTSR. Third, the HTSR transcriptional response is negatively regulated by extracellular proteins that function upstream of the transmembrane protein PTR-23/patched-related protein 23 and the GATA erythroid-like transcriptional factors ELT-2 and ELT-3. However, *ptr-23* is not required for all ORG expression and as such at least one *ptr-23* independent pathway must exist. It is unknown if this *ptr-23* independent

pathway functions through the GATA transcription factors. It also remains unknown if HTS itself can activate ELT-2/3 through an extracellular protein and *ptr-23* independent pathway. Finally, the O-GlcNAc transferase OGT-1 regulates GPDH-1 protein translation through a post-transcriptional pathway. *ogt-1* is required for *osm-8* and *osm-11* phenotypes, suggesting there is some crosstalk between the extracellular protein transcriptional pathway and the *ogt-1* post-transcriptional pathway. The TPR domain and not the catalytic domain of OGT-1 is required in this pathway. The precise mechanism by which *ogt-1* induces GPDH-1 protein expression is unknown, but it could include regulation of mRNA processing, mRNA export, initiation factor interactions, or ribosomal elongation. The output of both the transcriptional and post-transcriptional pathways is to mediate physiological adaptations that enable animals to survive and develop in hypertonic environments.

One notable finding from these studies of the *C. elegans* HTSR is that the genes and mechanisms identified in this relatively simple organism are not 'worm-specific'. Rather, they are ancient and highly conserved cellular pathways that impinge on critical aspects of cell physiology such as protein synthesis and folding, extracellular matrices, 3' mRNA processing, and novel functions of highly conserved proteins, such as OGT-1. However, much remains unknown about these HTSR regulatory pathways. The mechanisms by which cells sense HTS have yet to be described. Furthermore, in the transcriptional pathways, a transcription factor specific to the HTSR has not been identified and the signaling mechanism(s) by which this transcription factor becomes activated is unknown. One possibility is that HTS is sensed by the cell through the ECM. This paradigm occurs in the yeast Sho1 branch of the high osmolarity glycerol (HOG) pathway, where the OSM-8 – like, extracellular mucin domain – containing proteins, Msb2 and Hkr1 sense HTS to ultimately activate the master regulator of the yeast HTSR, Hog1 [115].

The post-transcriptional pathway through which OGT-1 functions to regulate the HTSR is also uncharacterized. OGT-1 could regulate GPDH-1 protein expression through mRNA processing, mRNA export, initiation factor interactions or ribosomal elongation. While the TPR

domain, and not catalytic activity, of OGT-1 is required to regulate GPDH-1 protein expression, the mechanism(s) by which this domain regulates the HTSR is currently unknown. Continued unbiased genetic screens, complemented by targeted biochemical and cell biological studies, will be instrumental towards further defining the cellular pathways regulating the *C. elegans* HTSR. The success of the genetic screening approaches used to characterize the role of ECM proteins, PTR-23, protein homeostasis, 3' mRNA processing, and OGT-1 in the HTSR indicate that such approaches are well suited to study this cellular stress response. Capturing unique missense alleles, identifying new genes, and describing new loss of function phenotypes through forward genetic screens in *C. elegans* will not only provide insight into the protein functions and cellular pathways regulating the HTSR, but will also reveal novel cell signaling paradigms that can be applied to other aspects of cellular physiology.

4.0 Methods

4.1 *C. elegans* strains and culture

Strains were cultured on standard NGM media with E.coli OP50 bacteria at 20˚C unless otherwise noted. The following strains were used; N2 Bristol WT, OG119 *drIs4 [gpdh-1p::GFP*; *col-12p::dsRed2*], VP223 *kbIs6* [*gpdh-1p::gpdh-1-GFP*], OG971 *ogt-1/nio-2(dr15);drIs4*, OG969 *ogt-1/nio-2(dr20);drIs4*, OG1034 *ogt-1(ok430);drIs4*, OG1035 *ogt-1(ok1474);drIs4*, OG968 *nio-5(dr13);drIs4*, OG970 *nio-6(dr19);drIs4*, OG972 *nio-1(dr14);drIs4*, OG975 *cpf-2/nio-3(dr16);drIs4*, OG976 *nio-5(dr18);drIs4*, OG978 *nio-4(dr17);drIs4*, OG995 *nio-5(dr22);drIs4*, OG996 *symk-1/nio-7(dr23);drIs4*, OG1066 *ogt-1(dr20 dr36);drIs4*, OG1064 *ogt-1(dr34);unc-119(ed3);kbIs6*, OG1115 *gpdh-1(dr81)* [*gpdh1::GFP*], OG1123 *gpdh-1(dr81);ogt-1(dr84)*, RB1373 *gpdh-1(ok1558)*, OG1048 *osm-8(dr9);unc-4(e120);drIs4*, OG1049 *osm-8(dr9);unc-4(e120);ogt-1(dr20):drIs4*, OG1111 *ogt-1(dr20);drIs4;drEx468* [*ogt-1p::ogt-1cDNA::ogt-1 3'utr; rol-6(su1006)]*, OG1119 *ogt-1(dr20);drIs4;drEx469* [*dpy-7p::ogt-1cDNA::ogt-1 3'utr; rol-6(su1006)]*, OG1120 *ogt-1(dr20);drIs4;drEx470* [*nhx-2p::ogt-1cDNA::ogt-1 3'utr; rol-6(su1006)*], OG1121 *ogt-1(dr20);drIs4;drEx471* [*myo-2p::ogt-1cDNA::ogt-1 3'utr; rol-6(su1006)*], OG1122 *ogt-1(dr20);drIs4;drEx472* [*rab-3p::ogt-1cDNA::ogt-1 3'utr; rol-6(su1006)*], OG1125 *ogt-1(dr20);drIs4;*drEx473 [*ogt-1p::human OGT isoform 1cDNA::ogt-1 3'utr; rol-6(su1006)]*, OG1126 *ogt-1(dr20);drIs4;drEx474* [*ogt-1p::human OGT isoform 1 H498AcDNA::ogt-1 3'utr; rol-6(su1006)*], OG1046 *ogt-1(dr20);drIs4;drEx465* [*ogt-1p::ogt-1 genomic*], TJ375 *gpIs1* [*hsp16.2p::GFP*], SJ4005 *zcIs4* [*hsp4p::GFP*] V, OG1081 *ogt-1(dr50);zcIs4*, MT3643 *osm-11(n1604)*, OG1083 *ogt-1(dr52);osm-11(n1604)*, OG1135 *ogt-*

1(dr86);drIs4, OG1140 *ogt-1(dr90);drIs4*, OG1124 *ogt-1(dr84)* [*ogt-1::GFP*], OG1139 *ogt-1(dr84 dr89)*, OG1141 *ogt-1(dr84 dr91)*, OG1156 *ogt-1(dr93);drIs4*, OG1157 *ogt-1(dr84 dr94)*, IG274 *frIs7* [*nlp-29p::GFP + col-12p::dsRed*2], OG975 *cpf-2(dr16);drIs4*, OG996 *symk-1(dr23);drIs4*. To create mutant combinations, we used either standard genetic crossing approaches or CRISPR/Cas9 genetic engineering (see below for CRISPR methods). The homozygous genotype of every strain was confirmed either by DNA sequencing of the mutant lesion, restriction digest, or a loss of function phenotype.

4.2 Genetic methods

4.2.1 ENU mutagenesis and mutant isolation

L4 stage *drIs4* animals (P_0) were mutagenized in 0.6 mM ENU diluted in M9 for 4 hours at 20˚C. One day after ENU mutagenesis, F1 mutagenized eggs were isolated by hypochlorite solution and hatched on NGM plates overnight. Starved ENU mutagenized F_1 *drIs4* L1 animals were washed twice in 1 x M9 and seeded onto 3–16 10 cm OP50 NGM plates. F2 synchronized larvae were obtained via hypochlorite synchronization and seeded onto OP50 NGM plates. Day one adult F_2 *drIs4* animals were transferred to 250 mM NaCl OP50 NGM plates for 18 hours. As controls, unmutagenized *drIs4* day 1 adults were also transferred to 50 mM NaCl and 250 mM NaCl OP50 NGM plates for 18 hours. After 18 hours, RFP and GFP fluorescence intensity, time of flight (TOF), and extinction (EXT) were acquired for each animal using a COPAS Biosort (Union Biometrica, Holliston, MA). Using the unmutagenized 50 mM NaCl NGM data as a reference, gate and sort regions for animals exposed to 250 mM NaCl were defined that isolated

rare mutant animals with GFP and RFP levels similar to the population of unmutagenized *drIs4* animals on 50 mM NaCl. These mutants were termed Nio mutants (no induction of osmolyte biosynthesis gene expression). Individual Nio mutant hermaphrodites were selfed and their F_3 and F_4 progeny re-tested to confirm the Nio phenotype.

4.2.2 Backcrossing and single gene recessive determination

Each *nio* mutant was backcrossed to *drIs4* males three times. F_1 progeny from these backcrosses were tested on 250 mM NaCl for 18 hours as day 1 adults. As expected for a recessive mutant, 100% of the crossed progeny were WT (non-Nio). F_1 heterozygous hermaphrodites from these crosses were selfed and their progeny (F_2) were tested on 250 mM NaCl for 18 hours as day 1 adults. As expected for a single gene recessive mutation, ~25% of progeny exhibited the Nio phenotype.

4.2.3 Complementation testing

nio/+ males were crossed with hermaphrodites homozygous for the mutation being complementation tested. The F_1 progeny from this cross were put on 250 mM NaCl OP50 NGM plates for 18 hours and screened for complementation. Crosses in which ~50% of these F_1 progeny were WT failed to complement (i.e. phenotype-causing mutations were alleles of the same gene). Crosses in which 100% of these F1 progeny were WT complemented (i.e. phenotype-causing mutations were alleles of different genes). Each mutant was complementation tested to every other mutant twice–as both a hermaphrodite and as a male.

4.2.4 Whole genome sequencing

DNA was isolated from starved OP50 NGM plates with WT (*drIs4*) or mutant animals using the Qiagen Gentra Puregene Tissue Kit (Cat No 158667). The supplementary protocol for "Purification of archive-quality DNA from nematode suspensions using the Gentra Puregene Tissue Kit" available from Qiagen was used to isolate DNA. DNA samples were sequenced by BGI Americas (Cambridge, MA) with 20X coverage and paired-end reads using the Illumina HiSeq X Ten System.

4.2.5 SNP and INDEL identification in mutants

A Galaxy workflow was used to analyze the FASTQ forward and reverse reads obtained from BGI. The forward and reverse FASTQ reads from the animal of interest, *C. elegans* reference genome Fasta file (ce11m.fa), and SnpEff download gene annotation file (SnpEff4.3 WBcel235.86) were input into the Galaxy workflow. The forward and reverse FASTQ reads were mapped to the reference genome Fasta files with the Burrows-Wheeler Aligner (BWA) for Illumina. The resultant Sequence Alignment Map (SAM) dataset was filtered using bitwise flag and converted to the Binary Alignment Map (BAM) format [506]. Read groups were added or replaced in the BAM file to ensure proper sequence analysis by downstream tools. To identify areas where the sequenced genome varied from the reference genome, the Genome Analysis Toolkit (GATK) Unified Genotyper was used. The types of variants identified with GATK were Single Nucleotide Polymorphisms (SNPs) and Insertion and Deletions (INDELs). The SnpEff4.3 WBcel235.86 gene annotation file was used to annotate the non-synonymous SNPs and INDELs that were identified as variants by GATK. The final list of all variants with annotated non-

synonymous variants was exported as a Microsoft Excel table. To identify mutations in the sequenced mutants that were not in the parent strain (*drIs4*), the MATCH and VLOOKUP functions in Microsoft Excel were used.

4.2.6 RNAi methods

Gravid adult animals on RNAi plates (NGM + 1mM IPTG + 25ug/ml carbenicillin) were hypochlorite treated. Synchronized L1s from the hypochlorite treatment were allowed to develop on RNAi plates until day one adult. Day 1 adults were seeded onto either 50 mM or 250 mM RNAi or OP50 NaCl plates. For the developmental timed RNAi experiment, hypochlorite synchronized L1 animals were seeded onto *ev(RNAi)* or *ogt-1(RNAi)*. At the indicated stages, animals were manually transferred from *ev(RNAi)* to *ogt-1(RNAi)*. For the adult-specific RNAi, day 1 adult animals were transferred from *ev(RNAi)* to *ogt-1(RNAi)* plates containing either 50 mM NaCl or 250 mM NaCl. The identity of all RNAi clones was confirmed by sequencing.

4.3 COPAS biosort acquisition and analysis

Day one adults from a synchronized egg lay or hypochlorite preparation were seeded on 50 or 250 mM NaCl OP50 or the indicated RNAi NGM plates. After 18 hours, the GFP and RFP fluorescence intensity, time of flight (TOF), and extinction (EXT) of each animal was acquired with the COPAS Biosort. The TOF is directly proportional to worm size. Events in which the RFP intensity of adult animals (TOF 400–1200) was <20 (dead worms or other objects) were excluded from the analysis. The GFP fluorescence intensity of each animal was normalized to its

RFP fluorescence intensity or TOF. To determine the fold induction of GFP for each animal, each GFP/RFP or GFP/TOF was divided by the average GFP/RFP or GFP/TOF of that strain exposed to 50 mM NaCl. The relative fold induction was determined by setting the fold induction of *drIs4* exposed to 250 mM NaCl to 1.

4.4 Molecular biology and transgenics

4.4.1 Reporter strains

The *drIs4* strain was made by injecting WT animals with *gpdh-1p::GFP* (20ng/µL) and *col-12p::dsRed2* (100ng/µL) to generate the extrachromosomal array *drEx73*, which was integrated using UV bombardment, followed by isolation of animals exhibiting 100% RFP fluorescence. The resulting strain was outcrossed five times to WT to generate the homozygous integrated transgene *drIs4*. *kbIs6* was generated from a Gene Gun bombardment of *unc-119(ed3)* animals with a *gpdh-1p::gpdh-1::GFP* plasmid and an *unc-119(+)* rescue plasmid (pMM051). The resulting strain was outcrossed five times to generate *kbIs6*. *drIs4* is integrated on LGIV. The integration site for *kbIs6* is unmapped.

The WT *gpdh-1p::GFP*, ΔCDS *gpdh-1p::GFP*, and Δ5' UTR *gpdh-1p::GFP* extrachromosomal reporter strains were made by cloning each *gpdh-1* promoter sequence into the pPD95.75 plasmid and injecting WT animals with 20 ng/µL of each construct. Animals were also injected with 2.5 ng/µL of a *myo2p::mCherry* construct as a co-injection marker. Animals expressing the *gpdh-1* promoter extrachromosomal arrays were maintained by picking animals expressing pharyngeal *myo2p::mCherry*.

4.4.2 Transgene rescue

The genomic *ogt-1* rescue construct (used in the *drEx465* extrachromosomal array) was made by amplifying *ogt-1* with 2 kb of sequence upstream of the start codon and 1 kb of sequence downstream of the stop codon. All other rescue constructs (used in extrachromosomal arrays *drEx468 –drEx474*) were made using Gibson Assembly. The *ogt-1* promoter, *ogt-1* cDNA, and *ogt-1* 3'UTR were cloned into the pPD61.125 vector through a four component Gibson Assembly reaction. This vector was used as the backbone for all other promoter and human OGT rescue constructs. All rescue constructs were confirmed by Sanger sequencing. Extrachromosomal array lines were made by injecting day one adult animals with the rescue construct (20 ng/μL) and *rol-6(su1006)* (100 ng/μL).

4.4.3 CRISPR/Cas9 genomic editing

CRISPR allele generation and TPR deletion was performed using the single-stranded oligodeoxynucleotide donors (ssODN) method [507, 508]. For identification of the *dr20* allele, we performed RFLP (restriction fragment length polymorphism) analysis using the *MboI* restriction enzyme, which cuts the WT allele, but not *dr20*. For identification of the *dr86, dr89, dr90*, and *dr91* alleles, we performed RFLP analysis using the *DdeI* restriction enzyme, which cuts the mutant alleles, but not WT. To make the *gpdh-1::GFP* CRISPR strain, we used a previously described double stranded DNA (dsDNA) asymmetric-hybrid donor method [507, 508]. To make the *ogt-1::GFP* CRISPR strain, we used a dsDNA donor method using Sp9 modified primers [509]. Homozygous CRISPR/Cas9 generated alleles were isolated by selfing heterozygotes to ensure that complex alleles were not obtained.

4.4.4 mRNA isolation, cDNA synthesis, and qPCR

Day one animals were plated on 50 mM or 250 mM NaCl OP50 NGM plates for 24 hours. Unless noted otherwise, after 24 hours, 35 animals were picked into 50 µL Trizol for mRNA isolation. RNA isolation followed a combined Trizol/RNeasy column purification method as previously described [324]. cDNA was synthesized from total RNA using the SuperScript VILO Master Mix. SYBR Green master mix, 2.5 ng input RNA, and the appropriate primers were used for each qPCR reaction. qPCR reactions were carried out using an Applied Biosystems 7300 Real Time PCR machine. *act-2* primers were used as a control for all qPCR reactions. At least three biological replicates of each qPCR reaction were performed with three technical replicates per biological replicate. qPCR data was analyzed through ΔΔCt analysis with all samples normalized to *act-2*. Data are represented as fold induction of RNA on 250 mM NaCl relative to on 50 mM NaCl.

4.4.5 Western blots

Cell lysates were prepared from hypochlorite synchronized day 1 adult animals exposed to 50 mM or 250 mM NaCl plates for 18 hours. 3–5 non-starved 10 cm plates were concentrated into a 100 µL mixture. NuPage LDS Sample Buffer (4X) and NuPAGE Sample Reducing Agent (10X) were added and the sample was frozen and thawed three times at -80˚C and 37˚C. Prior to gel loading, the sample was heated to 100˚C for 10 minutes and cleared by centrifugation at 4˚C, 12,000 x g for 15 minutes. The cleared supernatant was run on a 4–12% or 8% Bis-Tris Mini Plus gel and transferred to a nitrocellulose membrane using iBlot 2 NC Regular Stacks and the iBlot 2 Dry Blotting System. The membranes were placed on iBind cards and the iBind western device

was used for the antibody incubation and blocking. The Flex Fluorescent Detection (FD) Solution Kit or the iBind Solution Kit was used to dilute the antibodies and block the membrane. The following antibody dilutions were used: 1:1000 α-GFP, 1:2000 α-ß-Actin, 1:2000 α-mouse HRP, and 1:4000 Goat α-Mouse IgG (H+L) Cross-Absorbed Secondary DyLight 800. A C-DiGit Licor Blot Scanner (LI-COR Biosciences, Lincoln, NE) or an Odyssey CLx imaging System (LI-COR Biosciences, Lincoln, NE) were used to image membranes incubated with a chemiluminescent or fluorescent secondary antibody, respectively.

4.5 Microscopy

Worms were anesthetized (10mM levamisole) and mounted on either agar plates for low magnification stereo fluorescence microscopy or silicone greased slide chambers for high magnification wide-field microscopy. Images were collected on either a Leica MZ16FA fluorescence stereo dissecting scope with a DFC345 FX camera or a Leica DMI4000B inverted compound microscope with a Leica DFC 340x digital camera using the Leica Advanced Fluorescence software (Leica Microsystems, Wetzlar, Germany). Unless noted, images within an experiment were collected using the same exposure and zoom settings. Unless noted, images depict merged GFP and RFP channels of age matched day 1 adult animals exposed to 50 or 250 mM NaCl for 18 hours.

4.6 Immunofluorescence

Embryos from a hypochlorite preparation were freeze-cracked on a superfrost slide, fixed with 4% paraformaldehyde, blocked with bovine serum albumin (BSA), incubated with a 1:400 dilution of α-O-GlcNAc monoclonal antibody (RL2) overnight, and incubated with 1:400 dilution of 1:400 goat α-mouse IgG, IgM (H+L) Secondary Antibody, Alexa Fluor 488 for 4–6 hours [510]. Washes with PBS or antibody buffer were carried out between each incubation step. DNA was stained with 1 μg/mL Hoechst 33258 diluted in PBS. Exposure matched Z-stacks of images were processed using the following deconvolution parameters (Leica Application Suite Advanced Fluorescence, 2.1.0 build 4316): Method–blind, Total iterations– 10, Refractive index– 1.518, Resized to 16 bit depth. Images were scaled to the following intensities: RL2 maximum pixel intensity = 514, Hoechst 33258 maximum pixel intensity = 1028. Final images are represented as maximum Z-stack projections.

4.7 *C. elegans* assays

4.7.1 Acute adaptation assay.

Day one adult animals were transferred to five 50 mM NaCl OP50 NGM plates and five 200 mM NaCl OP50 plates. ~25 animals were transferred to each plate (i.e. ~125 animals total per condition per genotype). After 24 hours, 20 animals from each 50 mM or 200 mM plate were transferred to 600 mM NaCl OP50 NGM plates. Animals were scored for movement after 24 hours on the 600 mM NaCl OP50 NGM plates. The experimenter was blinded to genotype. To be

counted as moving, the animal had to move greater than half a body length. Animals that were not moving were lightly tapped on the nose to confirm that they were paralyzed or dead.

4.7.2 Chronic adaptation assay

5 L4 animals were transferred to 50 or 250 mM NaCl OP50 NGM plates. Plates were monitored over several days. For the brood and development assays, a single L4 animal was transferred to a 50 or 250 mM NaCl OP50 NGM plate. Embryos counts and transfer of the mother to a new plate were done daily until the mother stopped laying eggs. Progeny from each animal were allowed to develop and the number of L4s was counted. Percent of developed embryos was calculated by dividing the number of L4s on a plate by the number of embryos originally laid on that plate.

4.7.3 Survival assays and OSR assays

Survival and OSR assays were performed as previously described [324]. Briefly, for the survival assays, day 1 adults (24 hours post-L4) were placed on OP50 spotted NGM plates containing indicated concentrations of NaCl. The survival of each animal was determined after 24 hours at 20˚C. Animals that failed to respond to prodding with a platinum wire were scored as dead. For the OSR assay, animals were transferred from standard 50 mM NaCl OP50 spotted NGM plates to either 500 mM NaCl or 700 mM NaCl NGM plates without OP50. The percentage of animals moving after 10 minutes was determined by prodding with a platinum wire. Animals that failed to respond were scored as paralyzed.

4.8 Statistical analysis

Comparisons of means were analyzed with either a two-tailed Students t-test (2 groups) or ANOVA (3 or more groups) using the Dunnett's or Tukey's post-test analysis as indicated in GraphPad Prism 7 (GraphPad Software, Inc., La Jolla, CA). COPAS biosort data is nonparametric and was therefore analyzed using a Mann-Whitney test (2 groups) or Kruskal-Wallis test (3 or more groups) using the Dunn's post-test analysis in GraphPad Prism 7 (GraphPad Software, Inc., La Jolla, CA). p-values of <0.05 were considered significant. Data are expressed as mean ± S.D. with individual points shown.

Appendix A Supplementary Data

Appendix A.1 Investigating the role of the PQR/AQR/URX neurons in the physiological hypertonic stress response

Gradual upshifts (between 200 mOsm and 1 Osm) in extracellular osmolarity cause *C. elegans* to increase their turning rate [511]. Expression of the cGMP-gated channel subunit *tax-2* in the PQR, AQR, and URX sensory neurons is required to mediate this aversive behavioral response [511]. Importantly, this behavior is genetically distinct from the acute reversal phenotype *C. elegans* exhibits when it encounters extracellular osmolarities > 1 Osm, which depends on the expression of the TRPV homolog *osm-9* in the ASH sensory neurons [343].

Since the *C. elegans* physiological HTSR (i.e. osmosensitive gene upregulation and glycerol accumulation in the hypodermis and intestine) occurs in the same range of tonicities as the behavioral increase in turning rate that depends on the PQR/AQR/URX neurons [318, 511], I investigated if these neurons also mediate the physiological HTSR. Specifically, I hypothesized that if the PQR/AQR/URX neurons were required for the physiological HTSR, then *tax-2* mutants would have reduced survival during 24 or 48 h of exposure to HTS (Fig A.1). *osm-8(n1518)* mutants served as positive controls in these survival assays because they constitutively accumulate glycerol and therefore have increased survival during HTS compared to WT animals [329]. The initial 24 and 48 h survival curves suggested that *tax-2* may be required for *C. elegans* survival on 400 – 450 mM NaCl NGM plates (Fig A.1A). Therefore, I tested the survival of three *tax-2* LOF mutants and a *tax-2(p694)* mutant strain overexpressing *tax-2* in the PQR/AQR/URX neurons at 400 and 450 mM NaCl (Fig A.1B). The survival results were highly variable among the different

tax-2 alleles, salt conditions, and between experiments. Furthermore, the *tax-2(p694)* mutant strain overexpressing *tax-2* in the PQR/AQR/URX neurons did not consistently rescue the survival of *tax-2(p694)* mutants (Fig A.1B). Based on these results it is unlikely that the PQR/AQR/URX neurons regulate the physiological HTSR.

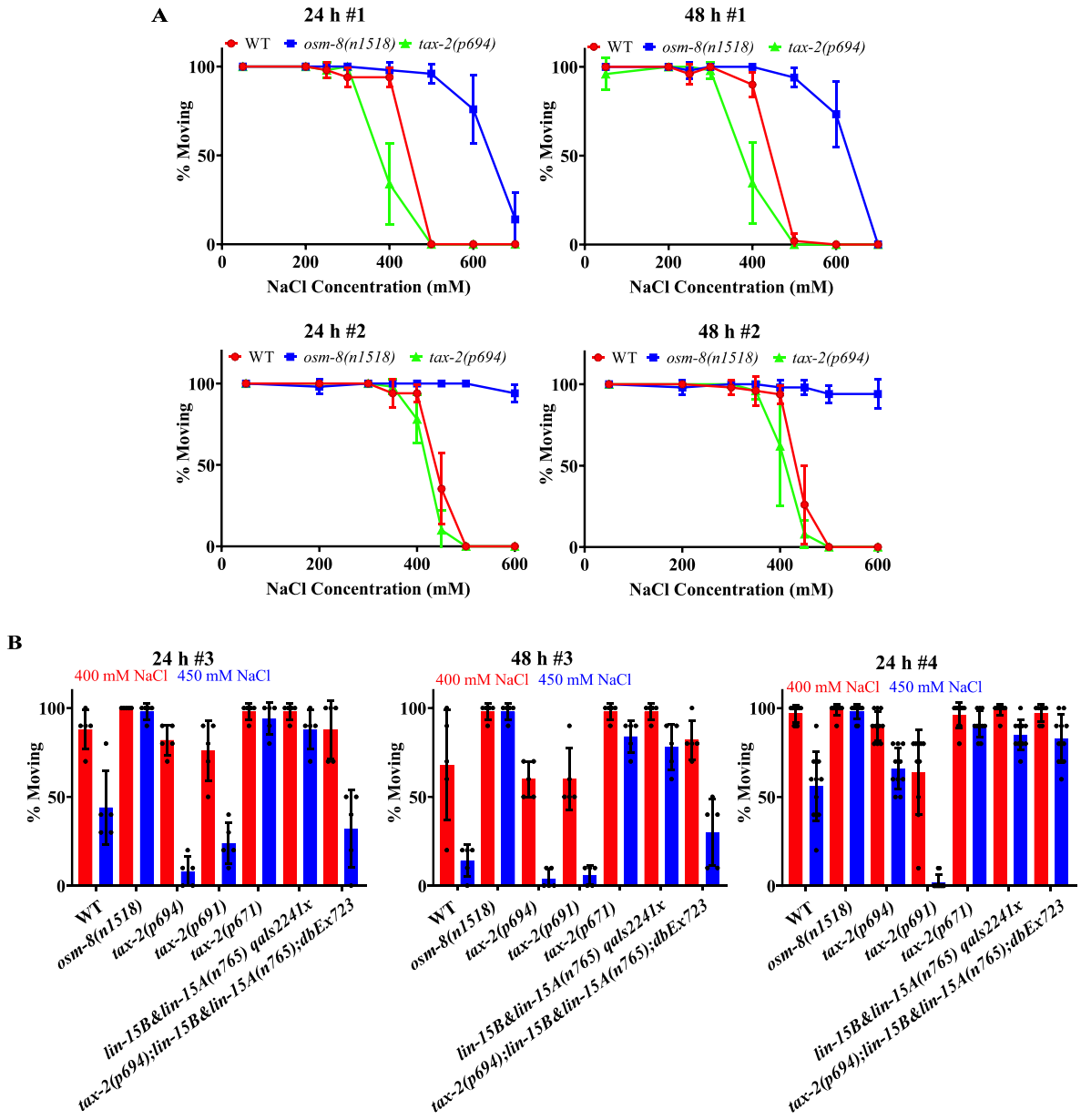

Figure A.1 *tax-2* expression in the PQR/AQR/URX neurons is not required for survival during HTS

(A) Percent survival of day 2 adult animals exposed to 100 – 600 or 700 mM NaCl NGM plates for 24 and 48 hours. Strains include WT, *osm-8(n1518)*, and *tax-2(p694)*. Data are expressed as mean ± S.D. N = 5 replicates of 20 animals for each salt concentration. The number above each graph indicates the duration of HTS and experiment number. (B) Percent survival of day 2 adult animals exposed to 400 or 450 mM NaCl for 24 and 48 hours. The *tax-2(p694);lin-15A&lin-15B(n765);dbEx723* strain is a *tax-2* rescue strain in which an extrachromosomal array containing the *tax-2* genomic sequence is expressed specifically in the PQR/AQR/URX neurons of *tax-2(p694)*

mutants. We included *lin-15A&lin-15B(n765)qals2241x* animals to test the background of this *tax-2* rescue strain. Data are expressed as mean ± S.D. N = 5 replicates of 20 animals for each salt concentration. The number of above each graph indicates the duration of HTS and experiment number.

Appendix A.2 Loss of *gpdh-1* impairs growth during hypertonic stress

I characterized the phenotype of the presumptive null *gpdh-1(ok1558)* mutant during HTS using a growth assay based on COPAS Biosort TOF measurements. In this assay, I seeded WT and *gpdh-1(ok1558)* mutant L1s on isotonic (50 mM NaCl) and hypertonic (400 mM NaCl) NGM plates and measured their size as adults. There was no difference in the size of WT and *gpdh-1(ok1558)* mutant animals exposed to isotonic conditions (Fig A.2A). However, when grown in hypertonic conditions for the same amount of time, *gpdh-1(ok1558)* mutants were significantly smaller than WT animals (Fig A.2B). This result suggests that GPDH-1 facilitates *C. elegans* growth during HTS.

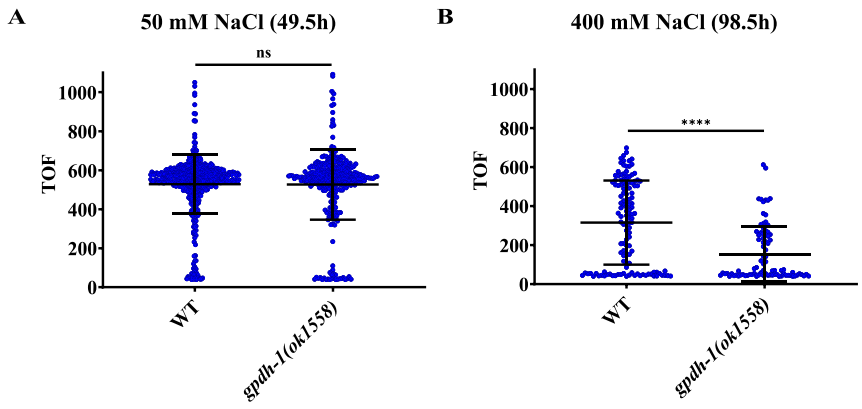

Figure A.2 *gpdh-1* is required for growth in hypertonic conditions

(A) COPAS Biosort quantification of the TOF of animals grown on 50 mM NaCl NGM plates. Animals were seeded on 50 mM NaCl NGM plates as L1s and data was acquired 49.5 hours later when these animals reached adulthood. Strains include WT and the presumptive *gpdh-1* null allele *gpdh-1(ok1558). ok1558* is an out-of-frame deletion allele that generates a premature stop codon in exon 2 of *gpdh-1* and is therefore a likely null allele. Data are expressed as mean ± S.D. ns = nonsignificant (Mann-Whitney test). N ≥ 313 for each group. (B) COPAS Biosort quantification of the TOF of animals grown on 400 mM NaCl NGM plates. Animals were seeded on 400 mM NaCl NGM plates as L1s and data was acquired 98.5 hours later when these animals reached adulthood. Strains include WT and the presumptive *gpdh-1* null allele *gpdh-1(ok1558).* Data are expressed as mean ± S.D. **** - $p < 0.0001$ (Mann-Whitney test). N ≥ 86 for each group.

Appendix A.3 *ogt-1* is required for full induction of the transcriptional *gpdh-1p::GFP (drIs4)* and translational *gpdh-1p::GPDH-1-GFP* (*kbIs6)* reporters during hypertonic stress

A western blot using a GFP antibody showed that *ogt-1(dr15)* and *ogt-1(dr20)* mutants expressed reduced amounts of the *gpdh-1p::GFP (drIs4)* transcriptional reporter (Fig A.3A) during HTS. Similarly, loss of *ogt-1* also reduced the hypertonic induction of the *gpdh-1p::GPDH-1-GFP* (*kbIs6)* translational reporter as measured by western blot (Fig A.3B). These

western blots in combination support the *gpdh-1p::GFP* fluorescence data for *ogt-1* mutants during HTS (Fig 2.2.1B, 2.2.1C, and 2.2.4A).

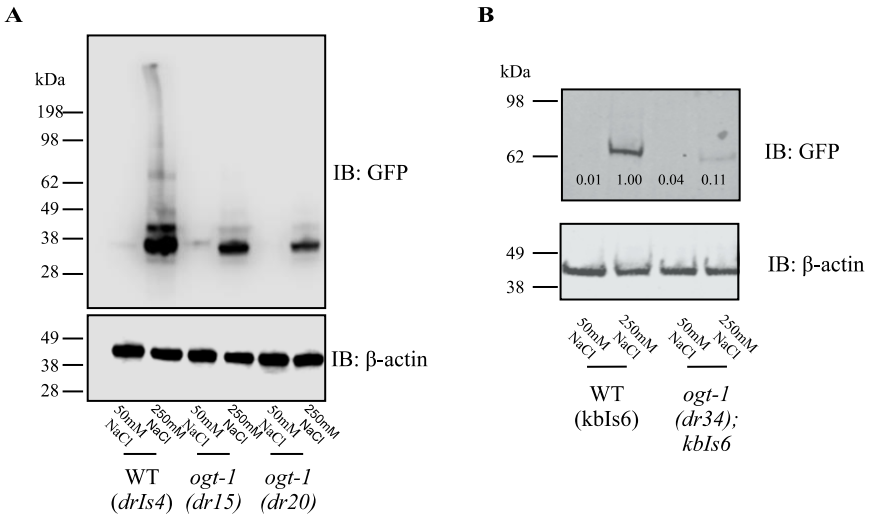

Figure A.3 *ogt-1* is required for full induction of the *gpdh-1p::GFP (drIs4)* and *gpdh-1p::GPDH-1-GFP* (*kbIs6)* reporters during HTS

(A) Immunoblot of GFP and *β*-actin in lysates from WT and *ogt-1* mutant animals expressing *drIs4* exposed to 50 or 250 mM NaCl NGM plates for 18 hours. (B) Immunoblot of GFP and *β*-actin in lysates from WT and *ogt-1(dr34)* animals expressing the *kbIs6* translational fusion exposed to 50 or 250 mM NaCl NGM plates for 18 hours. The *ogt-1(dr34)* allele carries the same homozygous Q600STOP mutation as the *ogt-1(dr20)* allele and was introduced using CRISPR/Cas9. Numbers under the GFP bands represent GFP signal normalized to *β*-actin signal for each sample, with the WT 250 mM NaCl sample set to 1.

Appendix A.4 Quantification of the hypertonic induction of *gpdh-1p::GFP (drIs4)* in a mixed age population of animals

Our Nio screen was done in adult *C. elegans* (500-1000 TOF). Here I tested if younger stage *ogt-1* mutants also had a Nio phenotype. *ogt-1* mutants within the 40-100 TOF, 100-200

TOF, and 300-500 TOF sizes were Nio (Fig A.4A, A.4B, and A.4D). However, *ogt-1* mutants within the 200-300 TOF size induced the *gpdh-1p::GFP (drIs4)* reporter similarly to WT animals suggesting that they were not Nio. Therefore, the Nio phenotype of *ogt-1* mutants may depend on developmental stage. However, this result has only been achieved once and thus this experiment needs to be repeated before robust conclusions can be made. The next time this experiment is done, it may be useful to more directly test the effect of developmental stage on hypertonic *gpdh-1p::GFP* induction instead of using COPAS Biosort size (TOF) as a proxy for developmental stage. Although more laborious, this can be achieved by growing up synchronized *C. elegans* to each larval stage and individually testing each group of animals on high salt. In this way, developmental stage can be directly linked to the ability to mount a HTSR in WT and *ogt-1* mutant animals.

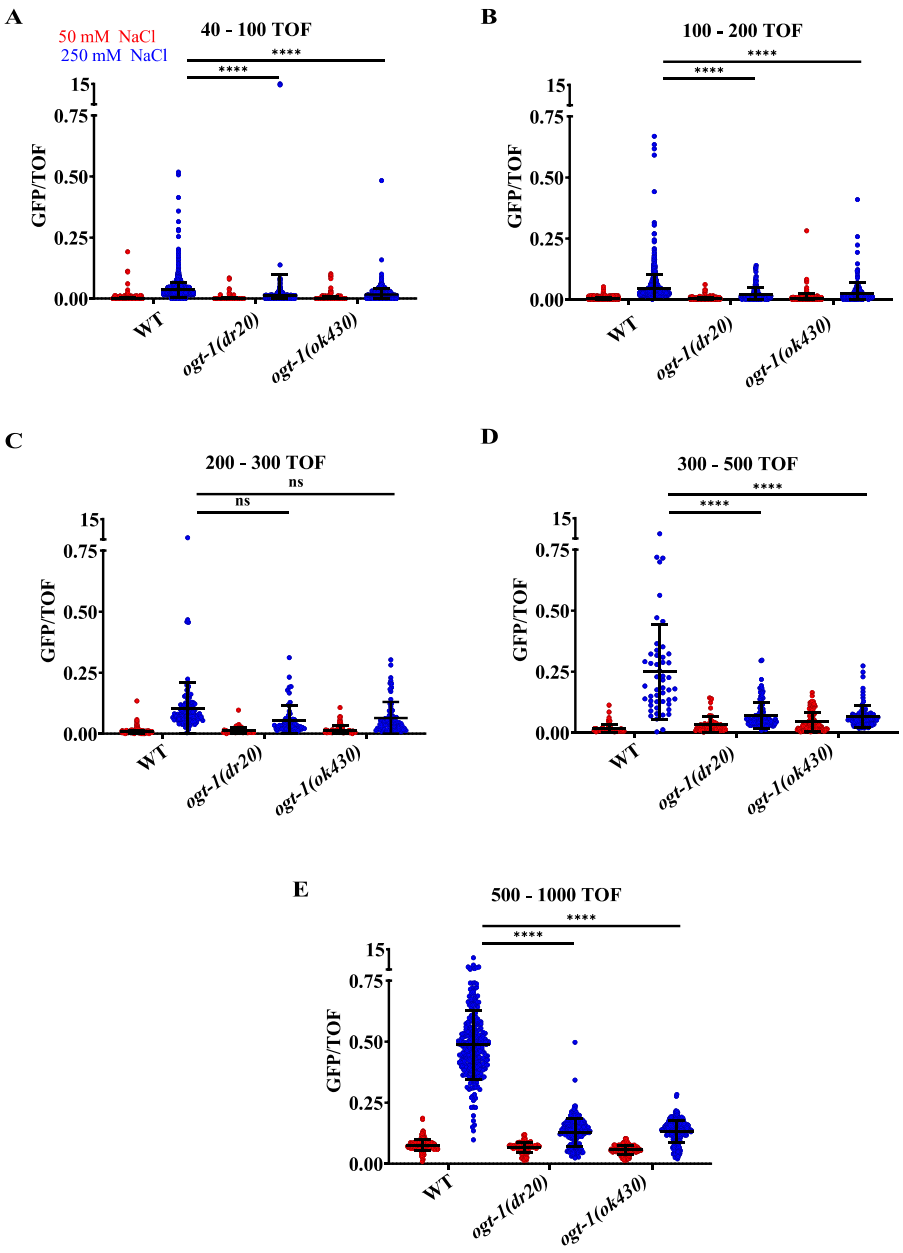

Figure A.4 The dependence of *gpdh-1p::GFP* expression on animal developmental stage

(A) COPAS Biosort quantification of GFP and TOF signal from animals that had a TOF between 40 and 100. Data are represented as the GFP/TOF ratio of animals exposed to 50 or 250 mM NaCl. Each point represents the quantified signal from a single animal. Data are expressed as mean ± S.D. **** - $p < 0.0001$ (Kruskal-Wallis test with post hoc Dunn's test). $N \geq 567$ for each group. (B) COPAS Biosort quantification of GFP and TOF signal from animals that had a TOF between 100 and 200. Data are represented as the GFP/TOF ratio of animals exposed to 50 or 250 mM

NaCl. Each point represents the quantified signal from a single animal. Data are expressed as mean ± S.D. **** - $p < 0.0001$ (Kruskal-Wallis test with post hoc Dunn's test). $N \geq 154$ for each group. (C) COPAS Biosort quantification of GFP and TOF signal from animals that had a TOF between 200 and 300. Data are represented as the GFP/TOF ratio of animals exposed to 50 or 250 mM NaCl. Each point represents the quantified signal from a single animal. Data are expressed as mean ± S.D. ns = nonsignificant (Kruskal-Wallis test with post hoc Dunn's test). $N \geq 53$ for each group. (D) COPAS Biosort quantification of GFP and TOF signal from animals that had a TOF between 300 and 500. Data are represented as the GFP/TOF ratio of animals exposed to 50 or 250 mM NaCl. Each point represents the quantified signal from a single animal. Data are expressed as mean ± S.D. **** - $p < 0.0001$ (Kruskal-Wallis test with post hoc Dunn's test). $N \geq 45$ for each group. (E) COPAS Biosort quantification of GFP and TOF signal from animals that had a TOF between 500 and 1000. Data are represented as the GFP/TOF ratio of animals exposed to 50 or 250 mM NaCl. Each point represents the quantified signal from a single animal. Data are expressed as mean ± S.D. **** - $p < 0.0001$ (Kruskal-Wallis test with post hoc Dunn's test). $N \geq 116$ for each group.

Appendix A.5 Intracellular glycerol measurements in *ogt-1, cpf-2,* and *symk-1* mutants

I measured whole worm glycerol concentration in *ogt-1*, *cpf-2*, and *symk-1* Nio mutants using the PicoProbe Free Glycerol Fluorometric Assay Kit (Biovision). We decided to utilize this new glycerol detection assay because it theoretically would allow us to measure whole animal glycerol content using a smaller number of worms and in a quicker fashion than previously used methods [318]. I measured they glycerol content of about fifty *C. elegans* per genotype per sample and normalized the glycerol concentration to protein concentration (measured with a BCA assay). The fifty *C. elegans* were picked directly from plates into glycerol assay buffer. In WT animals, I measured about a two-fold increase in glycerol levels during HTS (Fig A.5). This increase in glycerol accumulation was considerably smaller than expected based on previous experiments in which glycerol accumulation was increased on the order of hundreds fold. Glycerol accumulation

in the four Nio mutants was variable between experiments and I did not measure glycerol levels in these mutants in isotonic conditions (Fig A.5).

It is hard to draw conclusions from the results of this experiment because the small increase in glycerol concentration during HTS in WT animals suggests that the assay parameters are not optimized for accurate glycerol quantification. This smaller increase in glycerol concentration in WT animals could be due to the small number of animals or the sensitivity of the plate reader. Additionally, since the *C. elegans* were not washed prior to preparing the sample, bacterial contamination may have interfered with the fluorometric reaction, but there is currently no evidence that this was the case.

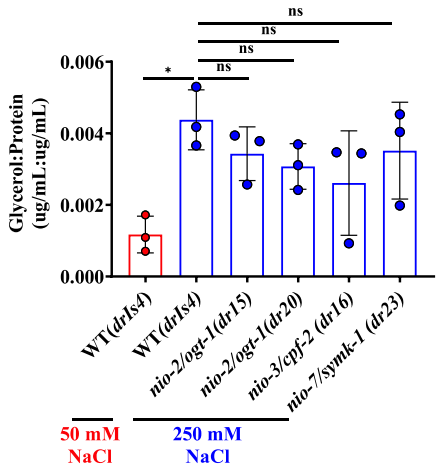

Figure A.5 Intracellular glycerol accumulation in *ogt-1*, *cpf-2*, and *symk-1* mutants

Whole worm glycerol concentration normalized to total protein concentration in day 2 adult animals exposed to 50 or 250 mM NaCl NGM plates for 18 hours. The PicoProbe Free Glycerol Fluorometric Assay Kit (Biovision) was used to measure glycerol concentration and the Pierce BCA Protein Assay Kit was used to measure protein concentration. Data are expressed as mean ± S.D. * - $p < 0.05$, ns = nonsignificant (One-way ANOVA with post hoc Tukey's test). N = 3 biological replicates of 50 animals each and three technical replicates within each biological replicate.

Appendix A.6 *empty vector(RNAi)* and *ogt-1(RNAi)* impact the acute adaptation of wild type animals

I performed an acute adaptation assay with WT *drIs4 (gpdh-1p::GFP)* and N2 Bristol *C. elegans* treated with either *ev(RNAi)* or *ogt-1(RNAi).* The rationale behind this experiment was to determine if *ogt-1(RNAi)* phenocopied the *ogt-1* LOF mutant adaptation phenotype. Surprisingly, my results suggested that RNAi was not compatible with the adaptation assay (Fig A.6). In both N2 and *drIs4* animals, the movement of *ogt-1(RNAi)*-treated unadapted animals was not fully suppressed (Fig A.6). Furthermore, a smaller percentage of adapted *drIs4* animals treated with *ev(RNAi)* were moving than expected based on previous adaptation assays (Fig 2.2.6A and A.6). Since *C. elegans* in RNAi experiments are fed a different strain of *E. coli* (HT115 *E. coli*) than non-RNAi experiments (OP50 *E.coli*), the discrepancies between the RNAi and mutant adaptation assays may be due to the different food sources. Alternatively, engagement of the RNAi machinery may desensitize *C. elegans* to HTS.

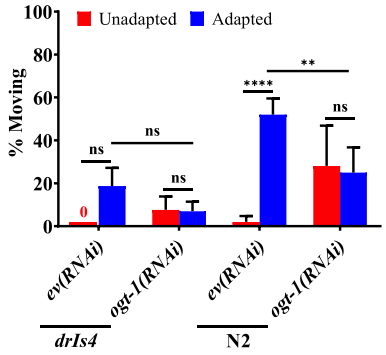

Figure A.6 Acute adaptation of WT animals treated with *empty vector(RNAi)* or *ogt-1(RNAi)*

Percent of moving unadpated and adapted day 3 adult animals exposed to 600 mM NaCl NGM plates for 24 hours. Strains include WT (N2) animals and WT animals expressing *drIs4*. Data are expressed an mean ± S.D. *** - $p < 0.001$, ** - $p < 0.01$, ns = nonsignificant (Two-way ANOVA with post hoc Tukey's test). N = 5 replicates of 20 animals for each strain.

Appendix A.7 *ogt-1* mutant acute adaptation assays with overexpressed transgenes

Since expression of an *ogt-1* cDNA transgene in *ogt-1* mutants rescued *gpdh-1p::GFP* reporter induction during HTS, I tested if it also rescued acute adaptation to HTS (Fig 2.2.1E, A.7A, and A.7B). In my initial experiments, I injected the rescue transgenes with a *rol-6(su1006)* marker. This marker causes a roller phenotype, which makes it possible to identify transgenic animals. Interestingly, I found that use of the *rol-6(su1006)* injection marker interfered with rescue of the adaptation phenotype (Fig A.7A). Expression *rol-6(su1006)* in *C. elegans* affects the cuticle to cause the roller phenotype. Since the cuticle is a critical component of the HTSR, expression of *rol-6(su1006)* may also influence the HTSR. In support of this hypothesis, when I injected the

rescue transgenes with a pharyngeal *myo2p::GFP* marker instead of the *rol-6(su1006)* marker, expression of an *ogt-1* cDNA transgene in *ogt-1* mutants rescued acute adaptation (Fig A.7B).

I also examined if expression of WT or catalytically inhibited H498A human OGT (*hOGT*) with the pharyngeal *myo2p::GFP* marker in *ogt-1* mutants rescued the acute adaptation phenotype (A.7C). Since expression of both WT and H498A *hOGT* in *ogt-1* mutants partially rescued hypertonic *gpdh-1p:GFP* induction, I hypothesized that these two constructs would also both partially rescue acute adaptation. However, the expression of neither WT nor H489A *hOGT* in *ogt-1* mutants rescued the acute adaptation phenotype (Fig A.7C). This result suggests that the partial rescue of hypertonic *gpdh-p::GFP* induction by WT or H498A *hOGT* in *ogt-1* mutants is not sufficient to facilitate acute adaptation to HTS.

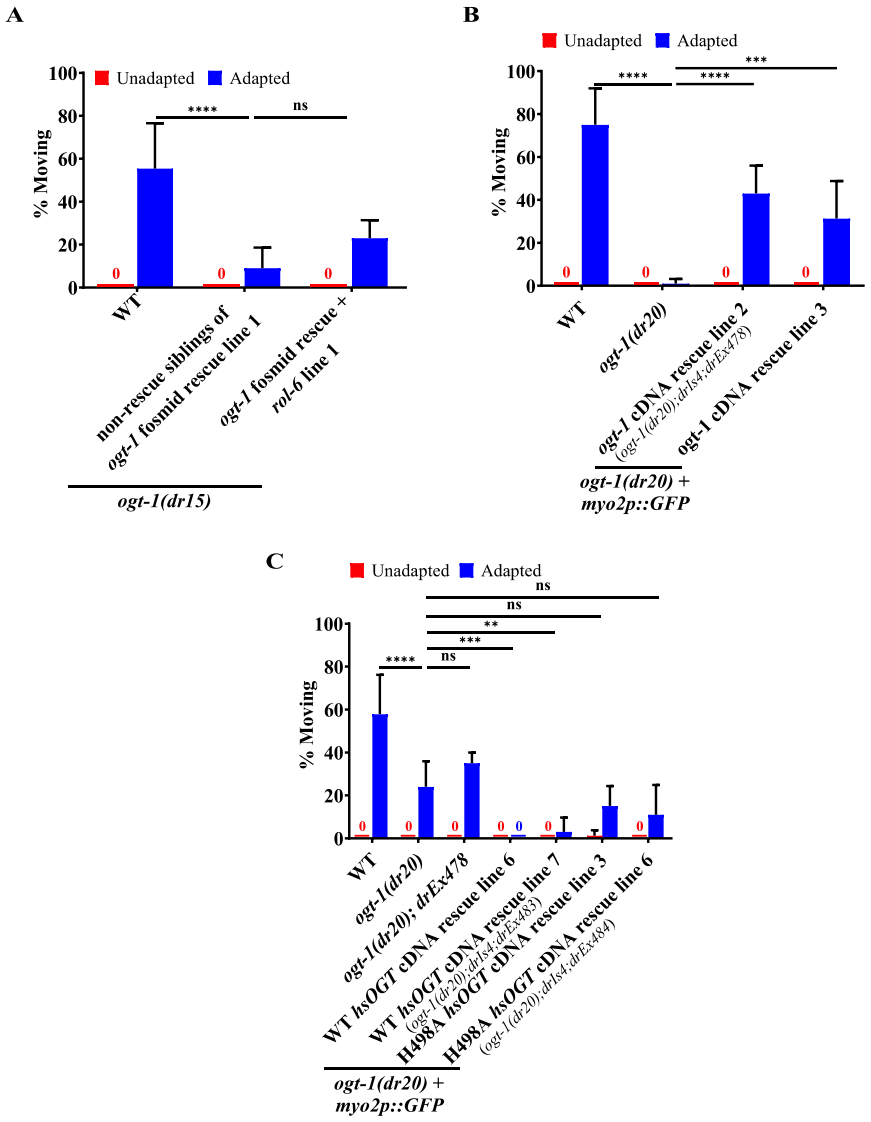

Figure A.7 Acute adaptation assays with *ogt-1* mutant rescue strains

(A) Percent of moving unadapted and adapted day 3 adult animals exposed to 600 mM NaCl NGM plates for 24 hours. Strains express *drIs4* and include WT, *ogt-1(dr15)* mutants expressing an extrachromosomal array with a roller marker (*rol-6(su1006)*) and a fosmid containing *ogt-1* genomic sequence, and *ogt-1(dr15)* mutant siblings that do not express this extrachromosomal array. Data are expressed an mean ± S.D. **** - $p < 0.0001$, ns = nonsignificant (Two-way ANOVA with post hoc Tukey's test). N = 5 replicates of 20 animals for each strain. (B) Percent of moving unadapted and adapted day 3 adult animals exposed to 600 mM NaCl NGM plates for 24 hours. Strains express *drIs4* and include WT, *ogt-1(dr20)*, and two separate lines of *ogt-1(dr20)* mutants expressing an extrachromosomal array with the pharyngeal *myo2p::GFP* marker and a plasmid containing the *ogt-1* cDNA sequence. Data are expressed an mean ±

S.D. **** - p < 0.0001, *** - p < 0.001 (Two-way ANOVA with post hoc Tukey's test). N = 5 replicates of 20 animals for each strain. (C) Percent of moving unadapted and adapted day 3 adult animals exposed to 600 mM NaCl NGM plates for 24 hours. Strains express *drIs4* and include WT, *ogt-1(dr20)*, *ogt-1(dr20)* mutants expressing an extrachromosomal array with the *myo2-GFP* pharyngeal marker and *ogt-1* cDNA (*ogt-1(dr20);drEx478),* and two separate lines each of *ogt-1(dr20)* mutants expressing an extrachromosomal array with the *myo2-GFP* pharyngeal marker and either WT *h. sapians OGT* cDNA or H498A *h. sapians OGT* cDNA. Data are expressed as mean ± S.D. **** - p < 0.0001, *** - p < 0.001, ** - p < 0.05, ns = nonsignificant (Two-way ANOVA with post hoc Tukey's test). N = 5 replicates of 20 animals for each strain.

Appendix A.8 *osm-8(dr9)* mutants have reduced *gpdh-1* RNA induction

ogt-1 is required for the constitutive expression of the *gpdh-1p::GFP* reporter and survival of *osm-8* LOF mutants during HTS (Fig 2.2.7A and 2.2.7C). These results suggests that *ogt-1* may function downstream of extracellular proteins such as OSM-8 during HTS to regulate *gpdh-1* expression. During HTS, *ogt-1* is not required for induction of osmosensitive mRNAs despite being required for osmosensitive protein expression. Here, I measured *gpdh-1* mRNA levels in *osm-8(dr9);ogt-1(dr20)* double mutants to test if *osm-8* is required for the expression of endogenous *gpdh-1* mRNA. Surprisingly, unlike during HTS, *ogt-1* is required for *gpdh-1* mRNA induction in *osm-8* mutants (Fig A.8A). In support of this results, *ogt-1* is also required for GFP mRNA induction from the *gpdh-1p::GFP* reporter in *osm-8* mutants (Fig A.8B). These results indicate that *ogt-1* may function through distinct pathways in *osm-8* mutants and during HTS.

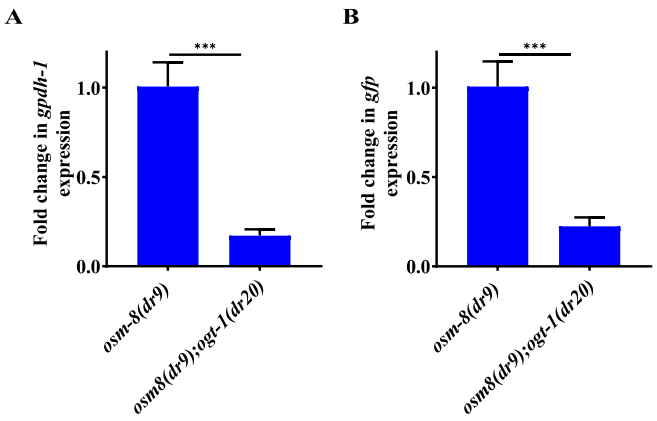

Figure A.8 *ogt-1* is required for constitutive upregulation of osmosensitive mRNAs in an *osm-8* mutant

(A) qPCR of *gpdh-1* mRNA from *osm-8(dr9)* and *osm-8(dr9);ogt-1(dr20)* mutant day 1 adult animals expressing *drIs4. osm-8(dr9)* was isolated in a previous genetic screen for new *osm-8* alleles but encodes the same mutation as the *n1518* reference allele. Data are represented as fold induction of RNA in *osm-8(dr9);ogt-1(dr20)* mutants relative to *osm-8(dr9)* mutants. Data are expressed as mean ± S.D. *** - $p < 0.001$ (Student's t-test). $N \geq 3$ biological replicates of 35 animals for each group. (B) qPCR of GFP mRNA from *osm-8(dr9)* and *osm-8(dr9);ogt-1(dr20)* mutant day 1 adult animals expressing *drIs4. osm-8(dr9)* was isolated in a previous genetic screen for new *osm-8* alleles but encodes the same mutation as the *n1518* reference allele. Data are represented as fold induction of RNA in *osm-8(dr9);ogt-1(dr20)* mutants relative to *osm-8(dr9)* mutants. Data are expressed as mean ± S.D. *** - $p < 0.001$ (Student's t-test). $N \geq 3$ biological replicates of 35 animals for each group.

Appendix A.9 Expression of *hOGT* cDNA with the *myo2p::GFP* marker does not rescue *gpdh-1p::GFP* induction in *ogt-1* mutants

Here, I measured hypertonic *gpdh-1p::GFP* induction in *ogt-1(dr20)* mutants injected with *hOGT* cDNA constructs and the *myo2p::GFP* marker. In contrast to the expression of *hOGT* cDNA with the *rol-6(su1006)* marker, which partially rescued hypertonic *gpdh-1p::GFP* induction

(Figure 2.2.9), expression of *hOGT* cDNA with the *myo2p::GFP* marker did not rescue hypertonic *gpdh-1p::GFP* induction in *ogt-1* mutants (Fig 2.2.9A, 2.2.9B, and A.9). Increasing the concentration of the injected *hOGT* cDNA construct from 20ng/µL to 100ng/µL also did not improve hypertonic *gpdh-1p::GFP* induction in *ogt-1* mutants (Fig A.9). These results suggest that increasing the injection concentration of the *hOGT* cDNA construct does not improve hypertonic *gpdh-1p::GFP* induction in *ogt-1* mutants. However, one important caveat in this experiment is that I only quantified the GFP/RFP signal for six *ogt-1(dr20)* mutants, which is a relatively small sample size, and the hypertonic *gpdh-1p::GFP* induction in these mutants was not significantly reduced compared to WT animals (Fig A.9). Therefore, this experiment needs to be redone with a larger *ogt-1(dr20)* sample size. If the results from this experiment stand, then they may explain why the *hOGT* constructs did not rescue the acute adaptation phenotype of *ogt-1(dr20)* mutants (Figure A.7). Additionally, this result would suggest that the *myo2p::GFP* marker masks the small rescue of *gpdh-1p::GFP* by the *hOGT* constructs in *ogt-1(dr20)* mutants.

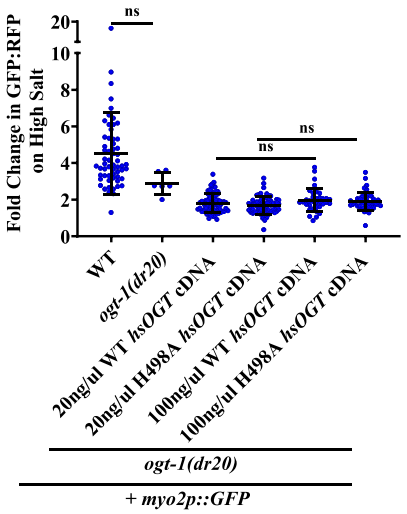

Figure A.9 Expression of *hOGT* cDNA with the pharyngeal *myo2p::GFP* marker does not rescue hypertonic *gpdh-1p::GFP* induction in *ogt-1* mutants

COPAS Biosort quantification of GFP and RFP signal in day 2 adult animals expressing *drIs4* exposed to 250 mM NaCl NGM plates for 18 hours. All strains express the pharyngeal *myo2p::GFP* marker. Data are represented as normalized fold induction of GFP/RFP ratio on 250 mM NaCl NGM plates relative to 50 mM NaCl NGM plates. Each point represents the quantified signal from a single animal. Data are expressed as mean ± S.D. ns = nonsignificant (Kruskal-Wallis test with post hoc Dunn's test). $N \geq 6$ for each group.

Appendix A.10 HB101 *E. coli* impairs hypertonic *gpdh-1p::GFP* induction in wild type animals

In addition to *rpn-8(RNAi)*, proteasomal activity in *C. elegans* can be inhibited by feeding it HB101 *E. coli* (Fig 2.2.4F) [494]. We thus fed WT and *ogt-1(dr20) C. elegans* HB101 *E. coli* to test if *ogt-1(dr20)* mutants have decreased hypertonic induction of GPDH-1 due to aberrant activation of the proteasome (Fig A.10). However, we found that HB101 bacteria impaired hypertonic *gpdh-1p::GFP* induction in WT animals (Fig A.10). Therefore, the results from this

experiment cannot be interpreted. We do not know why HB101 *E. coli* inhibits hypertonic *gpdh-1p::GFP* induction, but this finding suggests that the bacterial strain may influence the Nio phenotype.

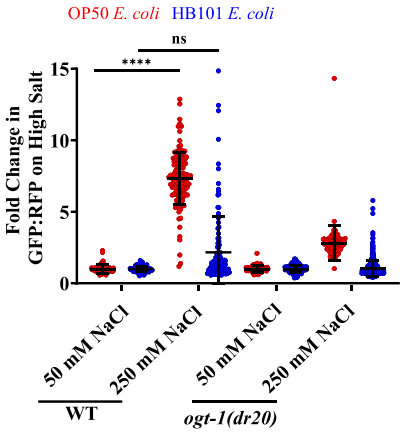

Figure A.10 Hypertonic *gpdh-1p::GFP* induction is impaired in WT and *ogt-1(dr20)* mutant animals fed HB101 *E. coli*

COPAS Biosort quantification of GFP and RFP signal in day 2 adult animals expressing *drIs4* exposed to 50 mM and 250 mM NaCl NGM plates for 18 hours. NGM plates were seeded with either the standard OP50 *E. coli* strain or the HB101 *E.coli* strain. Data are represented as normalized fold induction of GFP/RFP ratio on 50 or 250 mM NaCl NGM plates relative to 50 mM NaCl NGM plates. Each point represents the quantified signal from a single animal. Data are expressed as mean ± S.D. ns = nonsignificant (Kruskal-Wallis test with post hoc Dunn's test). $N \geq 81$ for each group.

Appendix A.11 TPRs 1-6 are required for hypertonic induction of *gpdh-1p::GFP* and acute adaptation to hypertonic stress

I used CRISPR/Cas9 to delete the first six TPRs of the endogenous *ogt-1* gene. Sequencing of the isolated ΔTPR_{1-6} allele revealed that it contained an in-frame deletion of the first six TPRs.

However, it was not the exact deletion that I engineered with my primers. Instead of a deletion spanning K127-E360 like I expected, the isolated ΔTPR$_{1-6}$ allele had a E130-N357 deletion. Additionally, the ΔTPR$_{1-6}$ allele contained a random eleven amino acid in-frame insertion sequence that did not introduce a stop codon. Therefore, although the ΔTPR$_{1-6}$ allele I isolated did not match the predicted sequence based on my CRISPR/Cas9 primers and a corrected allele needs to be made, it still appears to be a true TPR$_{1-6}$ deletion. We therefore carried out some preliminary experiments with this ΔTPR$_{1-6}$ allele.

Similarly to the full length ΔTPR allele (*ogt-1(dr93)*), the ΔTPR$_{1-6}$ *ogt-1* allele (*ogt-1(dr98))* completely suppressed the catalytic *O*-GlcNAcylation activity of OGT-1 (Fig 2.2.11A and A.11A). While we have not explicitly examined the expression levels of the *ogt-1(dr98)* allele, we predict that the TPR$_{1-6}$ deletion will not affect OGT-1 expression since the full length TPR deletion did not affect OGT-1 expression (Fig 2.2.11B) Additionally, like *ogt-1(dr93)*, *ogt-1(dr98)* animals had impaired hypertonic induction of *gpdh-1p::GFP* and adaptation to HTS (Fig 2.2.11C, 2.2.11D, 2.2.11E, A.11B, A.11C, and A.11D). While a ΔTPR$_{1-6}$ *ogt-1* allele with the correct sequence deletion needs to be made, these results suggest that the first six TPRs of OGT-1 are required for the HTSR.

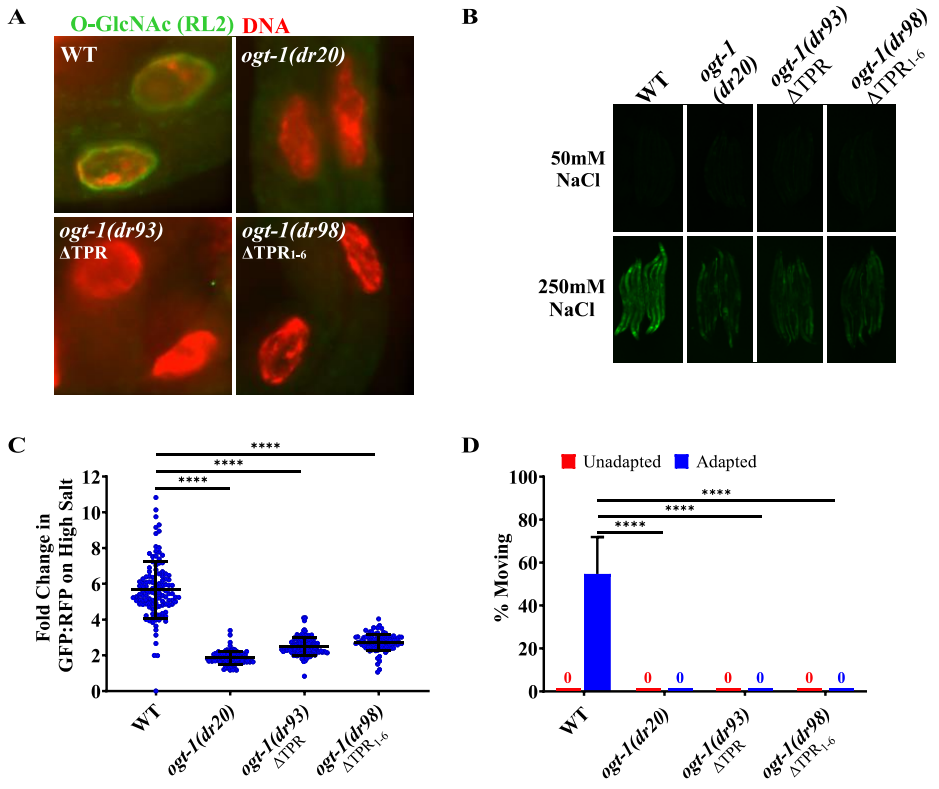

Figure A.11 TPRs 1-6 are required for hypertonic induction of *gpdh-1p::GFP* and acute adaptation to HTS

(A) Wide-field fluorescence microscopy of intestinal cells in fixed and stained day 1 adult animals. RL2 was used to stain for nuclear pore *O*-GlcNAc modifications and Hoechst 33258 was used to visualize the DNA. Images are exposure matched. (B) Wide-field fluorescence microscopy of day 2 adult animals expressing *drIs4* exposed to 50 or 250 mM NaCl NGM plates for 18 hours. Images depict the GFP channel only for clarity. The RFP channel was unaffected in these rescue strains (not shown). (C) COPAS Biosort quantification of GFP and RFP signal in day 2 adult animals expressing *drIs4* exposed to 250 mM NaCl NGM plates for 18 hours. Data are represented as the fold induction of normalized GFP/RFP ratio on 250 mM NaCl relative to on 50 mM NaCl NGM plates. Each point represents the quantified signal from a single animal. Data are expressed as mean ± S.D. **** - $p < 0.0001$ (Kruskal-Wallis test with post hoc Dunn's test). $N \geq 91$ for each group. (D) Percent of moving unadapted and adapted day 3 adult animals expressing *drIs4* exposed to 600 mM NaCl NGM plates for 24 hours. Data are expressed an mean ± S.D. **** - $p < 0.0001$ (Two-way ANOVA with post hoc Tukey's test). $N = 5$ replicates of 20 animals for each strain.

Appendix A.12 The protein expression of OGT-1 may increase in response to hypertonic stress

Previous microarray data suggests that *ogt-1* mRNA expression levels do not change during HTS [324]. However, preliminary data using a functional CRISPR/Cas9 GFP tagged *ogt-1* allele (OGT-1::GFP) indicates that the protein expression of OGT-1 may increase during HTS (Fig A12A and A12B). Exposure matched images indicate that OGT-1::GFP expression is increased during HTS (Fig A.12A). Furthermore, an anti-GFP western blot indicates this increase in OGT-1::GFP expression may be due to the formation of a new higher molecular weight OGT-1::GFP species (Fig A.12B). One possibility is that this higher molecular weight OGT-1::GFP species is due to the post-translational modification, such as the *O*-GlcNAcylation or phosphorylation, of OGT-1 during HTS. To test if OGT-1 is itself *O*-GlcNAcylated during HTS this western blot can be redone with the catalytically dead K957M OGT-1 allele. If the higher molecular weight OGT-1::GFP species goes away when the K957M mutation is introduced, this indicates that OGT-1 is *O*-GlcNAcylated during HTS. Alternatively, to test if OGT-1 is phosphorylated during HTS, phosphatase can be added to the protein lysate before the western blot. If the addition of phosphatase causes the higher molecular weight OGT-1::GFP species to disappear, this suggests that OGT-1 is phosphorylated during HTS.

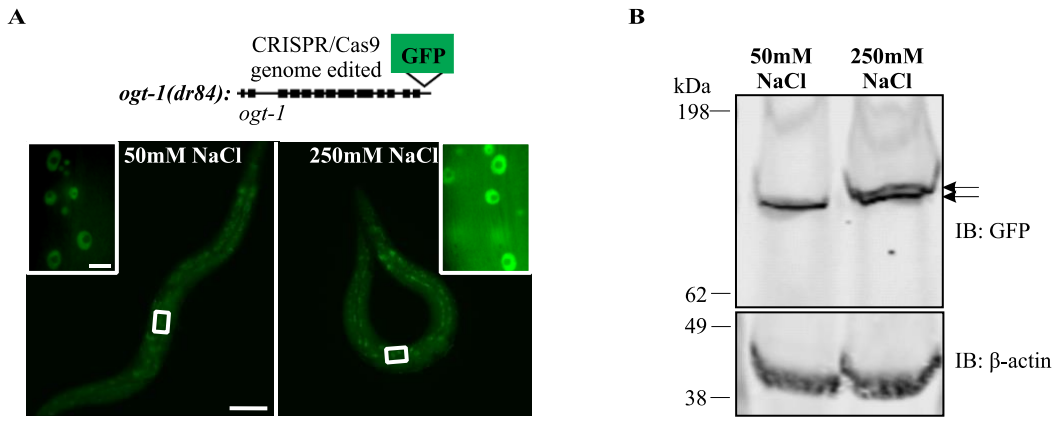

Figure A.12 The protein expression of OGT-1-GFP changes during hypertonic stress

(A) Wide-field fluorescence microscopy of WT day 2 adult animals expressing endogenously CRISPR/Cas9 GFP tagged OGT-1 exposed to 50 or 250 mM NaCl NGM plates. Scale bar = 100 microns. Images are exposure matched. *Inset:* Zoomed in images of the boxed area. Scale bar = 10 microns. (B) Immunoblot of GFP and *β*-actin in lysates from WT day 2 adult animals expressing endogenously CRISPR/Cas9 GFP tagged OGT-1 exposed to 50 or 250 mM NaCl NGM plates. Arrows point to the two OGT-1-GFP species present at 250 mM NaCl.

Bibliography

1. Burg, M.B., *Molecular basis of osmotic regulation.* Am J Physiol, 1995. **268**(6 Pt 2): p. F983-96.

2. Hippel, P.v. and T. Schleich, *The effects of neutral salts on the structure and conformational stability of macromolecules in solution.* Structure and stability of biological macromolecules, 1969. **2**: p. 417-574.

3. Borowitzka, L.J. and A.D. Brown, *The salt relations of marine and halophilic species of the unicellular green alga, Dunaliella. The role of glycerol as a compatible solute.* Arch Mikrobiol, 1974. **96**(1): p. 37-52.

4. Bowlus, R.D. and G.N. Somero, *Solute compatibility with enzyme function and structure: rationales for the selection of osmotic agents and end-products of anaerobic metabolism in marine invertebrates.* J Exp Zool, 1979. **208**(2): p. 137-51.

5. Best, L. and A.P. Yates, *Electrophysiological effects of osmotic cell shrinkage in rat pancreatic β-cells.* Islets, 2010. **2**(5): p. 303-7.

6. Ciano, C.D., et al., *Osmotic stress-induced remodeling of the cortical cytoskeleton.* American Journal of Physiology-Cell Physiology, 2002. **283**(3): p. C850-C865.

7. Cendoroglo, M., et al., *Necrosis and apoptosis of polymorphonuclear cells exposed to peritoneal dialysis fluids in vitro.* Kidney Int, 1997. **52**(6): p. 1626-34.

8. Terada, Y., et al., *Hyperosmolality activates Akt and regulates apoptosis in renal tubular cells.* Kidney Int, 2001. **60**(2): p. 553-67.

9. Bortner, C.D. and J.A. Cidlowski, *Absence of volume regulatory mechanisms contributes to the rapid activation of apoptosis in thymocytes.* American Journal of Physiology-Cell Physiology, 1996. **271**(3): p. C950-C961.

10. Galvez, A., et al., *A rapid and strong apoptotic process is triggered by hyperosmotic stress in cultured rat cardiac myocytes.* Cell Tissue Res, 2001. **304**(2): p. 279-85.

11. Michea, L., et al., *Cell cycle delay and apoptosis are induced by high salt and urea in renal medullary cells.* Am J Physiol Renal Physiol, 2000. **278**(2): p. F209-18.

12. Santos, B.C., et al., *A combination of NaCl and urea enhances survival of IMCD cells to hyperosmolality.* American Journal of Physiology-Renal Physiology, 1998. **274**(6): p. F1167-F1173.

13. Walter, A. and J. Gutknecht, *Permeability of small nonelectrolytes through lipid bilayer membranes.* J Membr Biol, 1986. **90**(3): p. 207-17.

14. Papahadjopoulos, D., S. Nir, and S. Oki, *Permeability properties of phospholipid membranes: effect of cholesterol and temperature.* Biochim Biophys Acta, 1972. **266**(3): p. 561-83.

15. Lande, M.B., J.M. Donovan, and M.L. Zeidel, *The relationship between membrane fluidity and permeabilities to water, solutes, ammonia, and protons.* J Gen Physiol, 1995. **106**(1): p. 67-84.

16. Agre, P., et al., *Aquaporin water channels--from atomic structure to clinical medicine.* J Physiol, 2002. **542**(Pt 1): p. 3-16.

17. Verkman, A.S., *Mammalian aquaporins: diverse physiological roles and potential clinical significance.* Expert Rev Mol Med, 2008. **10**: p. e13.

18. Agre, P., et al., *Purification and partial characterization of the Mr 30,000 integral membrane protein associated with the erythrocyte Rh(D) antigen.* J Biol Chem, 1987. **262**(36): p. 17497-503.

19. Preston, G.M., et al., *Membrane topology of aquaporin CHIP. Analysis of functional epitope-scanning mutants by vectorial proteolysis.* J Biol Chem, 1994. **269**(3): p. 1668-73.

20. Nielsen, S., et al., *Vasopressin increases water permeability of kidney collecting duct by inducing translocation of aquaporin-CD water channels to plasma membrane.* Proc Natl Acad Sci U S A, 1995. **92**(4): p. 1013-7.

21. Yang, B., et al., *Neonatal mortality in an aquaporin-2 knock-in mouse model of recessive nephrogenic diabetes insipidus.* J Biol Chem, 2001. **276**(4): p. 2775-9.

22. Krane, C.M., et al., *Salivary acinar cells from aquaporin 5-deficient mice have decreased membrane water permeability and altered cell volume regulation.* J Biol Chem, 2001. **276**(26): p. 23413-20.

23. Ishibashi, K., et al., *Cloning and functional expression of a new water channel abundantly expressed in the testis permeable to water, glycerol, and urea.* J Biol Chem, 1997. **272**(33): p. 20782-6.

24. Kishida, K., et al., *Aquaporin adipose, a putative glycerol channel in adipocytes.* J Biol Chem, 2000. **275**(27): p. 20896-902.

25. Hara-Chikuma, M., et al., *Progressive adipocyte hypertrophy in aquaporin-7-deficient mice: adipocyte glycerol permeability as a novel regulator of fat accumulation.* J Biol Chem, 2005. **280**(16): p. 15493-6.

26. Huang, C.G., et al., *Functional analysis of the aquaporin gene family in Caenorhabditis elegans.* Am J Physiol Cell Physiol, 2007. **292**(5): p. C1867-73.

27. Lohr, J.W. and J.J. Grantham, *Isovolumetric regulation of isolated S2 proximal tubules in anisotonic media.* J Clin Invest, 1986. **78**(5): p. 1165-72.

28. Hoffmann, E.K., I.H. Lambert, and S.F. Pedersen, *Physiology of cell volume regulation in vertebrates.* Physiol Rev, 2009. **89**(1): p. 193-277.

29. Strange, K., *Cellular volume homeostasis.* Adv Physiol Educ, 2004. **28**(1-4): p. 155-9.

30. Cheung, R.K., et al., *Volume regulation by human lymphocytes: characterization of the ionic basis for regulatory volume decrease.* J Cell Physiol, 1982. **112**(2): p. 189-96.

31. Hoffmann, E.K. and K.B. Hendil, *The role of amino acids and taurine in isosmotic intracellular regulation in Ehrlich ascites mouse tumour cells.* Journal of comparative physiology, 1976. **108**(3): p. 279-286.

32. Verbalis, J.G. and S.R. Gullans, *Hyponatremia causes large sustained reductions in brain content of multiple organic osmolytes in rats.* Brain Res, 1991. **567**(2): p. 274-82.

33. Strange, K. and P.S. Jackson, *Swelling-activated organic osmolyte efflux: a new role for anion channels.* Kidney Int, 1995. **48**(4): p. 994-1003.

34. Strange, K., *Molecular identity of the outwardly rectifying, swelling-activated anion channel: time to reevaluate pICln.* J Gen Physiol, 1998. **111**(5): p. 617-22.

35. Kirk, K., *Swelling-activated organic osmolyte channels.* J Membr Biol, 1997. **158**(1): p. 1-16.

36. Voss, F.K., et al., *Identification of LRRC8 heteromers as an essential component of the volume-regulated anion channel VRAC.* Science, 2014. **344**(6184): p. 634-8.

37. Oberleithner, H., et al., *Endothelial cell swelling by aldosterone.* J Membr Biol, 2003. **196**(3): p. 163-72.

38. Basavappa, S., et al., *Inhibition of Na+, K+-ATPase activates swelling-induced taurine efflux in a human neuroblastoma cell line.* J Cell Physiol, 1998. **174**(2): p. 145-53.

39. Ferrer-Martinez, A., et al., *Regulation of Na+,K(+)-ATPase and the Na+/K+/Cl- co-transporter in the renal epithelial cell line NBL-1 under osmotic stress.* Biochem J, 1996. **319 (Pt 2)**(Pt 2): p. 337-42.

40. Wehner, F., H. Sauer, and R.K. Kinne, *Hypertonic stress increases the Na+ conductance of rat hepatocytes in primary culture.* J Gen Physiol, 1995. **105**(4): p. 507-35.

41. Beck, F.X., A. Burger-Kentischer, and E. Müller, *Cellular response to osmotic stress in the renal medulla.* Pflugers Arch, 1998. **436**(6): p. 814-27.

42. Hebert, S.C., *Hypertonic cell volume regulation in mouse thick limbs. II. Na+-H+ and Cl(-)-HCO3- exchange in basolateral membranes.* Am J Physiol, 1986. **250**(6 Pt 1): p. C920-31.

43. Sone, M., et al., *Osmotic adaptation of renal medullary cells during transition from chronic diuresis to antidiuresis.* Am J Physiol, 1993. **264**(4 Pt 2): p. F722-9.

44. Yancey, P.H., et al., *Living with water stress: evolution of osmolyte systems.* Science, 1982. **217**(4566): p. 1214-22.

45. Sone, M., et al., *Restoration of urine concentrating ability and accumulation of medullary osmolytes after chronic diuresis.* Am J Physiol, 1995. **269**(4 Pt 2): p. F480-90.

46. Schmolke, M., F.X. Beck, and W.G. Guder, *Effect of antidiuretic hormone on renal organic osmolytes in Brattleboro rats.* Am J Physiol, 1989. **257**(5 Pt 2): p. F732-7.

47. Piechotta, K., J. Lu, and E. Delpire, *Cation chloride cotransporters interact with the stress-related kinases Ste20-related proline-alanine-rich kinase (SPAK) and oxidative stress response 1 (OSR1).* J Biol Chem, 2002. **277**(52): p. 50812-9.

48. Dowd, B.F. and B. Forbush, *PASK (proline-alanine-rich STE20-related kinase), a regulatory kinase of the Na-K-Cl cotransporter (NKCC1).* J Biol Chem, 2003. **278**(30): p. 27347-53.

49. López-Rodríguez, C., et al., *Loss of NFAT5 results in renal atrophy and lack of tonicity-responsive gene expression.* Proc Natl Acad Sci U S A, 2004. **101**(8): p. 2392-7.

50. Brown, A.D. and J.R. Simpson, *Water relations of sugar-tolerant yeasts: the role of intracellular polyols.* J Gen Microbiol, 1972. **72**(3): p. 589-91.

51. Yancey, P.H., *Organic osmolytes as compatible, metabolic and counteracting cytoprotectants in high osmolarity and other stresses.* J Exp Biol, 2005. **208**(Pt 15): p. 2819-30.

52. Burg, M.B. and J.D. Ferraris, *Intracellular organic osmolytes: function and regulation.* J Biol Chem, 2008. **283**(12): p. 7309-13.

53. Albertyn, J., S. Hohmann, and B.A. Prior, *Characterization of the osmotic-stress response in Saccharomyces cerevisiae: osmotic stress and glucose repression regulate glycerol-3-phosphate dehydrogenase independently.* Curr Genet, 1994. **25**(1): p. 12-8.

54. Shen, B., et al., *Roles of sugar alcohols in osmotic stress adaptation. Replacement of glycerol by mannitol and sorbitol in yeast.* Plant Physiol, 1999. **121**(1): p. 45-52.

55. Yancey, P.H., *Compatible and counteracting solutes: protecting cells from the Dead Sea to the deep sea.* Sci Prog, 2004. **87**(Pt 1): p. 1-24.

56. Pruski, A.M., et al., *Thiotaurine is a biomarker of sulfide-based symbiosis in deep-sea bivalves.* Limnology and Oceanography, 2000. **45**(8): p. 1860-1867.

57. Rosenberg, N.K., R.W. Lee, and P.H. Yancey, *High contents of hypotaurine and thiotaurine in hydrothermal-vent gastropods without thiotrophic endosymbionts.* J Exp Zool A Comp Exp Biol, 2006. **305**(8): p. 655-62.

58. Yancey, P.H., W.R. Blake, and J. Conley, *Unusual organic osmolytes in deep-sea animals: adaptations to hydrostatic pressure and other perturbants.* Comp Biochem Physiol A Mol Integr Physiol, 2002. **133**(3): p. 667-76.

59. Wolfe, G.V., *The chemical defense ecology of marine unicellular plankton: constraints, mechanisms, and impacts.* Biol Bull, 2000. **198**(2): p. 225-44.

60. DICKSON, D.M.J. and G.O. KIRST, *OSMOTIC ADJUSTMENT IN MARINE EUKARYOTIC ALGAE: THE ROLE OF INORGANIC IONS, QUATERNARY AMMONIUM, TERTIARY SULPHONIUM AND CARBOHYDRATE SOLUTES.* New Phytologist, 1987. **106**(4): p. 645-655.

61. Hanson, A.D., et al., *Comparative Physiological Evidence that beta-Alanine Betaine and Choline-O-Sulfate Act as Compatible Osmolytes in Halophytic Limonium Species.* Plant Physiol, 1991. **97**(3): p. 1199-205.

62. Yancey, P.H., M.B. Burg, and S.M. Bagnasco, *Effects of NaCl, glucose, and aldose reductase inhibitors on cloning efficiency of renal medullary cells.* Am J Physiol, 1990. **258**(1 Pt 1): p. C156-63.

63. Back, J.F., D. Oakenfull, and M.B. Smith, *Increased thermal stability of proteins in the presence of sugars and polyols.* Biochemistry, 1979. **18**(23): p. 5191-6.

64. Gekko, K. and S.N. Timasheff, *Thermodynamic and kinetic examination of protein stabilization by glycerol.* Biochemistry, 1981. **20**(16): p. 4677-86.

65. Tatzelt, J., S.B. Prusiner, and W.J. Welch, *Chemical chaperones interfere with the formation of scrapie prion protein.* Embo j, 1996. **15**(23): p. 6363-73.

66. Arakawa, T. and S.N. Timasheff, *The stabilization of proteins by osmolytes.* Biophys J, 1985. **47**(3): p. 411-4.

67. Auton, M., et al., *Osmolyte effects on protein stability and solubility: a balancing act between backbone and side-chains.* Biophys Chem, 2011. **159**(1): p. 90-9.

68. Hottiger, T., et al., *The role of trehalose synthesis for the acquisition of thermotolerance in yeast. II. Physiological concentrations of trehalose increase the thermal stability of proteins in vitro.* Eur J Biochem, 1994. **219**(1-2): p. 187-93.

69. Mayer, M.P. and B. Bukau, *Hsp70 chaperones: cellular functions and molecular mechanism.* Cell Mol Life Sci, 2005. **62**(6): p. 670-84.

70. Stock, A.M., V.L. Robinson, and P.N. Goudreau, *Two-component signal transduction.* Annu Rev Biochem, 2000. **69**: p. 183-215.

71. Schleyer, M., R. Schmid, and E.P. Bakker, *Transient, specific and extremely rapid release of osmolytes from growing cells of Escherichia coli K-12 exposed to hypoosmotic shock.* Arch Microbiol, 1993. **160**(6): p. 424-31.

72. Ruffert, S., et al., *Efflux of compatible solutes in Corynebacterium glutamicum mediated by osmoregulated channel activity.* Eur J Biochem, 1997. **247**(2): p. 572-80.

73. Martinac, B., et al., *Pressure-sensitive ion channel in Escherichia coli.* Proc Natl Acad Sci U S A, 1987. **84**(8): p. 2297-301.

74. Sukharev, S.I., et al., *A large-conductance mechanosensitive channel in E. coli encoded by mscL alone.* Nature, 1994. **368**(6468): p. 265-8.

75. Levina, N., et al., *Protection of Escherichia coli cells against extreme turgor by activation of MscS and MscL mechanosensitive channels: identification of genes required for MscS activity.* Embo j, 1999. **18**(7): p. 1730-7.

76. Peyronnet, R., et al., *Mechanosensitive channels: feeling tension in a world under pressure.* Front Plant Sci, 2014. **5**: p. 558.

77. Haswell, E.S., R. Phillips, and D.C. Rees, *Mechanosensitive channels: what can they do and how do they do it?* Structure, 2011. **19**(10): p. 1356-69.

78. Blount, P., M.J. Schroeder, and C. Kung, *Mutations in a bacterial mechanosensitive channel change the cellular response to osmotic stress.* J Biol Chem, 1997. **272**(51): p. 32150-7.

79. Perozo, E., et al., *Physical principles underlying the transduction of bilayer deformation forces during mechanosensitive channel gating.* Nat Struct Biol, 2002. **9**(9): p. 696-703.

80. Dinnbier, U., et al., *Transient accumulation of potassium glutamate and its replacement by trehalose during adaptation of growing cells of Escherichia coli K-12 to elevated sodium chloride concentrations.* Arch Microbiol, 1988. **150**(4): p. 348-57.

81. Miller, K.J., S.C. Zelt, and J.-H. Bae, *Glycine betaine and proline are the principal compatible solutes ofStaphylococcus aureus.* Current Microbiology, 1991. **23**(3): p. 131-137.

82. Csonka, L.N., *Physiological and genetic responses of bacteria to osmotic stress.* Microbiol Rev, 1989. **53**(1): p. 121-47.

83. Rhoads, D.B. and W. Epstein, *Cation transport in Escherichia coli. IX. Regulation of K transport.* Journal of General Physiology, 1978. **72**(3): p. 283-295.

84. Laimins, L.A., D.B. Rhoads, and W. Epstein, *Osmotic control of kdp operon expression in Escherichia coli.* Proc Natl Acad Sci U S A, 1981. **78**(1): p. 464-8.

85. Sutherland, L., et al., *Osmotic regulation of transcription: induction of the proU betaine transport gene is dependent on accumulation of intracellular potassium.* J Bacteriol, 1986. **168**(2): p. 805-14.

86. Walderhaug, M.O., et al., *KdpD and KdpE, proteins that control expression of the kdpABC operon, are members of the two-component sensor-effector class of regulators.* J Bacteriol, 1992. **174**(7): p. 2152-9.

87. Polarek, J.W., G. Williams, and W. Epstein, *The products of the kdpDE operon are required for expression of the Kdp ATPase of Escherichia coli.* J Bacteriol, 1992. **174**(7): p. 2145-51.

88. Nakashima, K., et al., *Phosphotransfer signal transduction between two regulatory factors involved in the osmoregulated kdp operon in Escherichia coli.* Mol Microbiol, 1992. **6**(13): p. 1777-84.

89. Nakashima, K., et al., *Signal transduction between the two regulatory components involved in the regulation of the kdpABC operon in Escherichia coli: phosphorylation-dependent functioning of the positive regulator, KdpE.* Mol Microbiol, 1993. **7**(1): p. 109-16.

90. Cairney, J., I.R. Booth, and C.F. Higgins, *Osmoregulation of gene expression in Salmonella typhimurium: proU encodes an osmotically induced betaine transport system.* J Bacteriol, 1985. **164**(3): p. 1224-32.

91. Cairney, J., I.R. Booth, and C.F. Higgins, *Salmonella typhimurium proP gene encodes a transport system for the osmoprotectant betaine.* J Bacteriol, 1985. **164**(3): p. 1218-23.

92. Mellies, J., A. Wise, and M. Villarejo, *Two different Escherichia coli proP promoters respond to osmotic and growth phase signals.* J Bacteriol, 1995. **177**(1): p. 144-51.

93. Xu, J. and R.C. Johnson, *Cyclic AMP receptor protein functions as a repressor of the osmotically inducible promoter proP P1 in Escherichia coli.* J Bacteriol, 1997. **179**(7): p. 2410-7.

94. Landis, L., J. Xu, and R.C. Johnson, *The cAMP receptor protein CRP can function as an osmoregulator of transcription in Escherichia coli.* Genes Dev, 1999. **13**(23): p. 3081-91.

95. Jovanovich, S.B., M.T. Record, Jr., and R.R. Burgess, *In an Escherichia coli coupled transcription-translation system, expression of the osmoregulated gene proU is stimulated at elevated potassium concentrations and by an extract from cells grown at high osmolality.* J Biol Chem, 1989. **264**(14): p. 7821-5.

96. Ramirez, R.M., et al., *In vitro reconstitution of osmoregulated expression of proU of Escherichia coli.* Proc Natl Acad Sci U S A, 1989. **86**(4): p. 1153-7.

97. Prince, W.S. and M.R. Villarejo, *Osmotic control of proU transcription is mediated through direct action of potassium glutamate on the transcription complex.* J Biol Chem, 1990. **265**(29): p. 17673-9.

98. Pratt, L.A., et al., *From acids to osmZ: multiple factors influence synthesis of the OmpF and OmpC porins in Escherichia coli.* Mol Microbiol, 1996. **20**(5): p. 911-7.

99. Nakae, T. and H. Nikaido, *Outer membrane as a diffusion barrier in Salmonella typhimurium. Penetration of oligo- and polysaccharides into isolated outer membrane vesicles and cells with degraded peptidoglycan layer.* J Biol Chem, 1975. **250**(18): p. 7359-65.

100. Sarma, V. and P. Reeves, *Genetic locus (ompB) affecting a major outer-membrane protein in Escherichia coli K-12.* J Bacteriol, 1977. **132**(1): p. 23-7.

101. Hall, M.N. and T.J. Silhavy, *Genetic analysis of the ompB locus in Escherichia coli K-12.* J Mol Biol, 1981. **151**(1): p. 1-15.

102. Hall, M.N. and T.J. Silhavy, *The ompB locus and the regulation of the major outer membrane porin proteins of Escherichia coli K12.* J Mol Biol, 1981. **146**(1): p. 23-43.

103. Aiba, H., et al., *Phosphorylation of a bacterial activator protein, OmpR, by a protein kinase, EnvZ, results in stimulation of its DNA-binding ability.* J Biochem, 1989. **106**(1): p. 5-7.

104. Delgado, J., et al., *Identification of a phosphorylation site and functional analysis of conserved aspartic acid residues of OmpR, a transcriptional activator for ompF and ompC in Escherichia coli.* Mol Microbiol, 1993. **10**(5): p. 1037-47.

105. Rampersaud, A., S.L. Harlocker, and M. Inouye, *The OmpR protein of Escherichia coli binds to sites in the ompF promoter region in a hierarchical manner determined by its degree of phosphorylation.* J Biol Chem, 1994. **269**(17): p. 12559-66.

106. Brewster, J.L., et al., *An osmosensing signal transduction pathway in yeast.* Science, 1993. **259**(5102): p. 1760-3.

107. Latterich, M. and M.D. Watson, *Evidence for a dual osmoregulatory mechanism in the yeast Saccharomyces cerevisiae.* Biochem Biophys Res Commun, 1993. **191**(3): p. 1111-7.

108. Lee, S.J., et al., *Osmolarity hypersensitivity of hog1 deleted mutants is suppressed by mutation in KSS1 in budding yeast Saccharomyces cerevisiae.* FEMS Microbiol Lett, 2002. **209**(1): p. 9-14.

109. Maeda, T., M. Takekawa, and H. Saito, *Activation of yeast PBS2 MAPKK by MAPKKKs or by binding of an SH3-containing osmosensor.* Science, 1995. **269**(5223): p. 554-8.

110. Maeda, T., S.M. Wurgler-Murphy, and H. Saito, *A two-component system that regulates an osmosensing MAP kinase cascade in yeast.* Nature, 1994. **369**(6477): p. 242-5.

111. Posas, F., et al., *Yeast HOG1 MAP kinase cascade is regulated by a multistep phosphorelay mechanism in the SLN1-YPD1-SSK1 "two-component" osmosensor.* Cell, 1996. **86**(6): p. 865-75.

112. Luyten, K., et al., *Fps1, a yeast member of the MIP family of channel proteins, is a facilitator for glycerol uptake and efflux and is inactive under osmotic stress.* Embo j, 1995. **14**(7): p. 1360-71.

113. Li, S., et al., *The eukaryotic two-component histidine kinase Sln1p regulates OCH1 via the transcription factor, Skn7p.* Mol Biol Cell, 2002. **13**(2): p. 412-24.

114. Brown, J.L., H. Bussey, and R.C. Stewart, *Yeast Skn7p functions in a eukaryotic two-component regulatory pathway.* Embo j, 1994. **13**(21): p. 5186-94.

115. Saito, H. and F. Posas, *Response to hyperosmotic stress.* Genetics, 2012. **192**(2): p. 289-318.

116. Nass, R. and R. Rao, *The yeast endosomal Na+/H+ exchanger, Nhx1, confers osmotolerance following acute hypertonic shock.* Microbiology, 1999. **145 (Pt 11)**: p. 3221-3228.

117. Proft, M. and K. Struhl, *MAP kinase-mediated stress relief that precedes and regulates the timing of transcriptional induction.* Cell, 2004. **118**(3): p. 351-61.

118. Rep, M., et al., *The transcriptional response of Saccharomyces cerevisiae to osmotic shock. Hot1p and Msn2p/Msn4p are required for the induction of subsets of high osmolarity glycerol pathway-dependent genes.* J Biol Chem, 2000. **275**(12): p. 8290-300.

119. Causton, H.C., et al., *Remodeling of yeast genome expression in response to environmental changes.* Mol Biol Cell, 2001. **12**(2): p. 323-37.

120. Gasch, A.P., et al., *Genomic expression programs in the response of yeast cells to environmental changes.* Mol Biol Cell, 2000. **11**(12): p. 4241-57.

121. Belli, G., et al., *Osmotic stress causes a G1 cell cycle delay and downregulation of Cln3/Cdc28 activity in Saccharomyces cerevisiae.* Mol Microbiol, 2001. **39**(4): p. 1022-35.

122. Albertyn, J., et al., *GPD1, which encodes glycerol-3-phosphate dehydrogenase, is essential for growth under osmotic stress in Saccharomyces cerevisiae, and its expression is regulated by the high-osmolarity glycerol response pathway.* Mol Cell Biol, 1994. **14**(6): p. 4135-44.

123. Tamas, M.J., et al., *Fps1p controls the accumulation and release of the compatible solute glycerol in yeast osmoregulation.* Mol Microbiol, 1999. **31**(4): p. 1087-104.

124. Han, J., et al., *A MAP kinase targeted by endotoxin and hyperosmolarity in mammalian cells.* Science, 1994. **265**(5173): p. 808-11.

125. Proft, M., et al., *Regulation of the Sko1 transcriptional repressor by the Hog1 MAP kinase in response to osmotic stress.* The EMBO Journal, 2001. **20**(5): p. 1123-1133.

126. de Nadal, E., L. Casadomé, and F. Posas, *Targeting the MEF2-like transcription factor Smp1 by the stress-activated Hog1 mitogen-activated protein kinase.* Mol Cell Biol, 2003. **23**(1): p. 229-37.

127. Rep, M., et al., *Osmotic stress-induced gene expression in Saccharomyces cerevisiae requires Msn1p and the novel nuclear factor Hot1p.* Mol Cell Biol, 1999. **19**(8): p. 5474-85.

128. Alepuz, P.M., et al., *Stress-induced map kinase Hog1 is part of transcription activation complexes.* Mol Cell, 2001. **7**(4): p. 767-77.

129. Han, J., et al., *Characterization of the structure and function of a novel MAP kinase kinase (MKK6).* J Biol Chem, 1996. **271**(6): p. 2886-91.

130. Murakami, Y., K. Tatebayashi, and H. Saito, *Two adjacent docking sites in the yeast Hog1 mitogen-activated protein (MAP) kinase differentially interact with the Pbs2 MAP kinase kinase and the Ptp2 protein tyrosine phosphatase.* Mol Cell Biol, 2008. **28**(7): p. 2481-94.

131. Horie, T., et al., *Phosphorylated Ssk1 prevents unphosphorylated Ssk1 from activating the Ssk2 mitogen-activated protein kinase kinase kinase in the yeast high-osmolarity glycerol osmoregulatory pathway.* Mol Cell Biol, 2008. **28**(17): p. 5172-83.

132. Tao, W., R.J. Deschenes, and J.S. Fassler, *Intracellular glycerol levels modulate the activity of Sln1p, a Saccharomyces cerevisiae two-component regulator.* J Biol Chem, 1999. **274**(1): p. 360-7.

133. Li, S., et al., *The yeast histidine protein kinase, Sln1p, mediates phosphotransfer to two response regulators, Ssk1p and Skn7p.* Embo j, 1998. **17**(23): p. 6952-62.

134. Tatebayashi, K., et al., *Transmembrane mucins Hkr1 and Msb2 are putative osmosensors in the SHO1 branch of yeast HOG pathway.* Embo j, 2007. **26**(15): p. 3521-33.

135. Tatebayashi, K., et al., *Osmosensing and scaffolding functions of the oligomeric four-transmembrane domain osmosensor Sho1.* Nat Commun, 2015. **6**: p. 6975.

136. Tanaka, K., et al., *Yeast osmosensors Hkr1 and Msb2 activate the Hog1 MAPK cascade by different mechanisms.* Sci Signal, 2014. **7**(314): p. ra21.

137. Ekiel, I., et al., *Binding the atypical RA domain of Ste50p to the unfolded Opy2p cytoplasmic tail is essential for the high-osmolarity glycerol pathway.* Mol Biol Cell, 2009. **20**(24): p. 5117-26.

138. Tatebayashi, K., et al., *Adaptor functions of Cdc42, Ste50, and Sho1 in the yeast osmoregulatory HOG MAPK pathway.* Embo j, 2006. **25**(13): p. 3033-44.

139. Raitt, D.C., F. Posas, and H. Saito, *Yeast Cdc42 GTPase and Ste20 PAK-like kinase regulate Sho1-dependent activation of the Hog1 MAPK pathway.* Embo j, 2000. **19**(17): p. 4623-31.

140. Lamson, R.E., M.J. Winters, and P.M. Pryciak, *Cdc42 regulation of kinase activity and signaling by the yeast p21-activated kinase Ste20.* Mol Cell Biol, 2002. **22**(9): p. 2939-51.

141. Wu, C., et al., *Functional characterization of the interaction of Ste50p with Ste11p MAPKKK in Saccharomyces cerevisiae.* Mol Biol Cell, 1999. **10**(7): p. 2425-40.

142. Choi, M.Y., et al., *Analysis of dual phosphorylation of Hog1 MAP kinase in Saccharomyces cerevisiae using quantitative mass spectrometry.* Mol Cells, 2008. **26**(2): p. 200-5.

143. Ferrigno, P., et al., *Regulated nucleo/cytoplasmic exchange of HOG1 MAPK requires the importin β homologs NMD5 and XPO1.* The EMBO Journal, 1998. **17**(19): p. 5606-5614.

144. Westfall, P.J. and J. Thorner, *Analysis of mitogen-activated protein kinase signaling specificity in response to hyperosmotic stress: use of an analog-sensitive HOG1 allele.* Eukaryot Cell, 2006. **5**(8): p. 1215-28.

145. Warmka, J., et al., *Ptc1, a type 2C Ser/Thr phosphatase, inactivates the HOG pathway by dephosphorylating the mitogen-activated protein kinase Hog1.* Mol Cell Biol, 2001. **21**(1): p. 51-60.

146. Jacoby, T., et al., *Two protein-tyrosine phosphatases inactivate the osmotic stress response pathway in yeast by targeting the mitogen-activated protein kinase, Hog1.* J Biol Chem, 1997. **272**(28): p. 17749-55.

147. Zhu, J.K., *Salt and drought stress signal transduction in plants.* Annu Rev Plant Biol, 2002. **53**: p. 247-73.

148. Acosta-Motos, J.R., et al., *Plant Responses to Salt Stress: Adaptive Mechanisms.* Agronomy, 2017. **7**(1): p. 18.

149. Haswell, E.S. and E.M. Meyerowitz, *MscS-like proteins control plastid size and shape in Arabidopsis thaliana.* Curr Biol, 2006. **16**(1): p. 1-11.

150. Veley, K.M., et al., *Mechanosensitive channels protect plastids from hypoosmotic stress during normal plant growth.* Curr Biol, 2012. **22**(5): p. 408-13.

151. Apse, M.P., et al., *Salt tolerance conferred by overexpression of a vacuolar Na+/H+ antiport in Arabidopsis.* Science, 1999. **285**(5431): p. 1256-8.

152. Shi, H., et al., *The Arabidopsis thaliana salt tolerance gene SOS1 encodes a putative Na+/H+ antiporter.* Proc Natl Acad Sci U S A, 2000. **97**(12): p. 6896-901.

153. Henry, C., et al., *Differential Role for Trehalose Metabolism in Salt-Stressed Maize.* Plant Physiol, 2015. **169**(2): p. 1072-89.

154. Slama, I., et al., *Diversity, distribution and roles of osmoprotective compounds accumulated in halophytes under abiotic stress.* Ann Bot, 2015. **115**(3): p. 433-47.

155. Yang, Y. and Y. Guo, *Unraveling salt stress signaling in plants.* J Integr Plant Biol, 2018. **60**(9): p. 796-804.

156. Shinozaki, K. and K. Yamaguchi-Shinozaki, *Gene Expression and Signal Transduction in Water-Stress Response.* Plant Physiol, 1997. **115**(2): p. 327-334.

157. Jia, W., et al., *Salt-stress-induced ABA accumulation is more sensitively triggered in roots than in shoots.* Journal of Experimental Botany, 2002. **53**(378): p. 2201-2206.

158. Pierce, M. and K. Raschke, *Correlation between loss of turgor and accumulation of abscisic acid in detached leaves.* Planta, 1980. **148**(2): p. 174-82.

159. Jia, W., J. Zhang, and J. Liang, *Initiation and regulation of water deficit-induced abscisic acid accumulation in maize leaves and roots: cellular volume and water relations.* Journal of Experimental Botany, 2001. **52**(355): p. 295-300.

160. Seo, M., et al., *The Arabidopsis aldehyde oxidase 3 (AAO3) gene product catalyzes the final step in abscisic acid biosynthesis in leaves.* Proc Natl Acad Sci U S A, 2000. **97**(23): p. 12908-13.

161. Qin, X. and J.A. Zeevaart, *The 9-cis-epoxycarotenoid cleavage reaction is the key regulatory step of abscisic acid biosynthesis in water-stressed bean.* Proc Natl Acad Sci U S A, 1999. **96**(26): p. 15354-61.

162. Iuchi, S., et al., *Regulation of drought tolerance by gene manipulation of 9-cis-epoxycarotenoid dioxygenase, a key enzyme in abscisic acid biosynthesis in Arabidopsis.* Plant J, 2001. **27**(4): p. 325-33.

163. Huang, Y., et al., *OsNCED5, a 9-cis-epoxycarotenoid dioxygenase gene, regulates salt and water stress tolerance and leaf senescence in rice.* Plant Sci, 2019. **287**: p. 110188.

164. Kushiro, T., et al., *The Arabidopsis cytochrome P450 CYP707A encodes ABA 8'-hydroxylases: key enzymes in ABA catabolism.* Embo j, 2004. **23**(7): p. 1647-56.

165. Umezawa, T., et al., *CYP707A3, a major ABA 8'-hydroxylase involved in dehydration and rehydration response in Arabidopsis thaliana.* The Plant Journal, 2006. **46**(2): p. 171-182.

166. Xiong, L., et al., *The Arabidopsis LOS5/ABA3 locus encodes a molybdenum cofactor sulfurase and modulates cold stress- and osmotic stress-responsive gene expression.* Plant Cell, 2001. **13**(9): p. 2063-83.

167. Fujii, H., P.E. Verslues, and J.K. Zhu, *Arabidopsis decuple mutant reveals the importance of SnRK2 kinases in osmotic stress responses in vivo.* Proc Natl Acad Sci U S A, 2011. **108**(4): p. 1717-22.

168. Yoshida, T., et al., *AREB1, AREB2, and ABF3 are master transcription factors that cooperatively regulate ABRE-dependent ABA signaling involved in drought stress tolerance and require ABA for full activation.* Plant J, 2010. **61**(4): p. 672-85.

169. Park, S.Y., et al., *Abscisic acid inhibits type 2C protein phosphatases via the PYR/PYL family of START proteins.* Science, 2009. **324**(5930): p. 1068-71.

170. Ma, Y., et al., *Regulators of PP2C phosphatase activity function as abscisic acid sensors.* Science, 2009. **324**(5930): p. 1064-8.

171. Vlad, F., et al., *Protein phosphatases 2C regulate the activation of the Snf1-related kinase OST1 by abscisic acid in Arabidopsis.* Plant Cell, 2009. **21**(10): p. 3170-84.

172. Mundy, J., K. Yamaguchi-Shinozaki, and N.H. Chua, *Nuclear proteins bind conserved elements in the abscisic acid-responsive promoter of a rice rab gene.* Proc Natl Acad Sci U S A, 1990. **87**(4): p. 1406-10.

173. Hattori, T., et al., *Experimentally determined sequence requirement of ACGT-containing abscisic acid response element.* Plant Cell Physiol, 2002. **43**(1): p. 136-40.

174. Abe, H., et al., *Role of arabidopsis MYC and MYB homologs in drought- and abscisic acid-regulated gene expression.* Plant Cell, 1997. **9**(10): p. 1859-68.

175. Abe, H., et al., *Arabidopsis AtMYC2 (bHLH) and AtMYB2 (MYB) function as transcriptional activators in abscisic acid signaling.* Plant Cell, 2003. **15**(1): p. 63-78.

176. Kazan, K. and J.M. Manners, *MYC2: The Master in Action.* Molecular Plant, 2013. **6**(3): p. 686-703.

177. Yamaguchi-Shinozaki, K. and K. Shinozaki, *TRANSCRIPTIONAL REGULATORY NETWORKS IN CELLULAR RESPONSES AND TOLERANCE TO DEHYDRATION AND COLD STRESSES.* Annual Review of Plant Biology, 2006. **57**(1): p. 781-803.

178. Stockinger, E.J., S.J. Gilmour, and M.F. Thomashow, *Arabidopsis thaliana CBF1 encodes an AP2 domain-containing transcriptional activator that binds to the C-repeat/DRE, a cis-acting DNA regulatory element that stimulates transcription in response to low temperature and water deficit.* Proc Natl Acad Sci U S A, 1997. **94**(3): p. 1035-40.

179. Haake, V., et al., *Transcription factor CBF4 is a regulator of drought adaptation in Arabidopsis.* Plant Physiol, 2002. **130**(2): p. 639-48.

180. Urao, T., et al., *A transmembrane hybrid-type histidine kinase in Arabidopsis functions as an osmosensor.* Plant Cell, 1999. **11**(9): p. 1743-54.

181. Tran, L.S., et al., *Functional analysis of AHK1/ATHK1 and cytokinin receptor histidine kinases in response to abscisic acid, drought, and salt stress in Arabidopsis.* Proc Natl Acad Sci U S A, 2007. **104**(51): p. 20623-8.

182. Bourque, C.W., *Central mechanisms of osmosensation and systemic osmoregulation.* Nat Rev Neurosci, 2008. **9**(7): p. 519-31.

183. Shirreffs, S.M., et al., *The effects of fluid restriction on hydration status and subjective feelings in man.* Br J Nutr, 2004. **91**(6): p. 951-8.

184. Saat, M., et al., *Effects of short-term exercise in the heat on thermoregulation, blood parameters, sweat secretion and sweat composition of tropic-dwelling subjects.* J Physiol Anthropol Appl Human Sci, 2005. **24**(5): p. 541-9.

185. Anderson, J.W., D.L. Washburn, and A.V. Ferguson, *Intrinsic osmosensitivity of subfornical organ neurons.* Neuroscience, 2000. **100**(3): p. 539-47.

186. Thrasher, T.N., L.C. Keil, and D.J. Ramsay, *Lesions of the organum vasculosum of the lamina terminalis (OVLT) attenuate osmotically-induced drinking and vasopressin secretion in the dog.* Endocrinology, 1982. **110**(5): p. 1837-9.

187. Oliet, S.H. and C.W. Bourque, *Properties of supraoptic magnocellular neurones isolated from the adult rat.* J Physiol, 1992. **455**: p. 291-306.

188. Zhang, Z. and C.W. Bourque, *Osmometry in osmosensory neurons.* Nature Neuroscience, 2003. **6**(10): p. 1021-1022.

189. Ciura, S., W. Liedtke, and C.W. Bourque, *Hypertonicity sensing in organum vasculosum lamina terminalis neurons: a mechanical process involving TRPV1 but not TRPV4.* J Neurosci, 2011. **31**(41): p. 14669-76.

190. Ciura, S. and C.W. Bourque, *Transient receptor potential vanilloid 1 is required for intrinsic osmoreception in organum vasculosum lamina terminalis neurons and for normal thirst responses to systemic hyperosmolality.* J Neurosci, 2006. **26**(35): p. 9069-75.

191. Mason, W.T., *Supraoptic neurones of rat hypothalamus are osmosensitive.* Nature, 1980. **287**(5778): p. 154-157.

192. Prager-Khoutorsky, M. and C.W. Bourque, *Mechanical basis of osmosensory transduction in magnocellular neurosecretory neurones of the rat supraoptic nucleus.* J Neuroendocrinol, 2015. **27**(6): p. 507-15.

193. Oliet, S.H. and C.W. Bourque, *Mechanosensitive channels transduce osmosensitivity in supraoptic neurons.* Nature, 1993. **364**(6435): p. 341-3.

194. Moriya, T., et al., *Full-length transient receptor potential vanilloid 1 channels mediate calcium signals and possibly contribute to osmoreception in vasopressin neurones in the rat supraoptic nucleus.* Cell Calcium, 2015. **57**(1): p. 25-37.

195. Prager-Khoutorsky, M., A. Khoutorsky, and C.W. Bourque, *Unique interweaved microtubule scaffold mediates osmosensory transduction via physical interaction with TRPV1.* Neuron, 2014. **83**(4): p. 866-78.

196. Rhodes, C.H., J.I. Morrell, and D.W. Pfaff, *Immunohistochemical analysis of magnocellular elements in rat hypothalamus: distribution and numbers of cells containing neurophysin, oxytocin, and vasopressin.* J Comp Neurol, 1981. **198**(1): p. 45-64.

197. Gizowski, C., E. Trudel, and C.W. Bourque, *Central and peripheral roles of vasopressin in the circadian defense of body hydration.* Best Pract Res Clin Endocrinol Metab, 2017. **31**(6): p. 535-546.

198. van Leeuwen, F.W., D.F. Swaab, and C. de Raay, *Immunoelectronmicroscopic localization of vasopressin in the rat suprachiasmatic nucleus.* Cell Tissue Res, 1978. **193**(1): p. 1-10.

199. Dunn, F.L., et al., *The role of blood osmolality and volume in regulating vasopressin secretion in the rat.* J Clin Invest, 1973. **52**(12): p. 3212-9.

200. Richard, D. and C.W. Bourque, *Synaptic activation of rat supraoptic neurons by osmotic stimulation of the organum vasculosum lamina terminalis.* Neuroendocrinology, 1992. **55**(5): p. 609-11.

201. Choe, K.Y., J.E. Olson, and C.W. Bourque, *Taurine release by astrocytes modulates osmosensitive glycine receptor tone and excitability in the adult supraoptic nucleus.* J Neurosci, 2012. **32**(36): p. 12518-27.

202. Hussy, N., et al., *Agonist action of taurine on glycine receptors in rat supraoptic magnocellular neurones: possible role in osmoregulation.* J Physiol, 1997. **502 (Pt 3)**(Pt 3): p. 609-21.

203. Sherlock, D.A., P.M. Field, and G. Raisman, *Retrograde transport of horseradish peroxidase in the magnocellular neurosecretory system of the rat.* Brain Res, 1975. **88**(3): p. 403-14.

204. Fisher, T.E. and C.W. Bourque, *Calcium-channel subtypes in the somata and axon terminals of magnocellular neurosecretory cells.* Trends Neurosci, 1996. **19**(10): p. 440-4.

205. Nishikawa, K., et al., *Structural Reconstruction of the Perivascular Space in the Adult Mouse Neurohypophysis During an Osmotic Stimulation.* J Neuroendocrinol, 2017. **29**(2).

206. Lim, N.F., M.C. Nowycky, and R.J. Bookman, *Direct measurement of exocytosis and calcium currents in single vertebrate nerve terminals.* Nature, 1990. **344**(6265): p. 449-51.

207. Lolait, S.J., et al., *Cloning and characterization of a vasopressin V2 receptor and possible link to nephrogenic diabetes insipidus.* Nature, 1992. **357**(6376): p. 336-9.

208. Robben, J.H., N.V. Knoers, and P.M. Deen, *Regulation of the vasopressin V2 receptor by vasopressin in polarized renal collecting duct cells.* Mol Biol Cell, 2004. **15**(12): p. 5693-9.

209. Katsura, T., et al., *Protein kinase A phosphorylation is involved in regulated exocytosis of aquaporin-2 in transfected LLC-PK1 cells.* Am J Physiol, 1997. **272**(6 Pt 2): p. F817-22.

210. Frindt, G., H. Sackin, and L.G. Palmer, *Whole-cell currents in rat cortical collecting tubule: low-Na diet increases amiloride-sensitive conductance.* Am J Physiol, 1990. **258**(3 Pt 2): p. F562-7.

211. Sevá Pessôa, B., et al., *Key developments in renin-angiotensin-aldosterone system inhibition.* Nat Rev Nephrol, 2013. **9**(1): p. 26-36.

212. Skeggs, L.T., Jr., et al., *The existence of two forms of hypertensin.* J Exp Med, 1954. **99**(3): p. 275-82.

213. Romero, C.A., M. Orias, and M.R. Weir, *Novel RAAS agonists and antagonists: clinical applications and controversies.* Nat Rev Endocrinol, 2015. **11**(4): p. 242-52.

214. Matsusaka, T., et al., *Liver angiotensinogen is the primary source of renal angiotensin II.* J Am Soc Nephrol, 2012. **23**(7): p. 1181-9.

215. Skeggs, L.T., Jr., J.R. Kahn, and N.P. Shumway, *The preparation and function of the hypertensin-converting enzyme.* J Exp Med, 1956. **103**(3): p. 295-9.

216. Giroud, C.J., J. Stachenko, and E.H. Venning, *Secretion of aldosterone by the zona glomerulosa of rat adrenal glands incubated in vitro.* Proc Soc Exp Biol Med, 1956. **92**(1): p. 154-8.

217. Laragh, J.H., et al., *Hypotensive agents and pressor substances. The effect of epinephrine, norepinephrine, angiotensin II, and others on the secretory rate of aldosterone in man.* Jama, 1960. **174**: p. 234-40.

218. Davis, J.O., et al., *Evidence for secretion of an aldosterone-stimulating hormone by the kidney.* J Clin Invest, 1961. **40**(4): p. 684-96.

219. Douglas, J., et al., *Receptor binding of angiotensin II and antagonists. Correlation with aldosterone production by isolated canine adrenal glomerulosa cells.* Circ Res, 1976. **38**(6 Suppl 2): p. 108-12.

220. Mulrow, P.J., *Angiotensin II and aldosterone regulation.* Regul Pept, 1999. **80**(1-2): p. 27-32.

221. Pearce, D., et al., *Collecting duct principal cell transport processes and their regulation.* Clin J Am Soc Nephrol, 2015. **10**(1): p. 135-46.

222. Asher, C., et al., *Expression of the amiloride-blockable Na+ channel by RNA from control versus aldosterone-stimulated tissue.* J Biol Chem, 1992. **267**(23): p. 16061-5.

223. Pácha, J., et al., *Regulation of Na channels of the rat cortical collecting tubule by aldosterone.* J Gen Physiol, 1993. **102**(1): p. 25-42.

224. Helman, S.I., et al., *Time-dependent stimulation by aldosterone of blocker-sensitive ENaCs in A6 epithelia.* Am J Physiol, 1998. **274**(4): p. C947-57.

225. Lopez-Rodríguez, C., et al., *NFAT5, a constitutively nuclear NFAT protein that does not cooperate with Fos and Jun.* Proc Natl Acad Sci U S A, 1999. **96**(13): p. 7214-9.

226. Zagórska, A., et al., *Regulation of activity and localization of the WNK1 protein kinase by hyperosmotic stress.* J Cell Biol, 2007. **176**(1): p. 89-100.

227. Moriguchi, T., et al., *WNK1 regulates phosphorylation of cation-chloride-coupled cotransporters via the STE20-related kinases, SPAK and OSR1.* J Biol Chem, 2005. **280**(52): p. 42685-93.

228. Vitari, A.C., et al., *The WNK1 and WNK4 protein kinases that are mutated in Gordon's hypertension syndrome phosphorylate and activate SPAK and OSR1 protein kinases.* Biochem J, 2005. **391**(Pt 1): p. 17-24.

229. Pacheco-Alvarez, D., et al., *The Na+:Cl- cotransporter is activated and phosphorylated at the amino-terminal domain upon intracellular chloride depletion.* J Biol Chem, 2006. **281**(39): p. 28755-63.

230. Boyd-Shiwarski, C.R., et al., *WNK1 Regulates Cell Volume via Crowding-Induced Phase Transitions.* The FASEB Journal, 2020. **34**(S1): p. 1-1.

231. Choe, K.P. and K. Strange, *Evolutionarily conserved WNK and Ste20 kinases are essential for acute volume recovery and survival after hypertonic shrinkage in Caenorhabditis elegans.* Am J Physiol Cell Physiol, 2007. **293**(3): p. C915-27.

232. Wehner, F., et al., *Cell volume regulation: osmolytes, osmolyte transport, and signal transduction.* Rev Physiol Biochem Pharmacol, 2003. **148**: p. 1-80.

233. Sizeland, P.C., et al., *Organic osmolytes in human and other mammalian kidneys.* Kidney Int, 1993. **43**(2): p. 448-53.

234. Weik, C., et al., *Compatible organic osmolytes in rat liver sinusoidal endothelial cells.* Hepatology, 1998. **27**(2): p. 569-75.

235. Grunewald, R.W., et al., *Rat renal expression of mRNA coding for aldose reductase and sorbitol dehydrogenase and its osmotic regulation in inner medullary collecting duct cells.* Cell Physiol Biochem, 1998. **8**(6): p. 293-303.

236. Lee, S.D., et al., *TonEBP stimulates multiple cellular pathways for adaptation to hypertonic stress: organic osmolyte-dependent and -independent pathways.* Am J Physiol Renal Physiol, 2011. **300**(3): p. F707-15.

237. Ridgway, N.D., *Chapter 7 - Phospholipid Synthesis in Mammalian Cells*, in *Biochemistry of Lipids, Lipoproteins and Membranes (Sixth Edition)*, N.D. Ridgway and R.S. McLeod, Editors. 2016, Elsevier: Boston. p. 209-236.

238. Kwon, H.M., et al., *Cloning of the cDNa for a Na+/myo-inositol cotransporter, a hypertonicity stress protein.* J Biol Chem, 1992. **267**(9): p. 6297-301.

239. Yamauchi, A., et al., *Hypertonicity stimulates transcription of gene for Na(+)-myo-inositol cotransporter in MDCK cells.* Am J Physiol, 1993. **264**(1 Pt 2): p. F20-3.

240. Schaffer, S., V. Solodushko, and J. Azuma, *Taurine-deficient cardiomyopathy: role of phospholipids, calcium and osmotic stress.* Adv Exp Med Biol, 2000. **483**: p. 57-69.

241. Lever, M. and S. Slow, *The clinical significance of betaine, an osmolyte with a key role in methyl group metabolism.* Clin Biochem, 2010. **43**(9): p. 732-44.

242. Uchida, S., et al., *Molecular cloning of the cDNA for an MDCK cell Na(+)- and Cl(-)-dependent taurine transporter that is regulated by hypertonicity.* Proc Natl Acad Sci U S A, 1993. **90**(15): p. 7424.

243. Ito, T., et al., *Expression of taurine transporter is regulated through the TonE (tonicity-responsive element)/TonEBP (TonE-binding protein) pathway and contributes to cytoprotection in HepG2 cells.* Biochem J, 2004. **382**(Pt 1): p. 177-82.

244. Yamauchi, A., et al., *Cloning of a Na(+)- and Cl(-)-dependent betaine transporter that is regulated by hypertonicity.* J Biol Chem, 1992. **267**(1): p. 649-52.

245. Uchida, S., et al., *Medium tonicity regulates expression of the Na(+)- and Cl(-)-dependent betaine transporter in Madin-Darby canine kidney cells by increasing transcription of the transporter gene.* J Clin Invest, 1993. **91**(4): p. 1604-7.

246. Zaccheo, O., et al., *Neuropathy target esterase and its yeast homologue degrade phosphatidylcholine to glycerophosphocholine in living cells.* J Biol Chem, 2004. **279**(23): p. 24024-33.

247. Gallazzini, M., et al., *Neuropathy target esterase catalyzes osmoprotective renal synthesis of glycerophosphocholine in response to high NaCl.* Proc Natl Acad Sci U S A, 2006. **103**(41): p. 15260-5.

248. Bauernschmitt, H.G. and R.K. Kinne, *Metabolism of the 'organic osmolyte' glycerophosphorylcholine in isolated rat inner medullary collecting duct cells. II. Regulation by extracellular osmolality.* Biochim Biophys Acta, 1993. **1150**(1): p. 25-34.

249. Marsh, D.J. and S.P. Azen, *Mechanism of NaCl reabsorption by hamster thin ascending limbs of Henle's loop.* Am J Physiol, 1975. **228**(1): p. 71-9.

250. Miyakawa, H., et al., *Tonicity-responsive enhancer binding protein, a rel-like protein that stimulates transcription in response to hypertonicity.* Proc Natl Acad Sci U S A, 1999. **96**(5): p. 2538-42.

251. Go, W.Y., et al., *NFAT5/TonEBP mutant mice define osmotic stress as a critical feature of the lymphoid microenvironment.* Proc Natl Acad Sci U S A, 2004. **101**(29): p. 10673-8.

252. Miyakawa, H., et al., *Cis- and trans-acting factors regulating transcription of the BGT1 gene in response to hypertonicity.* Am J Physiol, 1998. **274**(4): p. F753-61.

253. Cha, J.H., et al., *Hydration status affects nuclear distribution of transcription factor tonicity responsive enhancer binding protein in rat kidney.* J Am Soc Nephrol, 2001. **12**(11): p. 2221-30.

254. Woo, S.K., et al., *TonEBP/NFAT5 stimulates transcription of HSP70 in response to hypertonicity.* Mol Cell Biol, 2002. **22**(16): p. 5753-60.

255. Dasgupta, S., T.C. Hohman, and D. Carper, *Hypertonic stress induces alpha B-crystallin expression.* Exp Eye Res, 1992. **54**(3): p. 461-70.

256. Nahm, O., et al., *Involvement of multiple kinase pathways in stimulation of gene transcription by hypertonicity.* Am J Physiol Cell Physiol, 2002. **282**(1): p. C49-58.

257. Santos, B.C., et al., *Characterization of the Hsp110/SSE gene family response to hyperosmolality and other stresses.* Am J Physiol, 1998. **274**(6): p. F1054-61.

258. Kojima, R., et al., *Osmotic stress protein 94 (Osp94). A new member of the Hsp110/SSE gene subfamily.* J Biol Chem, 1996. **271**(21): p. 12327-32.

259. Hasler, U., et al., *Tonicity-responsive enhancer binding protein is an essential regulator of aquaporin-2 expression in renal collecting duct principal cells.* J Am Soc Nephrol, 2006. **17**(6): p. 1521-31.

260. Takenaka, M., et al., *The tonicity-sensitive element that mediates increased transcription of the betaine transporter gene in response to hypertonic stress.* J Biol Chem, 1994. **269**(47): p. 29379-81.

261. Ferraris, J.D., et al., *Functional consensus for mammalian osmotic response elements.* Am J Physiol, 1999. **276**(3): p. C667-73.

262. Dahl, S.C., J.S. Handler, and H.M. Kwon, *Hypertonicity-induced phosphorylation and nuclear localization of the transcription factor TonEBP.* Am J Physiol Cell Physiol, 2001. **280**(2): p. C248-53.

263. Tong, E.H., et al., *Regulation of nucleocytoplasmic trafficking of transcription factor OREBP/TonEBP/NFAT5.* J Biol Chem, 2006. **281**(33): p. 23870-9.

264. Zhang, Z., et al., *Ataxia telangiectasia-mutated, a DNA damage-inducible kinase, contributes to high NaCl-induced nuclear localization of transcription factor TonEBP/OREBP.* Am J Physiol Renal Physiol, 2005. **289**(3): p. F506-11.

265. Ferraris, J.D., et al., *Activity of the TonEBP/OREBP transactivation domain varies directly with extracellular NaCl concentration.* Proc Natl Acad Sci U S A, 2002. **99**(2): p. 739-44.

266. Lee, S.D., et al., *Multiple domains of TonEBP cooperate to stimulate transcription in response to hypertonicity.* J Biol Chem, 2003. **278**(48): p. 47571-7.

267. Burg, M.B., J.D. Ferraris, and N.I. Dmitrieva, *Cellular Response to Hyperosmotic Stresses.* Physiological Reviews, 2007. **87**(4): p. 1441-1474.

268. Ko, B.C., et al., *Fyn and p38 signaling are both required for maximal hypertonic activation of the osmotic response element-binding protein/tonicity-responsive enhancer-binding protein (OREBP/TonEBP).* J Biol Chem, 2002. **277**(48): p. 46085-92.

269. Irarrazabal, C.E., et al., *ATM, a DNA damage-inducible kinase, contributes to activation by high NaCl of the transcription factor TonEBP/OREBP.* Proc Natl Acad Sci U S A, 2004. **101**(23): p. 8809-14.

270. Irarrazabal, C.E., et al., *Phosphatidylinositol 3-kinase mediates activation of ATM by high NaCl and by ionizing radiation: Role in osmoprotective transcriptional regulation.* Proc Natl Acad Sci U S A, 2006. **103**(23): p. 8882-7.

271. Kapus, A., et al., *Cell shrinkage regulates Src kinases and induces tyrosine phosphorylation of cortactin, independent of the osmotic regulation of Na+/H+ exchangers.* J Biol Chem, 1999. **274**(12): p. 8093-102.

272. Kültz, D. and D. Chakravarty, *Hyperosmolality in the form of elevated NaCl but not urea causes DNA damage in murine kidney cells.* Proc Natl Acad Sci U S A, 2001. **98**(4): p. 1999-2004.

273. Urso, S.J. and T. Lamitina, *The C. elegans Hypertonic Stress Response: Big Insights from Shrinking Worms.* Cell Physiol Biochem, 2021. **55**(S1): p. 89-105.

274. Adrogué, H.J. and N.E. Madias, *Hypernatremia.* N Engl J Med, 2000. **342**(20): p. 1493-9.

275. Gullans, S.R. and J.G. Verbalis, *Control of brain volume during hyperosmolar and hypoosmolar conditions.* Annu Rev Med, 1993. **44**: p. 289-301.

276. Holliday, M.A., M.N. Kalayci, and J. Harrah, *Factors that limit brain volume changes in response to acute and sustained hyper- and hyponatremia.* J Clin Invest, 1968. **47**(8): p. 1916-28.

277. Arieff, A.I. and R. Guisado, *Effects on the central nervous system of hypernatremic and hyponatremic states.* Kidney Int, 1976. **10**(1): p. 104-16.

278. Hogan, G.R., et al., *Pathogenesis of seizures occurring during restoration of plasma tonicity to normal in animals previously chronically hypernatremic.* Pediatrics, 1969. **43**(1): p. 54-64.

279. Pasantes-Morales, H., et al., *Mechanisms counteracting swelling in brain cells during hyponatremia.* Arch Med Res, 2002. **33**(3): p. 237-44.

280. Arieff, A.I., F. Llach, and S.G. Massry, *Neurological manifestations and morbidity of hyponatremia: correlation with brain water and electrolytes.* Medicine (Baltimore), 1976. **55**(2): p. 121-9.

281. Suarez, J.I., et al., *Administration of hypertonic (3%) sodium chloride/acetate in hyponatremic patients with symptomatic vasospasm following subarachnoid hemorrhage.* J Neurosurg Anesthesiol, 1999. **11**(3): p. 178-84.

282. Sterns, R.H., D.J. Thomas, and R.M. Herndon, *Brain dehydration and neurologic deterioration after rapid correction of hyponatremia*. Kidney Int, 1989. **35**(1): p. 69-75.

283. Kalogeris, T., et al., *Cell biology of ischemia/reperfusion injury.* International review of cell and molecular biology, 2012. **298**: p. 229-317.

284. Fuller, W., et al., *Cardiac ischemia causes inhibition of the Na/K ATPase by a labile cytosolic compound whose production is linked to oxidant stress.* Cardiovasc Res, 2003. **57**(4): p. 1044-51.

285. Kim, M.J., et al., *Expression and activity of the na-k ATPase in ischemic injury of primary cultured astrocytes.* Korean J Physiol Pharmacol, 2013. **17**(4): p. 275-81.

286. Pike, M.M., M. Kitakaze, and E. Marban, *23Na-NMR measurements of intracellular sodium in intact perfused ferret hearts during ischemia and reperfusion.* Am J Physiol, 1990. **259**(6 Pt 2): p. H1767-73.

287. Ames, A., 3rd, et al., *Cerebral ischemia. II. The no-reflow phenomenon.* Am J Pathol, 1968. **52**(2): p. 437-53.

288. Cantu, R.C. and A. Ames, 3rd, *Experimental prevention of cerebral vasculature obstruction produced by ischemia.* J Neurosurg, 1969. **30**(1): p. 50-4.

289. Brenner, S., *The genetics of Caenorhabditis elegans*. Genetics, 1974. **77**(1): p. 71-94.

290. Sulston, J.E. and H.R. Horvitz, *Post-embryonic cell lineages of the nematode, Caenorhabditis elegans.* Dev Biol, 1977. **56**(1): p. 110-56.

291. Sulston, J.E., et al., *The embryonic cell lineage of the nematode Caenorhabditis elegans.* Dev Biol, 1983. **100**(1): p. 64-119.

292. Hedgecock, E.M., J.E. Sulston, and J.N. Thomson, *Mutations affecting programmed cell deaths in the nematode Caenorhabditis elegans.* Science, 1983. **220**(4603): p. 1277-9.

293. Ellis, H.M. and H.R. Horvitz, *Genetic control of programmed cell death in the nematode C. elegans.* Cell, 1986. **44**(6): p. 817-29.

294. Yuan, J., et al., *The C. elegans cell death gene ced-3 encodes a protein similar to mammalian interleukin-1 beta-converting enzyme.* Cell, 1993. **75**(4): p. 641-52.

295. Golde, T.E., *The therapeutic importance of understanding mechanisms of neuronal cell death in neurodegenerative disease.* Mol Neurodegener, 2009. **4**: p. 8.

296. Fire, A., et al., *Potent and specific genetic interference by double-stranded RNA in Caenorhabditis elegans.* Nature, 1998. **391**(6669): p. 806-11.

297. Leung, R.K. and P.A. Whittaker, *RNA interference: from gene silencing to gene-specific therapeutics.* Pharmacol Ther, 2005. **107**(2): p. 222-39.

298. Chalfie, M., et al., *Green fluorescent protein as a marker for gene expression.* Science, 1994. **263**(5148): p. 802-5.

299. Hughes, S.E., et al., *Genetic and pharmacological factors that influence reproductive aging in nematodes.* PLoS Genet, 2007. **3**(2): p. e25.

300. *Genome sequence of the nematode C. elegans: a platform for investigating biology.* Science, 1998. **282**(5396): p. 2012-8.

301. Hillier, L.W., et al., *Genomics in C. elegans: so many genes, such a little worm.* Genome Res, 2005. **15**(12): p. 1651-60.

302. Stricklin, S.L., S. Griffiths-Jones, and S.R. Eddy, *C. elegans noncoding RNA genes.* WormBook, 2005: p. 1-7.

303. Lai, C.H., et al., *Identification of novel human genes evolutionarily conserved in Caenorhabditis elegans by comparative proteomics.* Genome Res, 2000. **10**(5): p. 703-13.

304. Herman, M.A., *Hermaphrodite cell-fate specification.* WormBook, 2006: p. 1-16.

305. Muschiol, D., F. Schroeder, and W. Traunspurger, *Life cycle and population growth rate of Caenorhabditis elegans studied by a new method.* BMC Ecol, 2009. **9**: p. 14.

306. Corsi, A.K., B. Wightman, and M. Chalfie, *A Transparent Window into Biology: A Primer on Caenorhabditis elegans.* Genetics, 2015. **200**(2): p. 387-407.

307. Johnstone, I.L., *The cuticle of the nematode Caenorhabditis elegans: a complex collagen structure.* Bioessays, 1994. **16**(3): p. 171-8.

308. Pujol, N., et al., *Distinct innate immune responses to infection and wounding in the C. elegans epidermis.* Curr Biol, 2008. **18**(7): p. 481-9.

309. Kramer, J.M., *Extracellular Matrix*, in *C. elegans II*, D.L. Riddle, et al., Editors. 1997, Cold Spring Harbor Laboratory Press
Copyright © 1997, Cold Spring Harbor Laboratory Press.: Cold Spring Harbor (NY).

310. Dodd, W., et al., *A Damage Sensor Associated with the Cuticle Coordinates Three Core Environmental Stress Responses in Caenorhabditis elegans.* Genetics, 2018. **208**(4): p. 1467-1482.

311. Choe, K.P., A.J. Przybysz, and K. Strange, *The WD40 repeat protein WDR-23 functions with the CUL4/DDB1 ubiquitin ligase to regulate nuclear abundance and activity of SKN-1 in Caenorhabditis elegans.* Mol Cell Biol, 2009. **29**(10): p. 2704-15.

312. Wang, J., et al., *RNAi screening implicates a SKN-1-dependent transcriptional response in stress resistance and longevity deriving from translation inhibition.* PLoS Genet, 2010. **6**(8).

313. Lehrbach, N.J. and G. Ruvkun, *Proteasome dysfunction triggers activation of SKN-1A/Nrf1 by the aspartic protease DDI-1.* Elife, 2016. **5**.

314. Calfon, M., et al., *IRE1 couples endoplasmic reticulum load to secretory capacity by processing the XBP-1 mRNA.* Nature, 2002. **415**(6867): p. 92-6.

315. An, J.H. and T.K. Blackwell, *SKN-1 links C. elegans mesendodermal specification to a conserved oxidative stress response.* Genes Dev, 2003. **17**(15): p. 1882-93.

316. Oliveira, R.P., et al., *Condition-adapted stress and longevity gene regulation by Caenorhabditis elegans SKN-1/Nrf.* Aging Cell, 2009. **8**(5): p. 524-41.

317. Lamitina, T., C.G. Huang, and K. Strange, *Genome-wide RNAi screening identifies protein damage as a regulator of osmoprotective gene expression.* Proc Natl Acad Sci U S A, 2006. **103**(32): p. 12173-8.

318. Lamitina, S.T., et al., *Adaptation of the nematode Caenorhabditis elegans to extreme osmotic stress.* Am J Physiol Cell Physiol, 2004. **286**(4): p. C785-91.

319. Urso, S.J., et al., *The O-GlcNAc transferase OGT is a conserved and essential regulator of the cellular and organismal response to hypertonic stress.* PLoS Genet, 2020. **16**(10): p. e1008821.

320. Lenertz, L.Y., et al., *Properties of WNK1 and implications for other family members.* J Biol Chem, 2005. **280**(29): p. 26653-8.

321. Remize, F., L. Barnavon, and S. Dequin, *Glycerol export and glycerol-3-phosphate dehydrogenase, but not glycerol phosphatase, are rate limiting for glycerol production in Saccharomyces cerevisiae.* Metab Eng, 2001. **3**(4): p. 301-12.

322. Albertyn, J., A. van Tonder, and B.A. Prior, *Purification and characterization of glycerol-3-phosphate dehydrogenase of Saccharomyces cerevisiae.* FEBS Lett, 1992. **308**(2): p. 130-2.

323. Mráček, T., Z. Drahota, and J. Houštěk, *The function and the role of the mitochondrial glycerol-3-phosphate dehydrogenase in mammalian tissues.* Biochim Biophys Acta, 2013. **1827**(3): p. 401-10.

324. Rohlfing, A.K., et al., *Genetic and physiological activation of osmosensitive gene expression mimics transcriptional signatures of pathogen infection in C. elegans.* PLoS One, 2010. **5**(2): p. e9010.

325. Loewus, F.A. and P.P.N. Murthy, *myo-Inositol metabolism in plants.* Plant Science, 2000. **150**(1): p. 1-19.

326. Turner, B.L., et al., *Inositol phosphates in the environment.* Philos Trans R Soc Lond B Biol Sci, 2002. **357**(1420): p. 449-69.

327. Loewus, F.A. and M.W. Loewus, *myo-Inositol: Its Biosynthesis and Metabolism.* Annual Review of Plant Physiology, 1983. **34**(1): p. 137-161.

328. Dijksterhuis, J., M. Veenhuis, and W. Harder, *Ultrastructural study of adhesion and initial stages of infection of nematodes by conidia of Drechmeria coniospora.* Mycological Research, 1990. **94**(1): p. 1-8.

329. Rohlfing, A.K., et al., *The Caenorhabditis elegans mucin-like protein OSM-8 negatively regulates osmosensitive physiology via the transmembrane protein PTR-23.* PLoS Genet, 2011. **7**(1): p. e1001267.

330. Moronetti Mazzeo, L.E., et al., *Stress and aging induce distinct polyQ protein aggregation states.* Proc Natl Acad Sci U S A, 2012. **109**(26): p. 10587-92.

331. Burkewitz, K., K. Choe, and K. Strange, *Hypertonic stress induces rapid and widespread protein damage in C. elegans.* Am J Physiol Cell Physiol, 2011. **301**(3): p. C566-76.

332. Choe, K.P. and K. Strange, *Genome-wide RNAi screen and in vivo protein aggregation reporters identify degradation of damaged proteins as an essential hypertonic stress response.* Am J Physiol Cell Physiol, 2008. **295**(6): p. C1488-98.

333. Burkewitz, K., et al., *Characterization of the proteostasis roles of glycerol accumulation, protein degradation and protein synthesis during osmotic stress in C. elegans.* PLoS One, 2012. **7**(3): p. e34153.

334. Lee, E.C. and K. Strange, *GCN-2 dependent inhibition of protein synthesis activates osmosensitive gene transcription via WNK and Ste20 kinase signaling.* Am J Physiol Cell Physiol, 2012. **303**(12): p. C1269-77.

335. Cox, G.N., J.M. Kramer, and D. Hirsh, *Number and organization of collagen genes in Caenorhabditis elegans.* Mol Cell Biol, 1984. **4**(11): p. 2389-95.

336. Levy, A.D., J. Yang, and J.M. Kramer, *Molecular and genetic analyses of the Caenorhabditis elegans dpy-2 and dpy-10 collagen genes: a variety of molecular alterations affect organismal morphology.* Mol Biol Cell, 1993. **4**(8): p. 803-17.

337. von Mende, N., et al., *dpy-13: a nematode collagen gene that affects body shape.* Cell, 1988. **55**(4): p. 567-76.

338. Wheeler, J.M. and J.H. Thomas, *Identification of a novel gene family involved in osmotic stress response in Caenorhabditis elegans.* Genetics, 2006. **174**(3): p. 1327-36.

339. Komatsu, H., et al., *OSM-11 facilitates LIN-12 Notch signaling during Caenorhabditis elegans vulval development.* PLoS Biol, 2008. **6**(8): p. e196.

340. Solomon, A., et al., *Caenorhabditis elegans OSR-1 regulates behavioral and physiological responses to hyperosmotic environments.* Genetics, 2004. **167**(1): p. 161-70.

341. Culotti, J.G. and R.L. Russell, *Osmotic avoidance defective mutants of the nematode Caenorhabditis elegans.* Genetics, 1978. **90**(2): p. 243-56.

342. Bargmann, C.I., J.H. Thomas, and H.R. Horvitz, *Chemosensory cell function in the behavior and development of Caenorhabditis elegans.* Cold Spring Harb Symp Quant Biol, 1990. **55**: p. 529-38.

343. Colbert, H.A., T.L. Smith, and C.I. Bargmann, *OSM-9, a novel protein with structural similarity to channels, is required for olfaction, mechanosensation, and olfactory adaptation in Caenorhabditis elegans.* J Neurosci, 1997. **17**(21): p. 8259-69.

344. Blacque, O.E., et al., *Loss of C. elegans BBS-7 and BBS-8 protein function results in cilia defects and compromised intraflagellar transport.* Genes Dev, 2004. **18**(13): p. 1630-42.

345. Igual Gil, C., et al., *Neuronal Chemosensation and Osmotic Stress Response Converge in the Regulation of aqp-8 in C. elegans.* Front Physiol, 2017. **8**: p. 380.

346. Lee, E.C., et al., *Abnormal Osmotic Avoidance Behavior in C. elegans Is Associated with Increased Hypertonic Stress Resistance and Improved Proteostasis.* PLoS One, 2016. **11**(4): p. e0154156.

347. Nadkarni, V., et al., *Osmotic response element enhancer activity. Regulation through p38 kinase and mitogen-activated extracellular signal-regulated kinase kinase.* J Biol Chem, 1999. **274**(29): p. 20185-90.

348. Sheikh-Hamad, D., et al., *p38 kinase activity is essential for osmotic induction of mRNAs for HSP70 and transporter for organic solute betaine in Madin-Darby canine kidney cells.* J Biol Chem, 1998. **273**(3): p. 1832-7.

349. Pujol, N., et al., *Anti-fungal innate immunity in C. elegans is enhanced by evolutionary diversification of antimicrobial peptides.* PLoS Pathog, 2008. **4**(7): p. e1000105.

350. Banton, M.C. and A. Tunnacliffe, *MAPK phosphorylation is implicated in the adaptation to desiccation stress in nematodes.* J Exp Biol, 2012. **215**(Pt 24): p. 4288-98.

351. Gilleard, J.S. and J.D. McGhee, *Activation of hypodermal differentiation in the Caenorhabditis elegans embryo by GATA transcription factors ELT-1 and ELT-3.* Mol Cell Biol, 2001. **21**(7): p. 2533-44.

352. McGhee, J.D., et al., *ELT-2 is the predominant transcription factor controlling differentiation and function of the C. elegans intestine, from embryo to adult.* Dev Biol, 2009. **327**(2): p. 551-65.

353. Morton, E.A. and T. Lamitina, *Caenorhabditis elegans HSF-1 is an essential nuclear protein that forms stress granule-like structures following heat shock.* Aging Cell, 2013. **12**(1): p. 112-20.

354. Hart, G.W., *Nutrient regulation of signaling and transcription.* J Biol Chem, 2019. **294**(7): p. 2211-2231.

355. Torres, C.R. and G.W. Hart, *Topography and polypeptide distribution of terminal N-acetylglucosamine residues on the surfaces of intact lymphocytes. Evidence for O-linked GlcNAc.* J Biol Chem, 1984. **259**(5): p. 3308-17.

356. Holt, G.D. and G.W. Hart, *The subcellular distribution of terminal N-acetylglucosamine moieties. Localization of a novel protein-saccharide linkage, O-linked GlcNAc.* J Biol Chem, 1986. **261**(17): p. 8049-57.

357. Hanover, J.A., et al., *O-linked N-acetylglucosamine is attached to proteins of the nuclear pore. Evidence for cytoplasmic and nucleoplasmic glycoproteins.* J Biol Chem, 1987. **262**(20): p. 9887-94.

358. Holt, G.D., et al., *Erythrocytes contain cytoplasmic glycoproteins. O-linked GlcNAc on Band 4.1.* J Biol Chem, 1987. **262**(31): p. 14847-50.

359. Kreppel, L.K., M.A. Blomberg, and G.W. Hart, *Dynamic glycosylation of nuclear and cytosolic proteins. Cloning and characterization of a unique O-GlcNAc transferase with multiple tetratricopeptide repeats.* J Biol Chem, 1997. **272**(14): p. 9308-15.

360. Lubas, W.A., et al., *O-Linked GlcNAc transferase is a conserved nucleocytoplasmic protein containing tetratricopeptide repeats.* J Biol Chem, 1997. **272**(14): p. 9316-24.

361. Gao, Y., et al., *Dynamic O-glycosylation of nuclear and cytosolic proteins: cloning and characterization of a neutral, cytosolic beta-N-acetylglucosaminidase from human brain.* J Biol Chem, 2001. **276**(13): p. 9838-45.

362. Rahe, D.P. and O. Hobert, *Restriction of Cellular Plasticity of Differentiated Cells Mediated by Chromatin Modifiers, Transcription Factors and Protein Kinases.* G3 (Bethesda), 2019. **9**(7): p. 2287-2302.

363. Seo, H.G., et al., *Identification of the nuclear localisation signal of O-GlcNAc transferase and its nuclear import regulation.* Sci Rep, 2016. **6**: p. 34614.

364. Hanover, J.A., et al., *Mitochondrial and nucleocytoplasmic isoforms of O-linked GlcNAc transferase encoded by a single mammalian gene.* Arch Biochem Biophys, 2003. **409**(2): p. 287-97.

365. Lubas, W.A. and J.A. Hanover, *Functional expression of O-linked GlcNAc transferase. Domain structure and substrate specificity.* J Biol Chem, 2000. **275**(15): p. 10983-8.

366. Iyer, S.P. and G.W. Hart, *Roles of the tetratricopeptide repeat domain in O-GlcNAc transferase targeting and protein substrate specificity.* J Biol Chem, 2003. **278**(27): p. 24608-16.

367. Jínek, M., et al., *The superhelical TPR-repeat domain of O-linked GlcNAc transferase exhibits structural similarities to importin α.* Nature Structural & Molecular Biology, 2004. **11**(10): p. 1001-1007.

368. Kreppel, L.K. and G.W. Hart, *Regulation of a cytosolic and nuclear O-GlcNAc transferase. Role of the tetratricopeptide repeats.* J Biol Chem, 1999. **274**(45): p. 32015-22.

369. Bond, M.R. and J.A. Hanover, *A little sugar goes a long way: the cell biology of O-GlcNAc.* J Cell Biol, 2015. **208**(7): p. 869-80.

370. Love, D.C., et al., *Dynamic O-GlcNAc cycling at promoters of Caenorhabditis elegans genes regulating longevity, stress, and immunity.* Proc Natl Acad Sci U S A, 2010. **107**(16): p. 7413-8.

371. Yang, X., F. Zhang, and J.E. Kudlow, *Recruitment of O-GlcNAc transferase to promoters by corepressor mSin3A: coupling protein O-GlcNAcylation to transcriptional repression.* Cell, 2002. **110**(1): p. 69-80.

372. Ranuncolo, S.M., et al., *Evidence of the Involvement of O-GlcNAc-modified Human RNA Polymerase II CTD in Transcription in Vitro and in Vivo*.* Journal of Biological Chemistry, 2012. **287**(28): p. 23549-23561.

373. Lazarus, M.B., et al., *Structure of human O-GlcNAc transferase and its complex with a peptide substrate.* Nature, 2011. **469**(7331): p. 564-7.

374. Bashton, M. and C. Chothia, *The geometry of domain combination in proteins.* J Mol Biol, 2002. **315**(4): p. 927-39.

375. Sacoman, J.L., et al., *Mitochondrial O-GlcNAc Transferase (mOGT) Regulates Mitochondrial Structure, Function, and Survival in HeLa Cells.* J Biol Chem, 2017. **292**(11): p. 4499-4518.

376. März, P., et al., *Ataxin-10 interacts with O-linked beta-N-acetylglucosamine transferase in the brain.* J Biol Chem, 2006. **281**(29): p. 20263-70.

377. Haltiwanger, R.S., G.D. Holt, and G.W. Hart, *Enzymatic addition of O-GlcNAc to nuclear and cytoplasmic proteins. Identification of a uridine diphospho-N-acetylglucosamine:peptide beta-N-acetylglucosaminyltransferase.* J Biol Chem, 1990. **265**(5): p. 2563-8.

378. Olivier-Van Stichelen, S. and J.A. Hanover, *You are what you eat: O-linked N-acetylglucosamine in disease, development and epigenetics.* Curr Opin Clin Nutr Metab Care, 2015. **18**(4): p. 339-45.

379. Copeland, R.J., J.W. Bullen, and G.W. Hart, *Cross-talk between GlcNAcylation and phosphorylation: roles in insulin resistance and glucose toxicity.* American Journal of Physiology-Endocrinology and Metabolism, 2008. **295**(1): p. E17-E28.

380. Medford, H.M., J.C. Chatham, and S.A. Marsh, *Chronic ingestion of a Western diet increases O-linked-β-N-acetylglucosamine (O-GlcNAc) protein modification in the rat heart.* Life Sci, 2012. **90**(23-24): p. 883-8.

381. Taylor, R.P., et al., *Glucose deprivation stimulates O-GlcNAc modification of proteins through up-regulation of O-linked N-acetylglucosaminyltransferase.* J Biol Chem, 2008. **283**(10): p. 6050-7.

382. Cheung, W.D. and G.W. Hart, *AMP-activated protein kinase and p38 MAPK activate O-GlcNAcylation of neuronal proteins during glucose deprivation.* J Biol Chem, 2008. **283**(19): p. 13009-20.

383. Marotta, N.P., et al., *O-GlcNAc modification prevents peptide-dependent acceleration of α-synuclein aggregation.* Chembiochem, 2012. **13**(18): p. 2665-70.

384. Song, M., et al., *o-GlcNAc transferase is activated by CaMKIV-dependent phosphorylation under potassium chloride-induced depolarization in NG-108-15 cells.* Cell Signal, 2008. **20**(1): p. 94-104.

385. Kaasik, K., et al., *Glucose sensor O-GlcNAcylation coordinates with phosphorylation to regulate circadian clock.* Cell Metab, 2013. **17**(2): p. 291-302.

386. Bullen, J.W., et al., *Cross-talk between two essential nutrient-sensitive enzymes: O-GlcNAc transferase (OGT) and AMP-activated protein kinase (AMPK).* J Biol Chem, 2014. **289**(15): p. 10592-606.

387. Fan, Q., et al., *O-GlcNAc site-mapping of liver X receptor-α and O-GlcNAc transferase.* Biochem Biophys Res Commun, 2018. **499**(2): p. 354-360.

388. Liu, L., et al., *O-GlcNAcylation of Thr(12)/Ser(56) in short-form O-GlcNAc transferase (sOGT) regulates its substrate selectivity.* J Biol Chem, 2019. **294**(45): p. 16620-16633.

389. Cheung, W.D., et al., *O-linked beta-N-acetylglucosaminyltransferase substrate specificity is regulated by myosin phosphatase targeting and other interacting proteins.* J Biol Chem, 2008. **283**(49): p. 33935-41.

390. Wang, Z., M. Gucek, and G.W. Hart, *Cross-talk between GlcNAcylation and phosphorylation: site-specific phosphorylation dynamics in response to globally elevated O-GlcNAc.* Proc Natl Acad Sci U S A, 2008. **105**(37): p. 13793-8.

391. Dong, D.L., et al., *Cytoplasmic O-GlcNAc modification of the head domain and the KSP repeat motif of the neurofilament protein neurofilament-H.* J Biol Chem, 1996. **271**(34): p. 20845-52.

392. Kelly, W.G., M.E. Dahmus, and G.W. Hart, *RNA polymerase II is a glycoprotein. Modification of the COOH-terminal domain by O-GlcNAc.* J Biol Chem, 1993. **268**(14): p. 10416-24.

393. Comer, F.I. and G.W. Hart, *Reciprocity between O-GlcNAc and O-Phosphate on the Carboxyl Terminal Domain of RNA Polymerase II.* Biochemistry, 2001. **40**(26): p. 7845-7852.

394. Chou, T.Y., G.W. Hart, and C.V. Dang, *c-Myc is glycosylated at threonine 58, a known phosphorylation site and a mutational hot spot in lymphomas.* J Biol Chem, 1995. **270**(32): p. 18961-5.

395. Kamemura, K., et al., *Dynamic interplay between O-glycosylation and O-phosphorylation of nucleocytoplasmic proteins: alternative glycosylation/phosphorylation of THR-58, a known mutational hot spot of c-Myc in lymphomas, is regulated by mitogens.* J Biol Chem, 2002. **277**(21): p. 19229-35.

396. Dias, W.B., et al., *Regulation of calcium/calmodulin-dependent kinase IV by O-GlcNAc modification.* J Biol Chem, 2009. **284**(32): p. 21327-37.

397. Daou, S., et al., *Crosstalk between O-GlcNAcylation and proteolytic cleavage regulates the host cell factor-1 maturation pathway.* Proc Natl Acad Sci U S A, 2011. **108**(7): p. 2747-52.

398. Capotosti, F., et al., *O-GlcNAc transferase catalyzes site-specific proteolysis of HCF-1.* Cell, 2011. **144**(3): p. 376-88.

399. Wilson, A.C., M.G. Peterson, and W. Herr, *The HCF repeat is an unusual proteolytic cleavage signal.* Genes Dev, 1995. **9**(20): p. 2445-58.

400. Julien, E. and W. Herr, *Proteolytic processing is necessary to separate and ensure proper cell growth and cytokinesis functions of HCF-1.* The EMBO Journal, 2003. **22**(10): p. 2360-2369.

401. Julien, E. and W. Herr, *A switch in mitotic histone H4 lysine 20 methylation status is linked to M phase defects upon loss of HCF-1.* Mol Cell, 2004. **14**(6): p. 713-25.

402. Capotosti, F., J.J. Hsieh, and W. Herr, *Species selectivity of mixed-lineage leukemia/trithorax and HCF proteolytic maturation pathways.* Mol Cell Biol, 2007. **27**(20): p. 7063-72.

403. Liu, Y., M.O. Hengartner, and W. Herr, *Selected elements of herpes simplex virus accessory factor HCF are highly conserved in Caenorhabditis elegans.* Mol Cell Biol, 1999. **19**(1): p. 909-15.

404. Lazarus, M.B., et al., *HCF-1 is cleaved in the active site of O-GlcNAc transferase.* Science, 2013. **342**(6163): p. 1235-9.

405. Janetzko, J., et al., *How the glycosyltransferase OGT catalyzes amide bond cleavage.* Nat Chem Biol, 2016. **12**(11): p. 899-901.

406. Kapuria, V., et al., *Proteolysis of HCF-1 by Ser/Thr glycosylation-incompetent O-GlcNAc transferase:UDP-GlcNAc complexes.* Genes Dev, 2016. **30**(8): p. 960-72.

407. Liu, H., et al., *Inhibition of E-cadherin/catenin complex formation by O-linked N-acetylglucosamine transferase is partially independent of its catalytic activity.* Mol Med Rep, 2016. **13**(2): p. 1851-60.

408. Giles, A.C., et al., *A complex containing the O-GlcNAc transferase OGT-1 and the ubiquitin ligase EEL-1 regulates GABA neuron function.* J Biol Chem, 2019. **294**(17): p. 6843-6856.

409. Marshall, S., V. Bacote, and R.R. Traxinger, *Discovery of a metabolic pathway mediating glucose-induced desensitization of the glucose transport system. Role of hexosamine biosynthesis in the induction of insulin resistance.* J Biol Chem, 1991. **266**(8): p. 4706-12.

410. Vosseller, K., et al., *Elevated nucleocytoplasmic glycosylation by O-GlcNAc results in insulin resistance associated with defects in Akt activation in 3T3-L1 adipocytes.* Proc Natl Acad Sci U S A, 2002. **99**(8): p. 5313-8.

411. McClain, D.A., et al., *Altered glycan-dependent signaling induces insulin resistance and hyperleptinemia.* Proc Natl Acad Sci U S A, 2002. **99**(16): p. 10695-9.

412. Wang, S., et al., *Extensive crosstalk between O-GlcNAcylation and phosphorylation regulates Akt signaling.* PLoS One, 2012. **7**(5): p. e37427.

413. Hanover, J.A., et al., *A Caenorhabditis elegans model of insulin resistance: altered macronutrient storage and dauer formation in an OGT-1 knockout.* Proc Natl Acad Sci U S A, 2005. **102**(32): p. 11266-71.

414. Gandy, J.C., A.E. Rountree, and G.N. Bijur, *Akt1 is dynamically modified with O-GlcNAc following treatments with PUGNAc and insulin-like growth factor-1*. FEBS Letters, 2006. **580**(13): p. 3051-3058.

415. Kuo, M., et al., *O-glycosylation of FoxO1 increases its transcriptional activity towards the glucose 6-phosphatase gene.* FEBS Letters, 2008. **582**(5): p. 829-834.

416. Yang, X., et al., *Phosphoinositide signalling links O-GlcNAc transferase to insulin resistance.* Nature, 2008. **451**(7181): p. 964-9.

417. Park, S., et al., *Protein O-GlcNAcylation regulates Drosophila growth through the insulin signaling pathway.* Cellular and Molecular Life Sciences, 2011. **68**(20): p. 3377-3384.

418. Taub, D.G., M.R. Awal, and C.V. Gabel, *O-GlcNAc Signaling Orchestrates the Regenerative Response to Neuronal Injury in Caenorhabditis elegans.* Cell Rep, 2018. **24**(8): p. 1931-1938.e3.

419. Ardiel, E.L., et al., *Insights into the roles of CMK-1 and OGT-1 in interstimulus interval-dependent habituation in Caenorhabditis elegans.* Proc Biol Sci, 2018. **285**(1891).

420. Wheatley, E.G., et al., *Neuronal O-GlcNAcylation Improves Cognitive Function in the Aged Mouse Brain.* Curr Biol, 2019. **29**(20): p. 3359-3369.e4.

421. Wang, P. and J.A. Hanover, *Nutrient-driven O-GlcNAc cycling influences autophagic flux and neurodegenerative proteotoxicity.* Autophagy, 2013. **9**(4): p. 604-6.

422. Park, S., et al., *O-GlcNAc modification is essential for the regulation of autophagy in Drosophila melanogaster.* Cell Mol Life Sci, 2015. **72**(16): p. 3173-83.

423. Guo, B., et al., *O-GlcNAc-modification of SNAP-29 regulates autophagosome maturation.* Nat Cell Biol, 2014. **16**(12): p. 1215-26.

424. Li, H., et al., *O-GlcNAcylation of SKN-1 modulates the lifespan and oxidative stress resistance in Caenorhabditis elegans.* Sci Rep, 2017. **7**: p. 43601.

425. An, J.H., et al., *Regulation of the Caenorhabditis elegans oxidative stress defense protein SKN-1 by glycogen synthase kinase-3.* Proc Natl Acad Sci U S A, 2005. **102**(45): p. 16275-80.

426. Zhang, X., X.E. Shu, and S.B. Qian, *O-GlcNAc modification of eIF4GI acts as a translational switch in heat shock response.* Nat Chem Biol, 2018. **14**(10): p. 909-916.

427. Kazemi, Z., et al., *O-linked beta-N-acetylglucosamine (O-GlcNAc) regulates stress-induced heat shock protein expression in a GSK-3beta-dependent manner.* J Biol Chem, 2010. **285**(50): p. 39096-107.

428. Sohn, K.C., et al., *OGT functions as a catalytic chaperone under heat stress response: a unique defense role of OGT in hyperthermia*. Biochem Biophys Res Commun, 2004. **322**(3): p. 1045-51.

429. Jang, I., et al., *O-GlcNAcylation of eIF2alpha regulates the phospho-eIF2alpha-mediated ER stress response.* Biochim Biophys Acta, 2015. **1853**(8): p. 1860-9.

430. Bond, M.R., et al., *Conserved nutrient sensor O-GlcNAc transferase is integral to C. elegans pathogen-specific immunity.* PLoS One, 2014. **9**(12): p. e113231.

431. Ingham, P.W., *A gene that regulates the bithorax complex differentially in larval and adult cells of Drosophila.* Cell, 1984. **37**(3): p. 815-23.

432. O'Donnell, N., et al., *Ogt-dependent X-chromosome-linked protein glycosylation is a requisite modification in somatic cell function and embryo viability.* Mol Cell Biol, 2004. **24**(4): p. 1680-90.

433. Shafi, R., et al., *The O-GlcNAc transferase gene resides on the X chromosome and is essential for embryonic stem cell viability and mouse ontogeny.* Proc Natl Acad Sci U S A, 2000. **97**(11): p. 5735-9.

434. Watson, L.J., et al., *Cardiomyocyte Ogt is essential for postnatal viability.* American Journal of Physiology-Heart and Circulatory Physiology, 2014. **306**(1): p. H142-H153.

435. Yang, Y.R., et al., *O-GlcNAcase is essential for embryonic development and maintenance of genomic stability.* Aging Cell, 2012. **11**(3): p. 439-448.

436. Gloster, T.M., et al., *Hijacking a biosynthetic pathway yields a glycosyltransferase inhibitor within cells.* Nat Chem Biol, 2011. **7**(3): p. 174-81.

437. Boehmelt, G., et al., *Decreased UDP-GlcNAc levels abrogate proliferation control in EMeg32-deficient cells.* The EMBO Journal, 2000. **19**(19): p. 5092-5104.

438. Ortiz-Meoz, R.F., et al., *A small molecule that inhibits OGT activity in cells.* ACS Chem Biol, 2015. **10**(6): p. 1392-7.

439. Edmonds, M. and R. Abrams, *Polynucleotide biosynthesis: formation of a sequence of adenylate units from adenosine triphosphate by an enzyme from thymus nuclei.* J Biol Chem, 1960. **235**: p. 1142-9.

440. Edmonds, M., M.H. Vaughan, Jr., and H. Nakazato, *Polyadenylic acid sequences in the heterogeneous nuclear RNA and rapidly-labeled polyribosomal RNA of HeLa cells: possible evidence for a precursor relationship.* Proc Natl Acad Sci U S A, 1971. **68**(6): p. 1336-40.

441. Nevins, J.R. and J.E. Darnell, Jr., *Steps in the processing of Ad2 mRNA: poly(A)+ nuclear sequences are conserved and poly(A) addition precedes splicing.* Cell, 1978. **15**(4): p. 1477-93.

442. Zhao, J., L. Hyman, and C. Moore, *Formation of mRNA 3' ends in eukaryotes: mechanism, regulation, and interrelationships with other steps in mRNA synthesis.* Microbiol Mol Biol Rev, 1999. **63**(2): p. 405-45.

443. Huang, Y. and G.G. Carmichael, *Role of polyadenylation in nucleocytoplasmic transport of mRNA.* Mol Cell Biol, 1996. **16**(4): p. 1534-42.

444. Ford, L.P., P.S. Bagga, and J. Wilusz, *The poly(A) tail inhibits the assembly of a 3'-to-5' exonuclease in an in vitro RNA stability system.* Mol Cell Biol, 1997. **17**(1): p. 398-406.

445. Borman, A.M., et al., *Free poly(A) stimulates capped mRNA translation in vitro through the eIF4G-poly(A)-binding protein interaction.* J Biol Chem, 2002. **277**(39): p. 36818-24.

446. Shi, Y., et al., *Molecular architecture of the human pre-mRNA 3' processing complex.* Mol Cell, 2009. **33**(3): p. 365-76.

447. Mandel, C.R., Y. Bai, and L. Tong, *Protein factors in pre-mRNA 3'-end processing.* Cell Mol Life Sci, 2008. **65**(7-8): p. 1099-122.

448. Chan, S., E.A. Choi, and Y. Shi, *Pre-mRNA 3'-end processing complex assembly and function.* Wiley Interdiscip Rev RNA, 2011. **2**(3): p. 321-35.

449. Takagaki, Y. and J.L. Manley, *RNA recognition by the human polyadenylation factor CstF.* Mol Cell Biol, 1997. **17**(7): p. 3907-14.

450. Rüegsegger, U., K. Beyer, and W. Keller, *Purification and characterization of human cleavage factor Im involved in the 3' end processing of messenger RNA precursors.* J Biol Chem, 1996. **271**(11): p. 6107-13.

451. Zhao, J., et al., *Pta1, a component of yeast CF II, is required for both cleavage and poly(A) addition of mRNA precursor.* Mol Cell Biol, 1999. **19**(11): p. 7733-40.

452. Christofori, G. and W. Keller, *3' cleavage and polyadenylation of mRNA precursors in vitro requires a poly(A) polymerase, a cleavage factor, and a snRNP.* Cell, 1988. **54**(6): p. 875-89.

453. Meinhart, A. and P. Cramer, *Recognition of RNA polymerase II carboxy-terminal domain by 3'-RNA-processing factors.* Nature, 2004. **430**(6996): p. 223-226.

454. McCracken, S., et al., *The C-terminal domain of RNA polymerase II couples mRNA processing to transcription.* Nature, 1997. **385**(6614): p. 357-61.

455. Chen, F., C.C. MacDonald, and J. Wilusz, *Cleavage site determinants in the mammalian polyadenylation signal.* Nucleic Acids Res, 1995. **23**(14): p. 2614-20.

456. Wickens, M. and P. Stephenson, *Role of the conserved AAUAAA sequence: four AAUAAA point mutants prevent messenger RNA 3' end formation.* Science, 1984. **226**(4678): p. 1045-51.

457. Gil, A. and N.J. Proudfoot, *Position-dependent sequence elements downstream of AAUAAA are required for efficient rabbit beta-globin mRNA 3' end formation.* Cell, 1987. **49**(3): p. 399-406.

458. Keller, W., et al., *Cleavage and polyadenylation factor CPF specifically interacts with the pre-mRNA 3' processing signal AAUAAA.* Embo j, 1991. **10**(13): p. 4241-9.

459. Murthy, K.G. and J.L. Manley, *The 160-kD subunit of human cleavage-polyadenylation specificity factor coordinates pre-mRNA 3'-end formation.* Genes Dev, 1995. **9**(21): p. 2672-83.

460. Kaufmann, I., et al., *Human Fip1 is a subunit of CPSF that binds to U-rich RNA elements and stimulates poly(A) polymerase.* Embo j, 2004. **23**(3): p. 616-26.

461. Takagaki, Y. and J.L. Manley, *Complex protein interactions within the human polyadenylation machinery identify a novel component.* Mol Cell Biol, 2000. **20**(5): p. 1515-25.

462. MacDonald, C.C., J. Wilusz, and T. Shenk, *The 64-kilodalton subunit of the CstF polyadenylation factor binds to pre-mRNAs downstream of the cleavage site and influences cleavage site location.* Mol Cell Biol, 1994. **14**(10): p. 6647-54.

463. Mandel, C.R., et al., *Polyadenylation factor CPSF-73 is the pre-mRNA 3'-end-processing endonuclease.* Nature, 2006. **444**(7121): p. 953-6.

464. Wahle, E., et al., *Isolation and expression of cDNA clones encoding mammalian poly(A) polymerase.* Embo j, 1991. **10**(13): p. 4251-7.

465. Bienroth, S., W. Keller, and E. Wahle, *Assembly of a processive messenger RNA polyadenylation complex.* Embo j, 1993. **12**(2): p. 585-94.

466. Zhang, Z., J. Fu, and D.S. Gilmour, *CTD-dependent dismantling of the RNA polymerase II elongation complex by the pre-mRNA 3'-end processing factor, Pcf11.* Genes Dev, 2005. **19**(13): p. 1572-80.

467. Ruepp, M.D., et al., *Mammalian pre-mRNA 3' end processing factor CF I m 68 functions in mRNA export.* Mol Biol Cell, 2009. **20**(24): p. 5211-23.

468. Marzluff, W.F., *Metazoan replication-dependent histone mRNAs: a distinct set of RNA polymerase II transcripts.* Current Opinion in Cell Biology, 2005. **17**(3): p. 274-280.

469. Hoque, M., et al., *Analysis of alternative cleavage and polyadenylation by 3' region extraction and deep sequencing.* Nat Methods, 2013. **10**(2): p. 133-9.

470. Mangone, M., et al., *The landscape of C. elegans 3'UTRs.* Science, 2010. **329**(5990): p. 432-5.

471. Tian, B. and J.L. Manley, *Alternative polyadenylation of mRNA precursors.* Nat Rev Mol Cell Biol, 2017. **18**(1): p. 18-30.

472. Edwalds-Gilbert, G., K.L. Veraldi, and C. Milcarek, *Alternative poly(A) site selection in complex transcription units: means to an end?* Nucleic Acids Res, 1997. **25**(13): p. 2547-61.

473. Tian, B., et al., *A large-scale analysis of mRNA polyadenylation of human and mouse genes.* Nucleic Acids Research, 2005. **33**(1): p. 201-212.

474. Sandberg, R., et al., *Proliferating cells express mRNAs with shortened 3' untranslated regions and fewer microRNA target sites.* Science, 2008. **320**(5883): p. 1643-7.

475. Hogg, J.R. and S.P. Goff, *Upf1 senses 3'UTR length to potentiate mRNA decay.* Cell, 2010. **143**(3): p. 379-89.

476. Zheng, D., et al., *Cellular stress alters 3'UTR landscape through alternative polyadenylation and isoform-specific degradation.* Nat Commun, 2018. **9**(1): p. 2268.

477. Vorlová, S., et al., *Induction of antagonistic soluble decoy receptor tyrosine kinases by intronic polyA activation.* Mol Cell, 2011. **43**(6): p. 927-39.

478. Pan, Z., et al., *An intronic polyadenylation site in human and mouse CstF-77 genes suggests an evolutionarily conserved regulatory mechanism.* Gene, 2006. **366**(2): p. 325-34.

479. Takagaki, Y., et al., *The polyadenylation factor CstF-64 regulates alternative processing of IgM heavy chain pre-mRNA during B cell differentiation.* Cell, 1996. **87**(5): p. 941-52.

480. Ji, Z. and B. Tian, *Reprogramming of 3' untranslated regions of mRNAs by alternative polyadenylation in generation of pluripotent stem cells from different cell types.* PLoS One, 2009. **4**(12): p. e8419.

481. Beaudoing, E., et al., *Patterns of variant polyadenylation signal usage in human genes.* Genome Res, 2000. **10**(7): p. 1001-10.

482. Gruber, A.R., et al., *Cleavage factor Im is a key regulator of 3' UTR length.* RNA Biol, 2012. **9**(12): p. 1405-12.

483. Martin, G., et al., *Genome-wide analysis of pre-mRNA 3' end processing reveals a decisive role of human cleavage factor I in the regulation of 3' UTR length.* Cell Rep, 2012. **1**(6): p. 753-63.

484. Liu, Y., et al., *Cold-induced RNA-binding proteins regulate circadian gene expression by controlling alternative polyadenylation.* Scientific Reports, 2013. **3**(1): p. 2054.

485. Hung, L.H., et al., *Diverse roles of hnRNP L in mammalian mRNA processing: a combined microarray and RNAi analysis.* Rna, 2008. **14**(2): p. 284-96.

486. Tian, B., Z. Pan, and J.Y. Lee, *Widespread mRNA polyadenylation events in introns indicate dynamic interplay between polyadenylation and splicing.* Genome Res, 2007. **17**(2): p. 156-65.

487. Li, W., et al., *Systematic profiling of poly(A)+ transcripts modulated by core 3' end processing and splicing factors reveals regulatory rules of alternative cleavage and polyadenylation.* PLoS Genet, 2015. **11**(4): p. e1005166.

488. Müller-McNicoll, M., et al., *SR proteins are NXF1 adaptors that link alternative RNA processing to mRNA export.* Genes Dev, 2016. **30**(5): p. 553-66.

489. Hilgers, V., S.B. Lemke, and M. Levine, *ELAV mediates 3' UTR extension in the Drosophila nervous system.* Genes Dev, 2012. **26**(20): p. 2259-64.

490. Takagaki, Y. and J.L. Manley, *Levels of polyadenylation factor CstF-64 control IgM heavy chain mRNA accumulation and other events associated with B cell differentiation.* Mol Cell, 1998. **2**(6): p. 761-71.

491. LaBella, M.L., et al., *Casein Kinase 1δ Stabilizes Mature Axons by Inhibiting Transcription Termination of Ankyrin.* Dev Cell, 2020. **52**(1): p. 88-103.e18.

492. Sadek, J., et al., *Alternative polyadenylation and the stress response.* Wiley Interdiscip Rev RNA, 2019. **10**(5): p. e1540.

493. Tranter, M., et al., *Coordinated post-transcriptional regulation of Hsp70.3 gene expression by microRNA and alternative polyadenylation.* J Biol Chem, 2011. **286**(34): p. 29828-37.

494. Segref, A., S. Torres, and T. Hoppe, *A screenable in vivo assay to study proteostasis networks in Caenorhabditis elegans.* Genetics, 2011. **187**(4): p. 1235-40.

495. Jang, I., et al., *O-GlcNAcylation of eIF2α regulates the phospho-eIF2α-mediated ER stress response.* Biochim Biophys Acta, 2015. **1853**(8): p. 1860-9.

496. Rahman, M.M., et al., *Intracellular protein glycosylation modulates insulin mediated lifespan in C.elegans.* Aging (Albany NY), 2010. **2**(10): p. 678-90.

497. Su, L., et al., *ELT-2 promotes O-GlcNAc transferase OGT-1 expression to modulate Caenorhabditis elegans lifespan.* J Cell Biochem, 2020.

498. Mondoux, M.A., et al., *O-linked-N-acetylglucosamine cycling and insulin signaling are required for the glucose stress response in Caenorhabditis elegans.* Genetics, 2011. **188**(2): p. 369-82.

499. Kim, Y. and J. Choi, *Early life exposure of a biocide, CMIT/MIT causes metabolic toxicity via the O-GlcNAc transferase pathway in the nematode C. elegans.* Toxicol Appl Pharmacol, 2019. **376**: p. 1-8.

500. Hajduskova, M., et al., *MRG-1/MRG15 Is a Barrier for Germ Cell to Neuron Reprogramming in Caenorhabditis elegans.* Genetics, 2019. **211**(1): p. 121-139.

501. Shih, P.Y., et al., *Newly Identified Nematodes from Mono Lake Exhibit Extreme Arsenic Resistance.* Curr Biol, 2019. **29**(19): p. 3339-3344.e4.

502. Rouzaire-Dubois, B., S. O'Regan, and J.M. Dubois, *Cell size-dependent and independent proliferation of rodent neuroblastoma x glioma cells.* J Cell Physiol, 2005. **203**(1): p. 243-50.

503. Pendergrass, W.R., et al., *The relationship between the rate of entry into S phase, concentration of DNA polymerase alpha, and cell volume in human diploid fibroblast-like monokaryon cells.* Exp Cell Res, 1991. **192**(2): p. 418-25.

504. Pravata, V.M., et al., *Catalytic deficiency of O-GlcNAc transferase leads to X-linked intellectual disability.* Proc Natl Acad Sci U S A, 2019. **116**(30): p. 14961-14970.

505. Levine, Z.G. and S. Walker, *The Biochemistry of O-GlcNAc Transferase: Which Functions Make It Essential in Mammalian Cells?* Annu Rev Biochem, 2016. **85**: p. 631-57.

506. Li, H., et al., *The Sequence Alignment/Map format and SAMtools.* Bioinformatics, 2009. **25**(16): p. 2078-9.

507. Dokshin, G.A., et al., *Robust Genome Editing with Short Single-Stranded and Long, Partially Single-Stranded DNA Donors in Caenorhabditis elegans.* Genetics, 2018. **210**(3): p. 781-787.

508. Ghanta, K.S. and C.C. Mello, *Melting dsDNA Donor Molecules Greatly Improves Precision Genome Editing in Caenorhabditis elegans.* Genetics, 2020. **216**(3): p. 643-650.

509. Ghanta, K.S., et al., *5′ Modifications Improve Potency and Efficacy of DNA Donors for Precision Genome Editing.* bioRxiv, 2018: p. 354480.

510. Strome, S. and W.B. Wood, *Immunofluorescence visualization of germ-line-specific cytoplasmic granules in embryos, larvae, and adults of Caenorhabditis elegans.* Proc Natl Acad Sci U S A, 1982. **79**(5): p. 1558-62.

511. Yu, J., et al., *An Aversive Response to Osmotic Upshift in Caenorhabditis elegans.* eNeuro, 2017. **4**(2).